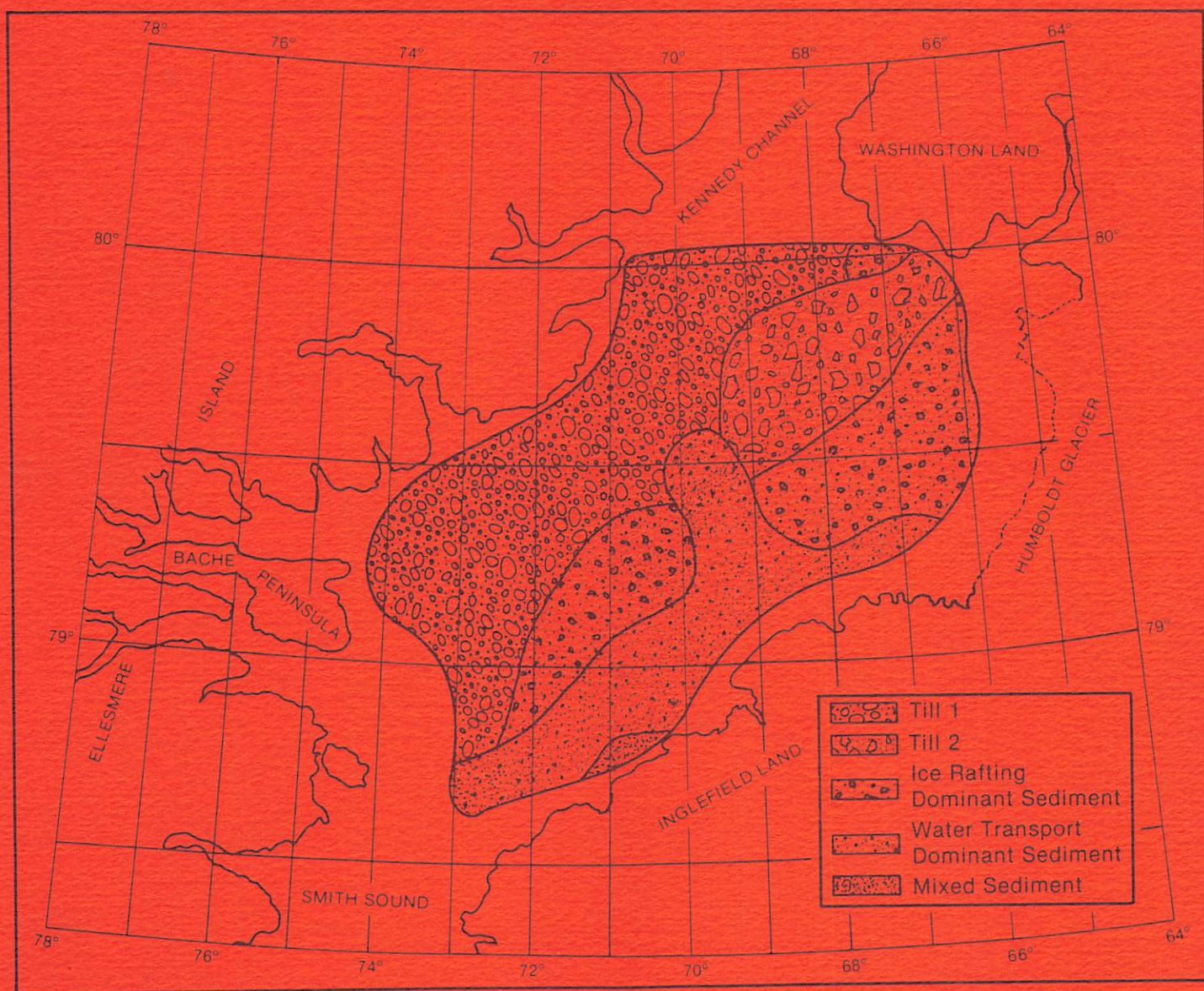


Sediments and Sediment Processes in Kane Basin, A High Arctic Glacial Marine Basin

By
Joseph Henry Kravitz



OCCASIONAL PAPER NO. 39
1982

INSTITUTE OF ARCTIC AND ALPINE RESEARCH • UNIVERSITY OF COLORADO

Sediments and Sediment Processes in Kane Basin,
A High Arctic Glacial Marine Basin

By

Joseph Henry Kravitz
Office of Marine Pollution Assessment
National Oceanic and Atmospheric Administration
Rockville, Maryland 20852

1982

University of Colorado
Institute of Arctic and Alpine Research
Occasional Paper 39

INSTAAR/OP - 39
ISSN 0069-6145

TABLE OF CONTENTS

	Page
PREFACE	v
ACKNOWLEDGEMENTS	vi
ABSTRACT	vii
LIST OF ILLUSTRATIONS	ix
LIST OF TABLES	x
 Chapter	
I. INTRODUCTION	1
Purpose	1
Regional Setting	1
Geological Setting	3
Bathymetry	10
Oceanography	12
Ice	14
Previous Studies of the Kane Basin	16
II. SHIPBOARD PROCEDURES	21
Navigation	21
Sediment Sampling	21
Underwater Camera Operations	22
Bathymetric Soundings	22
III. LABORATORY PROCEDURES	23
X-Radiography	23
Subsampling	23
Mass Physical Properties	24
Grain Size Analysis	29
Heavy and Light Mineral Analysis	30
Gravel Analysis	32
Mineral and Chemical Element Analysis of the < 2 μ m Sediment Fraction	32
Sediment Organic Carbon and Carbonate Content	39
Diatom Analysis	39
Statistical Procedures	40
Mapping and Plotting Procedures	42

Chapter	Page
IV. RESULTS	44
Radiograph Descriptions	44
Texture	44
Mass Physical Properties	53
Carbonate and Organic Carbon Content	70
Heavy and Light Mineral Composition	73
The Mineralogy of the < 2 μ m Sediment Fraction.	75
Chemical Elements in the < 2 μ m Sediment	
Fraction	83
Diatom Distribution	98
Factor Analysis	100
V. DISCUSSION	110
Factor Analysis	111
Radiograph Analysis	120
Texture	126
Mass Physical Properties	134
Carbonate and Organic Carbon Distribution	141
Gravel and Sand Composition	147
The Character and Distribution of the	
< 2 μ m Fraction Mineralogy	153
Chemical Elements in the	160
< 2 μ m Sediment Fraction	162
Diatom Distribution	
VI. CONCLUSIONS	165
REFERENCES CITED	177

PREFACE

Dr. Elisha Kent Kane, who led the second Grinnell expedition from the United States to the Arctic from 1853 to 1855, might be surprised to be told that, little over 100 years later, a ship would criss-cross the basin where he searched for Sir John Franklin, taking bottom sediment samples.

The Kane Expedition discovered the Humboldt Glacier, shown in this monograph to be so important in controlling the bottom sediments of the northeastern section of the Kane Basin. Kane's observations on ice conditions, geology, weather, climate, ice, snow, and biology were very acute; I believe that this controversial man would have enjoyed this monograph.

Dr. Kravitz's Occasional Paper fits with our intention for this series. It is written by an associate of the Institute of Arctic and Alpine Research and, with its origin as a doctoral dissertation, is too long and data intensive for publication in a research journal. It is nevertheless a well-produced, valuable document, which will be accessible to the scientific community.

Patrick J. Webber
Director
Institute for Arctic and Alpine Research

October 1982

ACKNOWLEDGEMENTS

This paper is part of a PhD dissertation submitted to The George Washington University. Thanks are extended to Drs. Roy C. Lindholm, Frederic R. Siegel, and Jack W. Pierce for assistance during the writing of this dissertation. Their council greatly improved the manuscript. The author is especially grateful for the guidance provided by Dr. Lindholm during the years of graduate study at The George Washington University. The author also thanks Dr. James V. Gardner of the U.S. Geological Survey for running the factor analysis programs and for valuable discussions concerning the resultant data. Various drafts of the dissertation were typed by Diane Bieber, Angie Smith, and Louise Flowers. Their efforts are sincerely appreciated. Funding to cover printing costs of this paper was provided by the Office of Marine Pollution Assessment, National Oceanic and Atmospheric Administration.

ABSTRACT

Textural parameters, mass physical properties, mineralogy, x-radiography and chemistry were used to identify and delineate lithofacies in the sediments of Kane Basin. Q-mode factor analysis was used to group the sediments into compositionally similar factors. This resulted in three factors which account for 91.7% of the variance. Detailed studies of the parameters making up the factors as well as an examination of sediment fabric allowed placement of the sediments into the following lithofacies:

Recent

- | | |
|----------|--|
| Factor I | { Sediments dominated by ice rafting |
| | { Sediments dominated by water transport |

Relict

- | | |
|------------|----------------------------------|
| Factor II | { Ellesmere Island till (till 1) |
| Factor III | { Greenland till (till 2) |

The sediments dominated by water transport occur near the Inglefield Land coast, and extend to the northwest. Sediments dominated by ice rafting are most abundant in the vicinity of the Humboldt Glacier. They are also present in the south central part of the Basin, northwest of Inglefield Land. The Ellesmere Island till (till 1) is found in the western Basin while the Greenland till (till 2) is located in the northeastern Basin along the topographic high, southwest of Washington Land, Greenland.

Examination of the areal and temporal (down core) distribution of the lithofacies indicates that the tills were deposited concomitantly. They differ primarily in terms of mineralogy and gravel composition. These differences reflect different source areas. Much of the Ellesmere Island till (till 1) originated from the materials making up the Tertiary outliers found in northeastern Ellesmere Island. The Greenland till (till 2) was derived from Paleozoic carbonate rocks of Washington Land, and the crystalline basement beneath the Humboldt Glacier.

The deposition of the tills was followed by a period when ice rafting was dominant. This was succeeded by an increase in the deposition of water-transported materials emanating primarily from Inglefield Land. Both ice rafting and water transport are going on at the present time.

LIST OF ILLUSTRATIONS

Figure	Page
1. Index Map of Kane Basin, Showing Location of Cores, Grabs and Camera Drops	2
2. General Bedrock Map of Land Areas Bordering Kane Basin . .	5
3. Location of Tertiary Outliers Along the Ellesmere Island Coast (after Miall, in press)	9
4. Bathymetric Map of the Floor of Kane Basin. Contours are in Meters Below Sea Level. Compiled by F. Sorensen, Naval Oceanographic Office.	11
5. Map of the Sedimentological Provinces of Kane Basin, Based on the Textural and Mineralogical Character of the Surficial Sediment Layer (after Kravitz, 1976) . . .	18
6. X-ray Diffractogram of Glycolated Slide Showing Method of Drawing Baseline. K=kaolinite, C=chlorite, A=amphibole.	35
7. X-ray Diffractogram of Slow Scan Showing Method of Drawing Baseline. Q=quartz, I=illite.	36
8. Univariate Maps of the Distribution of Gravel (A) and Sand (B) in the Surficial Sediment of the Kane Basin (after Kravitz, 1976).	48
9. Univariate Maps of the Distribution of Silt (A) and Clay (B) in the Surficial Sediment of the Kane Basin (after Kravitz, 1976).	49
10. Univariate Map of the Distribution of Wet Unit Weight Values in the Surface Sediment Layer	54
11. Univariate Map of the Distribution of Water Content (% Dry Weight) in the Surface Sediment Layer	55
12. Univariate Map of the Distribution of the Saturated Void Ratio Values of the Surface Sediment Layer.	57

Figure	Page
13. Univariate Map of the Distribution of Porosity Values in the Surface Sediment Layer.	58
14. Univariate Map Showing Near Surface Sediment Shear Strength in Kane Basin	59
15. Casagrande Plasticity Chart With Plots of Some Kane Basin Sediment Samples	65
16. Activity Chart With Plots of Some Kane Basin Sediment Samples.	67
17. Univariate Map of the Distribution of Carbonate Values in the Surface Sediment Layer.	71
18. Univariate Map of the Distribution of Organic Carbon Values in the Surface Sediment Layer	72
19. Univariate Map Depicting Distribution of Illite in the Surface Sediment Layer	76
20. Univariate Map Depicting Distribution of Expanding Lattice Clays in the Surface Sediment Layer.	78
21. Univariate Map Depicting Distribution of Kaolinite in the Surface Sediment Layer.	79
22. Univariate Map Depicting Distribution of Chlorite in the Surface Sediment Layer.	81
23. Univariate Map Showing Distribution of Rock Flour in the Surface Sediment Layer	82
24. Univariate Map Showing Distribution of Silicates in Rock Flour From the Surface Sediment Layer	84
25. Univariate Map Showing Distribution of Carbonates in Rock Flour From the Surface Sediment Layer	85
26. Univariate Map Showing Distribution of Fe in the < 2 μ m Fraction of the Surface Seiment Layer	86
27. Univariate Map Showing the Distribution of Mg in the < 2 μ m Fraction of the Surface Sediment Layer.	88
28. Univariate Map Showing Distribution of Mn in the < 2 μ m Fraction of the Surface Sediment Layer.	89

Figure	Page
29. Univariate Map Showing the Distribution of Cr in the < 2 μ m Fraction of the Surface Sediment Layer.	91
30. Univariate Map Showing the Distribution of Co in the < 2 μ m Fraction of the Surface Sediment Layer.	92
31. Univariate Map Showing the Distribution of Ni in the < 2 μ m Fraction of the Surface Sediment Layer.	93
32. Univariate Map Showing the Distribution of Zn in the < 2 μ m Fraction of the Surface Sediment Layer.	95
33. Univariate Map Showing the Distribution of Cu in the < 2 μ m Fraction of the Surface Sediment Layer.	96
34. Univariate Map Showing the Distribution of Ti in the < 2 μ m Fraction of the Surface Sediment Layer.	97
35. Map Showing Distribution of Diatoms in Surface Sediment Layer	99
36. Map Showing Distribution of Factor I Loading Values in Surface Sediment Layer	105
37. Map Showing Distribution of Factor II Loading Values in Surface Sediment Layer.	106
38. Map Showing Distribution of Factor III Loading Values in Surface Sediment Layer.	108
39. Composite Map of the Three Factors	109
40. Core Profiles of the Four Lithofacies.	121
41. X-radiograph of Core 16 Showing "Typical" Fabric of Ice Rafting Dominant Sediments	122
42. X-radiograph of Core 28 Showing "Typical" Fabric of Water Transport Dominant Sediments	124
43. X-radiograph of Core 25 Showing "Typical" Till 1 Fabric. .	127
44. X-radiograph of Core 26 Showing Sedimentary Structures in Upper Portions of Core and "Typical" Till Fabric in Lower Part of Core.	128

Figure	Page
45. Graph of Cumulative-Frequency Curves of Various Till and Glacial Marine Sediments (after Friedman and Sanders, 1978)	133
46. Graph of $M(\phi)$ vs. Inclusive Graphic Standard Deviation of Assorted Till and Glacial Marine Sediments (after Frakes and Crowell, 1973)	135
47. Graph of Wet Unit Weight Values for the Four Lithofacies .	141
48. Graph of Void Ratio Values for the Four Lithofacies. . . .	143
49. Inferred Direction of Ice Movement in Kane Basin	166
50. Areal Distribution of Four Lithofacies Found in Kane Basin	174

LIST OF TABLES

Table	Page
1. Thickness of Surficial Sediment Layer.	45
2. Standard Deviation Values.	51
3. Skewness Values.	52
4. Average Limit, Index, and Activity Values.	61
5. Diatom Abundances in Kane Basin Sediments.	101
6. The 42 Parameters Used in the Factor Analysis.	102
7. Characteristics of the Four Lithofacies.	112
8. Major Parameters Characterizing the Four Lithofacies . .	171

CHAPTER I

INTRODUCTION

Purpose

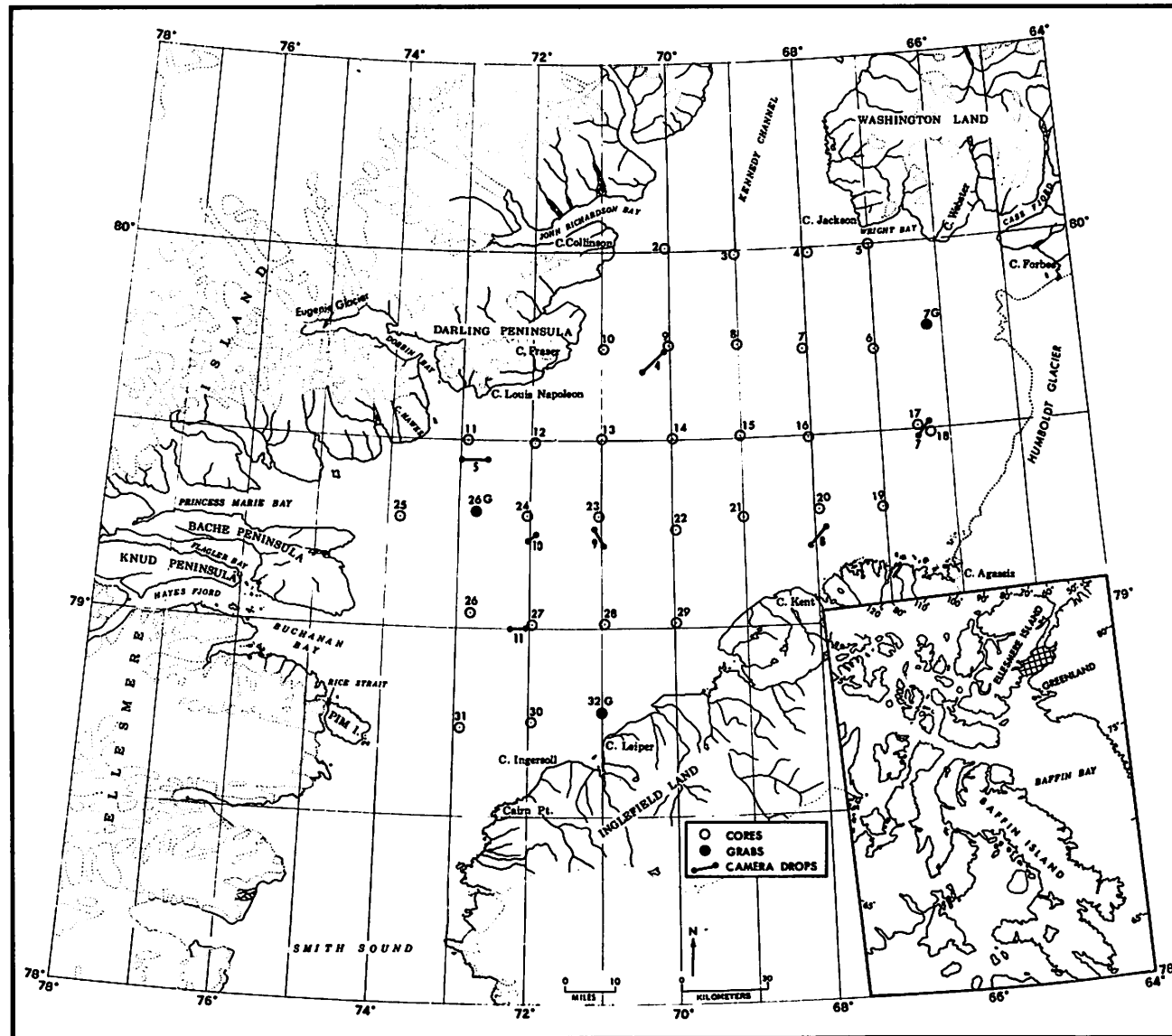
Little is known about the sedimentological processes taking place in the Arctic's shallow seas. This is due, in great part, to the inhospitable climate, severe sea-ice conditions, and the high cost of conducting oceanographic operations in these ice-covered remote areas. However, a high Arctic ocean survey conducted in the Kane Basin has resulted in the collection of sea bottom photographs and sediment cores ideally suited for sedimentological study (Kravitz and Sorensen, 1970).

The textural and heavy mineral character of the surficial sediment layer from these cores were determined previously (Kravitz, 1975). The present study examines samples from the deeper layers in the cores as well as the surficial sediment. Heavy mineral analysis and sediment texture analysis, x-ray diffraction analysis and chemical element analysis of the $< 2 \mu\text{m}$ fraction were carried out, as well as measurements of the sediment's mass physical properties and its total carbonate and organic carbon content. A diatom distribution study was also conducted. Areal and temporal variations of these parameters were studied to gain insight into both present and past sedimentary processes in glacial marine depositional environments, and the relationship of these processes to geologic events occurring in the Kane Basin and on the surrounding land mass. This research will supply additional evidence necessary for the correct identification of glacial and glacial marine environments in the geologic column.

Regional Setting

Kane Basin is part of an elongate body of water known as Nares Strait. The area is bordered by northwestern Greenland on the east, by Ellesmere Island on the west, and by Kennedy Channel and Smith Sound on the north and south, respectively (Figure 1).

Fig. 1. Index map of Kane Basin, showing location of cores, grabs and camera drops.



The Basin has an area of approximately 27,000 square kilometers (10,425 square miles), is about 170 kilometers (105 miles) long and at its broadest point (between Cape Louis Napoleon and Cape Agassiz) it is 124 kilometers (77 miles) wide. That part of Greenland bordering the Kane Basin is generally flat with a regular coastline. The Humboldt Glacier, 100 meters (328 feet) high and 100 kilometers (62 miles) long, extends from Cape Agassiz in the south to Cape Forbes in the north dividing the ice-free Greenland coastal strip into two segments. From Cairn Point, the eastern shore of Kane Basin trends east-northeast to Cape Agassiz, thence along the Humboldt Glacier to Cape Forbes. The coast line west-northwest from Cape Forbes to Cape Jackson, is quite irregular.

The western shore of the Kane Basin, along Ellesmere Island, trends north-northeast for about 140 kilometers (87 miles) from Rice Strait to Cape Collinson, and contains many deep indentations. Seven narrow fjords, generally oriented in an east-west direction, penetrate inland for nearly 100 kilometers (62 miles). The coast rises abruptly from sea level, forming irregular mountains with ice caps and talus covered slopes. The valleys contain many glaciers which discharge into the bays and fjords.

The eastern and western shores of Kane Basin have different amounts of ice and cloud cover. The western shore is approximately nine-tenths ice covered. This is attributed to the cold, northerly current which causes a continuous stream of ice to build up against Ellesmere Island's eastern shores. During the summer the current flowing along the Basin's Greenland coast is comparatively free of ice, (except in the Humboldt Glacier area), allowing open water to raise the general air temperature. The prevailing easterly winds also carry more moisture to the western side of the Basin which is often covered with fog in contrast to sunny conditions on the Greenland coast (Arctic Pilot, 1976).

Geological Setting

On the Greenland side of Kane Basin, Washington Land to the north and Inglefield Land to the south, are separated by the Humboldt Glacier (Figure 2). In Inglefield Land, large areas of Precambrian basement are exposed. According to Dawes (1976) the basement rocks can be separated

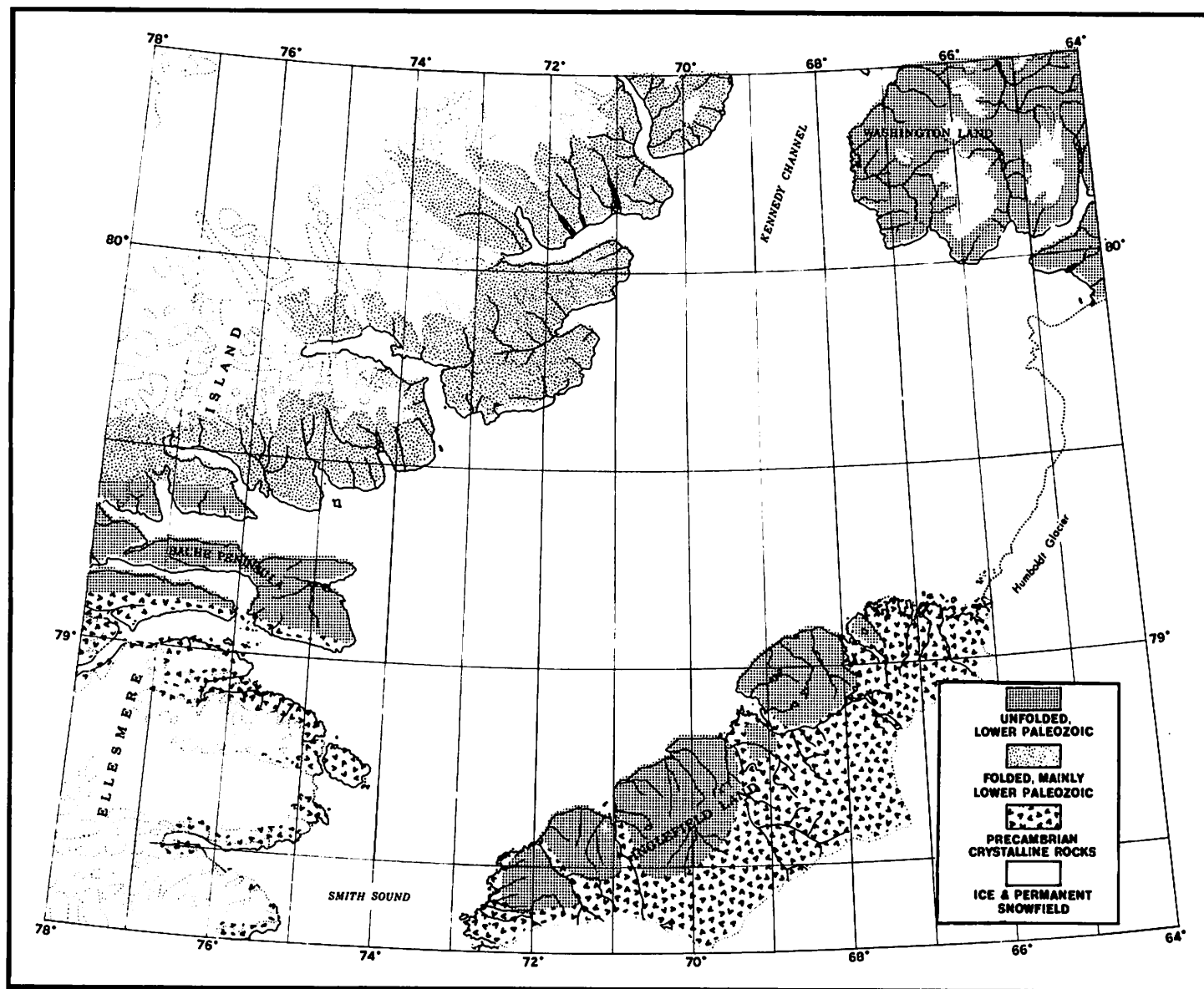
into three units; the Etah Group, the Etah Meta-igneous Complex, and the "variable associated gneisses."

The Etah Group is made up of light colored crystalline limestone, variable calc-silicate rocks, pelitic schists and minor psammitic rocks. These rocks are thought to be present throughout Inglefield Land (Precambrian rocks in Figure 2). Contact metamorphic mineral assemblages containing wollastonite, tremolite, diopside and spinel are common. The Etah Group is intruded by gabbroic to granitoid rocks known as the Etah Meta-igneous Complex. The rocks of this Complex vary from black, dark gray, and brown gabbro through diorite, quartz norite, quartz diorite and hypersthene tonalite to pink and red granodiorite and granite, as well as plagioclase-rich rocks resembling anorthosite. There is a gradation from these rocks to folded, veined gneisses and schists (Precambrian rocks in Figure 2).

The gneisses and schists vary in composition from amphibolitic and pyribolitic to quartzose gneisses and schists. The gneisses are composed of plagioclase and potash feldspar, orthopyroxene, biotite and hornblende. Garnet, cordierite, and sillimanite are also present. These probably are the gneisses first described by Koch (1929a, 1933) as being the dominant rocks in Inglefield Land's crystalline basement.

Overlying the Precambrian crystalline basement is a thin basal sequence, the Algonkian Thule Formation of Koch (1929a) and the Eocambrian Rensselaer Bay Formation of Troelsen (1950). This latter formation is made up of two members. The lower Hatherton Member contains purple ferruginous sandstones, shales and some dolomites. The upper Sverdrup Member contains cream, buff and yellow sandstones with siltstones. Above the Eocambrian Rensselaer Bay Formation are the gray to yellow, medium-to fine-grained dolomites of the Cape Leiper Formation below, and the Cape Ingersoll Formation above. These two formations are now considered to be of Early Cambrian age on the basis of correlation with strata in Ellesmere Island (Christie, 1967a and Kerr, 1967a). Unconformably overlying the Cape Ingersoll Formation is the Lower Cambrian Wulff River Formation consisting of conglomerates, glauconitic sandstones and limestone. Above this formation is a series of oolitic limestones, unfossiliferous dolomites, glauconitic sandstones, and shale known as the Cape Kent Formation. The Middle Cambrian is represented by

Fig. 2. General bedrock map of land areas bordering Kane Basin.



the Cape Wood Formation of Poulsen (1946) and Troelsen (1950). This formation is composed of conglomerates, glauconitic sandstone, argillaceous and arenaceous limestones, dolomites and breccia. The Upper Cambrian is not known in Inglefield Land. The only known Ordovician rocks in this area are the limestones and conglomerates which make up the Cass Fjord Formation (Dawes and Soper, 1973).

In Washington Land (Greenland) the Precambrian crystalline basement and the base of the Paleozoic strata are not exposed, but a rather complete succession of Cambrian, Ordovician and Silurian rocks crops out (unfolded Lower Paleozoic in Figure 2). The oldest strata exposed are yellow dolomites. Koch (1929b) has assigned these dolomites to the Thule Formation. The Cambrian (?) Cape Ingersoll and Cape Leiper Dolomites and the Cape Wood Formation are found in Washington Land as well as Inglefield Land. The Ordovician, which is represented in Inglefield Land only by the Cass Fjord Formation, is well represented in Washington Land and consists of both carbonate and clastic sedimentary rocks. Silurian rocks on Washington Land, but not present in Inglefield Land, are primarily biohermal and biostromal limestones as well as argillaceous limestones and shales.

Ellesmere Island borders Kane Basin on the west. That part of the Island facing Kane Basin is composed of Precambrian crystalline rocks, Lower Paleozoic sedimentary rocks and a variety of sedimentary deposits of Cenozoic age.

Bache Peninsula is located near the southeastern boundary of Kane Basin 81 kilometers (50 miles) west of Inglefield Land. Its Precambrian basement rocks are mainly biotite-quartz-feldspar gneisses, in part garnetiferous, with minor pegmatite quartz-feldspar intrusions or segregations. Massive red granites are present at the head of Flagler Bay. The gneiss is exposed at the mouth of Flagler Bay and along the south coast of Bache Peninsula. Similar rocks are exposed facing Bache Peninsula along the south shore of Alexandria Fjord. Pim Island, the southernmost point of the western boundary of Kane Basin is composed of Precambrian granites and allied plutonic rocks.

Overlying the Precambrian basement rocks of Bache Peninsula is a sequence of sedimentary rocks comprised of carbonate, evaporite and clastic components. Some of these rocks, including the Eocambrian

Rensselaer Bay, Lower Cambrian (?) Cape Leiper, Cape Ingersol, Cape Kent and Cape Wood Formations, and the Ordovician Cass Fjord Formation have been correlated with units exposed on Inglefield Land and Washington Land, Greenland. These rocks, mostly carbonates and coarse clastics, rest unconformably on the peneplaned surface of the crystalline basement and attain a total thickness of about 1250 meters (4,100 feet). The lowermost sedimentary units, intruded by two diabase sills, may be Precambrian in age.

Coal bearing Cenozoic clastics disconformably overlie the Palozoic rocks in down-faulted blocks. In addition, unconsolidated Pleistocene deposits are widespread. These include glacial boulders and cobbles composed of buff dolomite or dolomitic limestone, black limestone, dark gray quartzite, quartzose gneiss, red quartzite or sandstone, red granite, gray gneiss and white sandstone. A comprehensive geologic study of the Bache Peninsula has been published by Christie (1964).

The sedimentary rocks on eastern Ellesmere Island to the north of the Bache Peninsula were deposited in the Franklin Geosyncline. The Proterozoic Kennedy Channel Formation is made up of fine-grained quartzose sandstones, phyllites and some dolomite. Above the Kennedy Channel Formation is the Proterozoic Ella Bay Formation which consists primarily of dolomite. The Lower Cambrian is represented by the Ellesmere Group, a series of formations made up of clastic rocks.

Above the Ellesmere Group but still part of the Lower Cambrian is a series of dolomites with some shaly interbeds. The Middle Cambrian is represented by varicolored arenaceous carbonates (dolomite and limestone) which are associated with quartzose sandstones and shaly siltstones. Upper Cambrian rocks have not been found in eastern Ellesmere Island.

The Lower Ordovician contains gypsiferous, silty and shaly limestones and flatpebble conglomerates. The Middle and Upper Ordovician includes limestones and evaporites which grade upward into siltstones and shales. These rocks are overlain primarily by limestones. A great variety of sandstones, carbonates and shales make up the uppermost Ordovician to Upper Devonian sequences (Kerr 1967a, 1968).

The Allen Bay Formation consists almost entirely of sparsely fossiliferous dolomite whereas the overlying Read Bay Formation is more

varied. Although composed mainly of limestone, it contains a large clastic component. These two formations together constitute a carbonate unit that ranges in age from Late Ordovician (Richmondian) to probably Early Devonian. The unit grades westward into the largely equivalent shaly Cape Phillips Formation (Kerr, 1976).

The Lower Devonian is represented by the Imina Formation (Trettin, 1969), the Vendom Fjord Formation (Kerr, 1967b), and the Eids Formation (McLaren, 1963). The Imina Formation is a flysch-like succession of turbidites composed mainly of calcareous and dolomitic sandstone, siltstone and shale. The Vendom Fjord Formation is a red-bed unit which contains abundant clastic material and which grades westward into siltstone, limestone and limy shale. The Eids Formation is a thinly bedded calcareous siltstone, calcareous shale and shaly limestone.

Formations consisting of limestone, mudstone and sandstone make up the Middle Devonian sequence. The Upper Devonian is composed of a varicolored succession of largely nonmarine quartzose sandstone, sandy mudstone, and shale with very thin coal seams at certain horizons. Glacial debris, fluvial, lacustrine and marine deposits of Pleistocene and Quaternary age comprise the unconsolidated surficial materials.

Miall (in press) has found nonmarine Tertiary deposits at Carl Ritter Bay, Daly River and Pavy River on Judge Daly promontory, and at Watercourse Valley. These locations are on the northeast coast of Ellesmere Island along Kennedy Channel (Figure 3). At Carl Ritter Bay the section comprises four members: 1. coarse to pebbly sandstone; 2. fine grained sandstone, siltstone and shale; 3. siltstone and sideritic mudstone; 4. boulder conglomerate. At Daly River and Pavy River, sandstones comparable to member 1 at Carl Ritter Bay, are exposed. At Watercourse Valley, a basal breccia is followed by a succession of fine sandstone, siltstone and coal. Paleocurrent and petrographic evidence suggests that these deposits are outliers of an originally continuous unit deposited in the Judge Daly Basin. Limited biostratigraphic data indicate that all the strata are Paleocene in age.

Some of the sandstones have little matrix and others contain a green-brown, micaceous matrix. Sandstones of member 1 at Carl Ritter Bay contain volcanic fragments which include basalt, palagonite, glass, and individual grains of plagioclase, amphibole and clinopyroxene. The

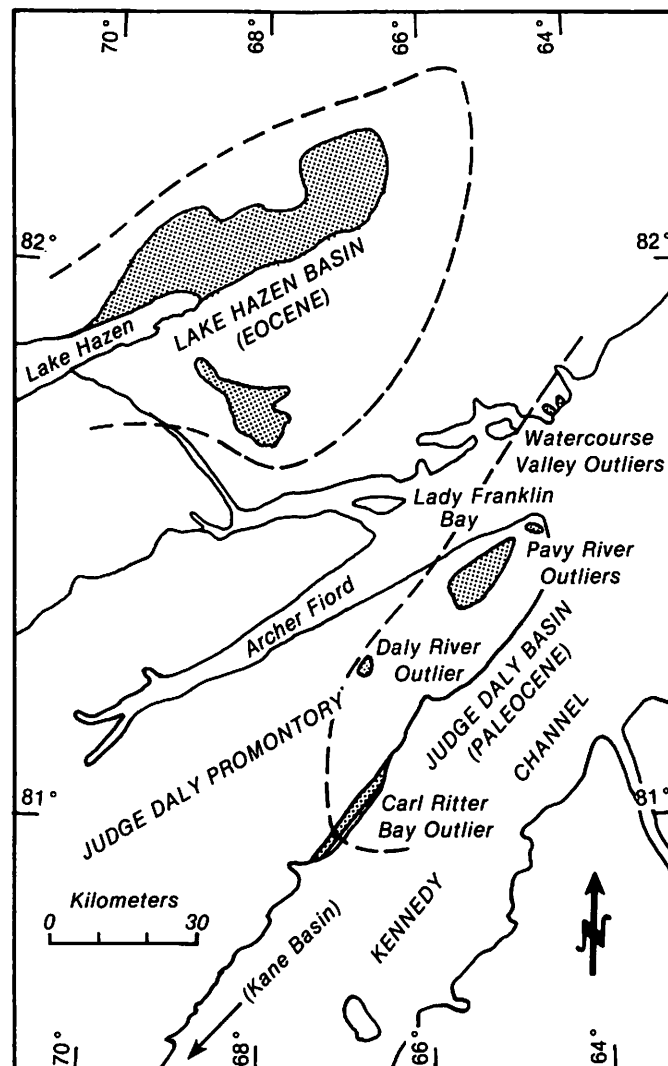


Fig. 3. Location of Tertiary outliers (stippled areas) along the Ellesmere Island coast (after Miall, in press).

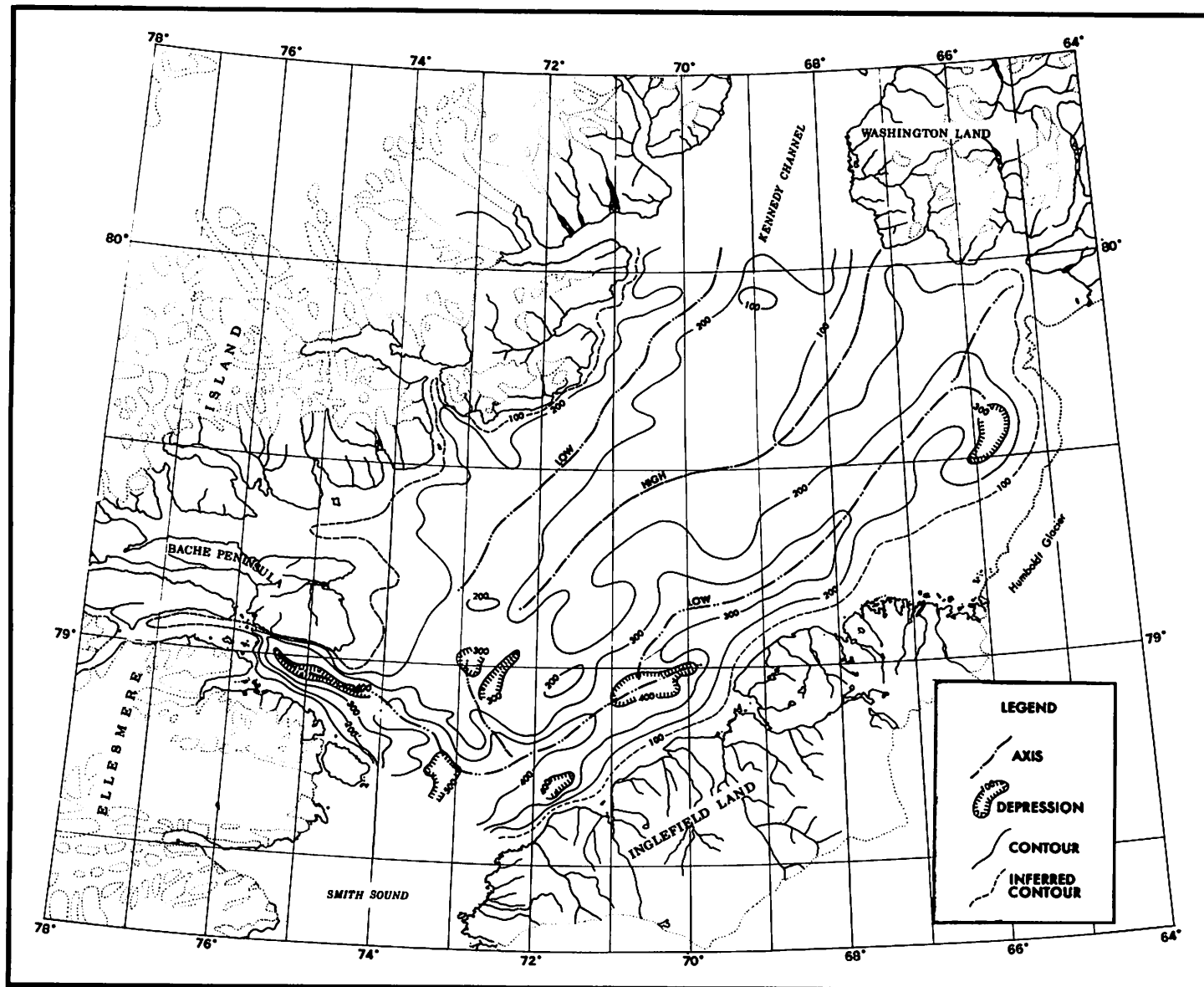
basalt fragments consist mainly of plagioclase microlites set in a glassy groundmass. The amphiboles and clinopyroxenes are believed to be phenocrysts from the basalt.

Some of the clay matrices of the sandstones are composed predominantly of mixed layer clays with minor illite. One sample from the Daly River outlier consisted of 34% montmorillonite. Most of the sandstones identified were lithic arenites with some lithic wackes, quartzose arenites and quartz arenites according to the classification of Okada (1971). Chloritic fragments, phyllite grains and detrital carbonates were also found in the sandstones. It is believed that most of the sediment was deposited by a fluvial system flowing northeastward, down the axis of the basin, with some input by transverse drainage entering from the margins.

Bathymetry

The submarine topography of the Kane Basin is characterized by two large shallow troughs. The troughs are separated by a broad topographic high with gentle slopes. This high plunges southwestward from Washington Land, Greenland toward Smith Sound (Figure 4). The eastern trough begins at the northern edge of Humboldt Glacier and extends to the southwest, where it gradually deepens from approximately 200 meters (109 fathoms) to over 500 meters (273 fathoms) toward Smith Sound. Within this trough are several small, closed depressions with depths between 300-400 meters (164-220 fathoms). The western trough is shallower than its eastern counterpart and runs parallel to Ellesmere Island. The bottom of this trough is slightly convex being shallower in the center, 200-300 meters (109-164 fathoms), and becoming deeper at either end (approximately 300 meters). A small, narrow, relatively deep trough, 400-500 meters (220-273 fathoms), located along the south side of Bache Peninsula, joins the other troughs at the northern end of Smith Sound. The limiting sill depth of 250 meters (136 fathoms) is in the western part of Kane Basin. From this point on, the depth gradually increases through Smith Sound into Baffin Bay. Pelletier (1966) proposed that the Kane Basin was at one time a drowned water shed with valley glaciers flowing south into Smith Sound and north into Kennedy Channel. Bathymetric data for this area are sparse due to its

Fig. 4. Bathymetric map of the floor of Kane Basin. Contours are in meters below sea level. Compiled by F. Sorensen, Naval Oceanographic Office.



remoteness and severe ice conditions, therefore, any interpretations of the origin of the submarine morphology are speculative.

Oceanography

Cold water of polar origin ($<0^{\circ}\text{C}$, $<33.50\text{‰}$) is found in the upper 200 meters (~ 100 fathoms) of the water column in Kane Basin, and makes up the major drift southward into Baffin Bay. The coldest water (-1.70°C) is found near the surface along the coast of Ellesmere Island. Beneath the surface, -1.50°C water is present from 25 to 50 meters (14 to 27 fathoms) in the southern part of the western trough, and down to 75 meters (41 fathoms) further north. Below 150 meters (82 fathoms) the temperature gradually increases with depth, and in places exceeds 0.25°C .

The surface waters of Kane Basin have low salinity, particularly on the east side near Humboldt Glacier where salinities as low as $<28.00\text{‰}$ have been reported (Sadler, 1976). At 100 meters (55 fathoms) water with a salinity of 33.50‰ is found in the deep channel of the western side. Below 100 meters (55 fathoms) salinity values exceeding 34.25‰ have been recorded. Salinities are higher (34.25‰) at 300 meters (164 fathoms) in Kane Basin than elsewhere in the northern Baffin Bay region (Muench, 1971a).

Nearly uniform distributions of temperature and salinity are found at the center of Kane Basin in the upper 150 meters (82 fathoms). Below 150 meters, the water is slightly warmer and more saline to the north. Masses of unusually low temperature and low salinity water, caused by local ice conditions and the admixture of fresh meltwater off the ice, are frequently found at the surface. These conditions cause considerable variability in the summer mean minimum temperature in the upper water column, and low and variable values of summer mean salinity.

The dissolved oxygen content in Kane Basin varies from super-saturated values (9.0 ml/l) near the surface to about 80% saturated (7.0 ml/l) below 100 meters (55 fathoms). The low salinities of the near surface waters can be attributed to the melting of sea ice and the summer runoff from the land. Particularly high oxygen contents have been found near Humboldt Glacier. This is due to the large air content of glacial ice which is released as tiny bubbles during the melting

process, resulting in a high level of dissolved oxygen in the surface layers. These observations were made during the summer months as reported by Moynihan (1972), and Sadler (1976).

Bailey (1956) stated that Arctic Ocean water enters Baffin Bay through Kane Basin and Smith Sound either as a slow and continuous flow or as a surge of dense water that sinks to the bottom. Collin (1965) showed, by density distribution, that the influx of high salinity ($<34.40\text{‰}$) Arctic Ocean water through Smith Sound is not continuous but probably takes place in intermittent pulses.

The circulation of water in Kane Basin has been interpreted from density data by Moynihan (1972). He determined that a southerly flow of Arctic water is concentrated on the western side through the trough "connecting" Kennedy Channel and Smith Sound. This passage is believed to contain the major flow of water between the Arctic Ocean and Baffin Bay. He goes on to state that, "A general counterclockwise circulation of the surface waters in Kane Basin is indicated by the slope of the isopycnals. . . "

Frictional effects of the wind and the bottom, and the effect of the tidal oscillations on the current through Kane Basin are unknown. The winds are extremely strong, especially in the winter when velocities of 50-100 knots can be measured. Dunbar (1971, 1979) reports that although the winds are varied in the southern part (south of 80°N) of Nares Strait there were many more days with a down-channel wind component than with an up-channel component, and the down-channel winds were appreciably stronger. It must be pointed out however that these observations were only for the winter months, from 1 December 1970 to 1 March 1971 and during October 1976 (Dunbar, 1979). Moynihan (1972) reports a relatively steady wind from 188°T (south-southwesterly) with a mean speed of 12.3 knots (range 0-20 knots), during July 1969. Based on observations taken in September 1970, Moynihan (1972) reports a relatively steady northeasterly wind (mean 10 knots, from 055°T) with velocities varying from 4 to 15 knots. This would induce a surface current transport to the southwest and would reduce the northeasterly flow into Kane Basin. However, this would only be a temporary condition with permanent and tidal current effects predominating.

Collin (1965) reported that tidal reversals of surface currents may occur in Smith Sound. Day (1968) stated that direct current measurements near $78^{\circ}27'N$, in Smith Sound in 1963 indicate a circulation dominated by semidiurnal tides with a net transport to the south. Muench, in Moynihan and Muench (1971b) found that current measurements from a fixed ice camp in Kane Basin during May 1969 indicate a general southward flow with less frequent flow reversal coinciding with the diurnal tidal currents.

The presence of Atlantic water in southeastern Smith Sound in 1963 and 1966 (Muench, 1971a), and as far north as $78^{\circ}03.2'N$, $73^{\circ}42.0'W$ in 1971 indicate incursions of Baffin Bay water at least as far north as Smith Sound (Sadler, 1976). The cause of these incursions, which range in depth from the surface to sill depth at 250 meters (136 fathoms) is unclear. However, no evidence has been found that they are caused by tidal motions or by the barometric gradient along Nares Strait.

In summary, it appears that there is a net southward flow of water out of Kane Basin which is somewhat more concentrated along the western side, with occasional "pulses" of northeasterly flowing water entering Smith Sound and possibly Kane Basin from Baffin Bay.

A detailed knowledge of currents in Kane Basin does not exist (Dunbar, 1979). Very few current measurements have been made at or near the surface and none have been made which would establish the presence and character of the bottom currents.

Ice

The Kane Basin is the most consistently icebound part of Nares Strait. Fast ice conditions begin in February-March and break up about July or August. The eastern part of the Basin, where the wind conditions are not as severe as the rest of Nares Strait, seems to be out of the main line of current and ice movement (Dunbar, 1979). Therefore, the eastern part of the Basin is usually more icebound than the western, northern and southernmost areas. The western half of the Basin, on a direct line from Kennedy Channel to Smith Sound, is more often open. Strong winds act on the heavy flows and keep breaking up the younger ice which forms between them until most of the available spaces are filled with heavily ridged first year ice.

The fast ice acts as an extension of the coast of Greenland, straightening it out and reducing the main channel to a fairly uniform width throughout its length. Since the lack of current activity in the eastern embayments is one of the reasons for the formation of the fast ice, it may be assumed that the main drift stream along the western side of the Basin keeps to its narrow path even when the fast ice is absent (Dunbar, 1979).

Summer conditions result in generally less ice in the eastern Basin and an increase in heavy ice near Ellesmere Island. These conditions can be attributed, in part, to easterly katabatic winds flowing from the Greenland ice cap across the Humboldt Glacier, and a net southward movement of ice through Nares Strait into Baffin Bay (Arctic Pilot 1976).

Three main types of ice are found in Kane Basin; icebergs, Arctic pack ice, and sea ice. A portion of the ice also comes from the rivers and fjords.

Icebergs form by the calving of ice at the terminus of glaciers. Most of these icebergs, with the major exception of ice calved from Humboldt Glacier, are initially deposited in the bays and fjords of Kane Basin. They eventually work their way into the main part of the Basin through the combined action of winds, storms, currents and tides.

The Arctic pack ice found in Kane Basin originated in the Arctic Basin. This dense, relatively old ice, slowly drifts through Nares Strait and over a period of years ends up in Baffin Bay.

Sea ice is the most common type of ice. It forms first in shallow water, near the coast or over shoals and banks, particularly in bays, inlets and straits in which there is little or no current, and also in regions with reduced salinity, such as those near the mouths of rivers and Humboldt Glacier. It spreads from these centers. Such ice is broken up and carried seaward by winds and currents where it starts further ice formation. Sea ice which has not melted during the previous season also acts as centers for new ice formation. Detailed descriptions of the various types of ice encountered in the ocean, and their processes of formation, can be found in Zubov (1945).

In a high latitude marine environment, ice plays an important geological role by eroding, transporting, and depositing sediment.

Glacial ice is probably the most significant agent in this respect followed closely by grounded ice (sea ice which forms along the coast and in shoal areas), ice formed in rivers, sea ice (formed in deep water), and Arctic pack ice. The latter two kinds of ice carry little sediment (unless it becomes grounded on shoals) except for wind borne materials (Kindle, 1924 and Hobbs, 1948). Glacial ice derives its sediment from medial moraines, superglacial and basal debris, and those parts of the glacier bordering on land. Grounded ice frozen to the coast and to the sea bottom breaks away carrying with it large amounts of rock and mud debris. In addition, during the warmer months, water flows from land onto the coastal ice and deposits sediments on its surface. River ice receives sediment in much the same way as grounded ice and during summer breakup can be a considerable force in erosion and transportation (Walker, 1969; Andrew and Kravitz, 1974; and Short et al., 1975). The term "gryazny" is used by the Russians to describe dirty ice containing gravel, sand, mud and alluvial material found off the Siberian coast.

Many descriptions of erosion, transport and deposition by ice in the Arctic can be found in the literature (Tarr, 1897; Kindle, 1924; Sverdrup, 1931; La Fond et al., 1949; Emery, 1949; and Ovenshine, 1970).

Previous Studies of The Kane Basin

The water column (Moynihan, 1972; Sadler, 1976) and ice conditions (Dunbar 1971, 1974, 1979) of Kane Basin have been studied. Bathymetric analysis has been undertaken by personnel of the Bedford Institute of Oceanography (Pelletier, 1966). With the lone exception of eight grab samples collected by the U.S.C.G.C. Evergreen in 1963 (Uchupi, 1964), no sampling of the Basin's floor was undertaken until the U.S.C.G.C. Southwind survey in the summer of 1969 (Kravitz and Sorensen, 1970).

Uchupi (1964) described the Kane Basin grab samples as gray to reddish-brown, poorly sorted, calcareous, sandy silts containing appreciable quantities of gravel. He identified the gravel clasts as angular to subrounded limestone, granite, sandstone and quartz diorite. The sand fraction was made up of angular to subangular quartz and feldspar grains along with some coal particles. He noted the close resemblance of the grain size distribution curves plotted for the Kane Basin samples

to the curves obtained from glacial tills. He concluded that the main type of sediment transport in the area was ice rafting.

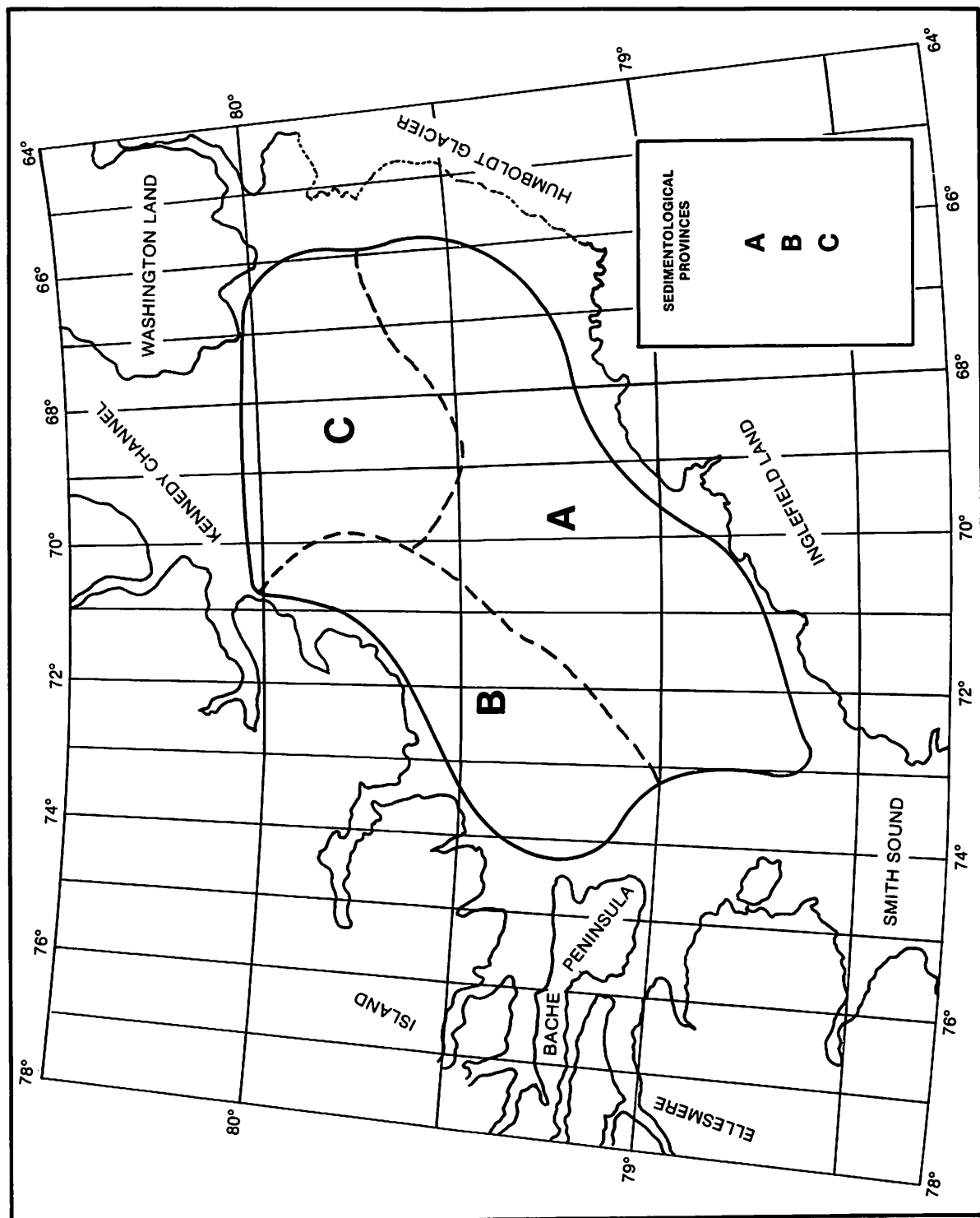
Kravitz (1976) identified three sediment provinces in Kane Basin (Figure 5). This was based on a study of the textural and mineralogical character of the surficial sediments.

Province A which makes up the eastern, central and southern Basin, contains both water- and ice-transported sediment. The sediments are poorly- to very poorly-sorted silts and clays with admixtures of sand and gravel. The gravels' clasts are mostly crystalline rocks. The heavy minerals are dominated by garnet and orthopyroxenes whose sources are the crystalline basement rocks exposed on Inglefield Land and underlying Humboldt Glacier. The ice-rafted sediments come from the Humboldt Glacier while Inglefield Land and Washington Land provide the water-transported materials.

Province B covers the western Basin from the western parts of the topographic high to Ellesmere Island. The sediments are extremely poorly sorted sands and silts with considerably more gravel than in Province A. The Recent sediments are mostly ice rafted from Ellesmere Island with subordinate stream transport. Relict sediments cover a considerable amount of bottom in this province. The Recent sediment is characterized by abundant clasts of carbonate rocks in the gravels and by grains of carbonate minerals in the sands, both originating from Ellesmere Island. The relict sediments have a gravel fraction dominated by clastic sedimentary rocks and a heavy mineral suite rich in clinopyroxene.

Province C, the shallowest area in Kane Basin includes the northernmost parts of the eastern and western troughs, and the northern topographic high from Kennedy Channel down to approximately 79°28'N. The sediments are the coarsest of the three provinces with large amounts of sand, gravel and silt, and very little clay. They are positively to slightly negatively skewed and very poorly to extremely poorly sorted. Both ice- and water-transported materials are well represented, with stream transported fines concentrated near Washington Land, and ice-transported sands, silts, and gravels on shoal areas farther to the west and south. The gravels and heavy minerals reflect the influence of province A and province B. Crystalline dominated gravels and garnets

Fig. 5. Map of the sedimentological provinces of Kane Basin, based on the textural and mineralogical character of the surficial sediment layer (after Kravitz, 1976). See text for description of sediment-allogical provinces A, B and C.



and orthopyroxenes characteristic of province A are found in the eastern and southern parts of province C. Recent carbonates and relict gravels containing clastic sedimentary rocks, along with clinopyroxene characteristic of province B, are found in the western part of province C.

Directly to the south, in Baffin Bay, sediments similar to those in Kane Basin have been studied. Grant (1965) examined a number of grab samples from northern Baffin Bay and discussed their distributional trends with emphasis on ice rafting. Marlowe (1968) presented a broad overview of Baffin Bay sediments. He noted that the relationship of the median grain size of the sediment to bottom topography is coarsest over topographic highs and finer in the central basin. Even though ice rafting occurs it does not mask the water deposited distribution patterns. Baker and Friedman (1973) conducted the most detailed textural analysis of Baffin Bay sediments to date. They found, as did Marlowe, that the sediments presently being deposited in many areas of Baffin Bay differ from those sediments found at greater depths in the cores. They also provided further evidence that the sandy layers which occur in the deeper areas of the Bay probably were formed by localized downslope movement of sediment rather than by the winnowing action of bottom currents. Aksu (1981) identified six lithofacies in Baffin Bay sediments; Facies A, sediments rich in detrital carbonates; Facies B, red sediments; Facies C, olive black gravelly-sandy mud; Facies D, sorted sand and silt; Facies E, fine muds; Facies F, reddish brown sediments. He characterized these facies on the basis of their mineralogical and sedimentological properties and identified potential source rocks and transporting/depositing mechanisms for them. Aksu (1981), using planktonic foraminiferal assemblages, volcanic ash and the distribution of ice rafted sediment together with oxygen isotope curves determined that during glacial periods one major current, caused by the northward advection of the North Atlantic subpolar water, dominated the circulation pattern. Interglacial periods were characterized by two currents flowing in opposite directions.

In Baffin Bay a cyclic sedimentation pattern was produced in response to climatic changes. The glacial strata were composed primarily of turbidites and debris flow deposits interbedded with ice rafted debris and hemipelagic sediment, whereas interglacial strata were

composed predominantly of ice rafted and hemipelagic sediments.
Sediments in the Nares Strait north of Kane Basin have not been studied.

CHAPTER 3

SHIPBOARD PROCEDURES

Navigation

Navigation was by dead reckoning, Loran A and radar. It was difficult to determine precise fixes because of the general problems encountered in polar navigation, and the datum differences between Greenland and Canada. Even when taking into consideration frequent land sightings, it is estimated that the ship maintained an average "on station" accuracy of no better than about five kilometers (three miles).

Sediment Sampling

Where possible, one core and one grab sample were collected at each station. However, coring in Kane Basin was difficult because of the extreme hardness of the basin floor. Where no cores were recovered (zero penetration) the composition of the surface sediment was determined from grab samples. Thirty cores and three grab samples were used in this study (Figure 1).

Station locations were plotted on a grid to provide sampling control. Ice conditions precluded strict adherence to the planned grid and sometimes necessitated taking samples at some distance from the scheduled sites. Four stations near Ellesmere Island and two stations in the vicinity of Humboldt Glacier were deleted because of heavy ice.

Grab samples were taken with shroud covered, "orange peel" type grab samplers. The sediment obtained from the grab samples was placed in large glass jars, marked and boxed for shipment. The cores were collected using "modified Ewing" open barrel gravity corers with barrels 3.4 m (11 feet) long that contained 6.35 cm (2.5 in) ID polycarbonate liners. The cores were capped, marked and stored vertically in large wooden boxes. Several layers of cushioning material was placed between the cores and the bottom of the boxes in an attempt to reduce the effect of the ship's vibration on the sediment.

Underwater Camera Operations

Photographs of the sea floor were taken with a single underwater camera (model 200A) and light source (model 210K), manufactured by EG & G International. The camera and light source were attached to a metal frame housing a sonic "pinger". The "pinger" emits signals which are picked up by the ship's AN UQN receiver and passed into an oscilloscope. By monitoring the signals on the oscilloscope the camera's distance from the sea floor can be determined and controlled. The camera system was equipped with a delay unit which triggered it at a pre-set time. The bottom was then photographed every 12 seconds until either all the film was used or the lowering was terminated. After each lowering, several strips of film were developed to ascertain the quality of the photographs and to determine whether the system was functioning properly. The eight camera stations are plotted on Figure 1.

Bathymetric Soundings

The Southwind's AN-UQN sonic depth recorder was used to record 2,060 kilometers (1,112 nautical miles) of continuous sonic profiles. The recorder was operated continuously between oceanographic stations as well as on station, except during camera drops. The 0-183 meters (0-100 fathoms) scale was used in waters less than 183 meters (100 fathoms). The 0-1097 meters (0-600 fathoms) scale was used in all other areas.

CHAPTER III

LABORATORY PROCEDURES

X-Radiography

All cores were x-rayed prior to sampling. The industrial x-ray unit employed was a Faxitron model 805, manufactured by Hewlett-Packard Corporation. It contains an automatic exposure meter, dual cabinets, copper target radiation, and inherent filtration of 0.81 mm (.025 inch) beryllium maximum. The unit was modified by cutting port holes in the lower cabinet so that cores of any length could be x-rayed. The cores were passed through the ports of the unit and x-rayed in 38 cm (1.25 feet) intervals. They rested on a low scatter shelf during exposure which reduced the amount of "burn out," or film overexposure, along the core edges. Kodak AA industrial x-ray film and a constant 3 milliamperere (Ma) setting with kilovoltages (KVP) ranging from 30 KVP to 100 KVP were used. The target to film distance (TFD) was 101.6 cm (40 inches). The resulting radiographs were viewed using a Mitchell X-Ray high intensity illuminator.

Subsampling

Sample intervals were initially selected using the core radiographs. The cores were then split longitudinally with a mica under-cutter (Kravitz, 1968), described and additional sample intervals selected by visual observation. Samples were selected on the basis of: marked film density differences, textural variations, presence or absence of stratification, sharp or gradational contacts, color changes and variations in compactness and water content. At least one sample was taken from each sedimentary unit; multiple samples were routinely taken from the thicker sedimentary units.

The thickness of the surface sediment layer at the various bottom sample locations in Kane Basin (Table 1) was determined by utilizing the criteria outlined above.

The sediment was sampled along the entire layer (unit), carefully avoiding the sediment-liner interface in order to prevent contamination. When a grab sample was used, the sediment was homogenized by hand using a spatula and then quartered according to Krumbein and Pettijohn (1938).

Mass Physical Properties

Each core was first sampled for analysis of mass physical properties in order to reduce the chance of evaporation.

Water Content

The sediment sample was put into a porcelain crucible, weighed on an analytical balance to three places, placed overnight in a "constant temperature" forced air drying oven at 110°C, cooled in a desiccator and reweighed. The percent water content (also called moisture content) was calculated from the formula:

$$w = \frac{W_1 - W_2}{W_2 - W_c} \times 100$$

where

- w = percent water content
- W₁ = total weight (1st weighing)
- W₂ = dry weight (2nd weighing)
- W_c = weight of crucible

and reported as a percentage of dry weight.

Specific gravity of solids

The procedures followed for determining the specific gravity of solids were essentially those outlined by the American Society for Testing and Materials (1964). Approximately 25 grams of ground up sediment was oven dried at 110°C overnight, cooled in a desiccator, weighed and placed in a volumetric flask containing air-free distilled water. Entrapped air was removed by subjecting the sample in the volumetric flask to a partial vacuum. Afterwards, the amount of air-free distilled water was increased and the flask reweighed. Specific gravity of solids, G_s, was determined from:

$$G_s = \frac{W_s G_t}{W_s - W_1 + W_2}$$

where

W_s = dry weight of solid particles

G_t = specific gravity of distilled water at temperature t

W_1 = weight of the volumetric flask, sediment, and air-free water

W_2 = weight of the volumetric flask and air-free water

Wet unit weight

The wet unit weight of a sediment mass is the weight of the solids plus pore water per unit volume, and can be expressed as:

$$\gamma = \frac{W}{V}$$

where

γ = wet unit weight

W = total weight of sample

V = total volume of sample

In the present study small sediment samples were often used, and it is inconvenient to measure the volume of such samples directly. Therefore, wet unit weight was computed from the following formula:

$$\gamma = \frac{G_s (1+w)}{G_s (w)+1}$$

where

γ = wet unit weight

G_s = specific gravity of solids

w = water content (expressed as a decimal)

All references to unit weight imply wet unit weight.

Saturation

Where the sediment units were large enough for volume determination, the percentage or degree of saturation (S_r) was determined. The formula used was:

$$Sr = \frac{w}{\gamma_w \left(V - \frac{W_s}{G_s \gamma_w} \right)}$$

where

$$\begin{aligned} w &= \text{water content} \\ \gamma_w &= \text{unit weight of water} \\ V &= \text{volume} \\ G_s &= \text{specific gravity of solids} \\ W_s &= \text{dry weight of solids} \\ V - \frac{W_s}{G_s \gamma_w} &= \text{the volume of voids, } V_v \end{aligned}$$

Saturated void ratio

Void ratio (e) is the volume of void space divided by the volume of solids in a given mass of sediment. The void ratio at 100% saturation is known as the saturated void ratio (e_{sat}) and was calculated according to Taylor (1948) as follows:

$$e_{sat} = \frac{W_w}{W_s} \frac{G_s}{S_r}$$

where W_w is the weight of water and saturation (S_r) is assumed to be 100%. All references to void ratio will assume saturated void ratio.

Porosity

Porosity (n) is the ratio in percentage of the volume of voids in a given mass to the volume of the sediment mass. It is normally calculated using the formula:

$$n = \frac{e}{1+e} \times 100$$

In this study e_{sat} replaced e in the formula. From the above expression the relation of porosity to void ratio can readily be seen.

Atterberg limits and indices

The Atterberg limits determined were liquid limit (LL) and plastic limit (PL). Liquid limit is the water content at which the sediment passes from a plastic to a liquid state. The plastic limit is the lowest water content at which the sediment is plastic. The plasticity index (PI) is the numerical difference between the liquid and plastic limits, $PI = LL - PL$. It is a good indication of the amount of water which must be gained or lost before the sediment becomes non-plastic. The ratio of the sediment's natural water, in excess of the plastic limit, to its plasticity index is known as the liquidity index (LI) and was computed from the formula:

$$LI = \frac{w-PL}{PI} \times 100$$

The procedures used to obtain the Atterberg limits were in general similar to those discussed by Lambe (1951) with several significant differences. A representative portion of the entire sample including all grain sizes was used; the samples were air-dried to slightly below their liquid limit rather than oven dried; and the liquid limit test was performed using the one-point method (Cooper and Johnson, 1950).

Activity

The activity (Ac) of a sediment is the ratio of the plasticity index to the percentage by weight of the clay size fraction smaller than 2 microns, or;

$$Ac = \frac{PI}{\text{clay \%} < 2 \mu\text{m}}$$

According to Skempton (1953), activity is a rough indication of the sediments geological history (i.e., Post-glacial marine, lacustrine and brackish water clays), its clay mineralogy and the degree of surface activity of the clay fraction with decreasing grain size.

Shear strength

In simple terms shear strength is the shear stress necessary to cause slippage on a surface through the sediment, or the maximum resistance to sliding of one sediment mass against another. During the 18th

Century the French scientist Coulomb developed an interest in the behavior of soils. His efforts resulted in the classic equation for shear strength:

$$s = c + \sigma \tan \phi$$

where in modern nomenclature

s denotes shear strength

c = apparent cohesion

σ = total pressure normal to shear plane (normal stress)

ϕ = angle of shearing resistance

Later modifications of this equation based primarily on the concept of effective stress (σ'), which is the difference between normal stress and pore water pressure, have resulted in the basic equation:

$$s = c + \sigma' \tan \phi$$

Detailed discussions of the evaluation of this equation and the terms in the various equations leading up to it are found in Terzaghi (1924), Hvorslev (1936 and 1937), and Skempton (1960).

In studies involving completely saturated sediments of low permeability, such as those found in ocean environments, shear strength is usually obtained under conditions of no change in water content. This procedure is called undrained or quick testing. During this testing the normal stress (σ) equals the pore pressure resulting in an effective stress (σ') of zero. The saturated sediments then behaves in response to the applied stresses at failure as a purely cohesive material with an angle of shearing resistance (ϕ) equal to zero. When this happens the equation for shear strength is expressed as:

$$s = c$$

These are the conditions assumed to exist in the sediments measured for shear strength during the present study.

The shear strength of marine sediments is most commonly determined by a miniature motorized laboratory vane device. In this study the measurements were made with the fall cone instead of the laboratory vane because the cores were split longitudinally and, therefore, it was not possible to insert the vane to a depth in the sediment sufficient to obtain accurate results. However, the results from the fall cone are

similar to those obtained from the laboratory vane in saturated sediments with low shear strengths (Kravitz, 1970).

The fall cone apparatus determines shear strength by measuring the depth a cone of known apex angle and weight penetrates the sediment. The test is carried out by placing a metal cone vertically over the sample with its apex just touching the top of the sediment. Depth of penetration is measured by visually lining up a horizontal disc attached to the cone's stem with the scale on the instrument.

The shear strength is then computed from the formula:

$$s = KQ/h^2$$

where

s = shear strength

K = a constant whose magnitude depends upon the cone angle and also the type of sediment sampler used

Q = the weight of the cone

h = depth of cone penetration

The instrument comes with four cones of varying weights and apical angles. Only the 60 gram (2.1 ounces) cone with the 60° apex angle and the 100 gram (3.5 ounces) cone with the 30° apex angle were used because of the shear strengths of the sediments.

Because the cores were cut longitudinally, the shear strength was a radial measurement conducted parallel to the sedimentary fabric rather than axial measurements made perpendicular to the fabric, as is usually the case. Comparisons of these shear strength values with those from other investigations must be made with this in mind. For the purposes of this study the values are considered index properties and used in a relative sense. Hansbo (1957) discusses the fall cone test and presents a series of tables relating depth of penetration to shear strength.

Grain Size Analysis

The moist samples were placed in beakers, covered and kept under refrigeration until analyzed. This procedure retarded evaporation, allowing the sediment particles to retain their water hulls and, thereby, making disaggregation less difficult. The sediment was soaked in a peptizer solution of sodium hexametaphosphate with a normality of 0.03, then mechanically dispersed by a sonic disruptor prior to wet sieving

(Kravitz 1966). The sand fraction was sieved and the silt and clay fractions were analyzed by the pipette technique outlined in Folk (1968). The resulting size distribution values were expressed in weight percent. Whole phi intervals were used. This is adequate to calculate grain size parameters for the poorly-sorted sediments from the Kane Basin.

Heavy and Light Mineral Analysis

That portion of the sand fraction of each sample resting on the 3 phi sieve (2 phi to 3 phi) and on the 4 phi sieve (3 phi to 4 phi) was poured into separate glass funnels containing tetrabromoethane (S.G. 2.97), while slowly stirring the liquid-sand mix with a glass stirring rod. The samples were restirred every thirty minutes over a six hour period. The procedure followed was similar to that outlined by Carver (1971). After washing with alcohol and drying, the heavy and light fractions were weighed and their respective percentages determined. The heavy minerals were then microsplit with a Sepor sample splitter and mounted in Lakeside 70 cement (R.I. 1.54) on microscope slides for petrographic study. All grains including opaques, alterites and aggregates, were counted on each slide until a total of 200 non-opaque grains was reached.

Petrographic identification was complemented by x-ray diffraction analysis. The x-ray diffraction mounts were made from that portion of the heavy minerals not utilized for petrographic analysis. The samples were x-rayed with a General Electric XRD-6 diffraction unit using copper target radiation at 45 KVP and 28 Ma. The scanning speed was $1^{\circ} 2\theta$ per minute.

A general identification of the light minerals from the surficial layer was made by Kravitz (1975). The 0.250 mm - 0.125 mm (2 phi to 3 phi) intervals of the light fractions from 10 widely spaced samples were split, mounted and identified both petrographically and by x-ray diffraction. The methodology used was the same as that for the heavy minerals. In addition, all sand fractions (280) were washed and examined with a binocular microscope. Further analysis of the light mineral fraction was not conducted.

The two main concepts of size separation for heavy mineral studies are normal analysis and fraction analysis. In normal analysis the abundance in an unsized sample is determined. In other words, all the various sizes present in the sand fraction which contain heavy minerals, are represented. This approach has been recommended by Doeglas (1940) and Van Andel (1950), among others. Loring and Nota (1973) suggest this procedure for the poorly-sorted sediments found in the Arctic. However, there are several disadvantages to this method.

The identification of heavy minerals with the petrographic microscope can be difficult and operator variation is a major source of error (Griffiths and Rosenfeld, 1954). The difficulty of identifying heavy minerals in grain mounts, and operator variation, is reduced if all grains are of approximately the same size because color, birefringence, and other optical properties tend to be more nearly constant for a given mineral species or variety (Rubey, 1933). Also, because of its very nature (non-fraction), a normal analysis can mask the effects of a particular mineral species flooding the sample, whereas in fraction analysis the mineral counts in two or more separate fractions can be compared and the presence or absence of bias from flooding determined.

In heavy mineral fraction analysis one or more size fractions are studied individually as opposed to studying the entire unsized suite. This technique was originally adopted to negate the "grain size effect" which simply stated is the fact that heavy minerals are hydraulically equivalent to light mineral grains of some larger size, depending on the specific gravity of the heavy mineral. Heavy mineral suites, therefore, vary in composition with grain size of the sample. One disadvantage of this method is that certain diagnostic minerals may be present in the size fractions not studied. Another disadvantage is that a standard size fraction has not been established. A detailed discussion of this problem is found in Carver (1971).

Rubey (1933) recommended two size grades, especially if the sands differ in texture; a fixed size grade for all samples and a relative size grade such as the size grade containing the mode. Two fixed size grades were used in this study, 0.250mm - 0.125mm (2phi-3phi) and 0.125mm - .062mm (3phi-4phi). These two size grades included the modal

size class of the sand fraction 90% of the time (173 out of 192 samples).

Counting of the heavy minerals was accomplished by the Ribbon method, where the slide is moved along the stage and all grains between the two lines are counted. If the width between the lines is considerably larger than the largest grains, the method may be considered to yield a number percentage. This procedure for counting grain mounts is preferred to the Fleet or Line methods for the reasons cited by Galehouse (1969). The heavy mineral percentages for the two size grades from each sample were combined, and the number percentage of sized suites method (Young, 1966) was used to provide the raw percentage data for statistical and factor analysis.

Gravel Analysis

The gravel fractions from the surficial layer were previously identified by macroscopic and microscopic examination (Kravitz, 1975). In that study the rocks were placed into three general categories: carbonate, (limestones and dolomites), clastic (sandstone, shale, siltstone, mudstone), and crystalline (igneous and metamorphic). Although in some instances the individual rocks could be more closely identified (i.e. pink granite), this was not routinely possible. Petrographic examination of the gravels was beyond the scope of the present study.

Mineral and Chemical Element Analysis of the < 2 μ m Sediment Fraction

Sediment samples were placed in 250 ml glass beakers and soaked in deionized/distilled water. The samples were stirred periodically with a glass rod and once the sediment settled out, the clear water was removed by decantation. This was done in order to get rid of as much salt as possible. After 48 hours (six treatments) the samples were poured into 1000 ml graduated cylinders, and deionized/distilled water added to the 1000 ml mark. The material was further dispersed mechanically by bubbling compressed air through the sediment-water column for approximately 10 minutes. No chemical dispersants were used. The samples were then allowed to settle for approximately 12-18 hours. The < 2 μ m material (withdrawal depth dependent on time and temperature) was drawn off by

suction and collected in 2,000 ml glass beakers. The 1000 ml graduated cylinders were again filled with deionized/distilled water and the entire process repeated until the amount of $< 2 \mu\text{m}$ material remaining in the samples was negligible. In order to reduce the large sediment-water volumes the mixtures were centrifuged and the clear supernatant liquid decanted. The remaining "clay" and water mixtures were then thoroughly stirred and shaken, and an aliquot of the material drawn off by micropipette and placed on warm glass slides and dried for clay mineral analysis. The glass slides were put on a hot plate under a bank of infrared lamps inside a fume hood. Care was taken to keep the drying temperature at or less than 100°C in an attempt to reduce any adverse effect heating might have on the clays. The sediment usually dried completely within a few minutes, limiting as much as possible the stratification effect caused by differential settlement of the clay minerals. The method of slide preparation for X-ray diffraction analysis recommended by Gibbs (1965) was not used because many of the samples had insufficient $< 2 \mu\text{m}$ material for Gibbs' smear technique and since semi-quantitative relative comparisons were to be made, it was considered preferable to standardize preparation of the slides.

Two slides were prepared for each sample. The remaining material was placed in large porcelain evaporating dishes and air dried. This sediment was then removed from the dishes and ground with an agate mortar and pestle to a fine powder. The powdered sediment was placed in glass vials and stored for chemical element analysis.

X-ray diffraction analysis

Analysis was conducted using a Picker Nuclear X-ray diffraction unit model 3668 set at 40 kilovolts (KV) and 15 milliamps (MA) with a ratemeter count of 3 and 1 K, and a Diano Corporation X-ray diffraction unit model XRD-7D set at 45 KV and 30 MA with a ratemeter count of 2.5 and 1 K. In both instances the X-ray diffraction patterns of the slides were run from 3° to $35^{\circ} 2\theta$ at $1^{\circ}/\text{minute}$ using Cu K_{α} Nickel-filtered radiation. The slides were then glycolated for 1 hour at 60°C and rescanned from 3° to $14^{\circ} 2\theta$ at $1^{\circ}/\text{minute}$ (within 15 minutes of being removed from the glycol atmosphere) and from 24° to $27^{\circ} 2\theta$ at $\frac{1}{2}^{\circ}/\text{minute}$.

The relative abundance of the expandable lattice clays, and illite were obtained by determining areas under the 17 \AA ($5.2^\circ 2\theta$), and 10 \AA ($8.8^\circ 2\theta$), peaks respectively. The relative abundances of kaolinite and chlorite were obtained by determining the area under the 7.1 \AA ($12.2^\circ 2\theta$) peak. The lower-angle scan of the glycol-treated slides was used to differentiate expandable lattice clays (smectite and mixed-layer clays group) from illite and chlorite, because the expanding lattice material expands from 15 \AA ($5.9^\circ 2\theta$) to a 17 \AA ($5.2^\circ 2\theta$) peak upon glycolation. This expandable peak is often very broad and occurs at a low 2θ angle, therefore, establishing a base line is difficult, making measurement of the peak area imprecise. For the sake of consistency of procedures the baseline for the 17 \AA peak was always drawn as shown in Figure 6.

The high-angle (24° to 27°) slow scan allows separation of kaolinite from chlorite by resolving the 3.5 \AA ($25.4^\circ 2\theta$) peak into the 3.54 \AA ($25.2^\circ 2\theta$) peak representing chlorite, and the 3.58 \AA ($24.8^\circ 2\theta$) peak representing kaolinite (Biscaye, 1964). A horizontal baseline was used and a vertical line drawn perpendicular to the baseline separated the 3.54 \AA peak from the 3.58 \AA peak (Figure 7). The amount of kaolinite and chlorite represented by the 7.1 \AA peak was then partitioned according to their relative contributions indicated by the 3.54 \AA and 3.58 \AA peaks.

Peaks used for other minerals present in the $< 2 \text{ }\mu\text{m}$ fraction were as follows: amphibole 8.33 \AA ($10.6^\circ 2\theta$), quartz 4.26 \AA ($20.8^\circ 2\theta$), potash feldspar 3.24 \AA ($27.5^\circ 2\theta$), plagioclase feldspar from 3.18 \AA ($28.04^\circ 2\theta$) to 3.20 \AA ($27.8^\circ 2\theta$), Mg calcite 2.99 \AA ($29.9^\circ 2\theta$) to calcite 3.04 \AA ($29.3^\circ 2\theta$), and dolomite 2.89 \AA ($30.9^\circ 2\theta$). The 4.26 \AA peak of quartz was used instead of the intense 3.34 \AA ($26.67^\circ 2\theta$) peak which coincides with the third-order 3.35 \AA ($26.6^\circ 2\theta$) illite peak. The effect of this illite peak (on the quartz peak) can be approximated from the clearly visible second-order 5.0 \AA ($17.7^\circ 2\theta$) illite peak which, in most samples, was very strong. The measured area under the 4.26 \AA quartz peak was multiplied by three. All peak areas were measured by a digitizer attached to an x-y plotter and interfaced with a 9820 Hewlett-Packard desk calculator. The computations were performed with an X-ray diffraction area program developed for use on the 9820 H-P calculator by the Smithsonian Institution's Division of Sedimentology. A number of

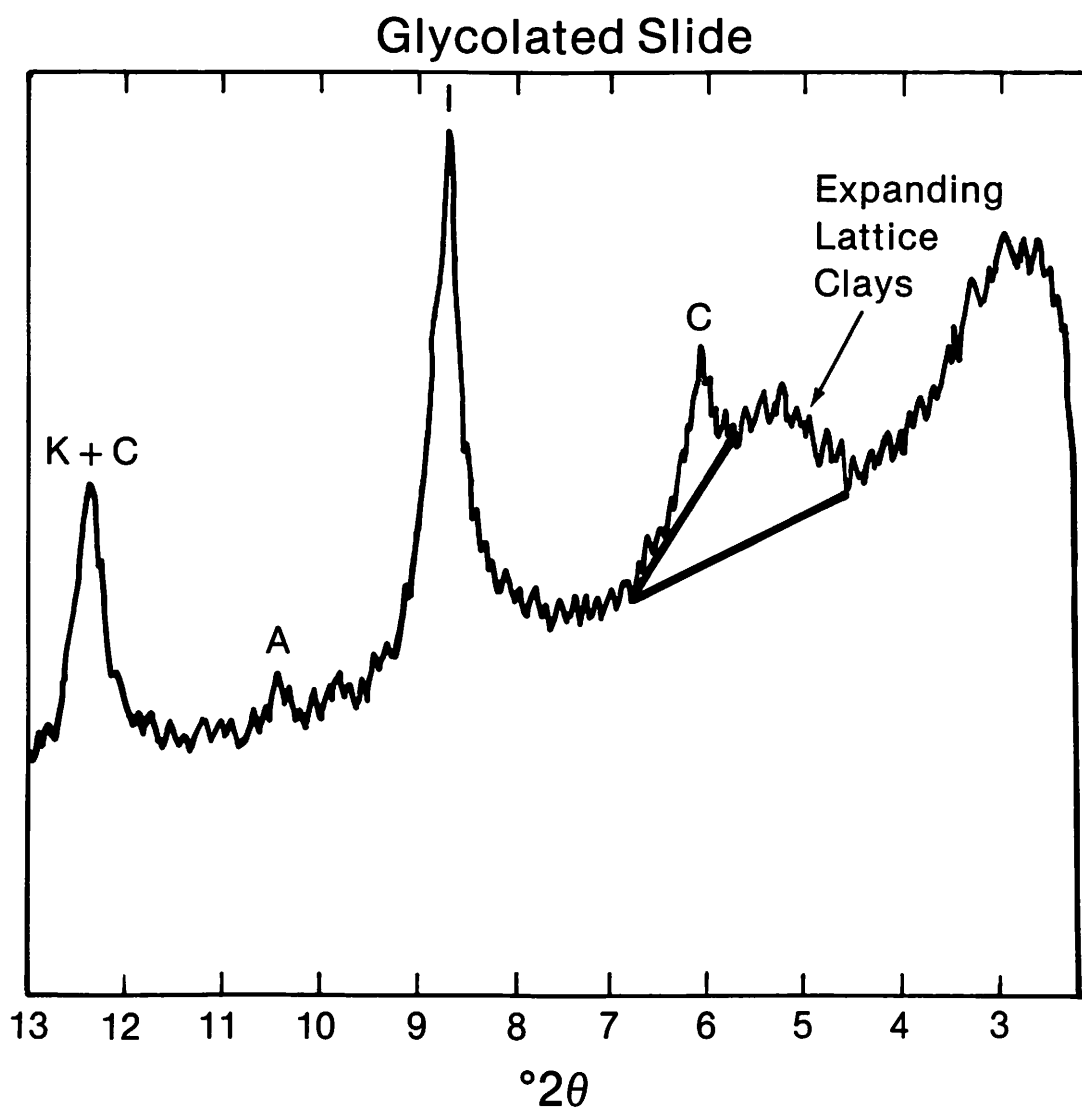


Fig. 6. X-ray diffractogram of glycolated slide showing method of drawing baseline. K=kaolinite, C=chlorite, I=illite, A=amphibole.

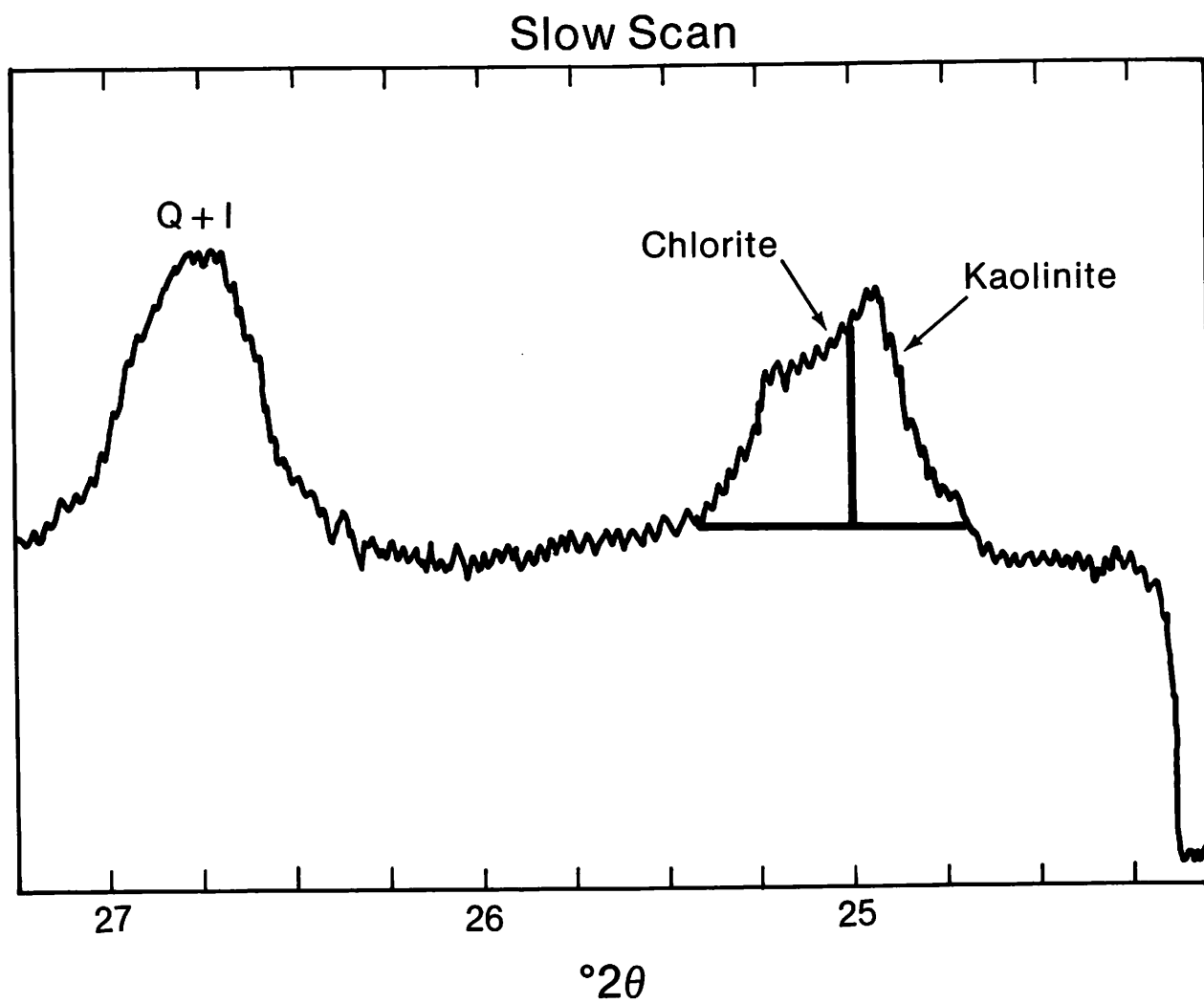


Fig. 7. X-ray diffractogram of slow scan showing method of drawing baseline. Q=quartz, I=illite.

samples were remeasured by a polar planimeter at the University of Colorado, and the peak areas hand calculated. In all cases the results from both methods were within $\pm 1\%$ peak area intensity.

Pierce and Siegel (1969) discussed the lack of a universally accepted method for quantifying clay minerals in sediments. They recommended tabulation of X-ray diffraction peak area intensities as the best way of presenting such data. However, in order to make any comparisons of clay minerals with most other studies that used the Biscaye (1965) weighting factors it is necessary to apply these factors to the peak areas. Therefore, peak area intensity percentages have been tabulated for all minerals present in the diffractograms of the $< 2 \mu\text{m}$ fraction, and in addition, weighted peak-area intensity percentages were tabulated for the clay minerals (illite, expanding lattice clays, kaolinite, and chlorite). These tabulations are found in Tables 11 and 12 in Kravitz, 1983.

Chemical element analysis

The chemical element analysis of the $< 2 \mu\text{m}$ fraction was conducted by atomic absorption and plasma analysis. Salts remaining after evaporation of interstitial water were removed by washing. The chemical analysis does not include cations from these waters or cations easily removed by the washing technique. The samples were prepared for analysis using the anhydrous lithium metaborate fusion technique (Medlin et al., 1969). In each case 0.1 grams of powdered sample was mixed with 0.5 grams of anhydrous lithium metaborate ($\text{LiBO}_2^+ \cdot 8\text{H}_2\text{O}$) and placed in a prefired graphite crucible. The mixture was heated in a muffle furnace for 10 minutes at $1,000^\circ\text{C}$. The resulting fluxed sample (in the form of a bead) was placed in a polypropylene beaker containing 40 ml of 3% nitric acid (HNO_3). A cover glass was placed over the beaker immediately in order to retard evaporation. The beaker's contents were stirred by a magnetic stirrer until the bead was completely dissolved. The solution was then passed through number 541 Whatman filter paper into 75 ml polyethylene vials. Initially the solution was diluted to 100 ml by adding deionized/ distilled water. However, in many instances the amount of a particular element was found to be below the detection limit of the atomic absorption instrument and, therefore, the concentrated

40 ml solution was routinely used with dilution carried out on a case by case basis.

The sediments were analyzed for the following elements: Fe, Mg, Mn, Cr, Co, Ni, Zn, Cu, Ti. The analysis for copper was conducted in the geochemistry laboratory at the University of Colorado with an Instrument Laboratory (IL) model 353 atomic absorption spectrophotometer, taking instrument settings from the manufacturer's handbook. The precision for copper analysis with this instrument and technique is $\pm 5\%$. Titanium analysis was carried out in the analytical laboratory of the Center for Environmental Sciences at the University of Colorado, Denver, by plasma emission utilizing an Applied Research Laboratories (ARL) model 35000c spectrometer. All other elements were analyzed by a Perkin Elmer model 5000 atomic absorption spectrophotometer in the same laboratory following analytical conditions recommended by the manufacturer. Accuracy of the elemental analysis was verified by analyzing U.S.G.S. Standards G-2 and AGV-1, and comparing the results thus obtained with those summarized by Flanagan (1973).

The analytical precision for Cr, Co and Ni was $\pm 15\%$; Ti $\pm 10\%$; Fe, Mg, Mn and Zn $\pm 5\%$. All standards were prepared in the laboratory and utilized within 90 days of preparation. No manufactured standards were used. The standards were diluted to the desired concentrations by the addition of a simple matrix solution composed of 40 ml of 3% nitric acid (HNO_3) per 0.5 grams of anhydrous lithium methaborate ($\text{LiBO}_2 \cdot 8\text{H}_2\text{O}$). In an attempt to maximize analytical accuracy, the instruments were calibrated within the following narrow range of values for each element:

Fe: .25 - 1 ppm (AA)	Ni: .5 - 2 ppm (AA)
Mg: .25 - .5 ppm (AA)	Zn: .1 - .3 ppm (AA)
Mn: .5 - 2 ppm (AA)	Cu: .5 - 2 ppm (AA)
Cr: .5 - 3 ppm (AA)	Ti: .5 - 20 ppm (Plasma)
Co: 1 - 4 ppm (AA)	

This approach helped eliminate the erratic instrument behavior and low repeatability experienced in earlier attempts at analyzing this suite of samples. The results are presented in parts per million (ppm) utilizing the following computational method:

$$\frac{X \text{ ug}}{\text{ml}} \times 40 \text{ ml} = Y \text{ ug}$$

$$\frac{Y \text{ ug}}{0.1 \text{ gm sediment}} = Z \text{ ug/gm} = Z \text{ ppm}$$

where

X = instrument reading in micro grams

Y = micro grams of element in 40 ml of solution

Z = amount of element in sediment in micro grams per gram or parts per million.

Sediment Organic Carbon and Carbonate Content

Organic Carbon

The percent of organic carbon in the samples was determined on the whole sample (excluding gravel) by the Allison titration method, which is based on the reduction of chromic acid (Allison, 1935).

Carbonate content

Carbonate content was determined by treating the whole samples with dilute HCl, filtering the solution, washing and drying the residue, and computing the percent insoluble residue (Twenhofel and Tyler, 1941). The use of replicate samples established the precision of this method as $\pm 5\%$. Care was taken to keep the pH of the solution above 3.0 in order to eliminate errors caused by the dissolution of chlorite.

Diatom Analysis

The sediments were examined for the presence of diatoms at the Lamont-Doherty Geological Observatory by the method described in Booth and Burckle (1976). After mounting, each slide was scanned at 400X under a light microscope. The slides were then categorized as:

1. No diatoms present to very rare diatom occurrence (less than one fragment of diatom present per field of view).
2. Rare to frequent diatoms present (at least one diatom or diatom fragment present in each field of view).
3. Common to very common diatoms present (at least three diatoms present per field of view; usually many more).

Statistical Procedures

The raw data from the sieve and pipette analysis were put through a slightly modified computer program developed by Rucker and Stewart (1966). The program provides weight percents for each whole phi interval and the sample mean, standard deviation, skewness, and kurtosis by moment computations.

Weight frequency data may be analyzed either by sample moment computation or by graphical (percentile) techniques. The moment measures have desirable statistical properties, if there are no errors induced by grouping or truncation. The grouping error was unimportant because the sieve interval is small compared to the sorting of the samples. Because much of the sample information concerning moment measures is in the tails of the distribution, even a small percentage of the total sample in a tail may greatly influence the computed values of the higher moments. Thus, the sample data from which the moments are computed should be complete and not open-ended. However, artificial truncation took place.

The graphical estimators use less of the sample data than do the moment measures and are therefore less efficient, implying greater variability. An additional source of variation is due to interpolation of percentiles from the cumulative curve. A serious problem with graphical techniques is that the graphic statistics are inter-related; skewness and kurtosis in the sample will alter the estimates of population mean, sorting, skewness and kurtosis (Jones, 1970).

Moment measure statistics were used to evaluate the grain size data because, in addition to reasons listed above, a large number of samples analyzed contained over 26% material smaller than 1 μm (10 Phi). This prevented the use of even the 75th percentile unless the cumulative percentage curve was arbitrarily extended, thereby creating additional errors.

The moment statistics applied to the grain size data are defined as follows:

$$\begin{aligned}
 \text{Mean} \quad \bar{x}\phi &= \frac{\sum fm}{n} \\
 \text{Standard deviation} \quad \sigma\phi &= \sqrt{\frac{\sum f (m - \bar{x}\phi)^2}{100}} \\
 \text{Skewness} \quad Sk &= \frac{\sum f (m - \bar{x}\phi)^3}{100 \sigma\phi^3} \\
 \text{Kurtosis} \quad K\phi &= \left[\frac{\sum f (m - \bar{x}\phi)^4}{100 \sigma\phi^4} \right] - 3
 \end{aligned}$$

Where f = weight percent (frequency) in each grain-size grade present
m = Midpoint of each grain-size grade in phi values
n = total number in sample which is 100 when f is in percent.

Correlation coefficients were used to compare various sediment properties to each other. They are effective in finding the degree of association that exists between two variables. A high correlation coefficient indicates the existence of a close mathematical relation between the variables, but it is important to realize that this does not necessarily imply causation. When a low correlation coefficient is obtained, the conclusion that the independent variable does not influence the quantity being measured is not necessarily correct. It is possible that other factors exist, masking or nullifying the effect of the independent variable on the dependent variable (Neville and Kennedy, 1968).

Q-mode factor analysis was used to characterize the sediment. It was decided to use Q-mode analysis instead of R-mode because in an R-mode study relationships between variables are compared on the basis of all samples; in the Q-mode, relationships between samples on the basis of all variables are established.

In order to do this, a modified factor analysis was applied to identify, in a data matrix, a set of end members (factors or reference vectors) of maximally different compositions that are represented by actual samples. The remaining samples are expressed in terms of proportional contributions of these factors. The main advantage of this

analysis is objectively arriving at an end-member classification for samples using a number of variables. This method does not introduce any variables to account for variations in composition and is intended to complement rather than to replace conventional techniques (Ross, 1971).

The best test of the geologic significance of the results of factor analysis is made by plotting the proportions (loading values) of the factors on a map or in profile (and interpreting the plots). If the pattern is systematic with respect to known geologic or hydrographic parameters, then the results may be both statistically and geologically significant. Factor analysis is discussed in greater detail by Imbrie and Van Andel (1964), and by Klován (1975).

A program developed by Dr. James Gardner of the USGS also was utilized. This program takes the variable vs factor output from the Q-mode analysis of surface samples and compares down-core data to it. This is done with matrix algebra as follows:

$$U_s = B_s F_s$$

where U_s is the matrix of surface samples vs variables; B_s is the matrix of surface samples vs surface factors and F_s is the matrix of surface variables vs surface factors. B_s and F_s are output from the surface Q-mode factor analysis. Because F_s and B_s have the same number of rows the equation can be rearranged to:

$$B_s = U_s F'_s$$

where F'_s is the transpose of F_s .

Next, U_d is substituted for U_s where U_d is the matrix of down-core samples vs variables and solved for B_s (more properly termed B_d) or the matrix of down-core samples vs the surface factors. In other words, we now have the fluctuation of the surface factors with time at each core site.

Mapping and Plotting Procedures

Much of the data were plotted as lithologic, single component (univariate), maps. This type of facies map shows the areal variation of one particular sediment characteristic. The characteristic may be expressed in terms of mineralogy (illite, kaolinite, chlorite, etc.),

mass physical properties (wet unit weight, porosity, etc.), or some other diagnostic property that can be quantitatively expressed. The maps are prepared by indicating the characteristic's value at each sampling point and using various patterns to illustrate the selected value intervals, or by contouring. The value intervals should be selected in order to present the data as clearly as possible. The selection of too small an interval can result in a "crowded" map which is difficult to interpret, conversely an overly large interval may "absorb" meaningful distributions. Patterns are used in this study primarily because the number of data points (33 sample points over 27,000 square kilometers) was insufficient to provide good control for contouring.

Data were also plotted in profile showing changes in properties with depth in the cores. The use of these core profiles allows for visual perception of temporal variations in the sediments' character.

CHAPTER IV

RESULTS

Sediment parameters were used to identify and delineate lithofacies in the sediments of the Kane Basin. The approximate thickness of the surface layer at the stations was estimated according to procedures previously outlined (Table 1). The distribution of the sediment parameters down the cores are detailed in Kravitz, 1983. A number of the parameters were employed in a Q-mode factor analysis. Tables 9-16 and Figures 51 to 188 are in Kravitz, 1983.

Radiograph Descriptions (pp. 214-222, Kravitz, 1983)

All references to texture (i.e., fine-grained, coarse-grained) in these descriptions are based on visual interpretations of the radiographs, and are not the result of the textural analysis. A fine-grained matrix, therefore, may include medium to fine sand as well as silt and clay sized materials. A coarse-grained matrix generally contains some silt and clay along with a preponderance of larger particles.

Texture

Surface distribution

The textural character of the surface sediment layer is discussed in Kravitz (1975) therefore only a brief synopsis will be given here.

Gravel is most abundant in the northeastern part of the Basin, along the topographic high south-southwest of Washington Land, and in the western trough, southeast of Dobbin Bay (Figure 8A). The smallest amounts of gravel (0-10%), are found in the eastern trough off Humboldt Glacier, and in that part of Kane Basin north of Inglefield Land. The amount of gravel in the surface samples ranges from none in two samples from the eastern trough to a high of 37% in a sample just east of Cape Hawks near the north of Dobbin Bay (Core 11).

TABLE 1
THICKNESS OF SURFICIAL SEDIMENT LAYER

BOTTOM SAMPLE	THICKNESS (CM)	BOTTOM SAMPLE	THICKNESS (CM)
2	20	19	22
3	20	20	21
4	16	21	12
5	56	22	36
6	10	23	68
7	10	24	23
8	20	25	5
9	38	26	9
10	18	27	16.5
11	5	28	20
12	32	29	14
13	12	30	68
14	90	31	8
15	12	7G	10
16	45	26G	10
17	34	32G	10
18	10		

Sand percentages of the surficial layer are highest in the northern and northeastern parts of Kane Basin, south to about 79°28'N; in the western trough, and on the western slopes of the topographic high (Figure 8B). The percentages of sand in the surface sediment ranges from 1% to 64%. With the exception of some scattered samples, the eastern, southeastern, and central areas of the Basin contain very little sand (<1% - 10%).

Silt concentrations are greatest off the coast of Inglefield Land and off Washington Land, from just slightly east of Cape Jackson to Cape Webster (Figure 9A). This latter zone of high silt content (> 40%) extends south of Wright Bay, down the east slope of the topographic high and into the northernmost part of the eastern trough. West and south of the zone is a broad belt of lower silt content (10 - 30%)

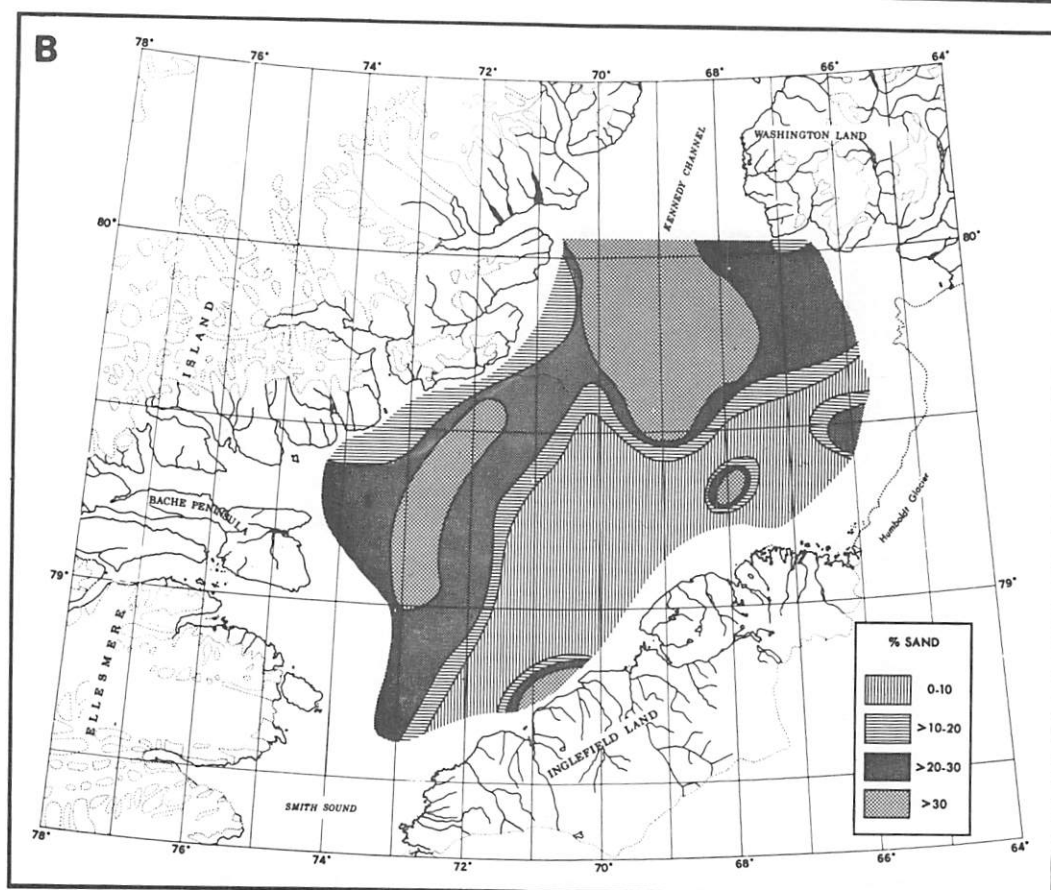
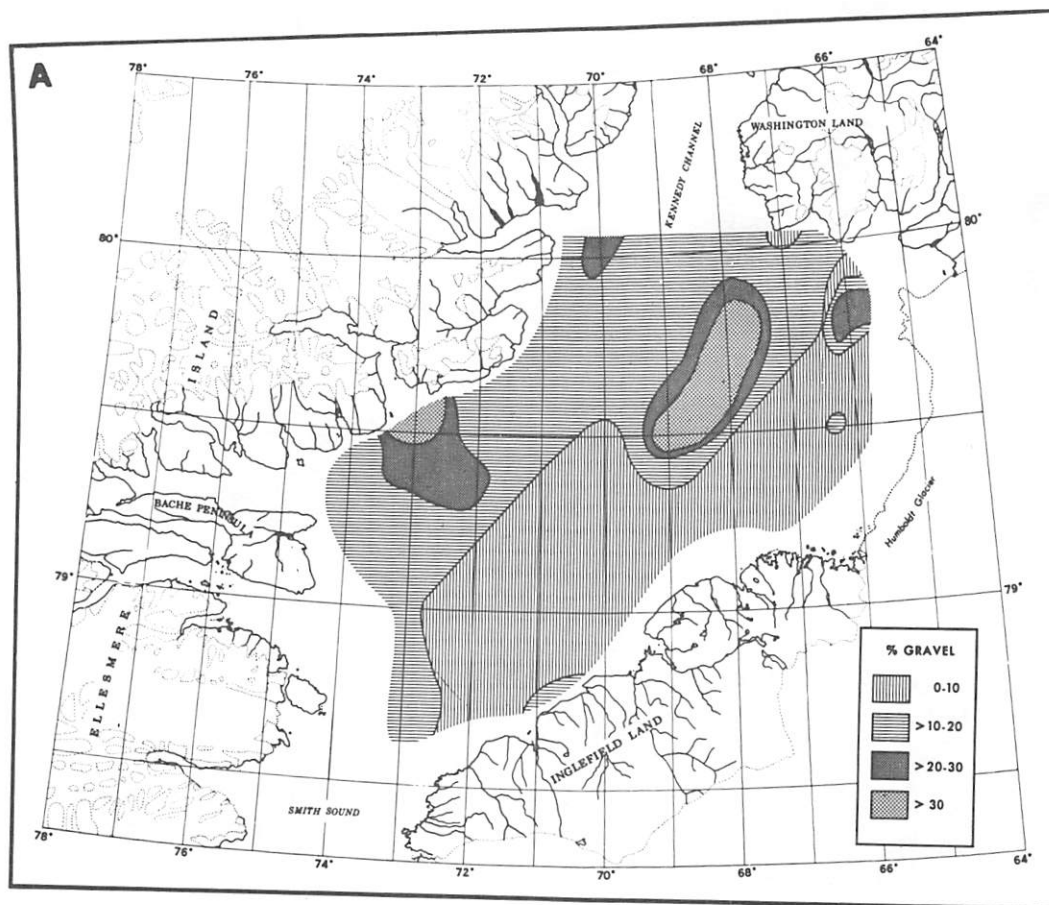
Silt is moderately abundant off the Ellesmere Island coast and throughout Kane Basin, except for the central part of the western trough and in the previously mentioned low concentration belt. Patches of sediment containing varying amounts of silt are present throughout the area. Silt is the most abundant size fraction of the surficial layer and ranges from 15% to 57% of the total.

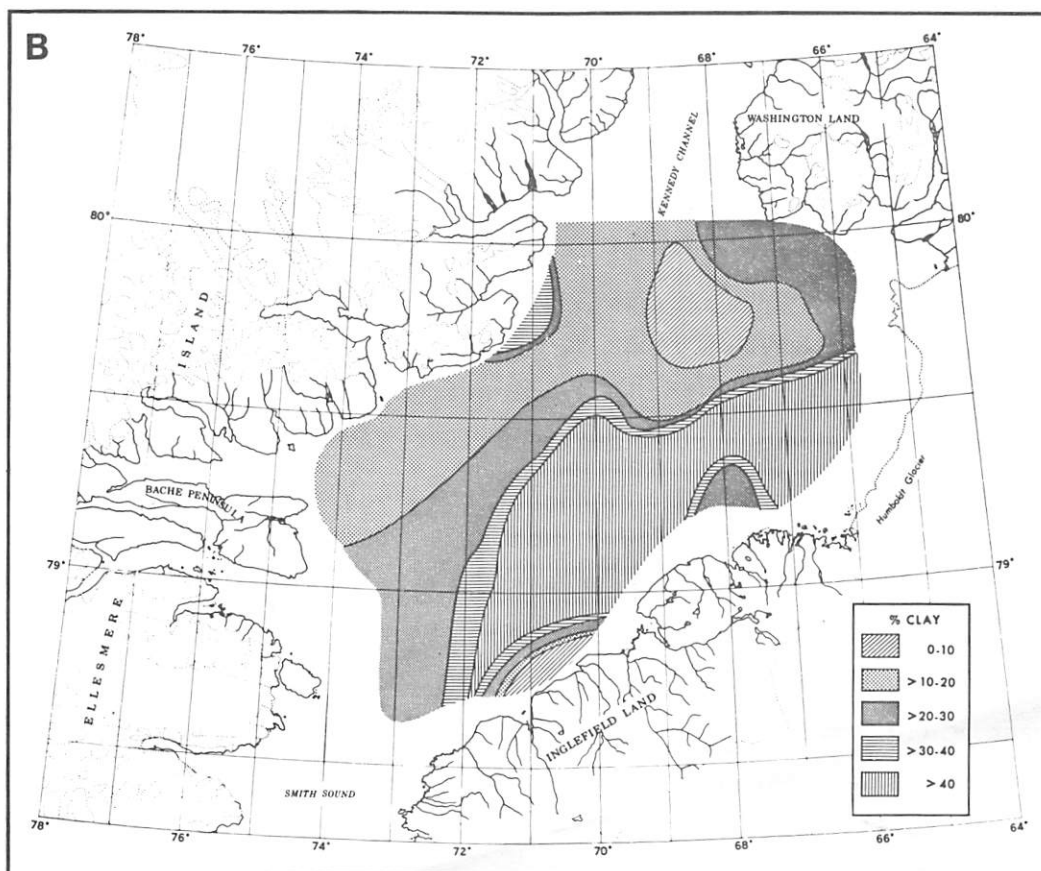
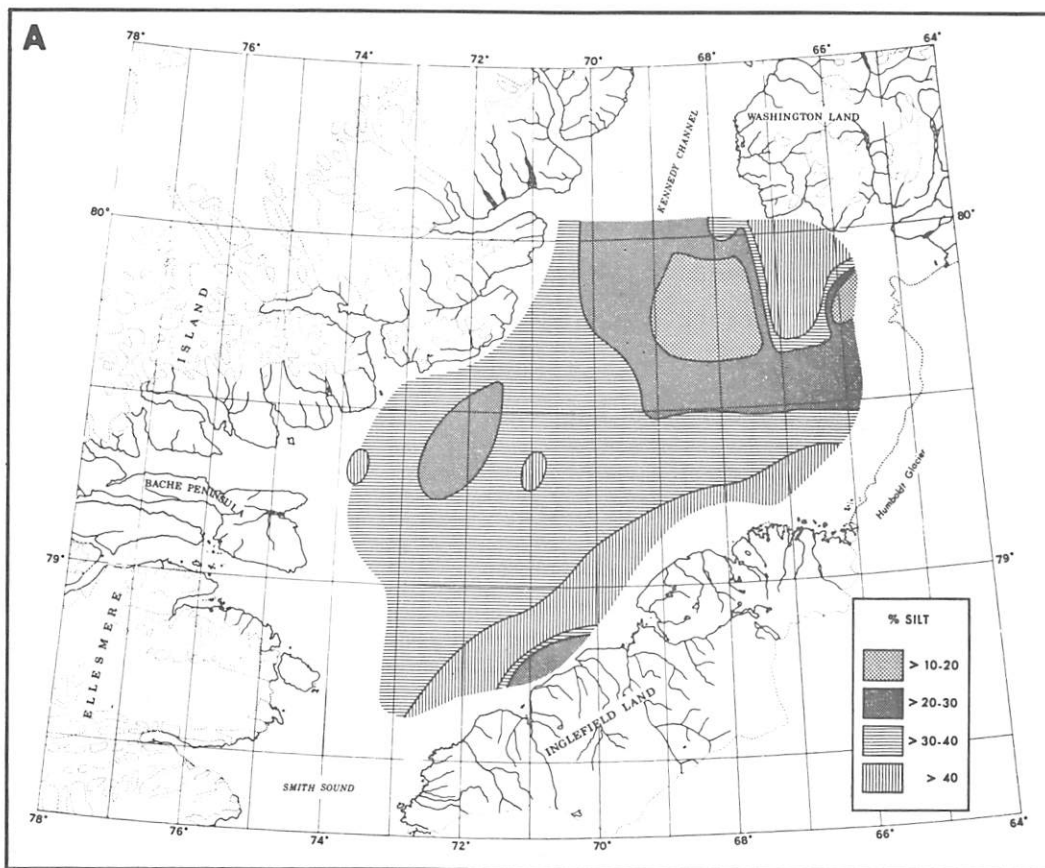
Clay is the second most abundant size fraction in the surficial layer of Kane Basin sediments (Figure 9B). It dominates (> 40%) the bottom sediment off Inglefield Land and Humboldt Glacier, including the central and southeastern part of the topographic high, and all but the northernmost area of the eastern trough. Moderate amounts of clay (>20% - 30%) are found just south of Washington Land, along the western parts of the topographic high, and in the eastern part of the western trough. The northern Basin off Ellesmere Island, including a large part of the western trough, has a low clay content (0 - 20%).

The surface sediments are poorly sorted (one sample) to extremely poorly sorted according to the sorting classifications of Folk and Ward (1957) and Friedman (1962). Standard deviations range from 1.7 phi to 5.2 phi. The sediments of the northern and northeastern Basin (primarily north of 79°30'N) and the western Basin are very poorly sorted (2 phi - 4 phi) to extremely poorly sorted (4 phi), using the sorting limits of Folk and Ward (1957). This includes the northern, northeastern and western topographic high and the western trough.

Fig. 8. Univariate maps of the distribution of gravel (A), and sand (B) in the surficial sediment of the Kane Basin (after Kravitz, 1976). (p. 48)

Fig. 9. Univariate maps of the distribution of silt (A) and clay (B) in the surficial sediment of the Kane Basin (after Kravitz, 1976). (p. 49)





In the area of Inglefield Land, sediments from the central and southern parts of the topographic high, and from the eastern trough are poorly sorted (1 phi - 2 phi) to very poorly sorted (2 phi - 4 phi). The sediments of the eastern trough off Humboldt Glacier are more poorly sorted than the sediments in the eastern trough off Inglefield Land. Standard deviation values for each core are summarized in Table 2.

The artificial truncation of the size distribution reduces the accuracy of the higher moments (skewness and kurtosis), especially kurtosis. It is important to keep this in mind when these properties are discussed.

Positively skewed sediments are concentrated in the north-central part of Kane Basin from Kennedy Channel south to approximately 79°28'N. This includes a large part of the northern topographic high. Sediments with positive skewness are also found near the mouth of Dobbin Bay and off Inglefield Land near Cape Leiper. The sediments from the areas off Inglefield Land, Washington Land, Humboldt Glacier and Ellesmere Island are negatively skewed.

Negative skewness of the sediments increases from west to east below 79°28'N. Most of the western trough contains slightly negatively skewed (-0.1 to 0) materials. The eastern edge of the western trough, and the southern and part of the western topographic high are covered with moderately negatively skewed (-0.2 to -0.1) sediments. The central and eastern topographic high and the eastern trough, except for its northernmost area, are covered with highly negatively skewed materials (≤ -0.2). The range and average skewness values for Kane Basin core and grab samples are found in Table 3.

The vast majority of the samples from the surficial layer are platykurtic (have very broad sediment distribution curves and negative kurtosis values). Only four samples; two on the northwestern part of the topographic high, one in the eastern trough, and one in the south of the Basin are leptokurtic (positive kurtosis values). The zone northwest of Inglefield Land between Cape Kent and Cape Leiper, which includes the southern half of the eastern trough has kurtosis values between -.110 and -.491. The remainder of the surface sediment of the Basin, excluding leptokurtic areas, contains kurtosis values ranging from -.50 to -1.170.

TABLE 2
STANDARD DEVIATION VALUES

CORE AND GRAB SAMPLES	STANDARD DEVIATION RANGE (ϕ)	STANDARD DEVIATION MEAN (ϕ)	SORTING CLASSIFICATION (Folk and Ward, 1957)
2		4.7*	Extremely poorly sorted
3		3.4*	Very poorly sorted
4		4.5*	Extremely poorly sorted
5	2.7 - 3.3	3.0	Very poorly sorted
6		3.9*	Very poorly sorted
7		4.0*	Extremely poorly sorted
8		3.3*	Very poorly sorted
9		3.7*	Very poorly sorted
10	3.5 - 4.4	3.9	Very poorly sorted
11	2.8 - 4.6	4.3	Extremely poorly sorted
12	3.2 - 4.3	3.9	Very poorly sorted
13		4.3*	Extremely poorly sorted
14	2.2 - 4.6	2.9	Very poorly sorted
15		4.5*	Extremely poorly sorted
16	3.3 - 6.6	4.4	Extremely poorly sorted
17	2.3 - 4.5	3.4	Very poorly sorted
18	2.3 - 5.5	3.7	Very poorly sorted
19	2.4 - 3.8	2.8	Very poorly sorted
20	3.7 - 3.8	3.8	Very poorly sorted
21	1.9 - 3.7	2.3	Very poorly sorted
22	2.9 - 4.6	3.8	Very poorly sorted
23	2.3 - 3.0	2.5	Very poorly sorted
24	4.1 - 5.4	4.7	Extremely poorly sorted
25	3.8 - 4.7	4.2	Extremely poorly sorted
26	3.8 - 5.2	4.3	Extremely poorly sorted
27	3.2 - 5.0	4.1	Extremely poorly sorted
28	1.7 - 2.1	1.9	Poorly sorted
29	2.2 - 4.2	2.6	Very poorly sorted
30	2.1 - 4.6	3.1	Very poorly sorted
31	2.6 - 4.8	3.7	Very poorly sorted
7G		5.2*	Extremely poorly sorted
26G		4.4*	Extremely poorly sorted
32G		3.7*	Very poorly sorted

*Value from single sample

TABLE 3
SKEWNESS VALUES

CORE AND GRAB SAMPLES	SKEWNESS RANGE	SKEWNESS AVERAGE	NATURE OF SKEWNESS
2		-0.016*	Slightly negative
3		0.327*	Positive
4		-0.185*	Moderately negative
5	0.077 to -0.040	0.018	Positive
6		-0.089*	Slightly negative
7		0.250*	Positive
8		0.362*	Positive
9		0.178*	Positive
10	-0.322 to -0.400	-0.361	Highly negative
11	0.074 to -0.867	-0.321	Highly negative
12	0.110 to -0.299	-0.151	Moderately negative
13		-0.200*	Moderately negative
14	0.331 to -0.764	-0.284	Highly negative
15		0.211*	Positive
16	-0.073 to -0.833	-0.402	Highly negative
17	-0.355 to -0.802	-0.510	Highly negative
18	-0.107 to -0.851	-0.438	Highly negative
19	-0.151 to -0.728	-0.406	Highly negative
20	0.102 to -0.064	-0.042	Slightly negative
21	-0.396 to -1.009	-0.591	Highly negative
22	0.025 to -0.402	-0.198	Moderately negative
23	0.080 to -0.565	-0.109	Moderately negative
24	0.030 to -0.130	-0.100	Slightly negative
25	-0.107 to -0.227	-0.145	Moderately negative
26	0.138 to -0.500	-0.147	Moderately negative
27	0.013 to -0.217	-0.108	Moderately negative
28	-0.328 to -0.993	-0.445	Highly negative
29	-0.085 to -0.494	-0.313	Highly negative
30	0.140 to -0.592	-0.176	Moderately negative
31	0.360 to -0.441	0.020	Positive
7G		-0.035*	Slightly negative
26G		-0.090*	Slightly negative
32G		0.083*	Slightly negative

*Value from single sample

Mass Physical Properties

Surface distribution of unit weight, water content, void ratio and porosity

The highest wet unit weight values ($>2.00 - 2.50$) for the surficial layer of Kane Basin sediments are found in two areas (Figure 10). The first is in the northern Kane Basin crossing the entrance to Kennedy Channel, between Cape Collinson on Ellesmere Island and Cape Jackson on Washington Land, and extending south-southeasterly to approximately $79^{\circ}28'N$. This area covers the northernmost part of the western trough, the northwestern slope of the topographic high, all of the northern topographic high and some of its northeastern slope. The other area is in the western Basin. It is a broad zone extending from just north of Cape Fraser on Darling Peninsula to approximately $79^{\circ}N$ off Bache Peninsula, and covers most of the western trough. These zones of high wet unit weight correspond to the areas of highest gravel and sand content in the Kane Basin sediments.

To the south and east of these two areas, the wet unit weight values decrease, with the lowest values ($<1.50 - 1.50$) occurring in an area extending from the southernmost part of Humboldt Glacier southwest along Inglefield Land, to Cairn Point.

The highest water content ($> 80\%$ dry weight) of Kane Basin's surficial sediment layer is found in a broad zone extending from a point northeast of Cape Agassiz southwest along the coast of Inglefield Land to Cairn Point, and extends northward as a lobe to $79^{\circ}32'N$, similar to the distribution of low values for wet unit weight (Figure 11). This zone contains the fine-grained sediment brought into Kane Basin by the streams emanating from Inglefield Land. These sediments with a high water content blanket most of the southern area in the eastern trough and a portion of the central topographic high.

The regional distribution of the sediments' water content shows zones decreasing in value to the north and west (where coarse-grained sediments dominate) with the lowest values ($> 0 - 20\%$ dry weight) found in an area between Cape Collinson and Cape Alexander. This zone of low water content extends south to approximately $79^{\circ}37'N$ and covers the northern tip of the western trough, a large part of the northwestern

Fig. 10. Univariate map of the distribution of wet unit weight values in the surface sediment layer.

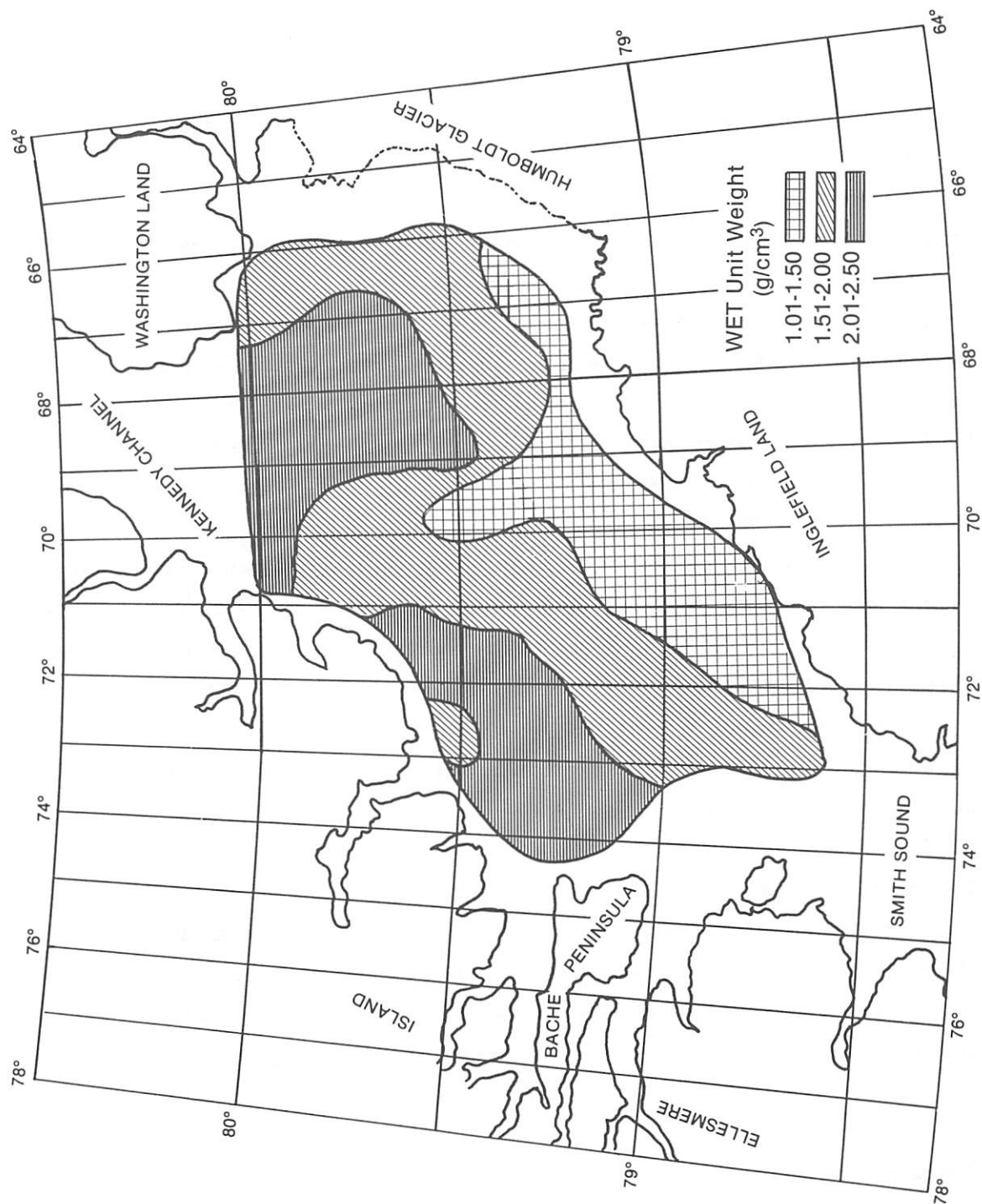
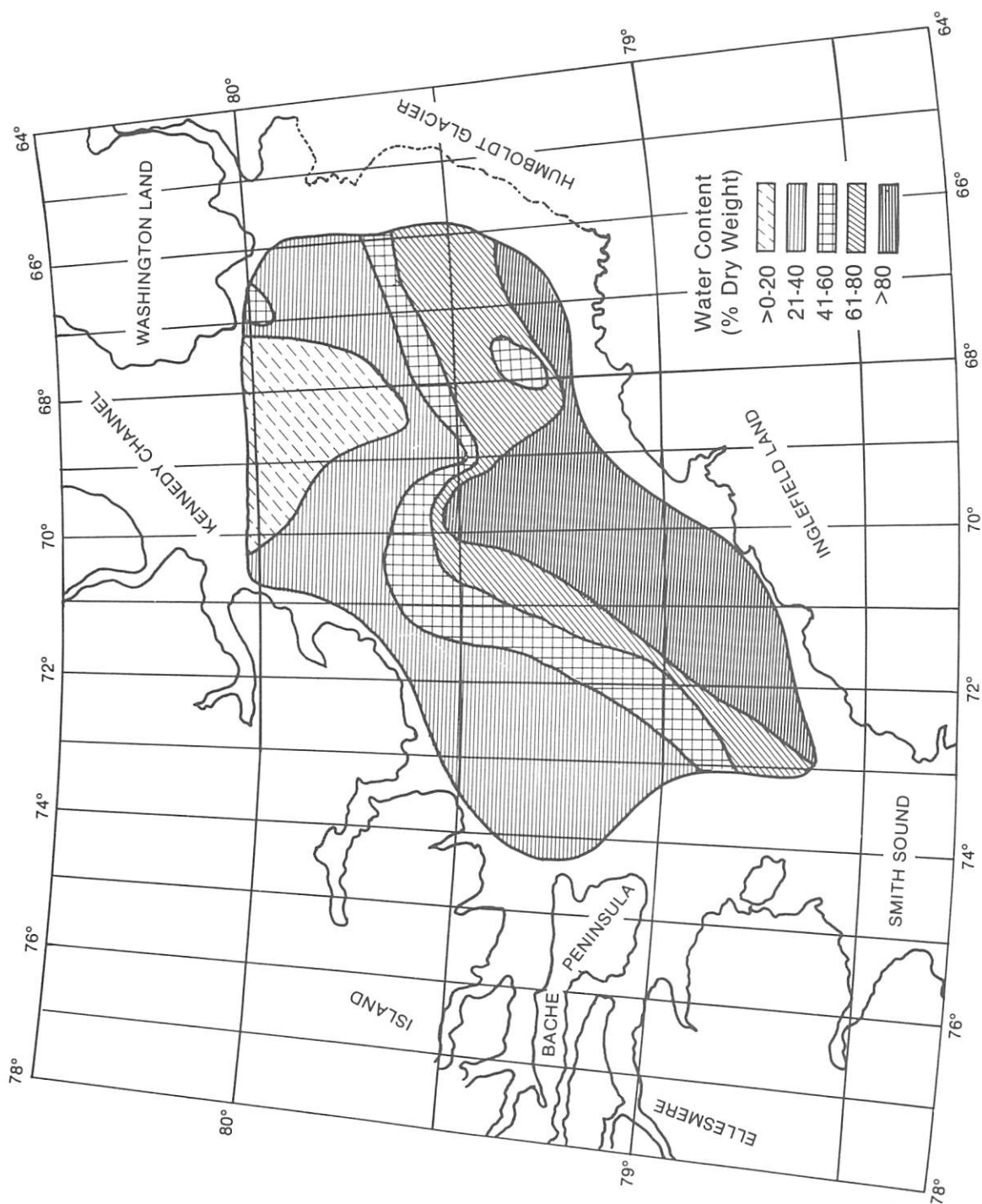


Fig. 11. Univariate map of the distribution of water content (% dry weight) in the surface sediment layer.



slope of the topographic high as well as the western half of the northern topographic high.

The regional trend of saturated void ratio values for the surface sediment is, as expected, very similar to that of the water content (Figure 12). The values decrease to the north and west with the highest values (2.1 to > 3.0) along the coast of Inglefield Land and most of Humboldt Glacier except for a pocket of low values (1.1 - 2.0) directly off the central part of the glacier.

The lowest void ratio values (0 - 1.0) are found in the coarse sediments in the northern and western areas of Kane Basin, which cover the northern topographic high, its northeastern and northwestern slopes, the western trough and the western slope of the topographic high down the length of Kane Basin.

As with water content and void ratio, the regional trend of porosity (Figure 13) is the opposite of the unit weight distribution pattern, with highest porosity values (71% to > 80%) off Inglefield Land. The high values are found in the finegrained sediments which cover the southern portion of the eastern trough and large parts of the central topographic high directly north of Inglefield Land. The porosity values are slightly lower (51% - 70%) off Humboldt Glacier in the central part of the eastern trough reflecting the presence of coarse sediments produced by the glacier.

The lowest porosity values (> 0 - 30% and 31 - 40%) are found in two south-southeasterly trending zones in the northern part of the Basin between Cape Collinson and Cape Alexander. These zones cover the northern tip of the western trough, most of the northern topographic high and its northwestern and northeastern slopes.

Surface distribution of shear strength

Shear strength was measured only on those core intervals where the sediment appeared to have a high clay content and low sand and gravel contents. This resulted in many unmeasured sediment intervals and a large number of cores being omitted entirely, due to the abundance of coarse-grained sediment. Consequently, Figure 14 does not always depict the shear strength value from the uppermost layer.

Fig. 12. Univariate map of the distribution of the saturated void ratio values of the surface sediment layer.

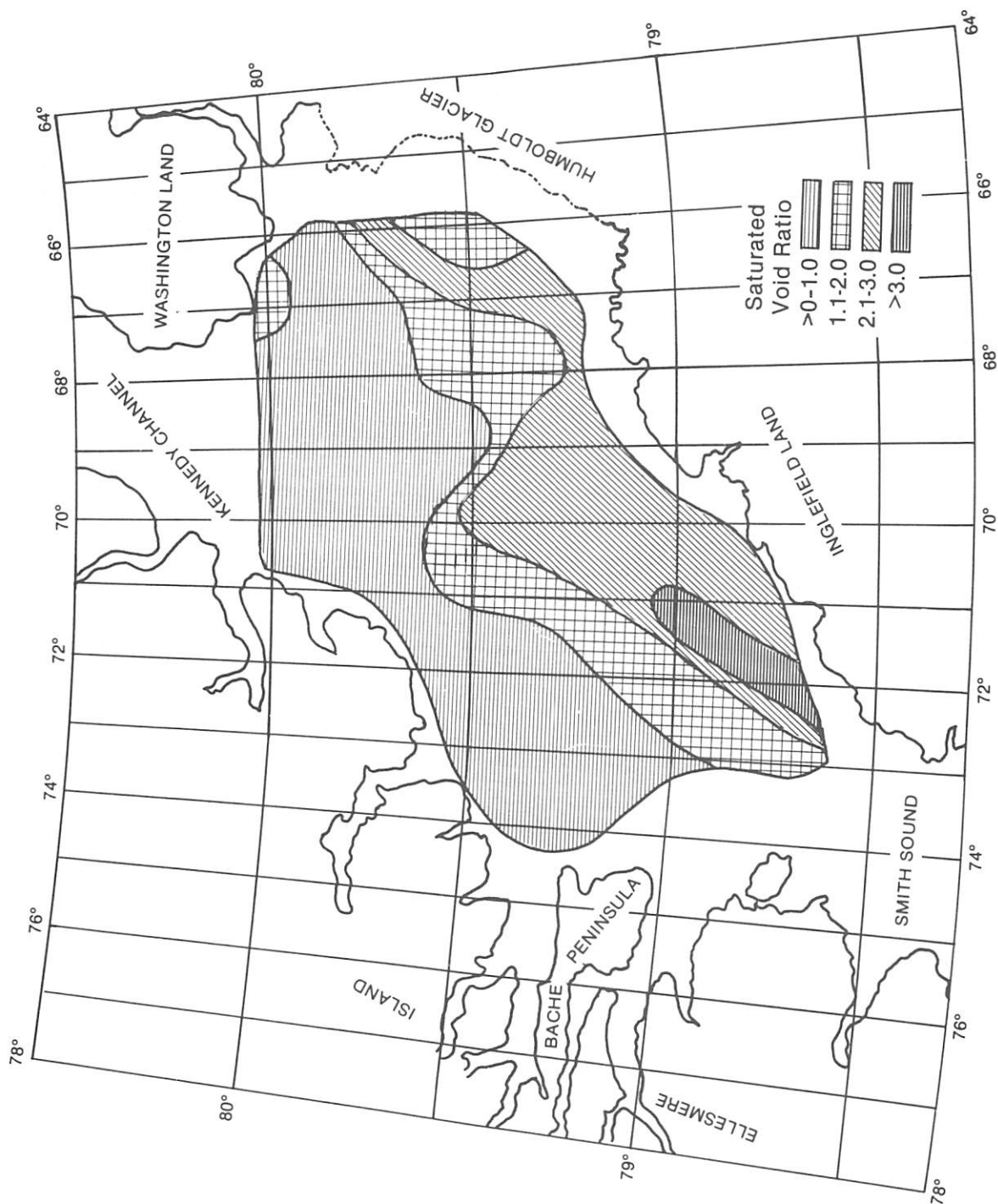


Fig. 13. Univariate map of the distribution of porosity values in the surface sediment layer.

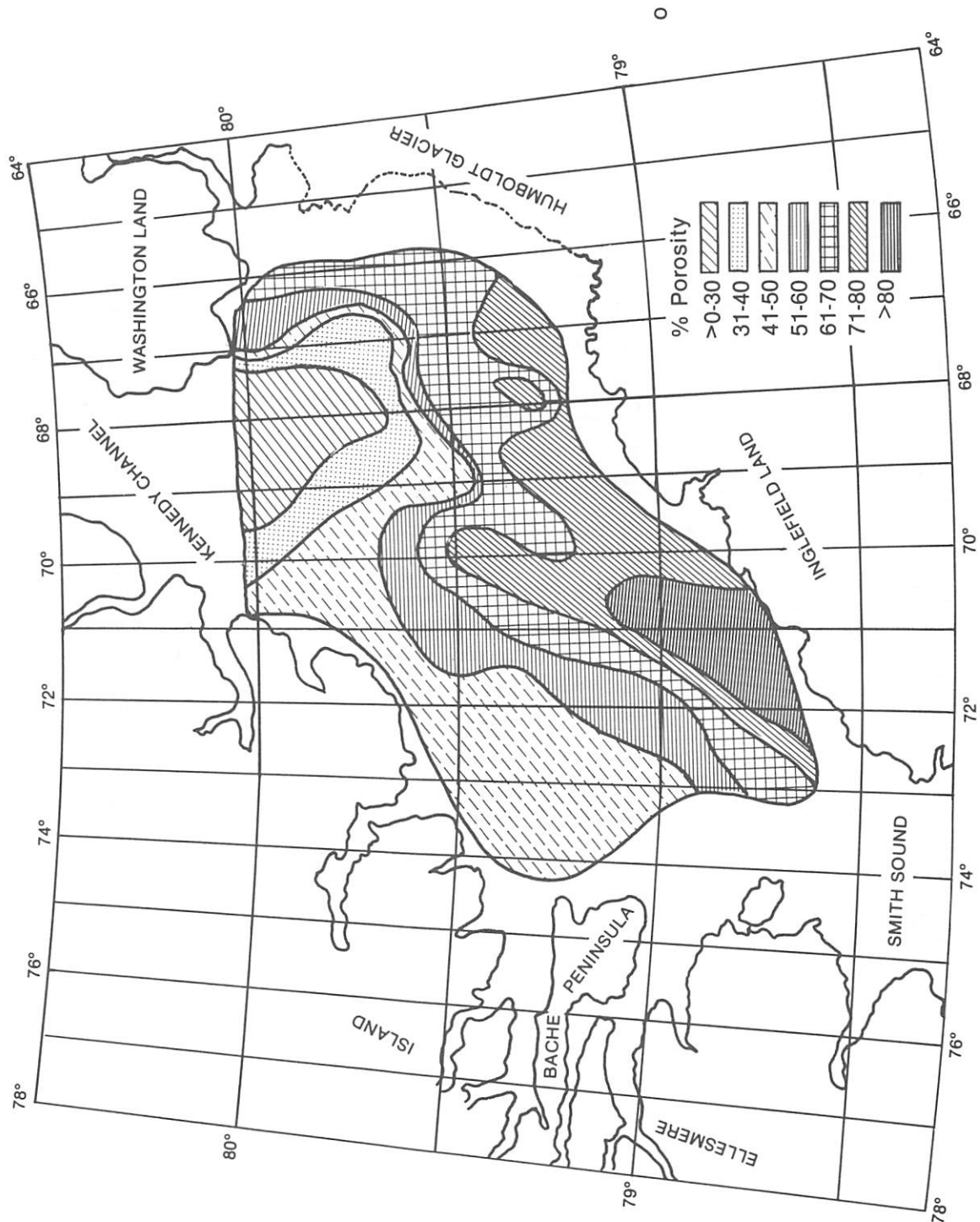
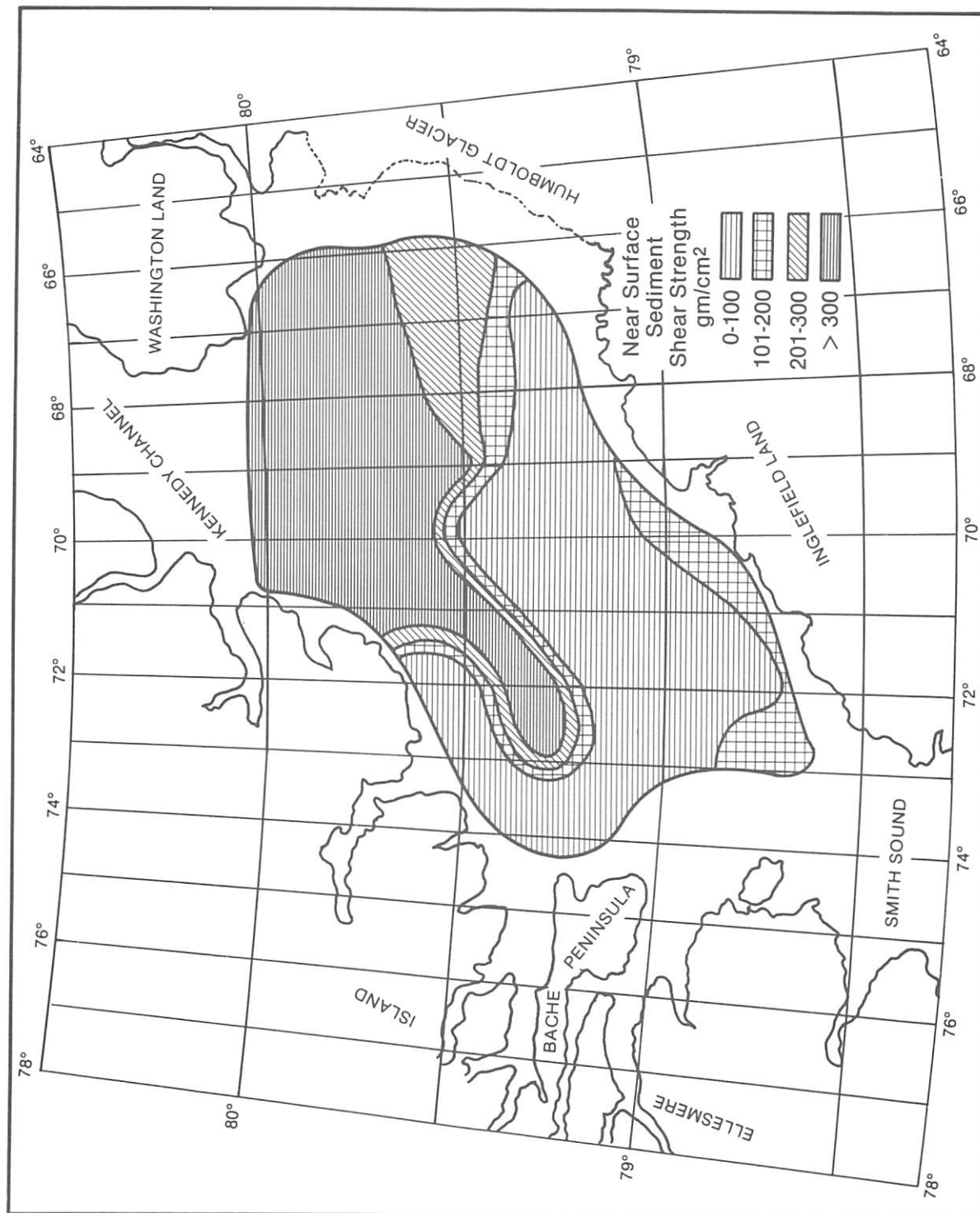


Fig. 14. Univariate map showing near surface sediment shear strength in Kane Basin.



Strengths in excess of 300 gm/cm^2^* are assumed values, since the sediment in those areas was too coarse to test with the fall cone, and because the materials were extremely resistant to coring (Kravitz and Sorensen, 1970). Therefore, the following interpretations must be considered no more than broad generalities. The mean shear strength distribution pattern is very similar to the surface shear strength pattern; mean shear strength distribution will not be discussed.

The areas with the highest sediment shear strengths ($> 300 \text{ gm/cm}^2$), and with the greatest resistance to corer penetration, are in the northern part of Kane Basin (Figure 14). This zone of high shear strength extends in a southwesterly direction as far south as Bache Peninsula. It covers the northern and western parts of the topographic high, its northwestern and northeastern slopes, much of the western trough and the northernmost section of the eastern trough. Shear strength decreases to the west, south and east of this zone with the lowest values ($0 - 100 \text{ gm/cm}^2$) in the western, central, and eastern parts of the Basin extending from Cape Louis Napoleon to Buchanan Bay and then to the east as far as Cape Agassiz. Shear strength values increase again ($101 - 200 \text{ gm/cm}^2$) off the coast of Inglefield Land south of Cape Kent, and there is a zone of higher shear strength values ($201 - 300 \text{ gm/cm}^2$) directly off Humboldt Glacier reflecting an increase in the coarseness of the sediment in this area.

Atterberg limits, indices, and activity

Many of the cores (and sediment intervals within cores) were too coarse for Atterberg limit testing; however, it was possible to determine Atterberg limits on 52 samples from 13 cores.

Liquid limit values range from 26 (core 11, 25 cm - 35 cm) to 135 (core 28, 20 cm - 30 cm). Plastic limit values range from 17 (core 17, 73 cm - 83 cm) to 61 (core 28, 45 cm - 60 cm). Plasticity index values range from 8 (core 11, 25 cm - 35 cm) to 88 (core 28, 0 - 20 cm). Cores 14, 21, 22, 28 and 29 have average plasticity indices in excess of 40 (Table 10, Kravitz, 1983) which, according to Burmister (1960) classifies their overall plasticity as very high. The average liquid limit values (Table 4) indicate that cores 5, 17 and 18 have medium plasticity (LL 30 - 50) and cores 14, 19, 21, 22, 23, 28, 29, 30 and 31 have high

* $1 \text{ gm/cm}^2 = .098060 \text{ kilopascals (kPa)}$

TABLE 4
AVERAGE LIMIT, INDEX, AND ACTIVITY VALUES

Core	LL	PL	PI	LI	Ac
5	36*	21*	15*	140	0.50*
11	26*	18*	8*	150	0.15*
14	80	32	48	123	0.85
17	44	20	24	160	0.39
18	39	22	17	310	0.28
19	72	33	39	150	0.75
21	82	35	47	124	0.72
22	72	31	41	120	0.77
23	55	35	20	215	0.49
28	128	53	75	144	1.11
29	95	43	52	142	0.86
30	82	43	39	186	1.05
31	63*	34*	29*	130	0.85*

* Value from single sample

LL = liquid limit
 PL = plastic limit
 PI = plasticity index
 LI = liquidity index
 Ac = activity

(LL > 50) plasticity (Terzaghi and Peck, 1948). The single sample from core 11 (25 - 35 cm) has a liquid limit of 26 and falls into the low plasticity range (LL < 30).

The above categorization pertains to inorganic clays (sediment with little clay-sized organic material present) and since a number of the cores contain at least some organic material the sediments were also classified according to their plasticity characteristics by plotting their liquid limits vs plasticity indices on the Casagrande plasticity chart (Casagrande, 1948). In this chart the A-line represents an important empirical boundary between typical inorganic clays generally above the line and plastic sediments containing organic colloids and typical inorganic silts (sediment with little silt-sized organic material present) and silty clays below it (Figure 15). Terzaghi (1955) demonstrated that the points representing different samples from a geologically well-defined sedimentary deposit will plot in a fairly straight line roughly parallel to the A-line, because of the likelihood of similar mineralogical composition of the clay-size fraction. If the plotted sediment samples are located on different lines or are on opposite sides of the A-line then the character of the sediment differs, implying a change in sediment source and/or some change in the sedimentation process. Using this chart the samples have been classified (see Figure 15 for descriptions of symbols) as:

SC - SF	{ 11(25-35) [11 = core number, 25-35 = sample interval in cm.]
SF - CL	{ 18(150-164), 18(164-170) 5(0-15), 5(30-45), 17(44-54),
CL	{ 17(54-64), 17(73-83), 18(97-107), 19(140-150), 19(180-204)
ML and OL - MN and OH	{ 23(50-60)
CH	{ 14(20-30), 14(40-50), 14(60-70), 19(0-10), 19(10-22), 19(22-30), 19(85-90), 21(12-20), 21(90-110), 21(110-120), 21(130-138), 21(175-182), 21(182-190), 21(210-220), 21(230-240), 22(0-11), 22(18-25), 23(0-10), 28(0-20), 28(20-30), 29(120-130)

$$\text{MH and OH} \quad \left\{ \begin{array}{l} 19(60-70), 21(0-12), 21(40-50), 21(80-90), \\ 21(138-145), 21(155-165), 28(45-60), 28(90-105), \\ 28(165-181.5), 29(0-7), 29(22-30), 29(45-60), \\ 29(75-90), 29(103-120), 30(0-6), 30(12-20), \\ 30(40-50), 30(60-68), 31(0-8) \end{array} \right.$$

The vast majority of the fine grained sediments in Kane Basin, according to the Casagrande (1948) classification, are inorganic clays of high plasticity, or micaceous, fine sandy and silty sediments, elastic silts and organic clays (sediment with clay-sized organic material present) of medium to high plasticity. The terms in this classification are used historically in the engineering literature to refer to a particular position on the plasticity chart and do not necessarily reflect the true composition of the sediment.

Terzaghi (1955) stated that marine clays in their original state have liquidity indices near 100%. When the liquidity index equals 100% the water content equals the liquid limit. Under these conditions the sediment is considered to be normally consolidated, that is it has never been under a pressure greater than the existing overburden load.

In the present study the water content exceeds the liquid limit for all the fine grained sediment, and the liquidity index exceeds 100% (see Table 10), indicating normally consolidated to under-consolidated conditions. There is no discernable decrease in the liquidity index values with depth in core, which is what would be expected in consolidated sediment (Skempton, 1970); for this reason the sediment is believed to be under-consolidated. This is not surprising considering the high rates of sedimentation (Charles Nittrouer, personal communication) in the southern and central Basin and off Humboldt Glacier.

It is widely recognized (Skempton, 1953) that the higher the plasticity index the more pronounced are the colloidal properties of a sediment. Moreover, the colloidal properties of a sediment are contributed largely by the finest particles and, in particular, by the clay fraction. Sediments which may have the same content of clay-sized materials can have widely different plastic indexes, depending on the mineralogical composition of the clay fraction. In these circumstances it would seem logical to assume that the sediment with the higher

Fig. 15. Casagrande plasticity chart with plots of some Kane Basin sediment samples. The symbols used on the chart are defined (Casagrande, 1948) as follows:

SC = Well graded sand with excellent clay binder.

SF = Sand with fine, silty sands, clayey sands, poorly graded sand-clay mixtures.

ML = Silts (inorganic) and very fine sands, rock flour, silty or clayey fine sands with slight plasticity.

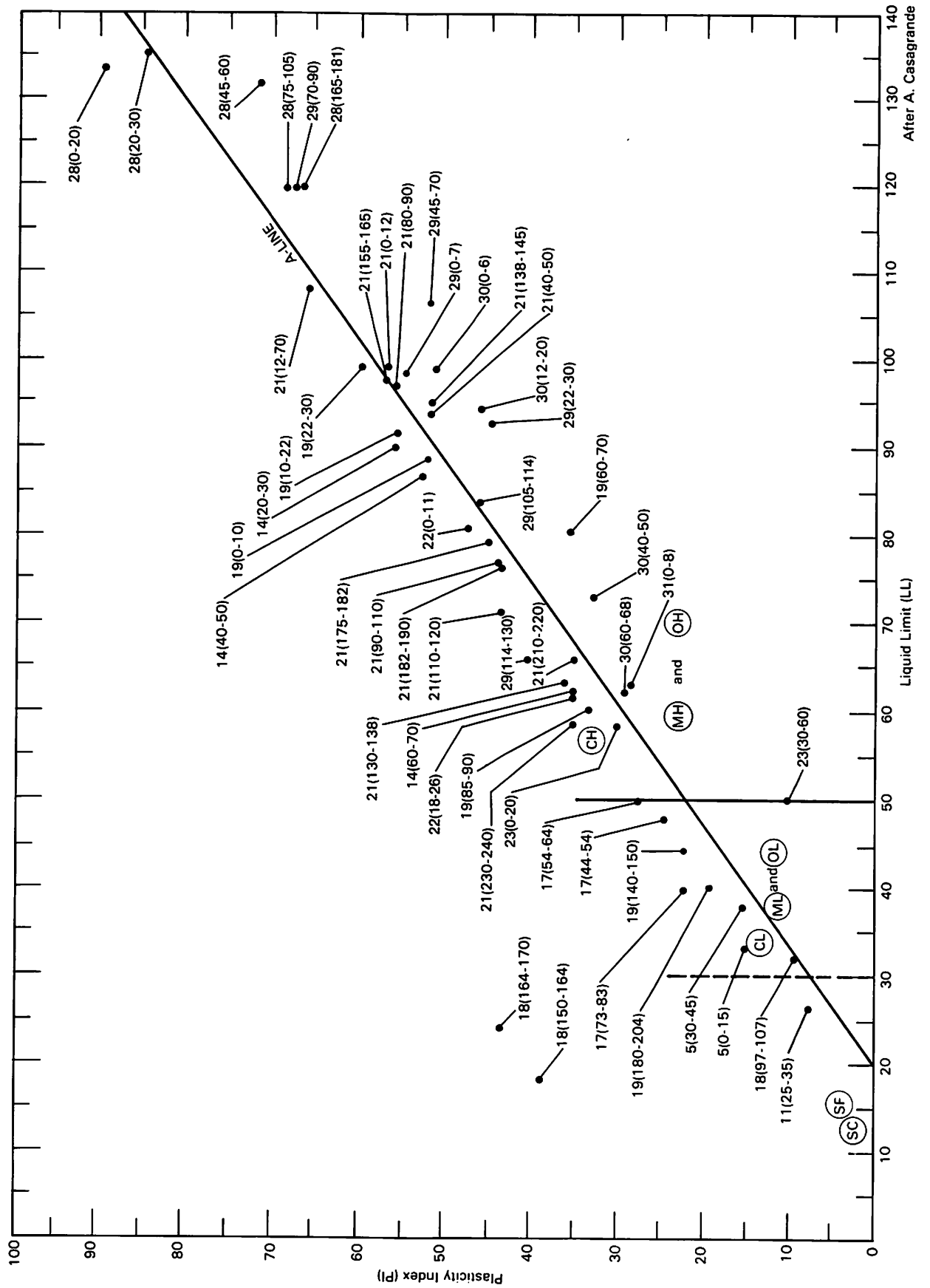
OL = Organic silts and organic silt-clays of low plasticity.

CL = Clays (inorganic) of low to medium plasticity, sandy clays, silty clays, lean clays.

CH = Clays (inorganic) of high plasticity, fat clays.

MH = Micaceous or diatomaceous fine sandy and silty soils, elastic silts.

OH = Organic clays of medium to high plasticity.



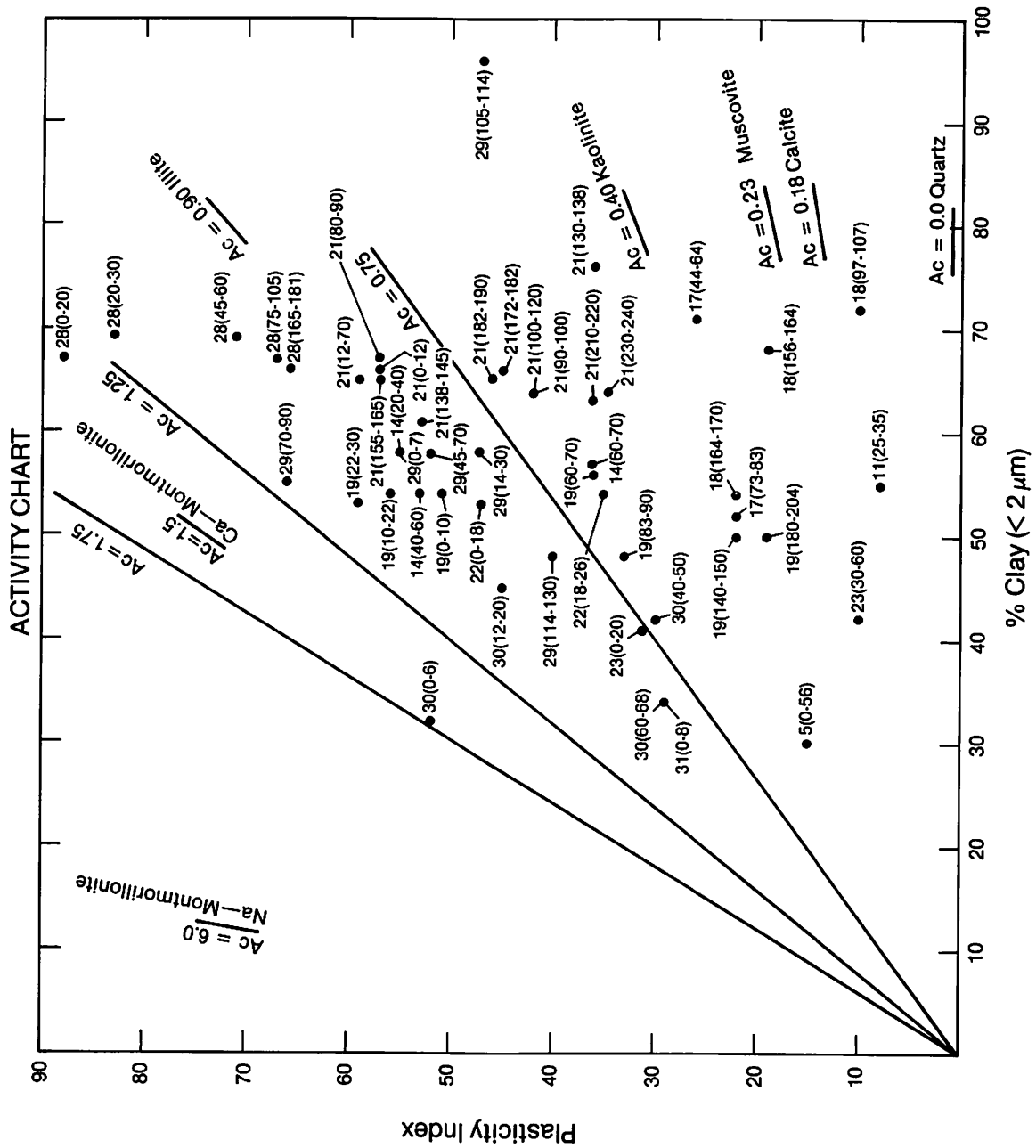
plasticity index, for a given clay fraction content, is more colloiddally active than the sediment with a lower plasticity index, for the same given clay content.

The relationship between plasticity index and clay fraction content for any particular sediment enables the degree of colloidal activity (simply termed, activity) to be expressed by the ratio of plasticity index to % clay fraction (see mass physical properties, Chapter III). Clay fractions containing abundant clay-sized quartz, feldspar, amphibole, calcite, and dolomite will have activities lower than clay fractions composed primarily of the clay minerals (expanding lattice clays, illite, chlorite and kaolinite). It follows that clay-sized materials derived largely by mechanical erosion of non-argillaceous rocks by ice should have low activities. Therefore, activity, as defined here is a sediment parameter useful in ascertaining the degree of influence glacial processes have on the sedimentology of the Kane Basin.

The activity (A_c) values of the fine grained sediments ranged from 0.14 and 0.15 (core 18, 97 cm - 107 cm and core 11, 25 cm - 35 cm respectively) to 1.63 (core 30, 0 cm - 6 cm). Mean activity values for the sediment cores analyzed can be found in Table 4 and interval values within the cores in Table 10. There is a general decrease in activity values with depth down core for cores 14, 19, 21, 22, 23, 28 and 30. Cores 18 and 29 show no discernable trends.

Skempton (1953) classified fine grained sediment (clays) based on their activity values, as inactive, $A_c < 0.75$; normal, $A_c = 0.75$ to 1.25 ; and active, $A_c > 1.25$. Using the mean activity values from Table 4, the sediments in cores 5, 11, 17, 18, 21, and 23 are inactive; and the sediments in cores 14, 19, 22, 28, 29, 30, and 31 are normal. None of the sediments in the cores are classified as active (mean $A_c > 1.25$). The mean activity values of the sediments do not adequately present the range of activity values encountered; therefore, the values determined were plotted on an activity chart, Figure 16. The activity chart was initially developed by Skempton (1953) who mixed quartz sand with individual, relatively pure, clay mineral species. Therefore, the chart should be used with caution when attempting to determine the mineralogical composition of naturally occurring sediments, based on activity

Fig. 16. Activity chart with plots of some Kane Basin sediment samples.



values. These materials contain a wide variety of minerals of differing concentration, all of which have some effect on the sediments activity.

This chart shows the differences in the activity values of the sediments within some of the cores and is an indication that down core variations exist in the nature of the sediments. The findings here strengthen the evidence, provided by the Casagrande A-line plots, that there are different sources supplying sediment to the Basin and/or there are changes in the sedimentation process, over the length of time represented by the analyzed cores. This is evident in the descriptions of the following cores.

All of the tested intervals of core 14 are classified as (CH), inorganic clays of high plasticity; however, the deepest measured interval (60 cm-70 cm) of core 14 has much smaller limits and lower plasticity index than the sediments from the upper part of the core. The material lower in the core is classified as inactive whereas the sediments above have normal activity values.

According to the plasticity chart (Figure 15) core 19 is composed of three distinct sediment types. The lowest measured intervals in the core, 140 cm - 150 cm and 180 cm - 204 cm, are (CL) inorganic clays of low to medium plasticity, sandy clays, silty clays, lean clays, and they are inactive ($Ac < 0.75$). The 85 cm to 90 cm interval is made up of (CH) inorganic clays of high plasticity, and fat clays. This sediment is also inactive ($Ac < 0.75$). Above this interval at 60 cm - 70 cm are (OH) inactive organic clays of medium to high plasticity and (MH) micaceous or diatomaceous fine sandy and silty sediments, elastic silts. The upper part of core 19 (0 cm - 30 cm) is composed of (CH) inorganic clays of high plasticity, fat clays. However, these clays have larger liquid limits and plasticity indices than the sediments farther down the core. They are also more active ($Ac = 0.75$ to 1.25). The sediments in the upper part of the core contain higher organic carbon values than the material farther down core (Table 9), which may account for their greater liquid limit values.

Core 21 is composed almost equally of (CH) inorganic clays of high plasticity, and (MH) micaceous or diatomaceous fine sandy and silty soils, elastic silts and/or (OH) organic clays of medium to high plasticity. From 175 cm to 240 cm the sediment is dominantly CH and

inactive. Above this interval to 138 cm the sediment is classified as MH/OH and has normal activity. From 138 cm upward to 90 cm the material is classified as CH and is inactive. Between 80 cm - 90 cm the sediment is again MH/OH and normally active. It then becomes CH and normally active up to 12 cm. The top of the core is MH/OH and normally active. We can see the previously discussed pattern occurring in core 21 even though CH and MH/OH sediments alternate. The inactive CH sediments, with relatively low liquid limits and plasticity indices, dominate the lower part of the core while the occurrence of MH/OH normally active sediments increases upward. From 90 cm to the surface the core consists of normally active CH and MH/OH materials.

Intervals 0 cm - 12 cm and 80 cm to 90 cm in core 21 are also rich in diatoms, with a common to very common abundance.

The apparently homogeneous core 28 is classified as MH/OH with normal activity from 45 cm to the bottom of the core. Above 45 cm the material is classified (CH) inorganic clay of high plasticity and active ($Ac > 1.25$). Below 30 cm diatoms are common to very common. Above 30 cm they are rare to frequent. Most of the sampled intervals in core 28 contain high organic carbon values compared to most other Kane Basin sediments.

The lower portion of core 29 is (CH) inorganic clays of high plasticity and normal ($Ac = 0.75 - 1.25$) activity. The remainder of the core is MH/OH of normal activity except for the 105 cm - 114 cm interval which has a large silt content and is classified as inactive ($Ac < 0.75$). Common to very common abundances of diatoms are present throughout the length of this core (except at the bottom, 130 cm - 140 cm), as are relatively large organic carbon values.

Core 30 is classified according to the plasticity chart as MH/OH down to 68 cm. Below this point the sediment was too coarse for Atterberg limits testing. As regards activity, intervals 12 cm - 20 cm and 60 cm - 68 cm are normal ($Ac = 0.75$ to 1.25); interval 40 cm - 50 cm is inactive; interval 0 cm - 6 cm is classified as active ($Ac > 1.25$). The reasons for these variations in activity are not known. The only core 31 interval measured (0 cm - 8 cm) is also classified as MH/OH. Its activity is normal.

Carbonate and Organic Carbon Content

The carbonate in Kane Basin sediments is predominantly detrital. Its highest concentration ($> 30\%$) in the surficial sediment layer is found along the Ellesmere Island coast extending from Cape Collinson down to Bache Peninsula, covering the westernmost portion of the western trough (Figure 17). The carbonate content decreases in an easterly direction with the lowest concentration ($0 - 10\%$) occurring in a zone stretching in a westerly direction from Humboldt Glacier over the central part of the eastern trough.

Another zone of fairly high carbonate ($21\% - 30\%$) is located off Washington Land and the northernmost tip of Humboldt Glacier. It extends southwest to just beyond 69° W latitude, blanketing most of the northern part of the topographic high and its northeastern slope. At the southwestern tip of this zone there is an area of high ($> 30\%$) carbonate content (core 15). There also is a small zone of fairly high ($21\% - 30\%$) carbonate near Cape Leiper, Inglefield Land.

The organic carbon content of the surface sediment has its greatest concentration ($> 1.0\%$) in two large zones, one in the western Basin, the other in the eastern Basin, as well as a patch in the southwestern part of the Basin (Figure 18). The zone in the western Basin is found between Cape Collinson and Cape Jackson, and extends in a southwesterly direction to approximately $79^\circ 12' \text{N}$. The concentrations of organic carbon decrease to the west, south and east of this zone. The western zone blankets the northernmost part of the western trough, its eastern side, some of the northern topographic high, and a large portion of the central and southern areas of the topographic high.

The area of high concentration on the eastern side of the Basin extends from the Humboldt Glacier along the Inglefield Land coast almost as far south as Cape Leiper, and covers a large portion of the eastern trough. The area of lowest organic carbon concentration ($0 - 0.50\%$) is on the eastern side of Kane Basin located between the zones of high concentration. This low organic carbon zone covers much of the northern part of the topographic high, its northeastern slope and a portion of both the eastern slope of the topographic high and some of the eastern trough. Pockets of equally low organic carbon are found at the mouth of Dobbin Bay and directly off the Humboldt Glacier.

Fig. 17. Univariate map of the distribution of carbonate values in the surface sediment layer.

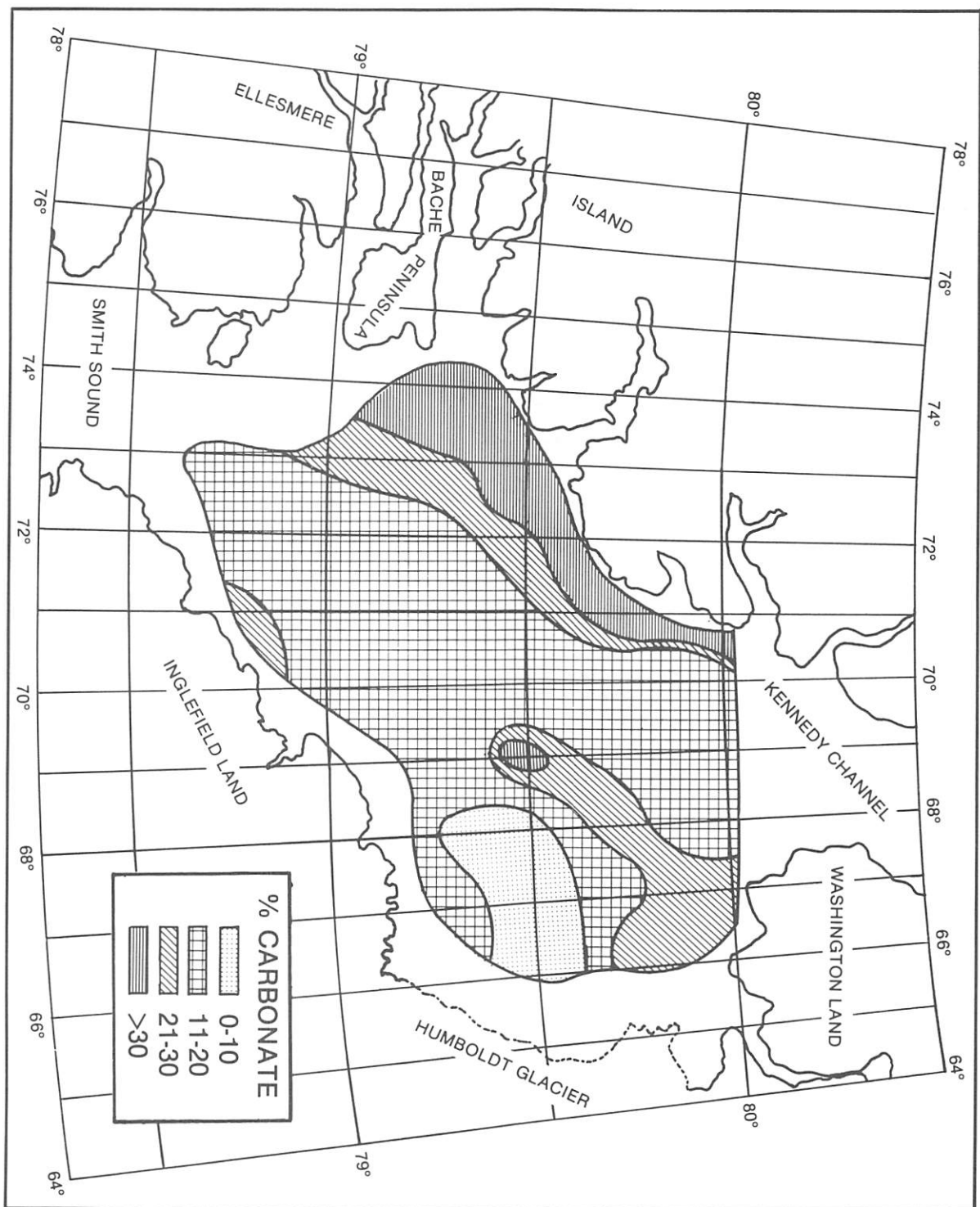
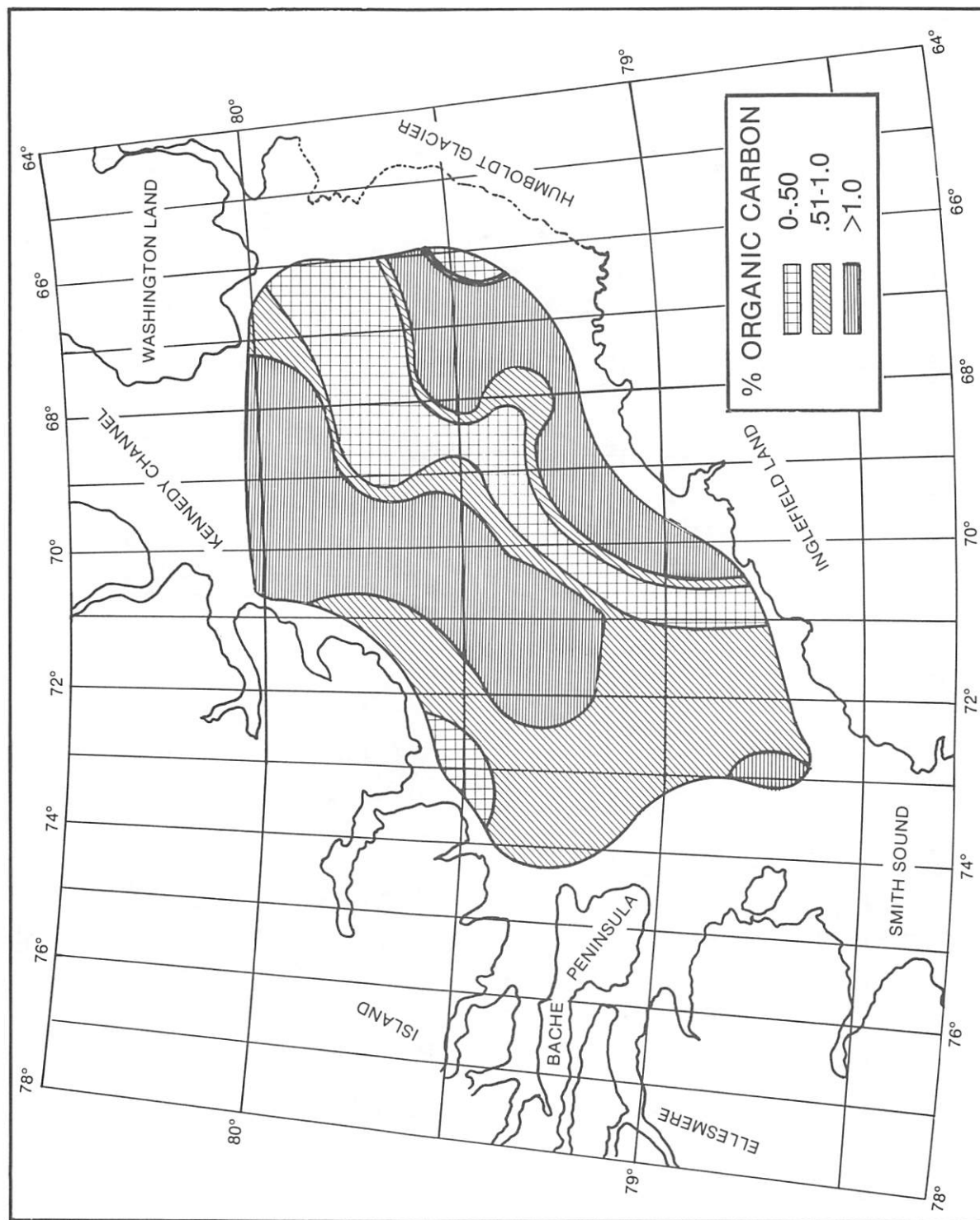


Fig. 18. Univariate map of the distribution of organic carbon values in the surface sediment layer.



Heavy and Light Mineral Composition

A detailed discussion of the mineralogy of Kane Basin's surficial sediment layer is found in Kravitz (1975), however, an abbreviated version is presented here for the sake of completeness.

Non-opaque grains dominate the heavy mineral fractions with opaques, aggregates, and alterites following in decreasing order of abundance (Table 13). In the surficial layer, the greatest percentages (12% - 41%) of aggregates (those particles composed of two or more grains, either monomineralic or polymineralic, including rock fragments), are found in the northern and western parts of Kane Basin, i.e., the area off Ellesmere Island including the northwestern and western topographic high and the western trough. The highest concentration of aggregates is found in a strip covering the northernmost part of the western trough, and the western topographic high from approximately 80°N down to about 79°28'N. The rest of the Basin's surface sediment layer contains very low percentages of aggregates (1-5%). No distinct patterns are present in the surficial distribution of alterites, opaques, and non-opaques. The most abundant heavy minerals are garnet, orthopyroxene, clinopyroxene and amphibole. Apatite, zircon, tourmaline, rutile, kyanite, dolomite, sphene, epidote, staurolite, chlorite, spinel and "other" make up the less abundant minerals. The minerals classified as "other" are mostly unidentified.

The garnets are clear or pink, with some red and yellow grains present. Most are angular to subangular and are fresh in appearance. Some contain inclusions; some are etched or stained. The orthopyroxenes, mostly hypersthene, are angular to subangular, sometimes rounded, with characteristic pink to green pleochroism ranging from strong to weak. In some of the hypersthene, schiller-structure is present. Augite is the dominant clinopyroxene, followed in abundance by diopside and other less common clinopyroxenes. They are angular to subangular with some subrounded grains. A number of the augite grains are marked by fine ruling structure (variety diallage). The amphiboles consist primarily of common hornblende with lesser amounts of blue-green hornblende, oxyhornblende and tremolite-actinolite. The grains are usually elongate, angular to subangular, infrequently rounded, often ragged, and sometimes showing dentate edges.

Of the less abundant minerals, apatite is found in the largest amounts (0.2% - 6%). It is usually subangular to subrounded and fresh in appearance. Very stable minerals such as zircon, rutile and tourmaline are uncommon, and their combined percentages amounts to less than 4% (except core 14) and rarely exceed 3% of the non-opaque mineral fraction. Tourmaline, zircon and rutile frequently appear weathered and are mostly rounded to subrounded with occasional angular grains and with some grains showing crystal faces. The dolomites usually occur as rhombohedra which are often altered. The total percentage of the less abundant minerals never exceeds 24% and frequently makes up less than 10% of the non-opaque suite.

Factor analysis of the heavy mineral component of the surface layer, conducted previously by Kravitz (1975), showed that three reference vectors (factors) explain 99.58% of the variance. Vector I (garnet, orthopyroxene), with a sample variance of 64, is the dominant mineralogic assemblage. Vector II (clinopyroxene) accounts for a significant amount of sample variance (33.10) not explained by vector I. Vector III (amphibole) has a sample variance of only 2.48.

Vector I is dominant in the surficial sediments of the northeastern, eastern, central and southern Kane Basin. The vector is strongest off Humboldt Glacier and northeastern Inglefield Land, and extends westward as far as the western edge of the topographic high. The loading values decrease to the southwest along the Inglefield Land coast, and northward in the direction of Washington Land (Kravitz, 1975). Along the western part of the topographic high is a zone where mixing of vector I and vector II minerals occur.

Vector II dominates the western part of Kane Basin. This includes the entire western trough and northwestern and southwestern parts of the topographic high. Vector II is more dominant than vector I in the zone of mixing previously referred to. Vector II is insignificant in other areas of Kane Basin.

The greatest effect of vector III occurs south of Washington Land along the northern topographic high and, to a lesser extent, in an easterly trending lobe off Dobbin Bay and Darling Peninsula. Vector III has little influence in the rest of the Basin.

The sample variance that vector III accounts for is so minimal (2.48) that it is probably mostly noise and might be disregarded. However, its largest values are clustered in two locations (especially south of Washington Land) and this may indicate some geological significance.

The light minerals present are mostly quartz, feldspar and detrital calcite. Occasional shell fragments, foram tests, diatoms, mica, pieces of coal, plant material, and aggregates also are present, usually in amounts of < 10%.

Quartz is generally angular to subangular, and contains inclusions (bubble trains, rod-like inclusions, acicular inclusions). Staining is common and some of the grains are corroded and round. A small number of composite grains occur in all samples. A few grains had a wormy appearance and may be myrmekite.

The feldspars are dominantly plagioclase with the potassium feldspars less common. Much of the feldspar is sericitized and some grains show a cloudy alteration (vacuolization or kaolinization?). Twinning, when present, is usually of the albite type. Some of the feldspars are stained and are usually subangular to subrounded.

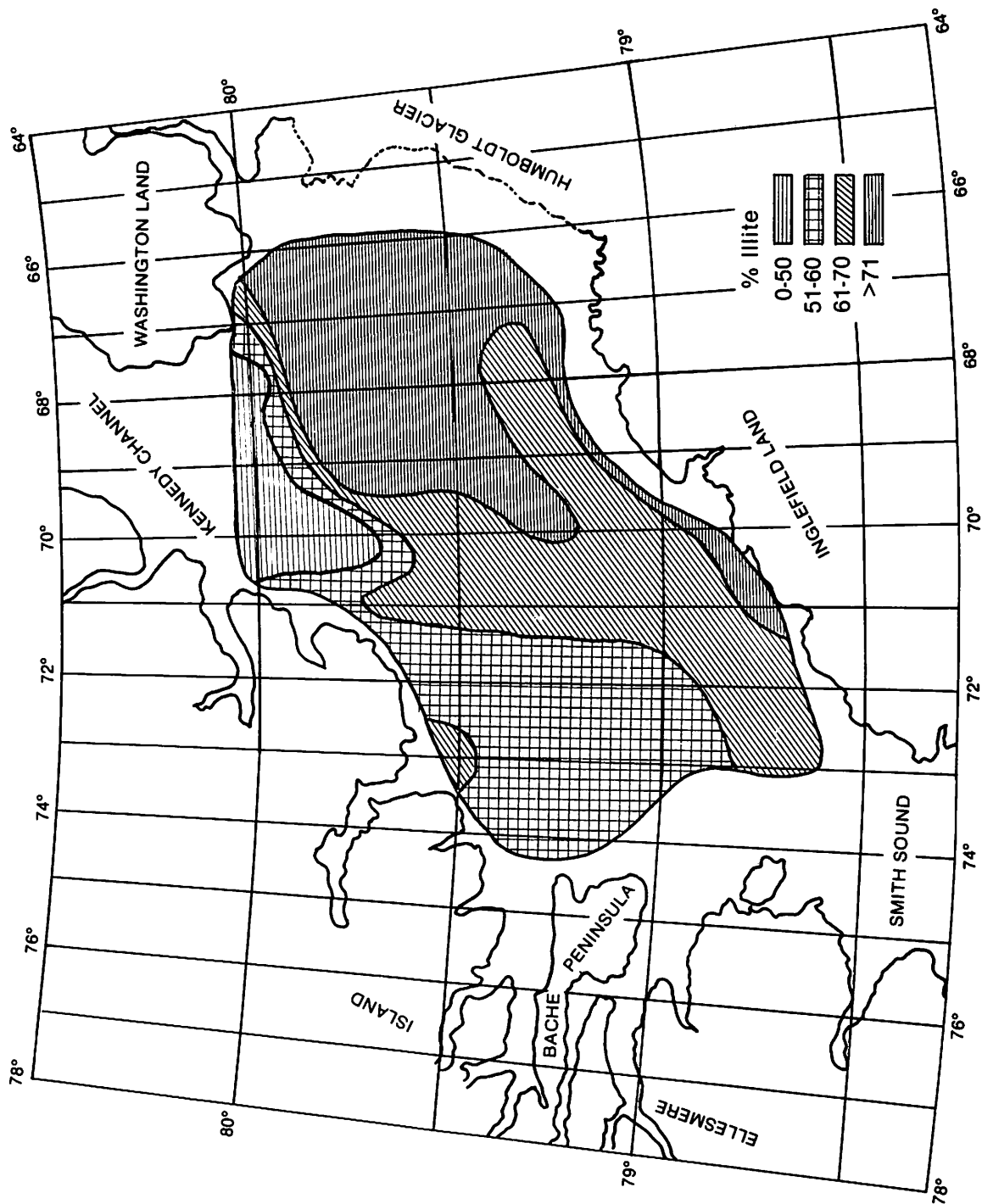
Some calcite and dolomite grains are rhomb shaped but they more commonly occur as subangular to subrounded grains. Many appeared altered. The samples containing the highest calcite and dolomite percentages in the surficial layer are usually samples whose gravel fractions contain carbonates as the dominant rock type. Coal was most abundant off Ellesmere Island and plant fragments are common near Inglefield Land. Foram tests are found primarily on the eastern side of Kane Basin.

The Mineralogy of the < 2 μ m Sediment Fraction

Surface distribution

Illite is the most ubiquitous and abundant clay mineral found in Kane Basin. It has its greatest surface concentration (> 70% of the clay mineral fraction) in the eastern part of the Basin off Humboldt Glacier and in a narrow strip just off Inglefield Land (Figure 19). This includes the northern part of the topographic high, its

Fig. 19. Univariate map depicting distribution of illite in the surface sediment layer.



northeastern slope and the northern part of the eastern trough. This zone of high illite concentration extends in a southwest trending lobe midway down the topographic high and then down onto its eastern slope.

Illite content in the sediments decreases to the west and northwest. Its lowest concentration ($\leq 50\%$) is found along the 80° parallel between Washington Land and Ellesmere Island, just south of Kennedy Channel. The area of low concentration extends as a lobe-shaped zone essentially confined to the western trough, south to approximately $79^\circ 45'N$.

The second most plentiful clay mineral group is the expanding lattice clays, whose highest concentrations ($> 20\%$) are found along the length of the western trough from Kennedy Channel to Smith Sound (Figure 20). They decrease in abundance to the east and west with their lowest concentrations ($0 - 10\%$) in the eastern part of the Basin, including the eastern and northern parts of the topographic high, and the eastern trough off Humboldt Glacier. In the eastern Basin there are relatively moderate amounts ($11\% - 20\%$) of expanding lattice clays off Washington Land's Wright Bay, between Cape Jackson and Cape Webster, directly off Humboldt Glacier, and in a zone off Inglefield Land.

The overall pattern is one of north-south trending bands of decreasing concentration on either side of the western trough with slight anomalies in concentration near Inglefield Land, Washington Land and in an isolated patch near Humboldt Glacier.

Kaolinite is the least abundant of the clay minerals occurring in the area. The largest concentrations ($12\% - 57\%$) of kaolinite in the surficial layer are found in a lobe at latitude $80^\circ N$ at the entrance to Kennedy Channel, and in an isolated zone (11%) on the southeastern part of the topographic high (Figure 21). The lowest concentrations ($0 - 5\%$) are found in a zone extending along Ellesmere Island from just north of Princess Marie Bay to Cape Collinson and then eastward in an arc as far as Washington Land's Wright Bay. At this point it trends directly south in a narrow zone, across the topographic high, to approximately $79^\circ 28' N$ latitude. The remainder, and greatest area of the Basin is covered with a surface layer containing between 6% and 10% kaolinite.

The largest percentages of chlorite in the surficial layer ($\geq 16\%$) are confined to a broadly undulating zone extending from just north of

Fig. 20. Univariate map depicting distribution of expanding lattice clays in the surface sediment layer.

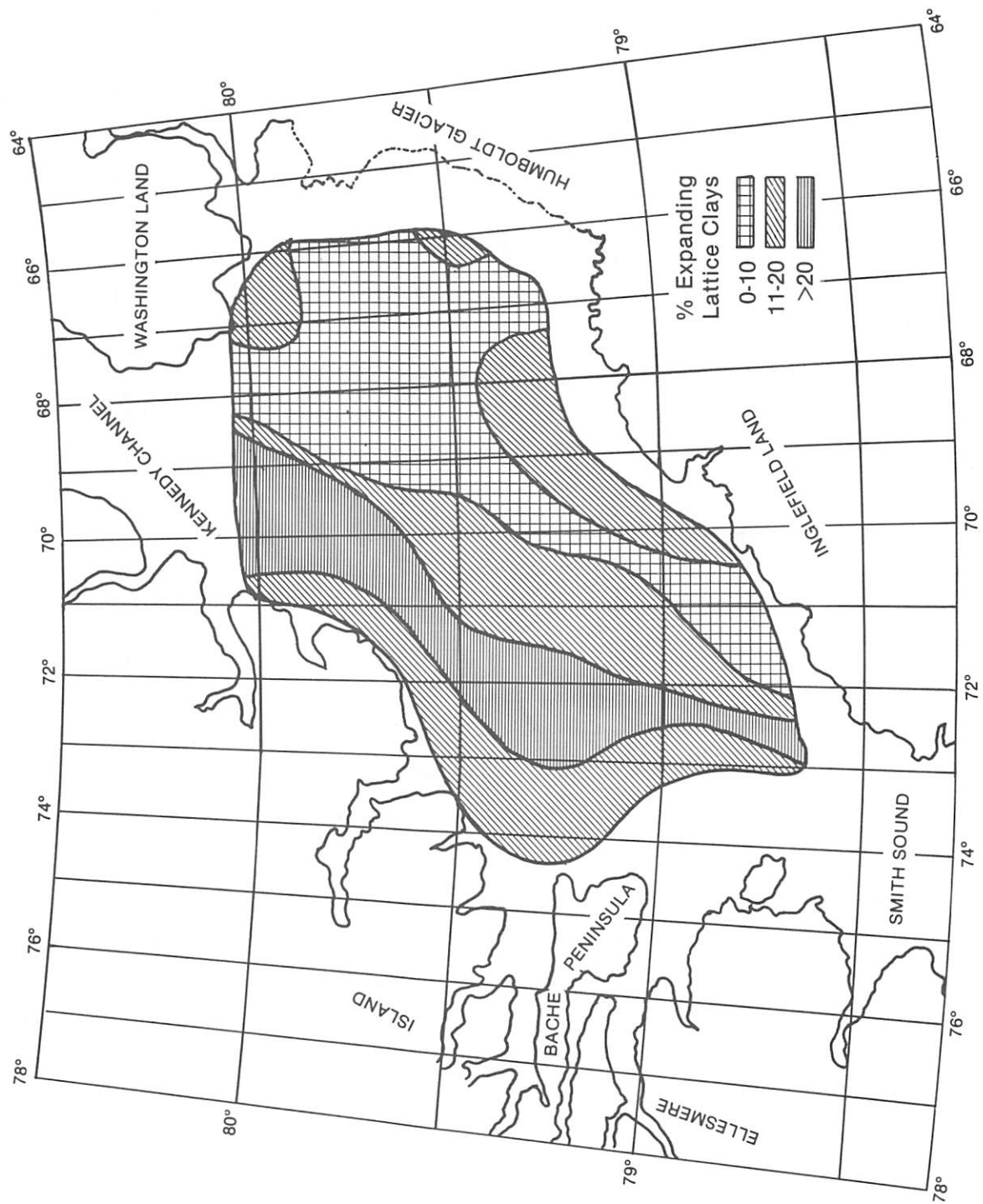
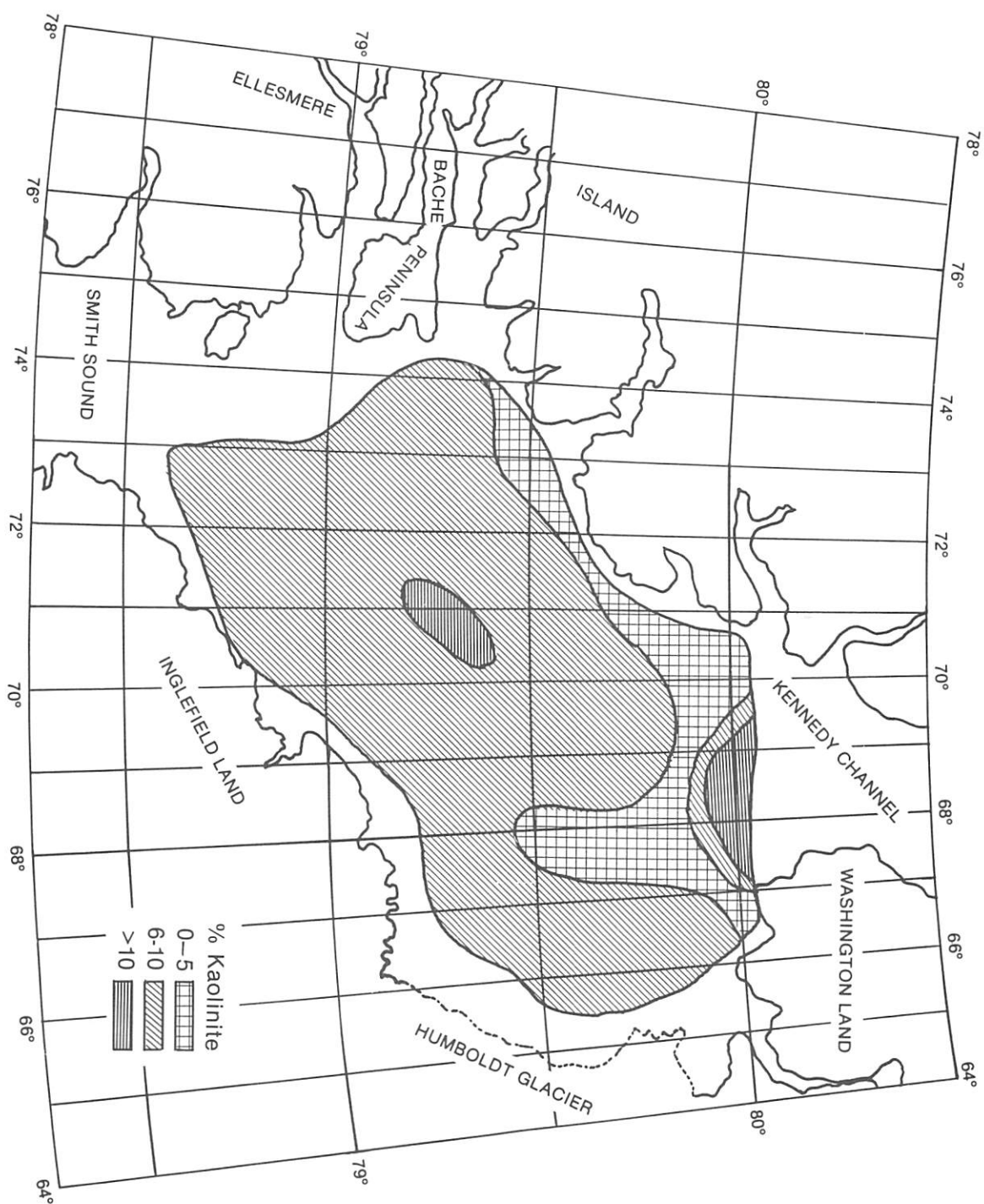


Fig. 21. Univariate map depicting distribution of kaolinite in the surface sediment layer.



Princess Marie Bay along Ellesmere Island to Cape Collinson and eastward to approximately 66°45' W; then trending in a southeasterly direction in a narrow irregular lobe as far as 79°29' N. This zone of high chlorite concentration covers the western and northern part of the western trough, a portion of the northern topographic high down into the northern section of the eastern trough. This corresponds to the area of low kaolinite concentration.

The chlorite values decrease to the north, south and east of this zone with the lowest chlorite concentrations (0% - 10%) in a band near 80°N latitude between Greenland (Washington Land) and Ellesmere Island, a zone off the northern tip of the Humboldt Glacier, and a large irregular zone covering a considerable portion of southeastern Kane Basin off Inglefield Land, which includes much of the eastern part of the topographic high and the eastern trough (Figure 22).

In this study the rock flour component of the < 2 μ m sediment fraction is defined as that portion of this fraction consisting of the carbonate and silicate minerals (excluding clay minerals). The silicates in this case are made up predominantly of quartz and feldspar with minor amphibole. The carbonate minerals are calcite and dolomite. The assumption being made here is that most of these materials occur in the < 2 μ m fraction in the Kane Basin primarily as the result of glacial processes and that their abundance in the clay fraction would be much less in this area if glacial conditions did not exist.

The < 2 μ m fraction was selected to represent rock flour excluding silt, because considerable silt can be produced by other processes in the high arctic i.e. congelifraction (Tedrow, 1968). The inclusion of this size fraction (silt) might mask the effects of glacial action in the production of rock flour.

A rock flour lobe emanates from Humboldt Glacier (Figure 23). Rock flour is relatively abundant in an elongate band along the Ellesmere Island coast from Cape Collinson down to approximately 78°59' N, east of Buchanan Bay.

The lowest concentration (0 - 5%) of rock flour in the surface sediment layer is found off Washington Land in a small area extending from Cape Webster to slightly west of Cape Jackson. This is followed to the west and southwest by a zone of only slightly higher concentration

Fig. 22. Univariate map depicting distribution of chlorite in the surface sediment layer.

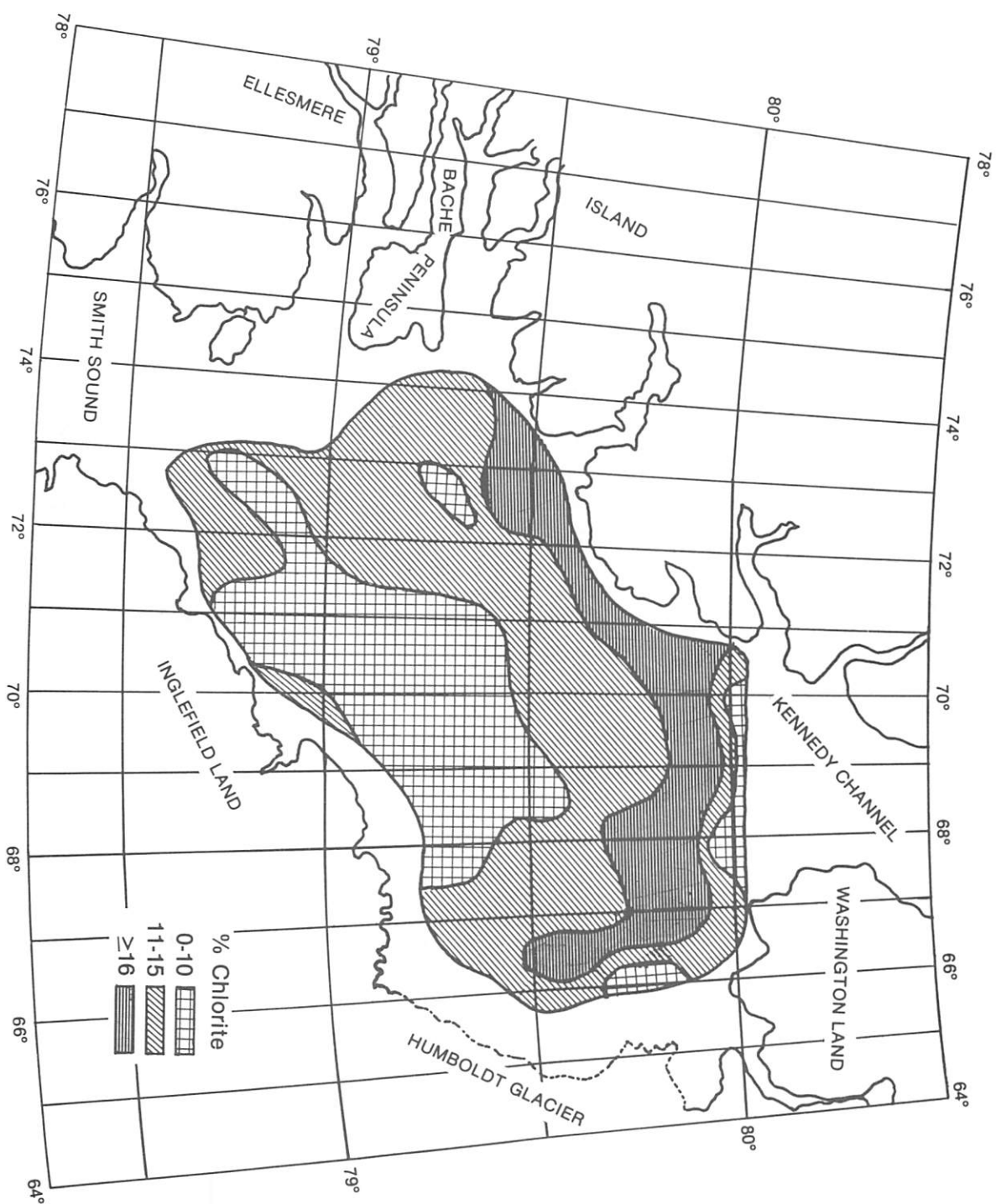
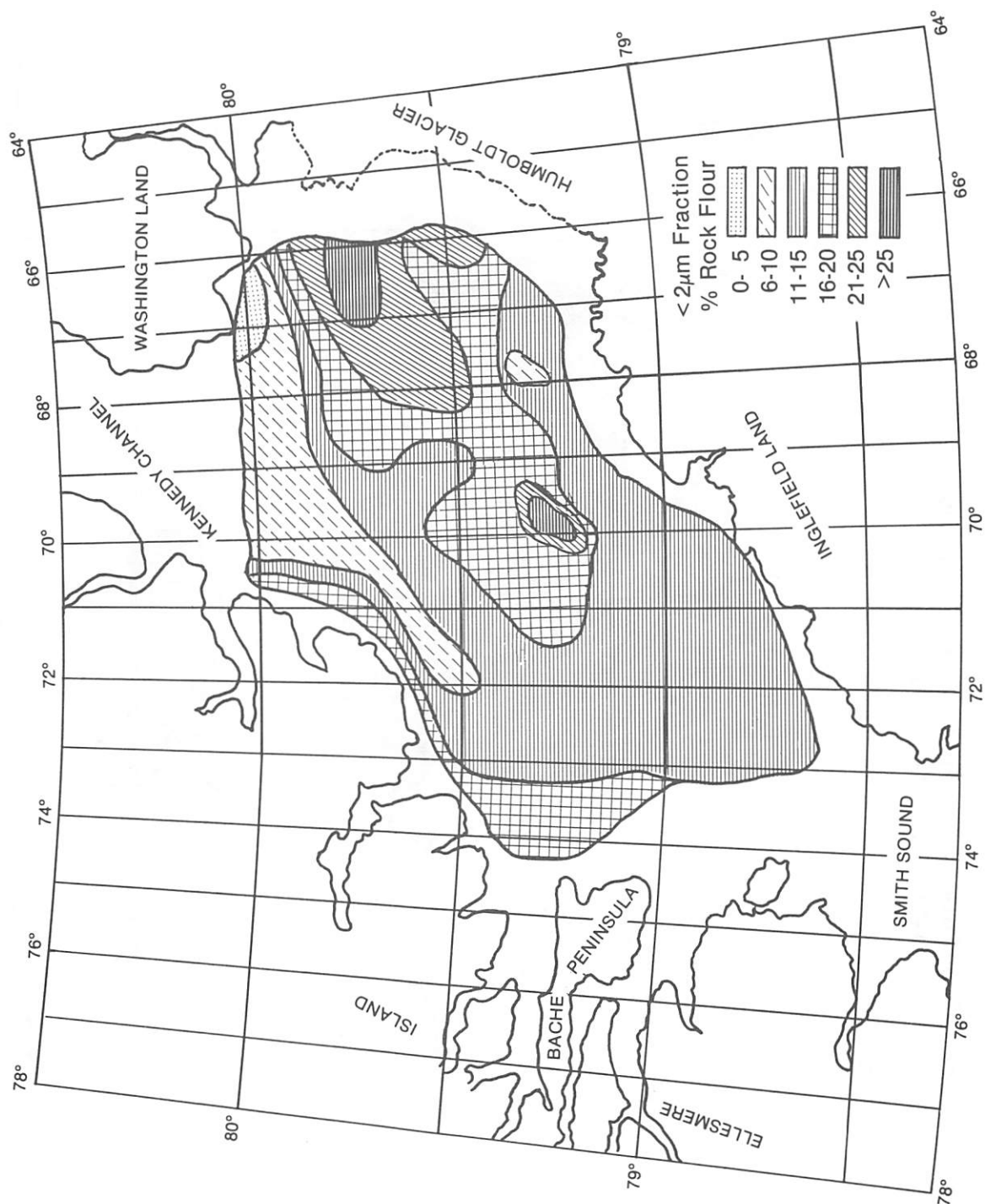


Fig. 23. Univariate map showing distribution of rock flour in the surface sediment layer.



(6% - 10%) which extends almost the width of Kennedy Channel, and then as a thin elongate lobe down into the western trough.

Silicate minerals are the dominant components in the rock flour of the surficial layer of Kane Basin. Their greatest concentration (91% - 100%) is off Humboldt Glacier. Silicates blanket most of the eastern trough and a large portion of the eastern side of the topographic high. They decrease slightly in concentration to the west in northeast-southwest trending zones. The area of lowest silicate content is in the northern and westernmost part of the Basin including a large portion of the western trough (Figure 24).

The carbonate component of the rock flour has its greatest surface sediment concentration (> 40%) in the western and northern parts of the Basin (Figure 25). This high concentration zone extends from Wright Bay to Cape Collinson and then southwestward along Ellesmere Island down to 78°59' N off Buchanan Bay. Carbonate content in the rock flour generally decreases to the south and east; lowest concentration (0 - 10%) occurs in the eastern Basin off Humboldt Glacier and Inglefield Land. As with the silicate rock flour, the zones of concentration trend in a general northeast-southwest direction.

Chemical elements in the < 2 μ m Sediment Fraction

Surface distribution

Core 27, near the southernmost extension of the topographic high (Figure 26), contains the highest concentration of iron (Fe), 140,000 ppm (14%), in the surficial sediment layer of the Kane Basin. The lowest concentrations of Fe occur in core 4 (17,000 ppm [1.7%]) west of Washington Land's Cape Jackson, and in grab sample 26G (16,000 ppm [1.6%]) in the vicinity (just east) of Princess Marie Bay.

From the low values in the northern part of the Basin, the Fe values increase in the form of a series of southwest trending zones which extend over most of the northern topographic high including its northeastern and northwestern slopes. A zone of higher Fe content (61,000 to 80,000 ppm [6.1% - 8.0%]) surrounds these lobes on the east, south and west including large portions of the eastern and western troughs. This zone extends to the southwest along the central part of

Fig. 24. Univariate map showing distribution of silicates in rock flour from the surface sediment layer.

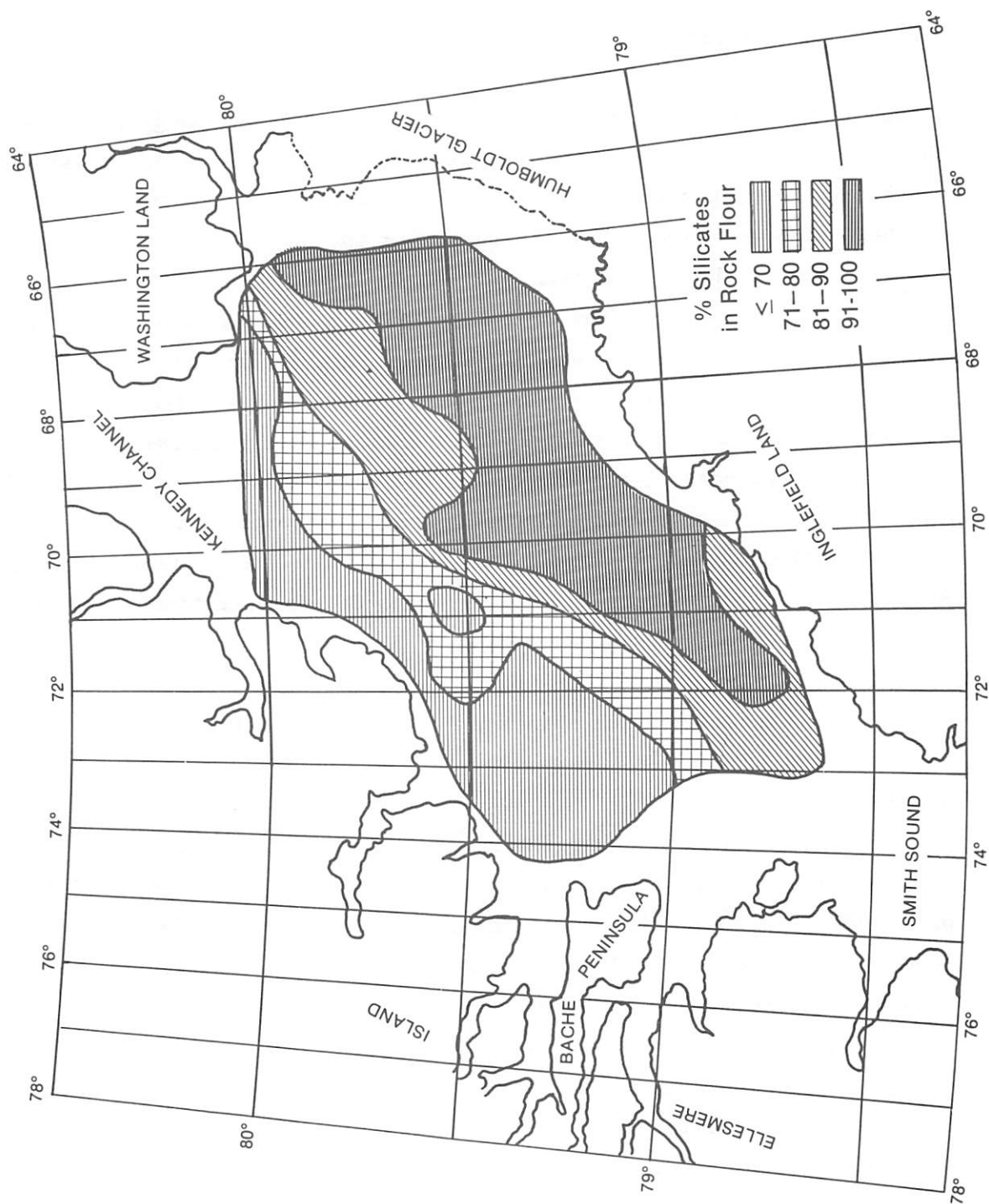


Fig. 25. Univariate map showing distribution of carbonates in rock flour from the surface sediment layer.

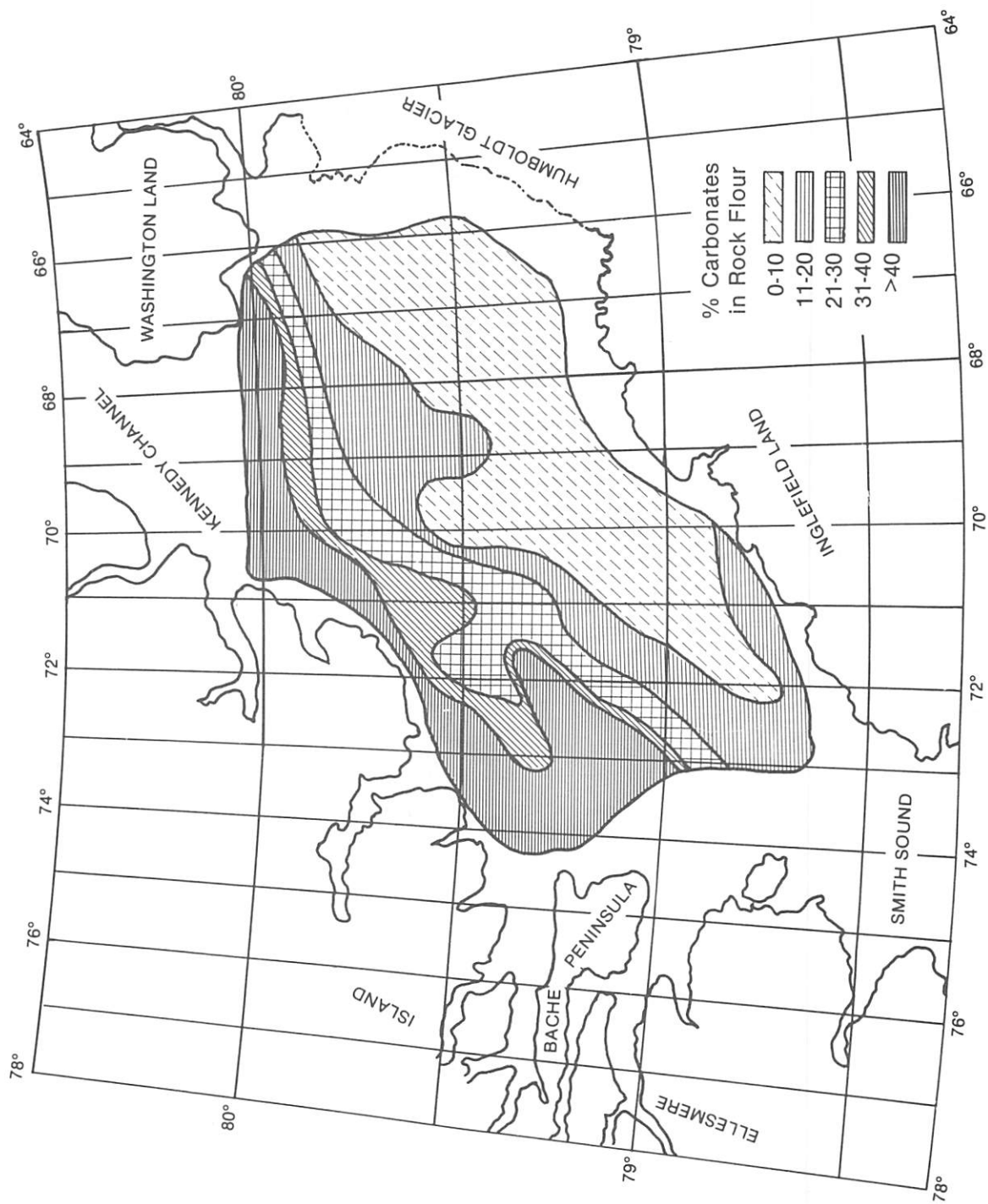
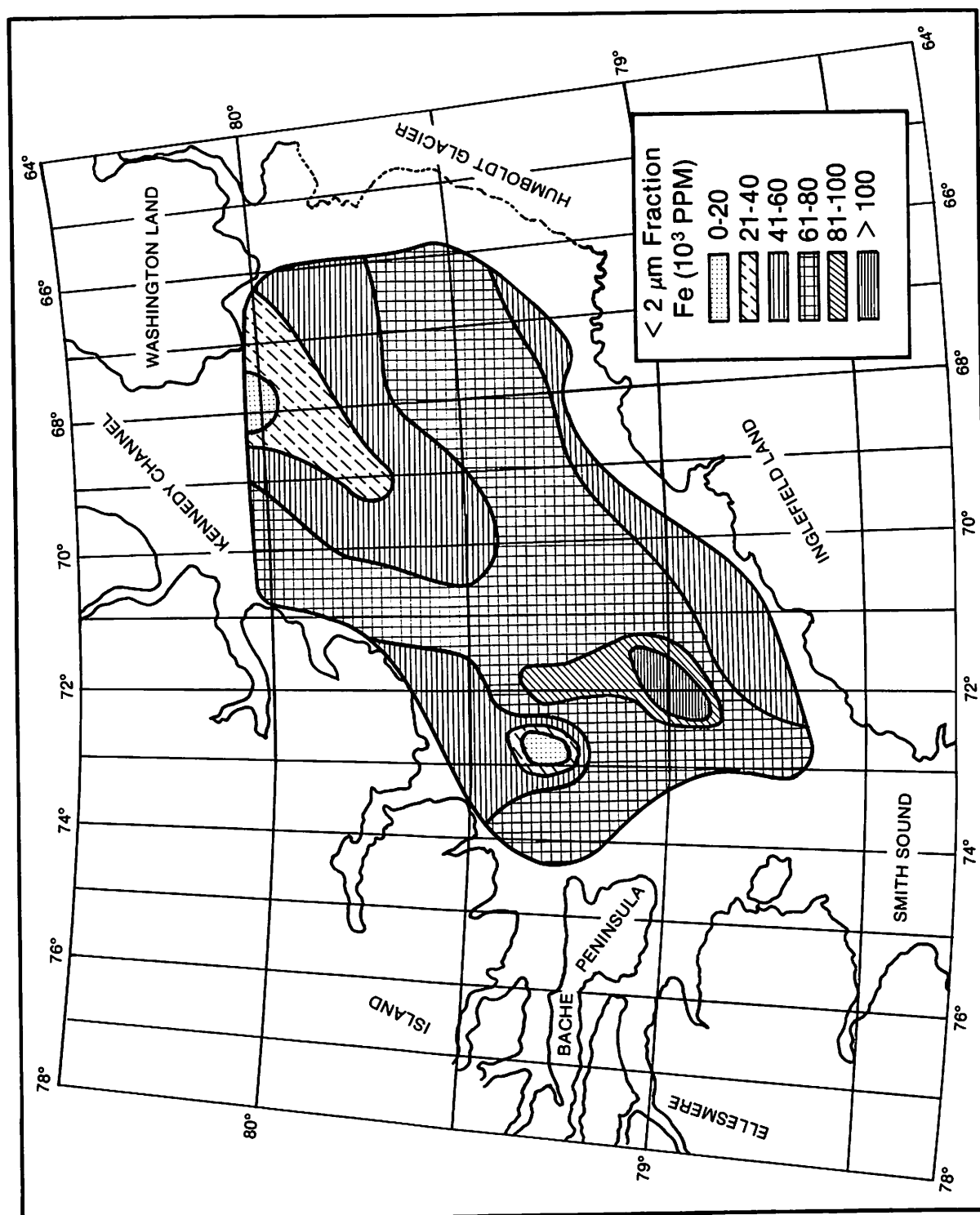


Fig. 26. Univariate map showing distribution of Fe in the $< 2 \mu\text{m}$ fraction of the surface sediment layer.



the topographic high covering most of the Basin except for a strip of lower Fe content (41,000 to 60,000 ppm [4.1% - 6.0%]) along the Inglefield Land coast. A zone of similar and lower concentration extends south from Dobbin Bay.

The regional trend of magnesium (Mg) in the surface layer shows high concentrations in the western Basin decreasing to the east (Figure 27). The highest concentrations of Mg are present as patches on the map surrounded by sediment with lower Mg values. These high concentrations are in core 2 (38,000 ppm [3.8%]) in the northwesternmost part of Kane Basin off Ellesmere Island near Cape Collinson; core 12 (40,000 ppm [4.0%]) south of Cape Louis Napoleon, Ellesmere Island; core 27 (38,000 ppm [3.8%]) at 79° N and 72° W, the site of the highest Fe content in the surface layer; and core 15 (36,000 ppm [3.6%]) located at approximately 79°30' N and 69° W near the axis of the topographic high. The first three high Mg areas are located in a broad zone of relatively high Mg content (31,000 - 35,000 ppm [3.1% - 3.5%]), which extends along the Ellesmere Island coast from Cape Collinson to just northeast of Pim Island. This zone covers the western trough, and most of the western slope and the southern tip of the topographic high. Directly to the east of this zone is a zone of lesser Mg concentration (26,000 - 30,000 ppm [2.6% - 3.0%]) followed by another zone of still lower Mg concentration (21,000 - 25,000 ppm [2.1% - 2.5%]) which occurs off Humboldt Glacier and the Inglefield Land coast. This easternmost zone covers much of the eastern trough.

The least Mg is in core 4 (9,900 ppm [0.99%]) which also has a relatively low Fe content. This sample is located just west of Cape Jackson, Washington Land. There is an obvious relationship between Mg (Figure 27) and carbonate (Figure 17). Stations 2, 12 and 15 also have high carbonate contents. The western Basin along Ellesmere Island has greater concentrations of both Mg and carbonate than the rest of the Basin.

Manganese (Mn) concentrations in the surface layer decrease from west to east in NE-SW trending zones with the highest concentrations (> 400 ppm) found along the Ellesmere Island coast extending from Cape Collinson down to Cape Hawks (Figure 28). This zone and the zone of slightly lower concentrations (301-400 ppm) directly to the east cover

Fig. 27. Univariate map showing the distribution of Mg in the $< 2 \mu\text{m}$ fraction of the surface sediment layer.

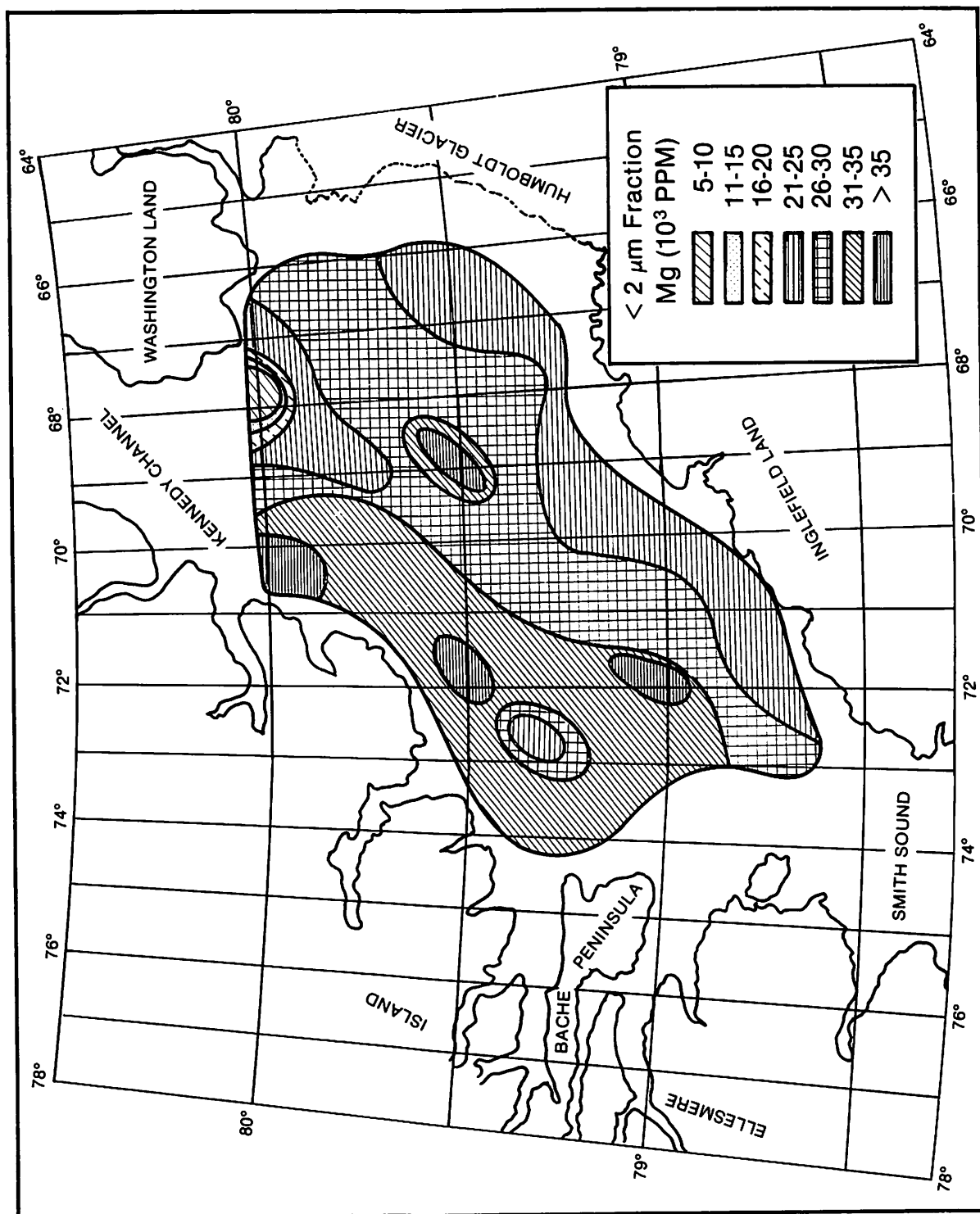
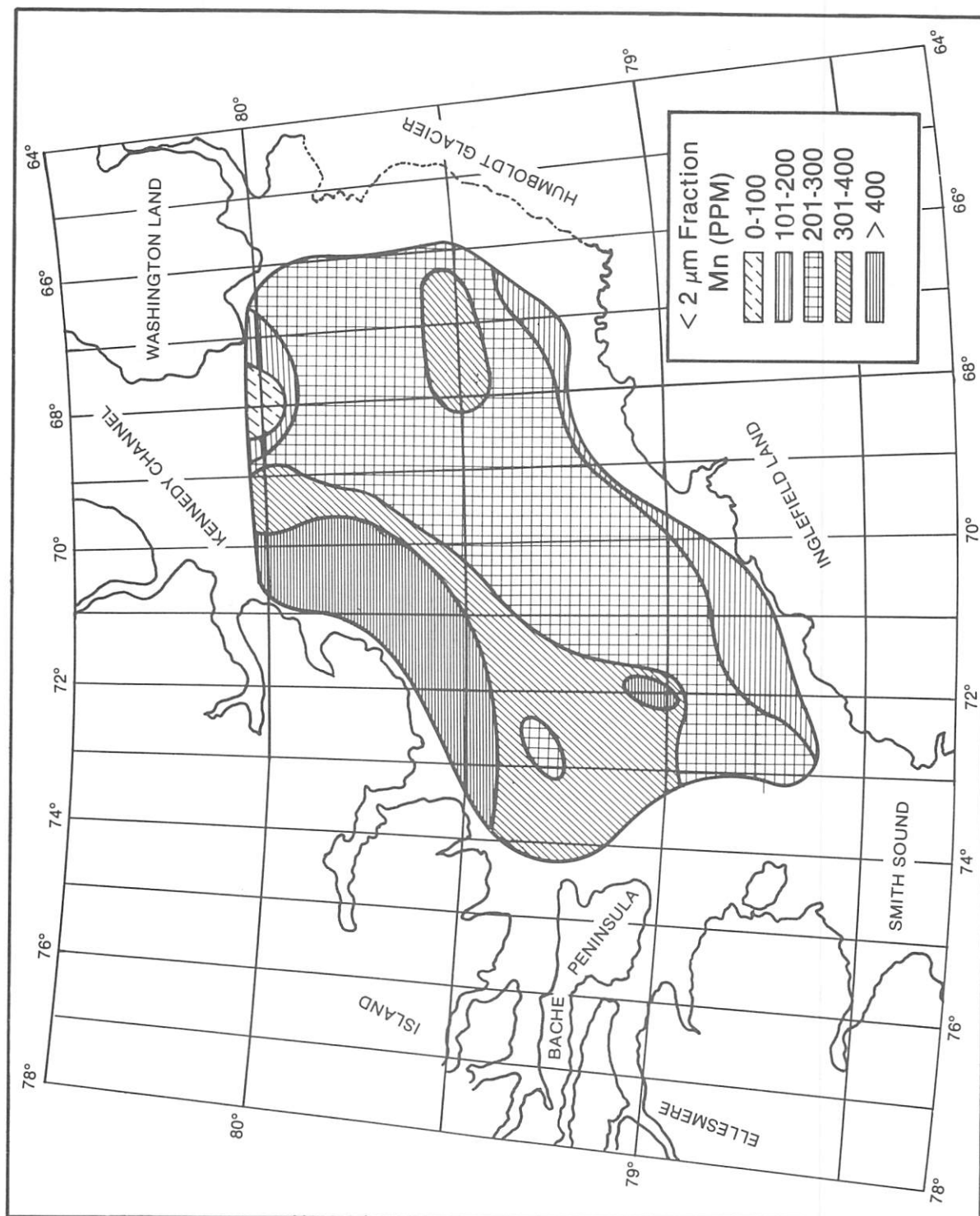


Fig. 28. Univariate map showing distribution of Mn in the $< 2 \mu\text{m}$ fraction of the surface sediment layer.



the western part of the Basin. The area of lowest concentration (core 4, containing 50 ppm Mn), is located along the northern part of the topographic high. Core 27 once again shows a high elemental value in its surface layer (Mn, 440 ppm) as was the case for Fe and Mg. Along the Inglefield Land coast and off the lower part of Humboldt Glacier is a narrow zone of low Mn concentration (101 - 200 ppm), its greatest seaward extension occurring off Cape Ingersoll. Concentrations of Fe and Mg also are low in the sediments of this zone.

The highest concentration (250-300 ppm) of chromium (Cr) is found in the western trough along its axis, extending from Darling Peninsula down below Cape Hawks (Figure 29). From this zone of high concentration, Cr content in the sediments decreases to the north, south, east and west; however, the largest amounts (151 - 300 ppm) of Cr are still confined to the western trough and to the southern part of the Basin.

The smallest amounts of Cr in the Basin's surface layer are found in core 4 (37 ppm) off Washington Land; in a southwest trending zone (51 - 100 ppm) covering the northernmost part of the topographic high, its northwestern slope and a northern section of the eastern trough; and in a strip (51 - 100 ppm) extending along the Inglefield Land coast from Cairn Point in the south just north of Cape Agassiz next to Humboldt Glacier.

The largest amounts of cobalt (Co) are found, as with most of the previous elements, in the western part of Kane Basin. In the case of Co the greatest concentration (> 100 ppm) is in a broad area extending from Cape Collinson, Ellesmere Island, in a series of zones of diminishing concentrations, as far south as approximately 78°50'N. These zones cover a large portion of the western trough (Figure 30). The lowest concentration of this element is in a small area directly to the south and west of Washington Land, with core 4 once again having the lowest concentration (18 ppm) of the surface sediment layer.

Core 10 off the Darling Peninsula contains the largest nickel (Ni) content (320 ppm) of the Kane Basin surface sediment. The next highest Ni content (201-250 ppm) is located in a strip stretching in a south-westerly direction from approximately 81°N to about 79°10'N and then eastward as far as the Inglefield Land coast north of Cape Leiper (Figure 31). This zone appears to run along and parallel to the western

Fig. 29. Univariante map showing the distribution of Cr in the $< 2 \mu\text{m}$ fraction of the surface sediment layer.

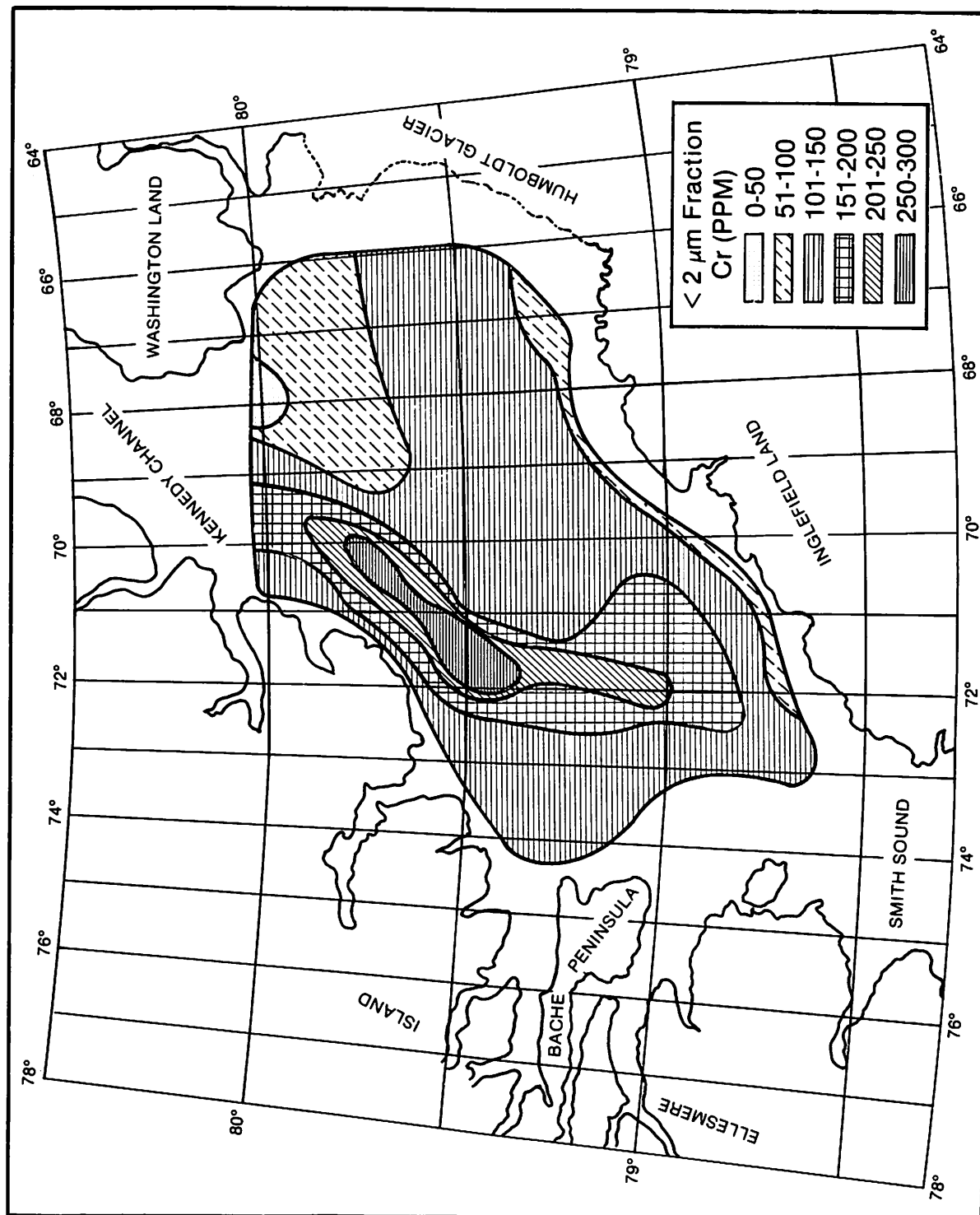


Fig. 30. Univariate map showing the distribution of Co in the $< 2 \mu\text{m}$ fraction of the surface sediment layer.

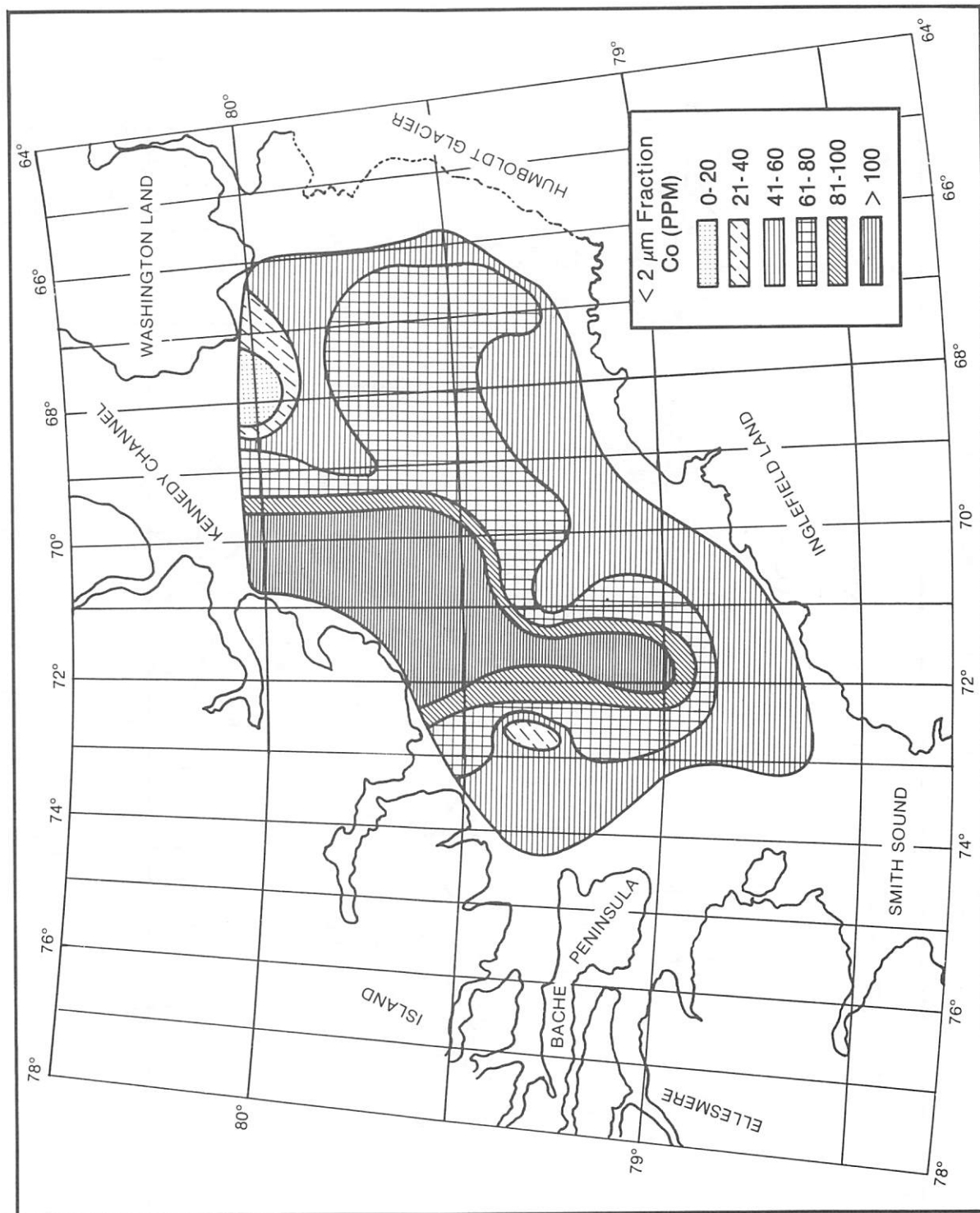
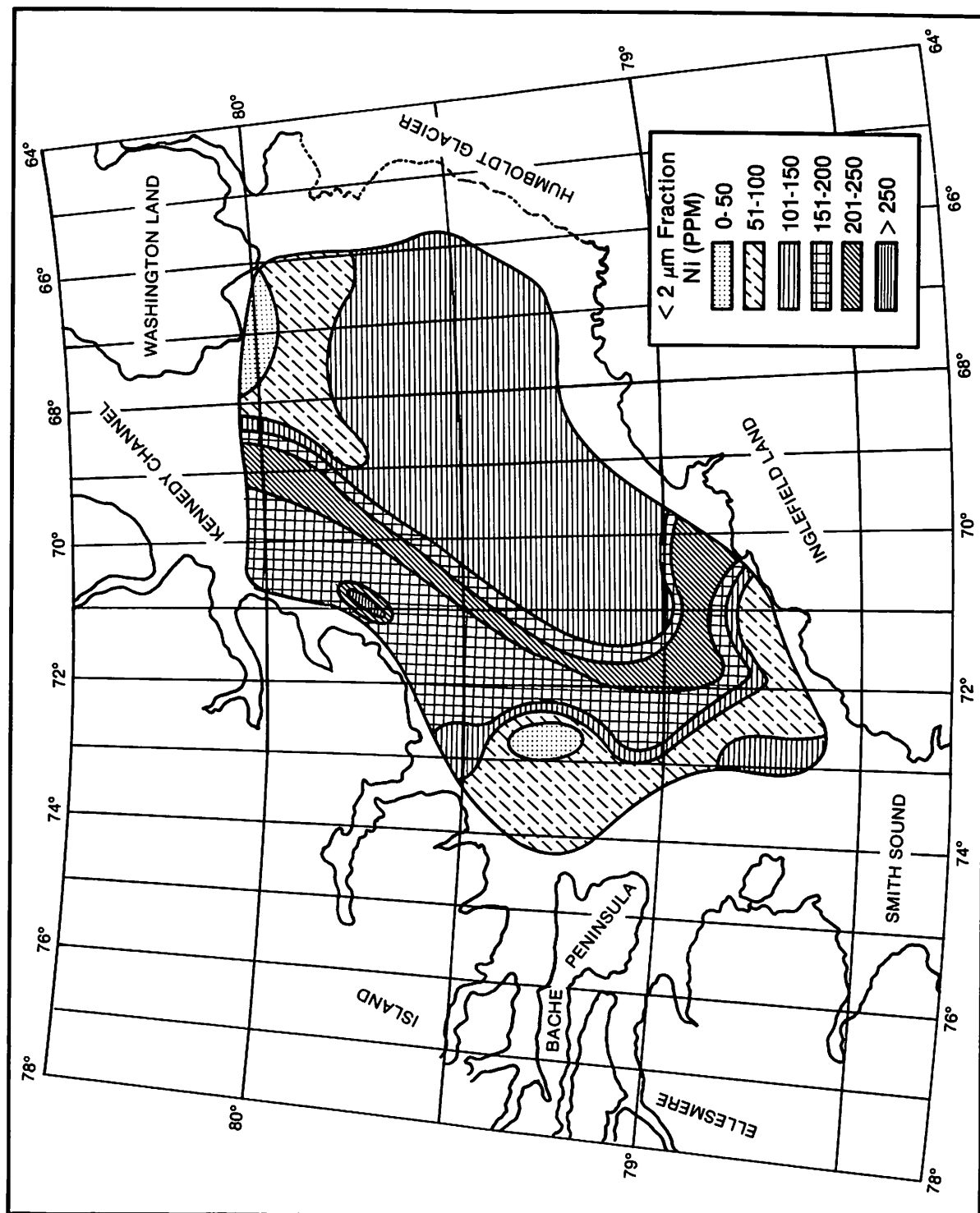


Fig. 31. Univariate map showing the distribution of Ni in the $< 2 \mu\text{m}$ fraction of the surface sediment layer.



slope of the topographic high, cutting across the south tip of the high in its sweep to the east. The lowest Ni values are found on the northern topographic high (core 4, 52 ppm) accompanied by the usual southwest trending zone of slightly higher (51 - 100 ppm) concentration. The vast majority of eastern Kane Basin contains relatively moderate amounts of Ni.

The maximum amount of zinc (Zn) in the sediment surface layer is found at two locations in the western Kane Basin; the core 30 site (510 ppm) off Darling Peninsula, and the core 27 site (630 ppm). With the exception of these two unusually high values the rest of western Kane Basin has low (101 - 200 ppm) Zn concentration in the sediments relative to the central and eastern areas, where the values generally range from 201 - 300 ppm. An exception to this is a 101 - 100 ppm zone northwest of Cape Agassiz (Figure 32). The lowest Zn content in the surface layer is found in core 4 (73 ppm) west of Cape Jackson, Washington Land.

The distribution of copper (Cu) in the sediment surface samples appears erratic; however, some trends are recognizable. The highest Cu contents are found in core 12 (512 ppm) and core 27 (272 ppm), both located in the western Basin inside a zone of lower (151 - 200 ppm) Cu concentration (Figure 33).

A zone moderately high (201 - 250 ppm) in Cu extends from Cape Collinson south as far as the Inglefield Land coast between Cape Leiper and 70° W longitude. This zone covers the northern part of the western trough, crosses the central topographic high and enters the southern end of the eastern trough. The lowest Cu value in the surface layer is in core 5 (20 ppm) just south of Cape Jackson.

As with most of the previously discussed elements, titanium (Ti) values are greatest in the western part of Kane Basin (Figure 34). The highest values (> 15,000 ppm) are found in a southward trending zone which extends from Cape Collinson to below Cape Hawks and covers most of the western trough in the area. This zone is within another zone of lower (10,000 - 15,000 ppm) Ti values which extends as far south as Pim Island. The lowest Ti values (0 - 5,000 ppm), are found along the northernmost part of the topographic high and extend from Cape Webster west several kilometers beyond Cape Jackson.

Fig. 32. Univariate map showing the distribution of Zn in the $< 2 \mu\text{m}$ fraction of the surface sediment layer.

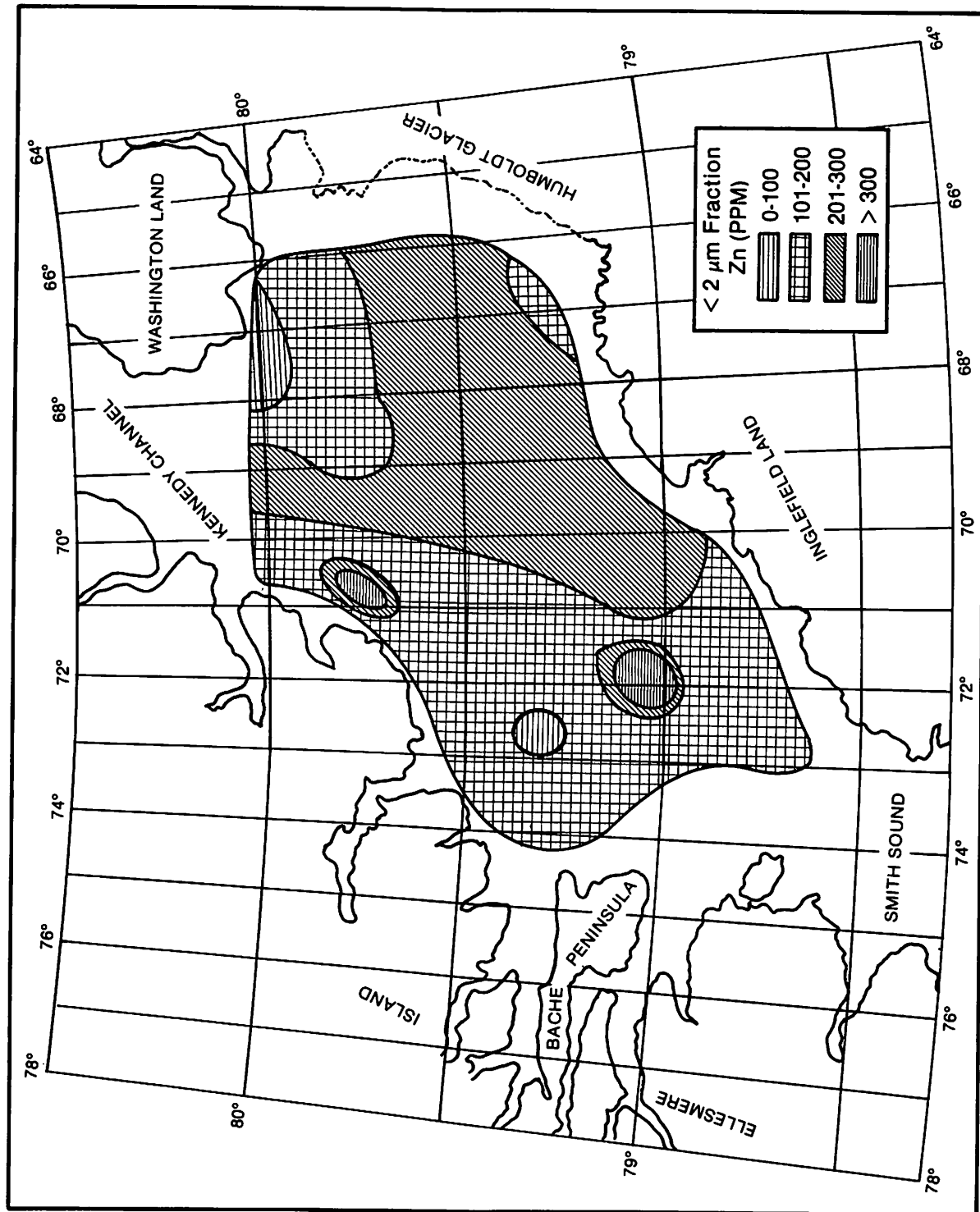


Fig. 33. Univariate map showing the distribution of Cu in the $< 2 \mu\text{m}$ fraction of the surface sediment layer.

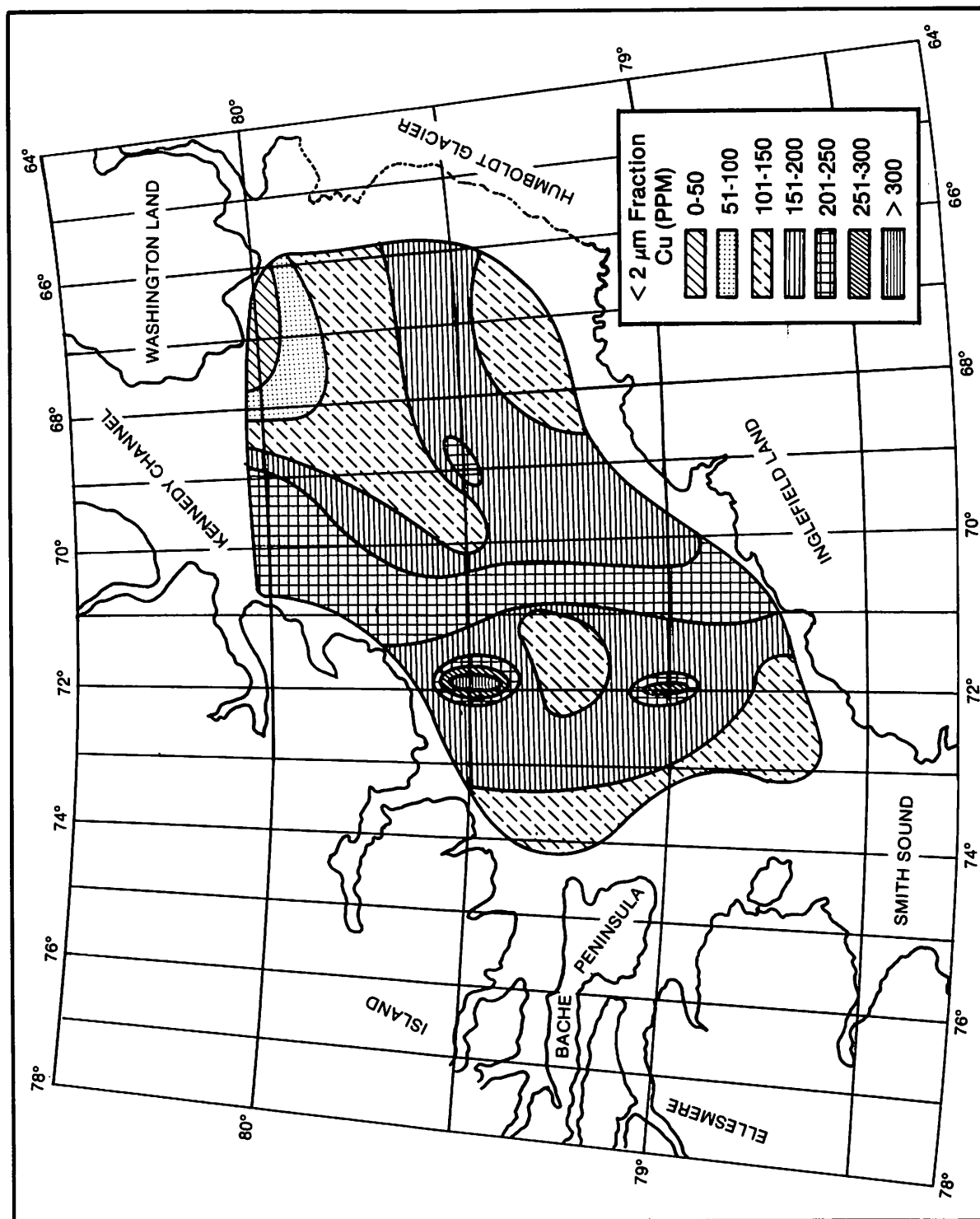
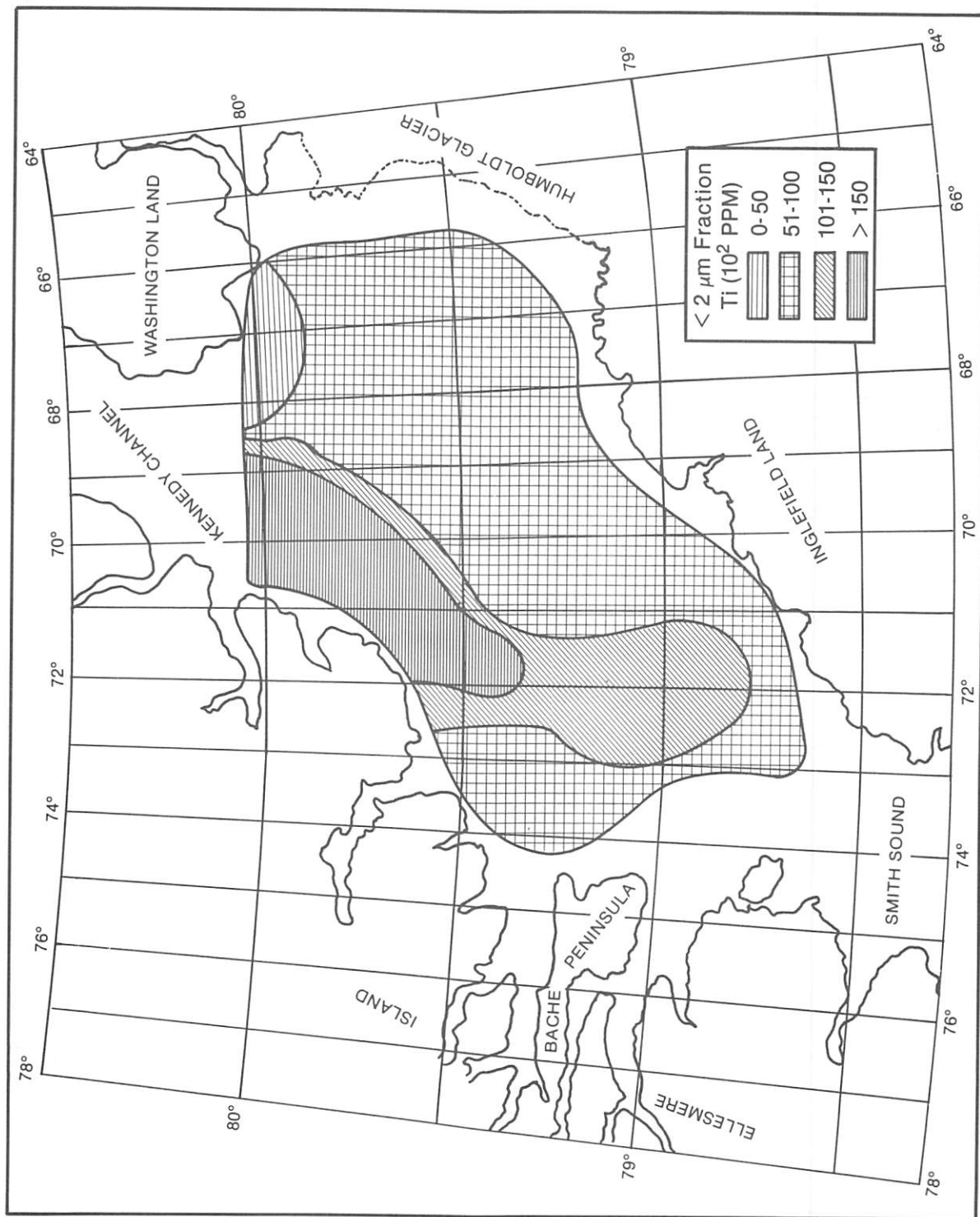


Fig. 34. Univariate map showing the distribution of Ti in the $< 2 \mu\text{m}$ fraction of the surface sediment layer.



Except for Fe and Zn, the highest concentrations of the chemical elements occur in the western side of the Basin. This part of the Basin is the area where relict sediment was previously discovered (Kravitz, 1975). The relict sediment is comprised of sand-sized aggregates, stained gravels composed largely of clastic rock fragments (including litharenite fragments containing particles of basalt), chlorite, expanding lattice clays and a heavy mineral suite dominated by clinopyroxenes. The sediments in the area of low chemical element concentration (core 4) on the northern topographic high, contain abundant kaolinite.

Concentrations of some of the chemical elements in the 0-6 cm interval of core 30 were unusually high relative to the rest of the core. It was suspected that evaporation or contamination of the sample solution may have taken place, therefore, Chauvenet's criterion for rejection of outliers was applied;

$$\left(\frac{s_m - \bar{x}}{s} \right)$$

where: s_m = value of the suspected outlier

\bar{x} = sample mean

s = estimate of the standard deviation

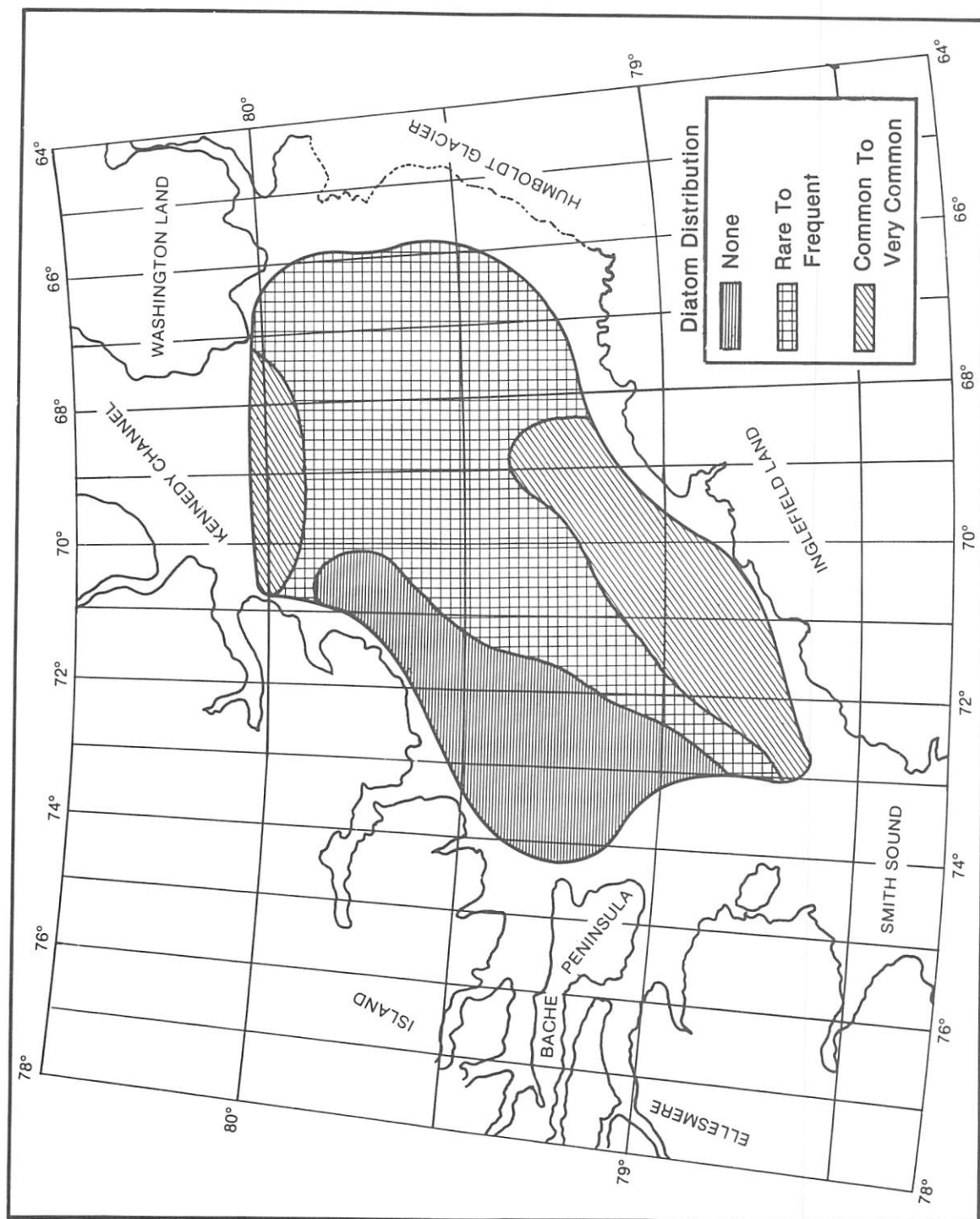
Based on this criterion seven of the nine element values were rejected; therefore all chemical data of the $< 2 \mu\text{m}$ fraction from this particular interval is questionable.

Diatom Distribution

The emphasis here is on the relative abundance of diatoms. The various types of diatoms found in Kane Basin were not identified.

Diatoms are concentrated in two areas in the Kane Basin (Figure 35). The first is directly off Inglefield Land extending to the southwest from the vicinity of Cape Kent to approximately $73^{\circ}10'W$ longitude, and covering the southern part of the eastern trough; the other is in the northernmost part of the Basin in a narrow zone located between Cape Collinson, and Cape Jackson. This latter area stretches across the entrance to Kennedy Channel and covers a small part of the northern topographic high, some of its northwestern slope and the northern end of

Fig. 35. Map showing distributon of diatoms in surface sediment layer.



the western trough. An area where surface sediments contain no diatoms is present in the western Basin extending from Darling Peninsula as far south as Pim Island, covering most of the western trough and the southwestern tip of the topographic high. Diatom presence ranges from rare to frequent in the rest of the Basin. The distribution of diatoms in the sediments of Kane Basin is tabulated in Table 5.

Factor Analysis

A Q - mode factor analysis was used to ascertain the regional grouping of similar sediment based on measured compositional variables. The data set used consisted of 42 variables from each of 192 samples and included textural parameters, mass physical properties, mineralogy of the $< 2 \mu\text{m}$ fraction (including % rock flour and % clay minerals), components of the heavy mineral fraction, heavy mineral species, % carbonate in the total sample, and % organic carbon in the total sample (Table 6). Variables such as the chemical elements in the $< 2 \mu\text{m}$ fraction, shear strength, Atterberg limits, indices based on the Atterberg limits, and activity were not included in the data base for factor analysis because it was not possible to determine these particular variables on all the samples (see previous discussions).

The 42 variables were scaled to range from zero to one, so that those variables having large values (means and variances) relative to variables with small values (e.g. porosity with a value of 70% and organic carbon with a value of 0.2%), should not have an inordinate effect and thereby determine the outcome. The data were then normalized so that the sum of squares of each row in the data matrix was unity (Klovan, 1975).

It was found that 91.7% of the variance in the scaled and row-normalized data was accounted for by three factors. The addition of a fourth factor accounted for only an additional 1.1% of the explained variance; therefore, the three factor model was used.

Factor I has a sample variance of 36.735. Its composition, as roughly determined from the columns of the scaled varimax factor score matrix (Klovan, 1975), is primarily made up of the following variables:

TABLE 5

DIATON ABUNDANCES IN KANE BASIN SEDIMENTS

BOTTOM SAMPLE (cm)	DIATOM ABUNDANCE	BOTTOM SAMPLE (cm)	DIATOM ABUNDANCE
2	common to very common	20 (6-40)	none
3	common to very common	21 (0-90)	common to very common
4	common to very common	21 (130-138)	none
5	rare to frequent	21 (138-246)	rare to frequent
6	rare to frequent	22 (0-11)	none
7	rare to frequent	22 (18-26)	rare to frequent
8	rare to frequent	22 (36-42)	none
9 (0-10)	rare to frequent	23 (0-68)	rare to frequent
9 (10-38)	none	24	none
10	none	25	none
11	none	26	none
12	none	27 (5-16.5)	none
13	rare to frequent	27 (25-38)	rare to frequent
14 (0-10)	rare to frequent	28 (0-10))	rare to frequent
14 (10-132)	none	28 (30-181)	common to very common
15	rare to frequent	29 (0-130)	common to very common
16 (0-45)	rare to frequent	29 (130-142)	none
16 (45-79)	none	30 (6-12)	common to very common
17 (4-14)	rare to frequent	30 (60-88)	rare to frequent
17 (64-91)	none	30 (88-101)	none
18 (4-14)	rare to frequent	31 (0-8)	rare to frequent
18 (14-200)	none	31 (8-79)	none
19 (0-10)	rare to frequent	7G	rare to frequent
19 (70-83)	common to very common	26G	none
19 (130-204)	none	32G	common to very common
20 (0-6)	rare to frequent		

TABLE 6
THE 42 PARAMETERS USED IN THE FACTOR ANALYSIS

HEAVY MINERAL SPECIES (%)	MINERALOGY OF THE < 2 μ m FRACTION (%)
Garnet	Expanding lattice clays
Orthopyroxene	Illite
Clinopyroxene	Chlorite
Amphibole	Kaolinite
Apatite	Quartz
Zircon	Feldspar
Rutile	Amphibole
Tourmaline	Carbonate
Kyanite	Clay minerals
Dolomite	Rock flour
Sphene	Carbonate in rock flour
Chlorite (sand-sized)	Silicate in rock flour
Spinel	
MASS PHYSICAL PROPERTIES	TEXTURAL PARAMETERS
Wet unit weight	% gravel
Water content	% sand
Void ratio	% silt
Porosity	% clay
	M ϕ
	Skewness
	Kurtosis
MAJOR COMPONENTS OF THE HEAVY MINERAL FRACTION (%)	CHEMISTRY
Non-opaques	% carbonate in total sample
Aggregates	% organic carbon in total sample
Alterites	
Opaques	

Physical Parameters

M(ϕ)
 Porosity
 % clay
 Void ratio
 % silt

Mineralogical Parameters

Garnet
 Orthopyroxene
 Illite
 Non-opaques
 % feldspar in < 2 μ m fraction

Factor II has a sample variance of 31.482. Its general composition, also determined from the scaled varimax factor score matrix, is comprised of the variables:

Physical Parameters

Aggregates
 Unit weight
 Skewness
 % sand

Mineralogical Parameters

% clay minerals in < 2 μ m fraction
 % carbonate in rock flour*
 Clinopyroxene
 % carbonate in < 2 μ m fraction**
 Expanding lattice clays
 Sphene
 Rutile

Factor III's sample variance is 15.861; its composition was determined in the same way as the previous two factors, and consists of the variables:

Physical Parameters

% gravel
 Unit weight
 Skewness
 % sand

Mineralogical Parameters

% silicate in rock flour
 Non-opaques
 % feldspar in < 2 μ m fraction
 Illite
 Amphibole
 Orthopyroxene
 Garnet

*The variable, % carbonate in rock flour, is the amount of carbonate minerals expressed as a percent of the silicate and carbonate portion of the < 2 μ m fraction, exclusive of the clay minerals (see definition of rock flour, this chapter).

**The variable, % carbonate in the < 2 μ m fraction, is the amount of carbonate minerals expressed as a percent of the total < 2 μ m fraction, including the clay minerals.

Table 16 (Kravitz, 1983), is a listing of the factor (varimax) loadings which give the relative importance of each factor for each of the 192 samples. The degree of similarity of any sample to each of the theoretical end member samples (factors) is proportional to the square of that sample's loading on the factor in question. Therefore, a sample with a loading value of 1.0 on factor I would be identical in properties to factor I. A sample with a loading of 0.7 on factor I and 0.7 on factor II, would be intermediate in properties between factor I and factor II. Individual factors may reflect either a single environmental condition or a group of conditions (Van Andel and Veevers, 1967). The factor loadings for the surficial sediment layer are plotted in Figures 36 through 39.

Surface distribution

Figure 36 is a map of the areal distribution of factor I in the upper sediment layer of Kane Basin. The highest loading values for this factor ($> .70$) occur off Humboldt Glacier and the entire coast of Inglefield Land. It blankets a large part of the eastern trough and much of the central portion of the topographic high. There is an area of slightly lower loading values (.50 to .70) within this zone, near Cape Leiper. Factor I decreases in importance to the north and west with its lowest loading values ($< .3$) found in the northwest part of the Basin between Cape Collinson and Cape Jackson. This zone extends as far south as Cape Fraser, Ellesmere Island, and covers the northern section of the western trough and the northwestern slope of the topographic high.

Factor II is most dominant on the western side of Kane Basin (Figure 37). Its area of highest loading values is a narrow, tapering zone which extends from the entrance to Kennedy Channel in the north to as far south as Bache Peninsula, and mantles a large part of the topographic high's western slope and the northern and central parts of the western trough. Factor II generally weakens in an easterly direction and the lowest loading values for this factor are in the eastern Basin in a broad area off Humboldt Glacier and Inglefield Land, to approximately $70^{\circ}50'W$ longitude. This area includes most of the eastern trough and a large part of the central topographic high, reminiscent of the zone of high factor I loading values.

Fig. 36. Map showing distribution of Factor I loading values in surface sediment layer.

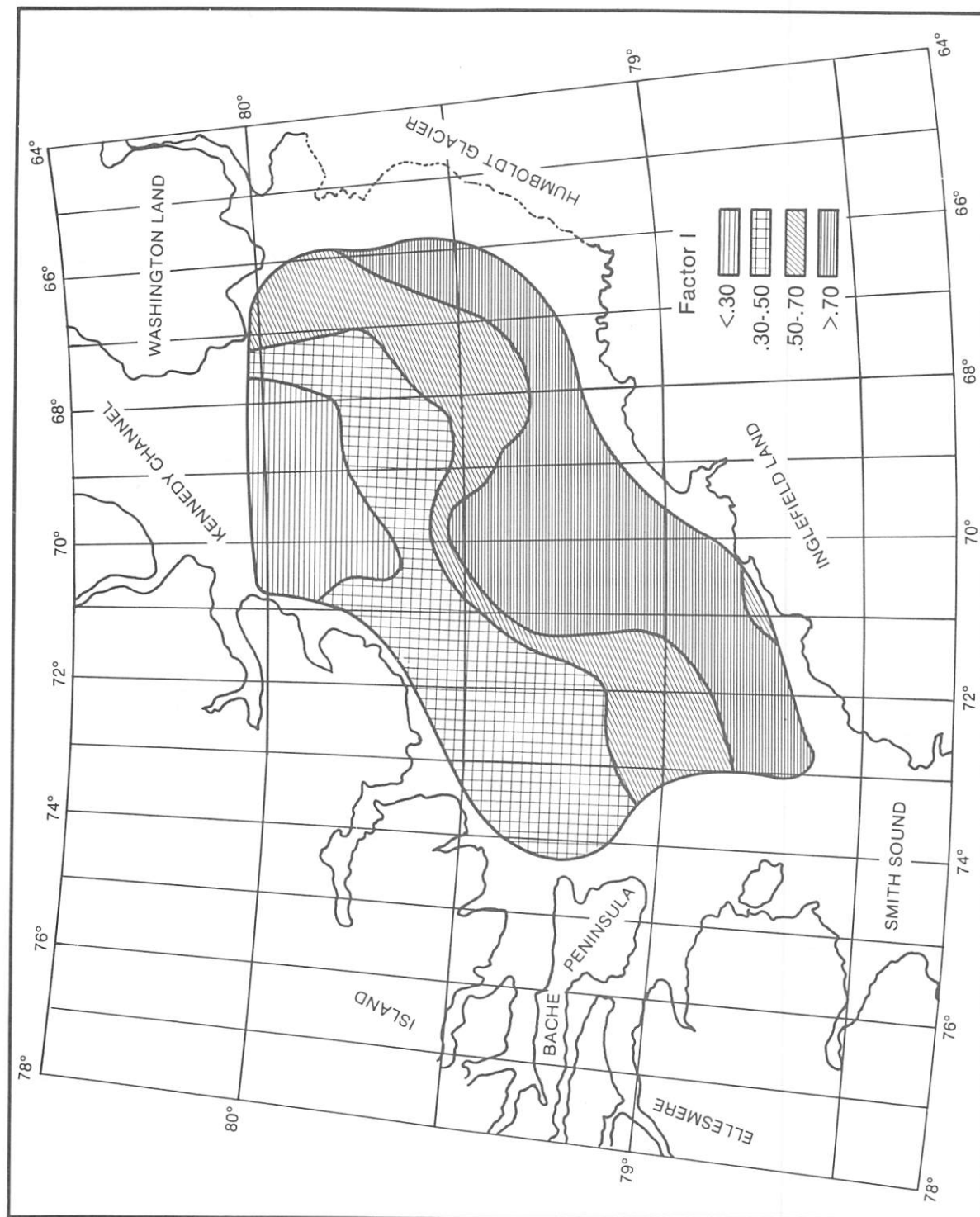
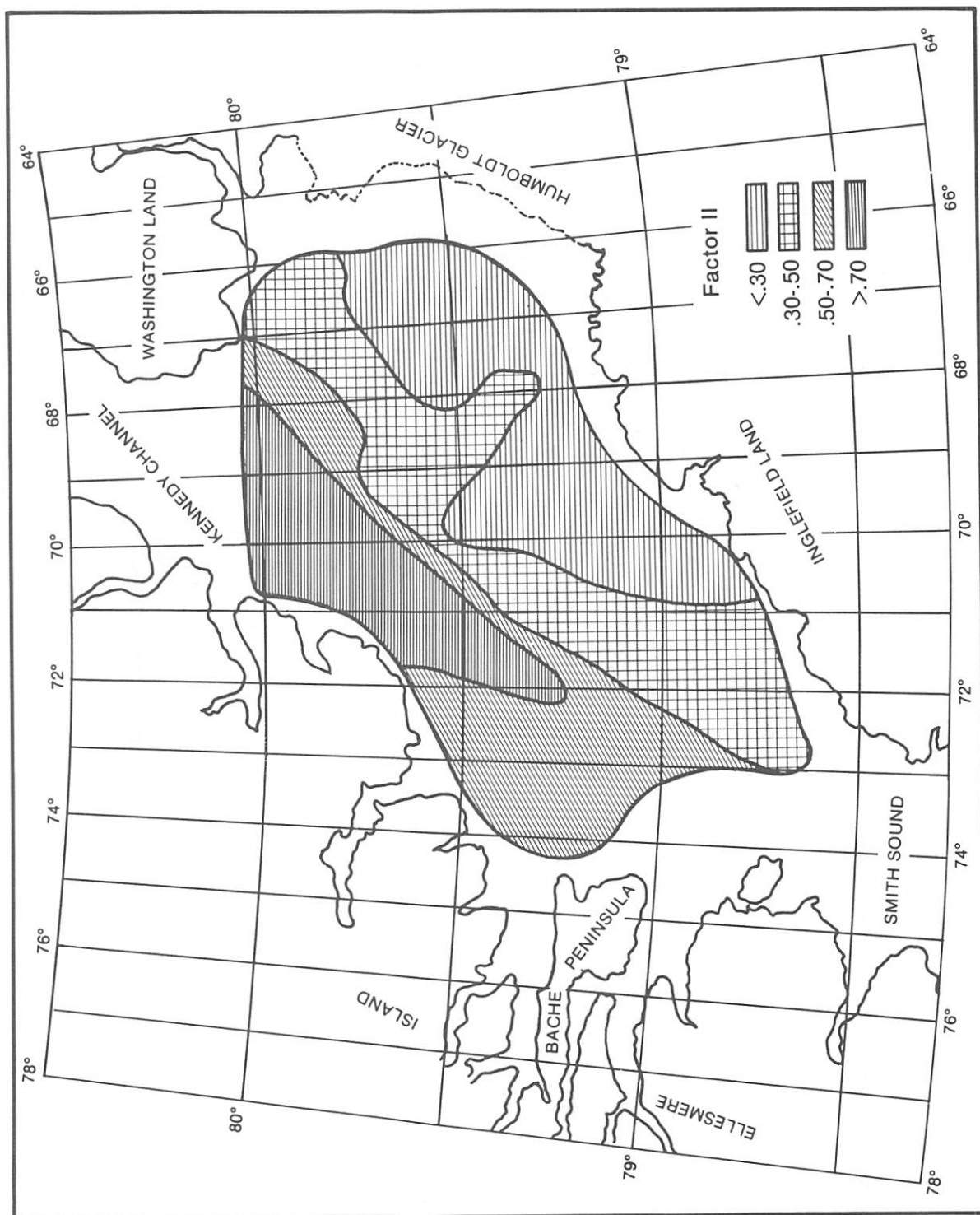


Fig. 37. Map showing distribution of Factor II loading values in surface sediment layer.



The highest factor III loading values ($> .60$) in the Kane Basin's surface sediment layer are found in the northeastern part of the Basin (Figure 38). This zone covers most of the northern topographic high and much of its northeastern and northwestern slopes. A southwesterly trending zone of lower loading values ($.40$ to $.60$) surrounds the primary zone on three sides.

The area of lowest factor III loading values ($< .20$) is a broad zone found in the western Basin. This zone spreads over most of the western trough, and the western slope of the topographic high. There is an area of slightly higher factor III loading values ($.20$ to $.40$) off Dobbin Bay. Similar values also are present in the area directly off the Inglefield Land Coast including the southern and southeastern parts of the Basin.

A composite map of the three factors shows the areas of dominance of each in the surface sediment layer of Kane Basin (Figure 39). Factor I is strongest in the eastern Basin including the eastern trough, the eastern slope of the topographic high, and the eastern topographic high below $79^{\circ}30'N$. It extends slightly onto the western part of the topographic high above this latitude. Factor II is dominant in the western Basin covering the western trough, parts of the western topographic high and most of its western slope. Factor III, prevalent in a portion of the northeast Basin, blankets most of the northern topographic high, including large parts of its northeastern and northwestern slopes.

Fig. 38. Map showing distribution of Factor III loading values in surface sediment layer.

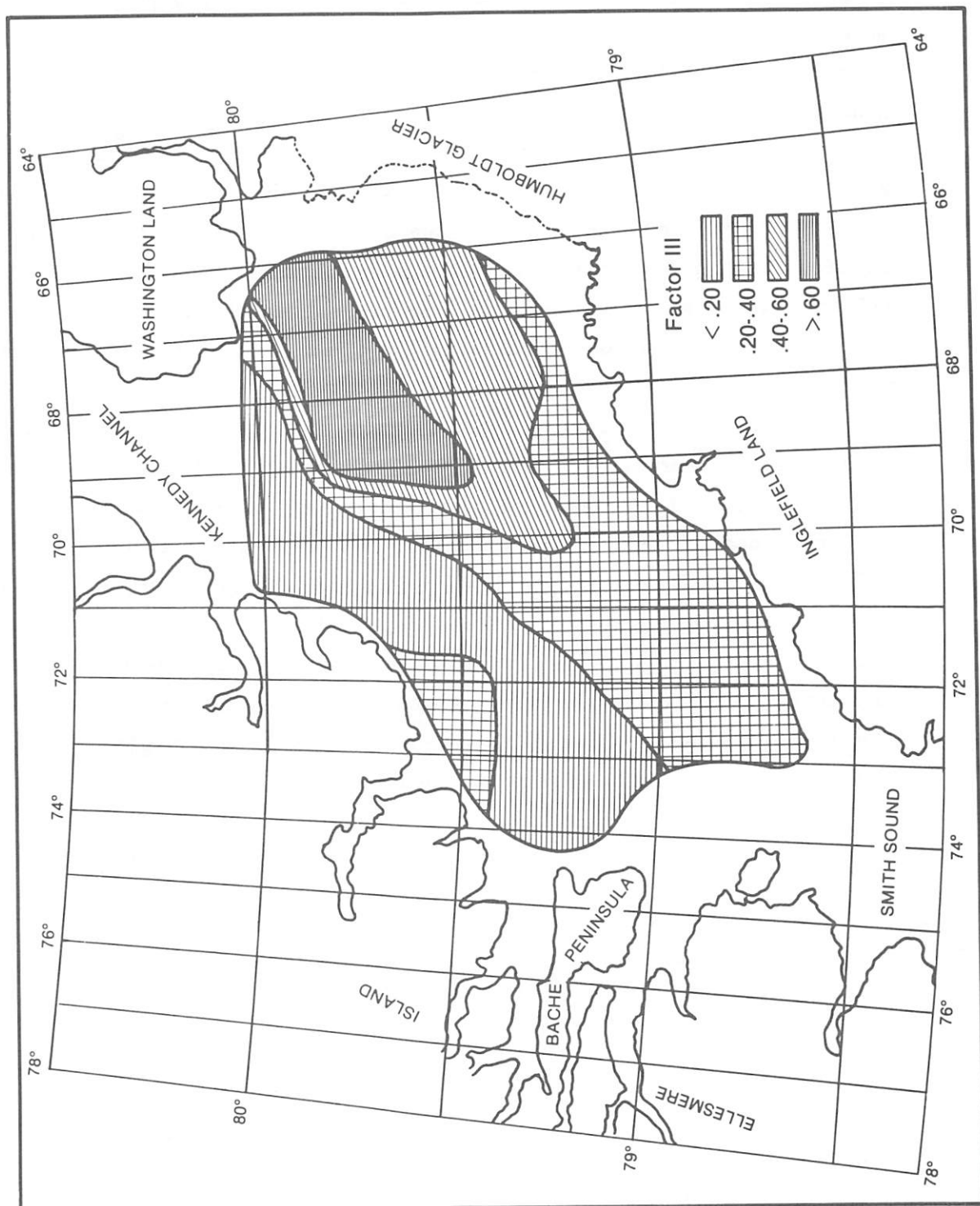
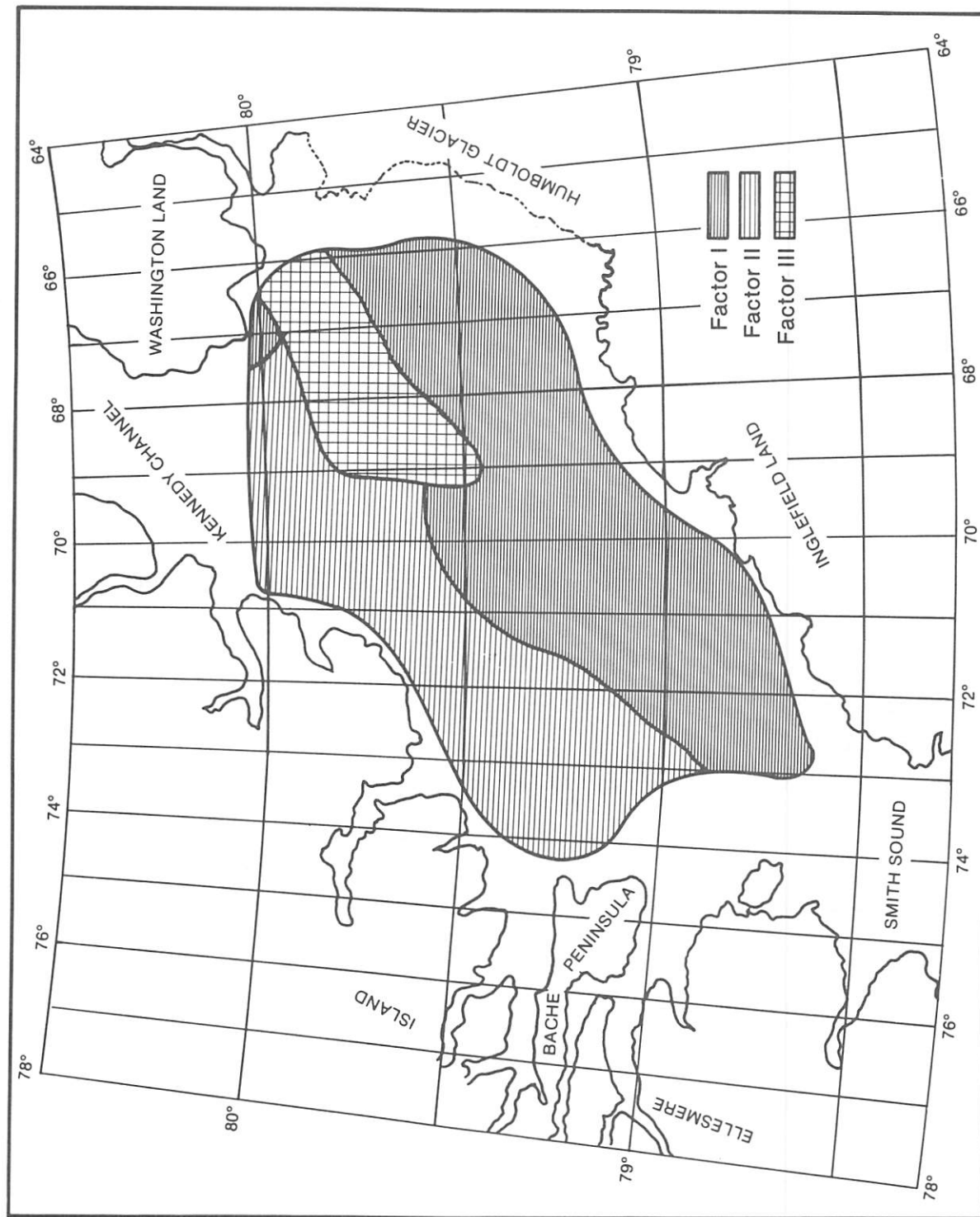


Fig. 39. Composite map of the three factors.



CHAPTER V

DISCUSSION

Q-mode factor analysis places the Kane Basin sediments into three distinct groupings designated as factors I, II and III.

Factor I sediments are characterized by higher water contents (larger void ratios and porosities) and a finer-grained texture than either factor II or factor III sediments. Factor II and III sediments have higher unit weights, larger skewness values and are coarser grained than factor I sediments. Factor II sediments contain more aggregates than the other sediments. Gravel is a major component in factor III sediments (see Chapter IV).

The mineralogy of factor I and factor III sediments is very similar. Important components of both factors are garnet, orthopyroxene, illite, non-opaque minerals and % feldspar in the $< 2 \mu\text{m}$ fraction. However, amphibole and % silicate in rock flour, major components of factor III sediments, are not important in factor I sediments.

The major mineralogical components of factor II sediments are; % clay minerals in the $< 2 \mu\text{m}$ fraction, % carbonate in rock flour, % carbonate in the $< 2 \mu\text{m}$ fraction, expanding lattice clays, clinopyroxene, sphene and rutile. Therefore, the mineralogical character of factor II sediments differs considerably from factor I and factor III sediments.

Factor I is interpreted to characterize recent sediments and factors II and III, relict sediments (till). Factor I sediments were further divided into a facies composed of sediment dominated by ice rafting and a facies composed of sediment dominated by water transport. This division was based on examination of the radiographs of the sediment cores (in order to determine the gross fabric of the sediment) along with an evaluation of the textural characteristics and mass physical properties of the sediments.

The sediment fabric, deduced from the radiographs, and the textural and physical properties of factor II and factor III sediments categorize them as tills. The major mineral components of the factor II and factor III sediments coupled with an examination of their gravel compositions and their chemistry, were used to classify factor II and factor III sediments as Ellesmere Island till (Till 1) and Greenland till (Till 2), respectively.

The following discussion of the factors and the various sediment parameters provides insight into the identification, distribution, and provenance of the four lithofacies. Table 7 lists the parameters studied, their values, and the sediment samples making up each lithofacies.

Factor Analysis

Factor I (Sediments dominated by ice rafting)

In sediments dominated by ice rafting the following down core relationships apply. Cores 5, 16, 17, 20, 22 (0 cm - 38 cm), 23, 30 (78 cm - 101 cm), and 31 (8 cm - 41.5 cm) all show a down core increase in factor III. This is usually accompanied by a corresponding decrease in factor I, implying that a shallow cover of factor I materials (in this case the ice rafted sediments) overlays factor III (till 2) sediment. The down core patterns for cores 18 and 27 are variable and have no definite trends; however, the variations in the factor loading values can be easily correlated with changes in their physical and mineralogical parameters. To some degree these changes are caused by current activity.

Factor I (Sediments dominated by water transport)

In the sediments dominated by water transport core 28 shows a slight down core increase in factor I loading values but relatively little change in factors II and III. However, in cores 19, 21, 29 and 30 (0 cm - 78 cm) the factor I loading values decrease down core and, with the exception of core 29, factor III loading values increase. This is the same overall pattern found in the ice rafted sediments and indicates that the water transported materials also overlie coarser, higher

TABLE 7
CHARACTERISTICS OF THE FOUR LITHOFACIES

	Till 1 (Ellesmere Island Till)	Till 2 (Greenland Till)	Ice rafting dominant	Water transport dominant
Bottom samples	2, 3, 4, 9, 10, 11, 12, 13, 14(108 cm-132 cm), 24, 25 26(27 cm-73 cm), 26G	6, 7, 8, 15, 22(36 cm-44 cm)	5, 16, 17, 18, 20, 22(0 cm-36 cm), 23, 27, 30(78 cm-101 cm), 31(8 cm-41.5 cm), 7G	14(0 cm - 90 cm), 19, 21, 28, 29, 30(0 cm - 78 cm), 31(0 cm - 8 cm)
Factors	II	III	I	I
Sedimentary structures	None	None	Coarse bedding Laminae Cross-laminae	Coarse bedding Laminae Cross-laminae
Pebble orientation	No	No	Yes	Yes
Bioturbation	None	None	Weak	Strong
Single burrows	None	None	None	Yes
Shell material	None	None	Yes	Yes
Diatoms	Surface only	Surface only	Surface and occasionally down core	Surface and common down core
% Gravel	15	22	7	< 1

TABLE 7
(continued)

113

	Till 1 (Ellesmere Island Till)	Till 2 (Greenland Till)	Ice rafting dominant	Water transport dominant
% Sand	33	41	20	4
% Silt	29	23	31	44
% Clay	23	14	42	52
M(ϕ)	Very fine sand (4.0)	Fine sand (2.7)	Medium silt (5.8)	Very fine silt (7.9)
Standard deviation	Extremely poorly sorted (4.2)	Extremely poorly sorted (4.0)	Very poorly sorted (3.8)	Very poorly sorted (2.5)
Skewness	Slightly negative (-0.055)	Positive (0.153)	Moderately negative (-0.206)	Highly negative (-0.325)
Kurtosis	Platykurtic (-0.671)	Platykurtic (-0.445)	Platykurtic (-0.542)	Leptokurtic (0.072)
Wet unit weight (gm/cm ³)	2.06	2.15	1.75	1.48
Water content (% dry weight)	23	20	50	101
Saturated void ratio	0.60	0.52	1.36	2.59

TABLE 7
(continued)

	Till 1 (Ellesmere Island Till)	Till 2 (Greenland Till)	Ice rafting dominant	Water transport dominant
Porosity (%)	38	33	56	72
Total carbonate (%)	25	18	16	15
Total organic carbon(%)	1.07	0.20	0.54	1.04
Illite(%)	51	72	70	67
Expanding lattice clays(%)	22	8	10	13
Kaolinite(%)	15	8	8	8
Chlorite(%)	12	12	12	12
% Calcite and dolomite in the rock flour	57	24	15	6
% Quartz in the rock flour	29	40	41	51
% Feldspar in the rock flour	14	36	41	40
% Amphibole in the rock flour	0	0	3	3

TABLE 7
(continued)

	Till 1 (Ellesmere Island Till)	Till 2 (Greenland Till)	Ice rafting dominant	Water transport dominant
% Rock flour in < 2 μ m fraction	14	25	19	15
% Clay minerals in < 2 μ m fraction	86	75	81	85
Non-opaques	53	79	77	77
Alterites	7	5	5	6
Opagues	14	13	15	14
Aggregates	26	3	3	3
% Silicate in rock flour	46	76	84	93
% Carbonate in rock flour	54	24	16	7
Dominant rock types in gravel fraction	Clastics and Carbonates	Carbonates	Crystallines	Crystallines
% Garnet	13	40	44	42
% Orthopyroxene	7	23	23	23

TABLE 7
(continued)

	Till 1 (Ellesmere Island Till)	Till 2 (Greenland Till)	Ice rafting dominant	Water transport dominant
% Clinopyroxene	55	8	9	12
% Amphibole	15	22	17	16
% Apatite	3	3	2	2
% Zircon	0.71	0.67	0.50	0.89
% Tourmaline	0.76	0.18	0.41	0.31
% Rutile	0.60	0.18	0.50	0.39
% Kyanite	0.43	0.03	0.19	0.15
% Epidote	0.57	0.10	0.30	0.36
% Sphene	0.33	0.15	0.19	0.30
% Spinel	0.51	0.21	0.25	0.10
% Staurolite	0.17	0	0.15	0.04
% Chlorite (ss)	0.17	0.05	0.14	0.22
% Dolomite	1.40	0.12	1.40	1.43
Fe(ppm)	55,395 (5.54%)	50,167 (5.02%)	72,248 (7.23%)	60,518 (6.05%)

TABLE 7
(continued)

	Till 1 (Ellesmere Island Till)	Till 2 (Greenland Till)	Ice rafting dominant	Water transport dominant
Mg(ppm)	33,853 (3.38%)	30,633 (3.06%)	27,845 (2.78%)	26,139 (2.61%)
Mn(ppm)	485	288	302	250
Cr(ppm)	154	91	126	129
Co(ppm)	90	63	69	64
Ni(ppm)	177	115	134	136
Zn(ppm)	251	188	255	235
Cu(ppm)	197	154	146	170
Ti(ppm)	17,325 (1.73%)	6,523 (0.65%)	15,265 (1.53%)	7,713 (0.77%)

density (till 2) sediments. Factor II shows a definite increase down core only in core 14, and is usually subordinate to factor III in the sediments of the eastern Basin (major exception, core 31).

Factor II (Till 1)

Factor II, the dominant factor in the western Basin, increases down core in all the cores containing till 1 sediments, except core 12 where it decreases. These increases are accompanied by lower loading values for factors I and III with the exception of core 10. In this core all factors increase down core. The smaller factor II loading values in the upper part of this core are attributed to the influence of limited reworking of Recent sediments into the upper layers of the till (cores 11, 25, 26). The difference between the factor II loading values in core 10 is inconsequential and, therefore, the factor II variation in this short core is essentially non-existent.

The upper sediments in core 12, in comparison to the materials below 32 cm, have higher sand and gravel contents, a more positive skewness, larger wet unit weights, higher $< 2 \mu\text{m}$ carbonate, expanding lattice clays, clinopyroxene, epidote, staurolite and spinel values, and lower garnet and orthopyroxene contents. Therefore, factor II shows an upward increase in loading values. The reason for this may just be a natural heterogeneity in the till or perhaps an influx of sediment with till 1 parameters.

In core 14, sediments classified as factor II (till 1) are found below factor I (the water transported component) sediments. These factor II sediments are mineralogically quite different from other factor II sediments (see discussion under Gravel and Sand Composition, this chapter). The mineralogical difference indicates a different source for this sediment than for other factor II sediments.

The factor analysis classification of this material as till 1 is based on its textural and mass physical properties, which are quite similar to the other factor II sediments. Because of the mineralogical differences, however, the three factors do not account for a very large proportion of the variation in this particular sediment.

Factor III (Till 2)

The largest factor III (till 2) loading values are found in surface cores 6, 7, 8 and 15 along the topographic high. In each of these cores factor I loading values are higher than factor II loading values. Core 22 (36 cm - 44 cm) is an almost equal mixture of factor III and factor I sediments with subordinate amounts of factor II sediment. The texture and mass physical properties are much closer to till 2, than to the ice rafting materials, therefore, this sample is classified as a till.

There is an interesting aspect of the down core trends of factor I (the ice rafted sediment) and factor III (till 2) which needs further comment. In certain cases (cores 18, 27 and 31 [8 cm - 41.5 cm]) where factor III increases at the expense of factor I the cause is attributed to current activity, which removes the finer-grained material and results in higher sand and gravel contents, a more positive skewness and a larger wet unit weight. Since the mineralogy of factor I and factor III is similar it is conceivable that till 2 is not a till at all but is actually a winnowed lag deposit of ice rafted, factor I material. However, other sediments with equivalent factor III values are intimately mixed with factor I and/or factor II materials and show no indication of current activity (core 22 [36 cm - 44 cm] and core 31 [41.5 cm - 79 cm]). In addition, the temporal relationship of factor II and factor III (factor III is never found as the dominant sediment overlying factor II and vice versa) and the areal relationship (factor III is stronger than factor II in the eastern Basin while factor II dominates the western Basin) indicate contemporaneous deposits with reasonably distinct lines of demarcation. This, coupled with the strong similarity of the mass physical and textural properties of factors II and III favor the interpretation of factor III material as a till (possibly winnowed).

Core 31 is located in the southernmost part of Kane Basin southwest of the topographic high and is almost evenly spaced between Greenland and Ellesmere Island (Figure 1). In this core factor I (ice rafted sediment from 41 cm to 8 cm, water transported sediment from 8 cm to the sediment-water interface) increases upward. Above 41 cm factor I fluctuates in an erratic fashion while both factors II and III fluctuate in

direct opposition to it (Figure 188, Kravitz, 1983). These irregular profiles were caused by currents whose resultant sedimentary structures are apparent on the radiographs.

From about 41 cm to the surface of core 31, factor I is dominant. Below 41 cm the three factors are approximately equal. This equivalency of the factors is believed to be due to a coalescence of the glacial ice in the low lands south of the topographic high where components of tills 1 and 2 were mixed together. This was followed by deposition of ice rafted sediments, reworked in their upper parts (8 cm - 41.5 cm) and finally blanketed by water transport dominant sediments (0 cm - 8 cm). Core 31 is, in effect, a microcosm of the sedimentary events occurring in Kane Basin (Figure 40).

Factor analysis was very useful in providing a broad characterization and grouping of the sediments under study, and a close examination of the factors loading values does identify sediment samples in which the factors do not account for a very large portion of the variation. However, the factor analysis as used here does not differentiate between sediments influenced by ice rafting and sediments influenced by water transport, nor does it clearly point out the exact nature of the subtle differences in the sediments making up factor II (till 1). Therefore, in addition to factor analysis, the parameters--sediment fabric (as determined by x-radiography), texture, mass physical properties, carbonate and organic carbon content, mineralogy and element chemistry--were used to help differentiate the lithofacies.

Figure 40 presents the resultant down core profiles of the 4 lithofacies. A discussion of these lithofacies and their parameters follows.

Radiograph Analysis

Sediments dominated by ice rafting

The ice rafted sediments contain a large number of dropstones in fine to coarse grained (medium to high radiograph densities) matrices. The cores nearest Humboldt Glacier (16, 17 and 18) contain stringers, pockets and poorly formed beds and laminae of coarse material (Figure 41). This is indicative of large amounts of coarse material being deposited from the glacier, and then being slightly reworked by

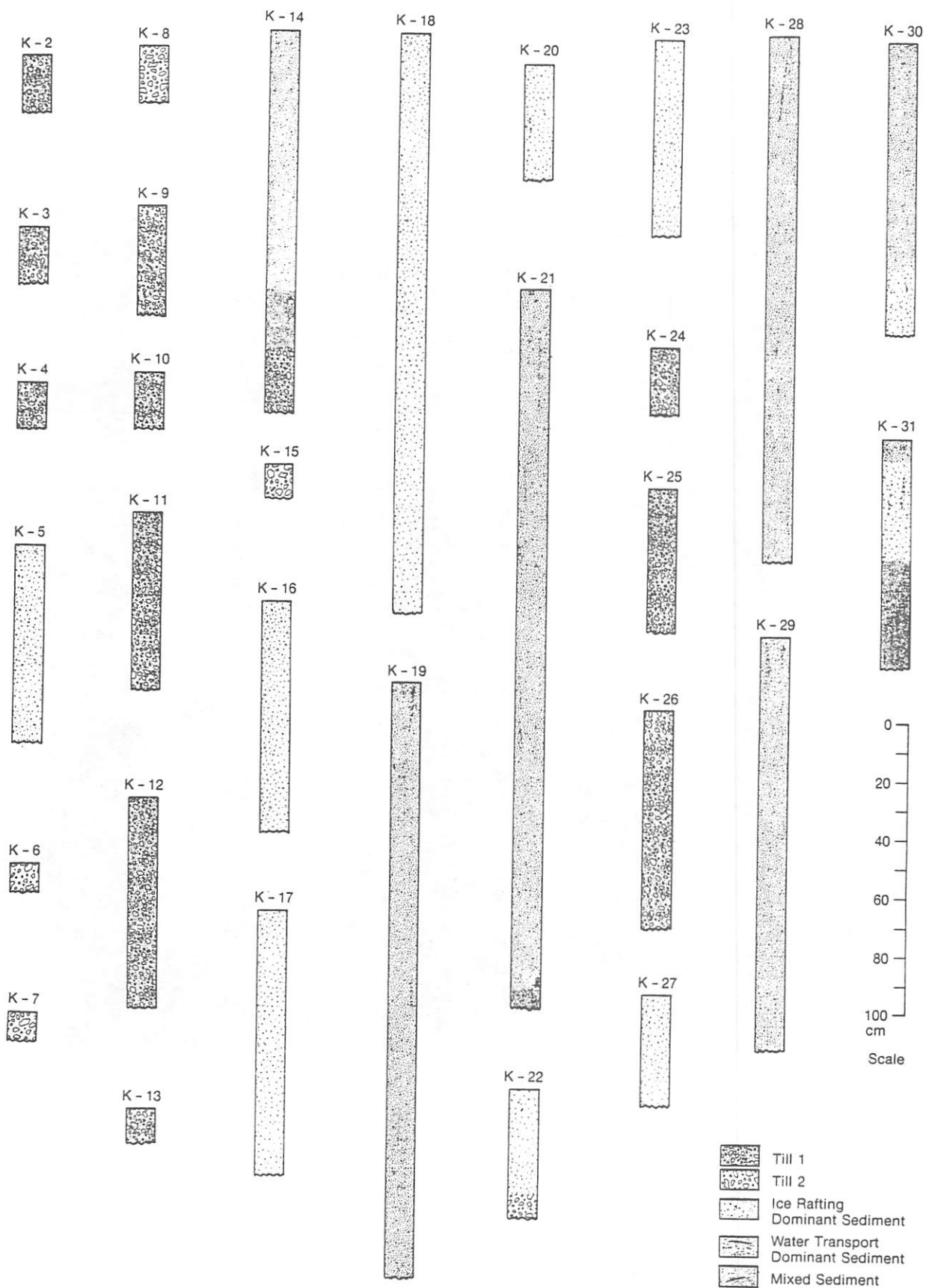


Fig. 40. Core profiles of the four lithofacies.

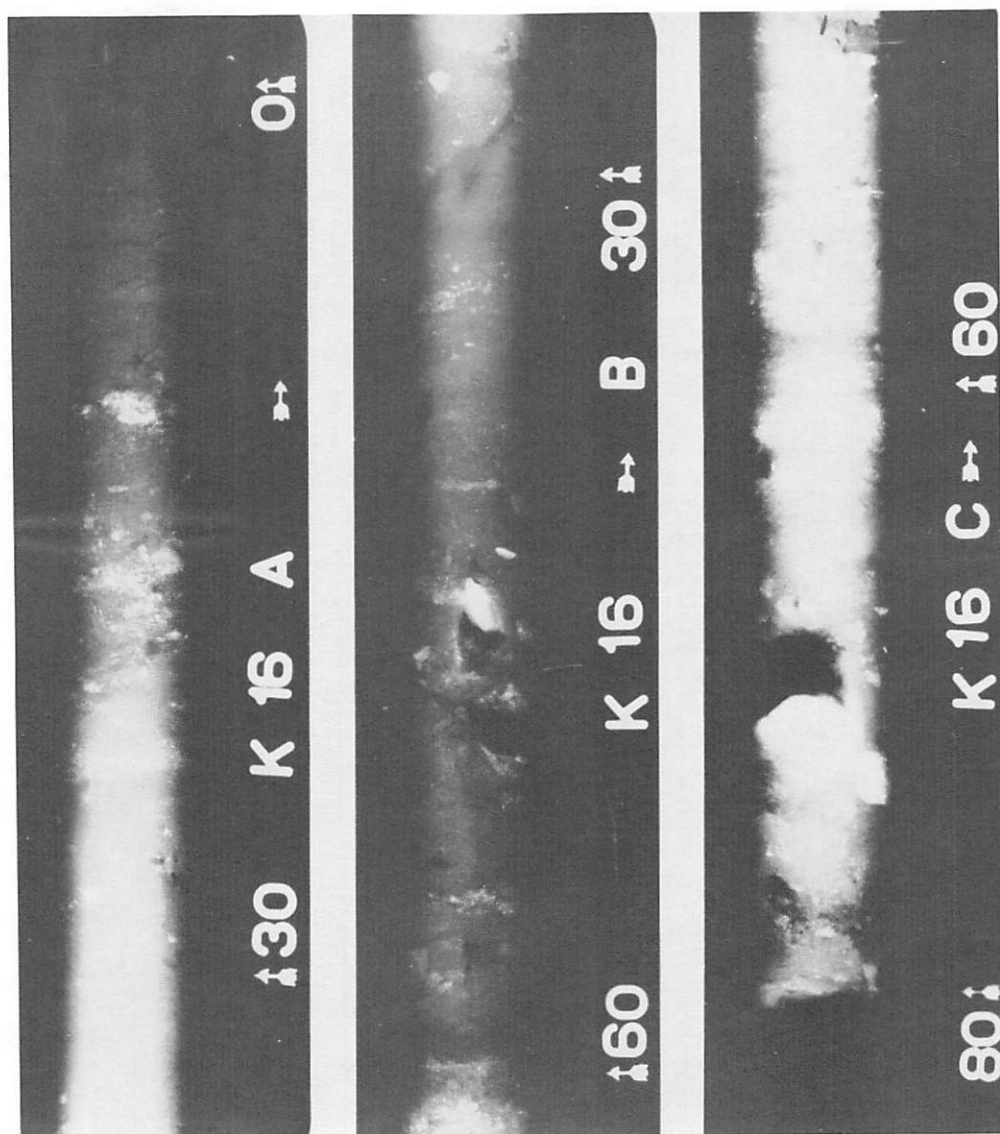


Fig. 41. X-radiograph of core 16 showing "typical" fabric of ice rafting dominant sediments. Scale (numbers with arrows) in cm.

erratic, weak current activity. The origin of these currents is not certain. Edwards (1978) states that rapid mixing of fresh water and sea water adjacent to ice tunnel mouths may produce a high density underflow capable of transporting sand-size sediment and occasionally coarser material. The formation of brines derived from freezing at the base of the ice also may result in current activity, as the high density brines move along the bottom.

The current activity is more pronounced close to the glacier, as evidenced by some cross-lamination and somewhat better defined sedimentary structures in core 18. In the vicinity of core 16 the presence of only a few poorly formed laminae indicate weaker, more irregular currents.

Bottom currents have also reworked the ice rafted sediments in cores 20, 22 (0 cm - 36 cm), and 31 (8 cm - 41.5 cm) as evidenced by the presence of bedding, definite alternating laminae, and pebbles oriented to the horizontal. Core 27 shows slight pebble orientation in some of its coarse layers while cores 5, 23 and 30 (78 cm - 101 cm) have no sedimentary structures except for some possible bioturbation in core 23, and therefore, show no indication of reworking by bottom currents.

Sediments dominated by water transport

The water transport dominant sediments have fine-grained (medium radiograph densities) matrices with small numbers of dropstones scattered throughout. In some of the cores laminae, distorted by the dropstones, are evident. Sedimentary structures, such as crude bedding, thin high density laminae and some cross-lamination are present in a few of the cores [19, 29 and 30 (0 cm - 78 cm)]. Some high density (silt and/or fine sand) stringers, which do not always extend across the width of the cores, occur in most of the water transport dominant sediment. The presence of the stringers is perhaps due to the relatively sparse coarse fraction of these sediments and a current regime which is not strong enough to produce definite, areally extensive, sedimentary structures. Bioturbation, distinct horizontal and non-horizontal burrows, occasional shells and "mycelia" also are common in the majority of the water transported sediment cores (Figure 42).

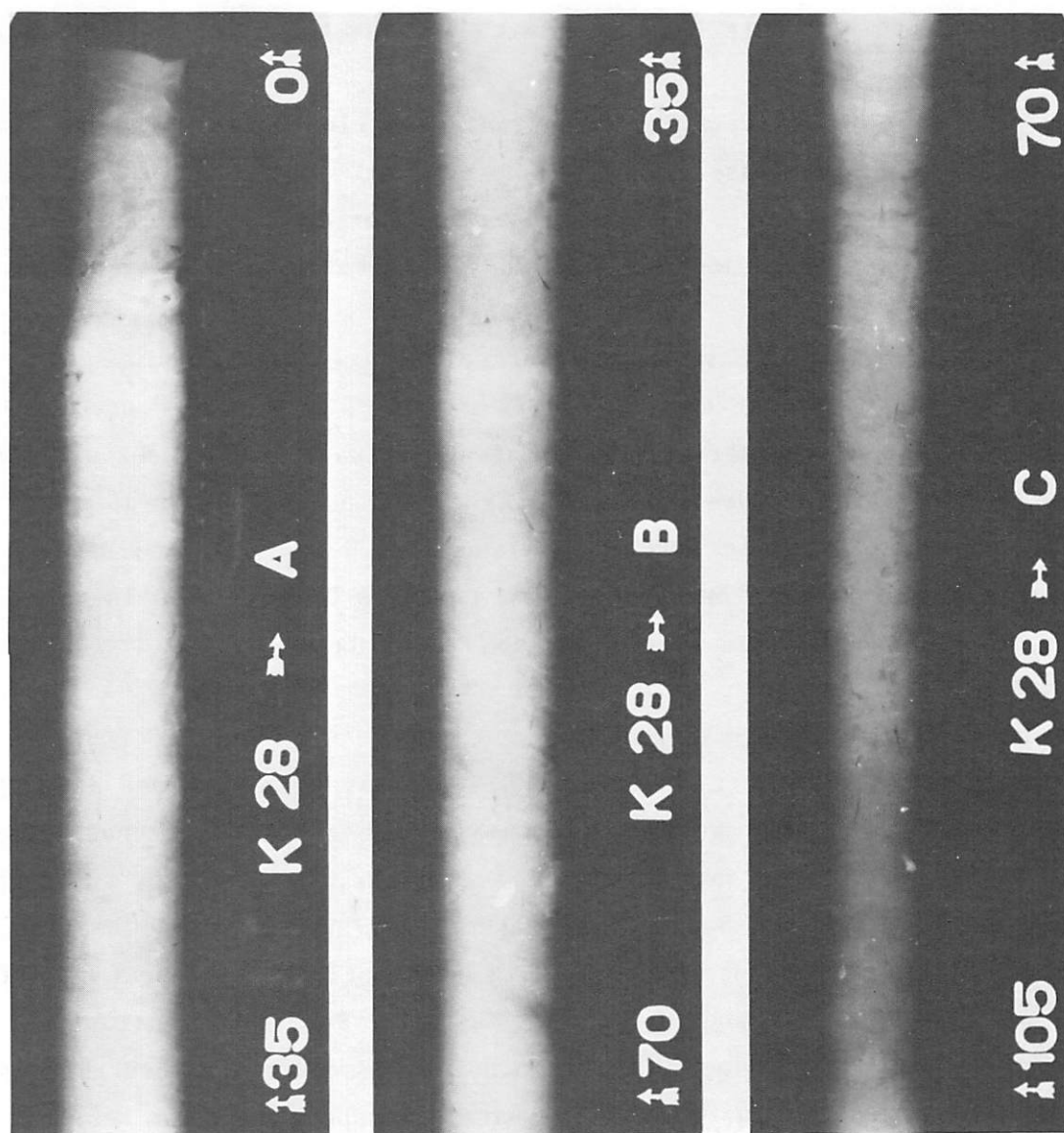


Fig. 42. X-radiograph of core 28 showing "typical" fabric of water transport dominant sediments. Scale (numbers with arrows) in cm.

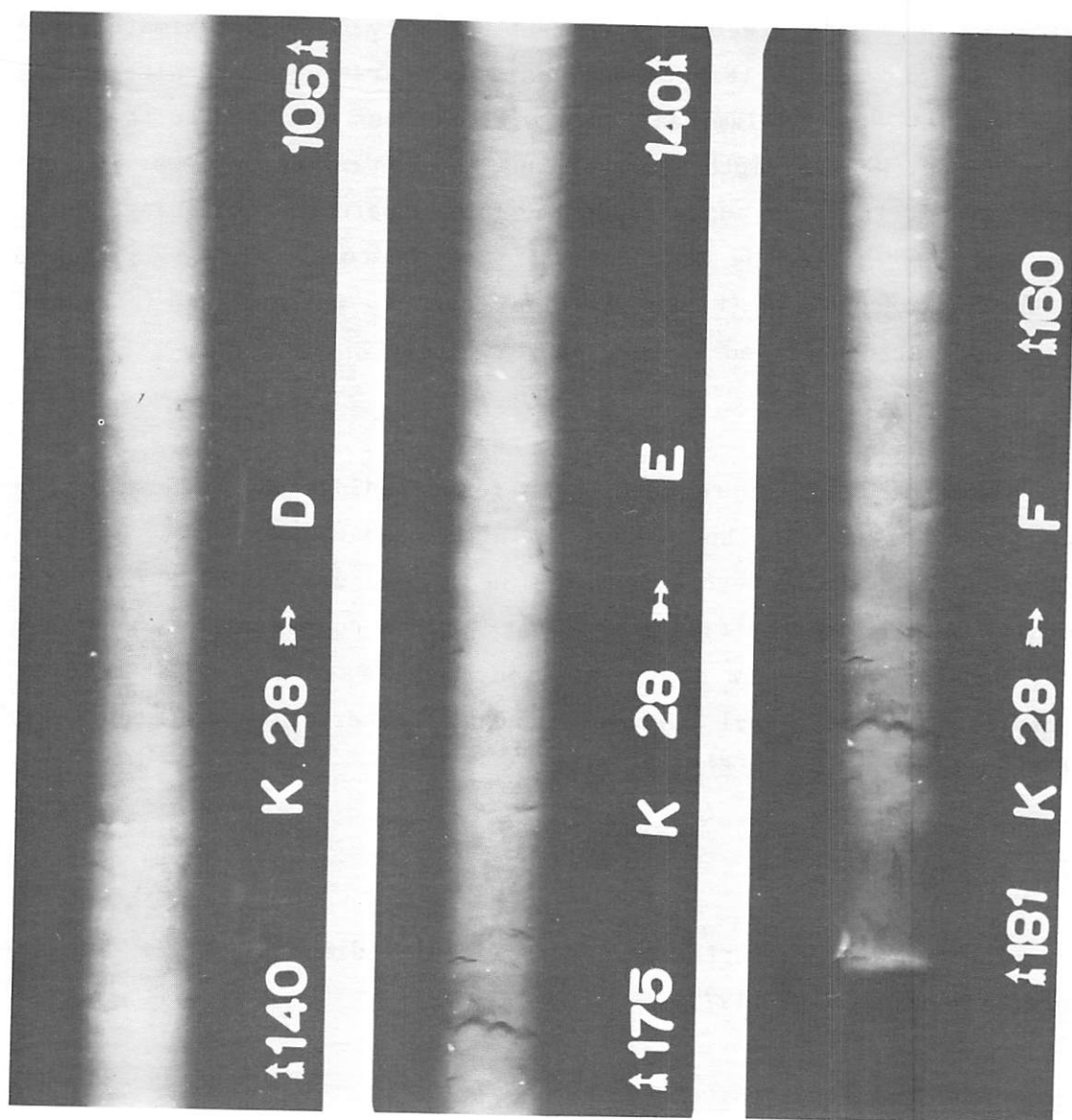


Fig. 42. (continued)

Till 1

Till 1 contains abundant pebbles which show no preferred pebble orientation and, except for two cores, no sedimentary structures (Figure 43). The matrix is generally coarse grained but in a few cases it is fine grained. Core 12 contains a layer between 30 cm - 33 cm which may be a bed created by current activity, and approximately the top 27 cm of core 26 (Figure 44) contains coarse beds and alternating high and low density laminae, some with pebbles oriented to the horizontal. Below this depth there are no sedimentary structures. Current reworking of the previously deposited till apparently took place during the time represented by the upper part of the core. This is supported by the factor profile (Figure 183) for core 26 which shows increased mixing of factors II and I above approximately 27 cm.

Till 2

Cores of till 2 were unsuitable for x-radiography because of the low penetrability of the sediment, which resulted in short, highly disturbed samples. However, core 22 (36 cm - 44 cm) has material structurally similar to the till 1 sediments with a coarse matrix containing many pebbles which show no orientation, and no sedimentary structures. Bioturbation, individual burrows, and shell material were absent in all of the sediments identified as tills.

Texture

The textural character of the surficial sediment layer is described in detail in Kravitz (1975).

Sediments dominated by ice rafting

The gravel content for the sediments dominated by ice rafting is 7%. The occasional high concentrations of coarse sediments showing up in cores 18 and 27 are attributed to two processes having varying degrees of influence; the deposition of coarse material from ice, and the concentration of coarse sediment by current activity. The increase in gravel in the lower part of core 22 is the result of the presence of till 2 sediment (Figure 180, Kravitz, 1983).

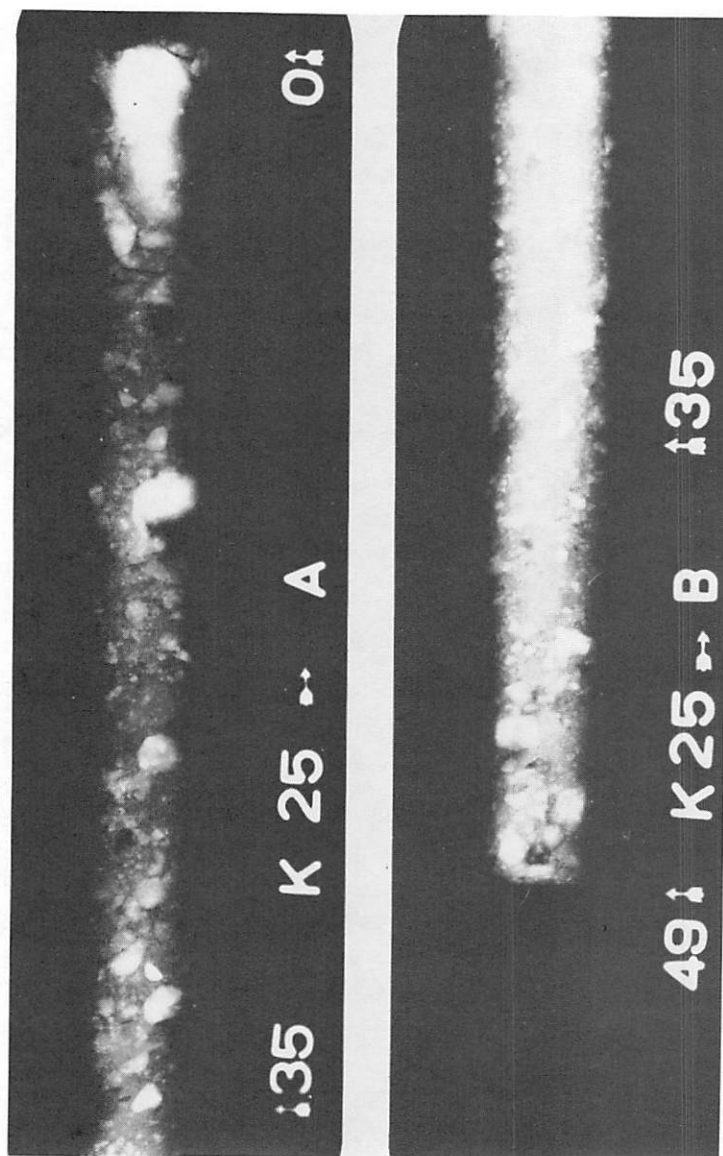


Fig. 43. X-radiograph of core 25 showing "typical" till fabric. Scale (numbers with arrows) in cm.

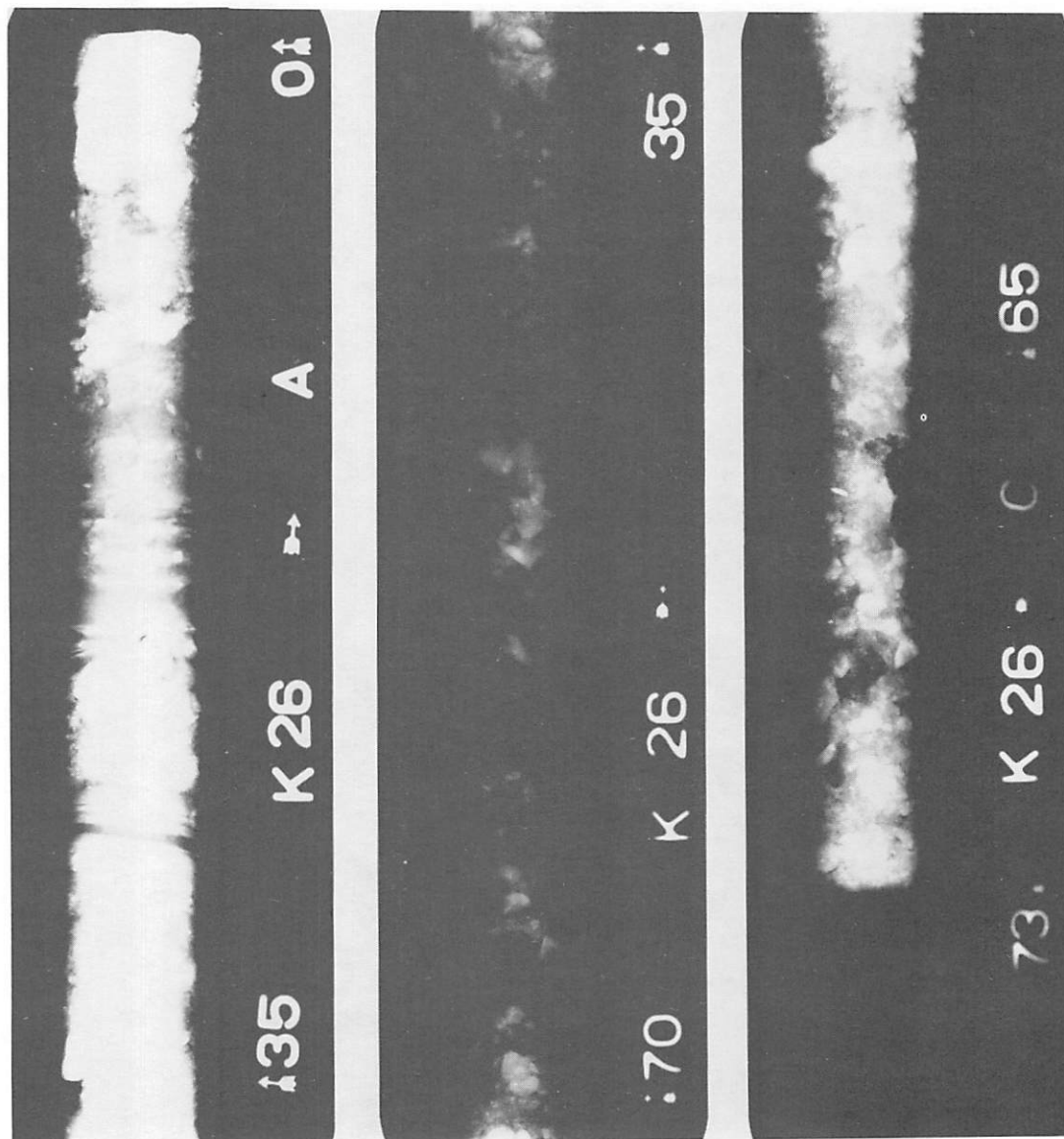


Fig. 44. X-radiograph of core 26 showing sedimentary structures in upper portions of core and "typical" till fabric in lower part of core. Scale (numbers with arrows) in cm.

Sand is more abundant than gravel in the ice rafted sediment with a mean value of 20%. In core 20 the downcore increase in sand content is the result of current activity. This activity removed the finer material and resulted in the formation of laminae and cross-bedding. The increase in sand content at the bottom of cores 5 and 22 represents the influence of till 2 sediments, which are in close proximity to the overlying ice rafted material (Figures 169 and 180, Kravitz, 1983). Sand content increases upward in core 17. This indicates greater recent deposition of sand-sized material at this location. The explanation for the zones of high sand content in core 18 is the same as that offered for the gravel distribution in this core (see preceding comments).

Silt is the second most dominant size fraction (31%) in the ice rafted facies. It decreases downward in cores 5 and 23, as the sand and gravel content increases. The silt content increases down core 18. Its fluctuations in this core are similar to the fluctuations in sand content. This is explained by the presence of cross-laminae composed of these two size fractions. The variations in silt downward in cores 27 and 31 (8 cm- 41.5 cm) change in opposition to gravel and sand concentrations. Clay is the most abundant size fraction (42%) in the ice rafted sediments. Its variations within the cores are opposite to those of sand and gravel. In most instances, where current activity has taken place, the clay concentration shows (as expected) a marked decrease due to winnowing. The average mean grain size for these sediments is 5.8ϕ (0.018 mm, coarse silt). The mean grain size has a strong covariance with clay content and a weak covariance with silt content. Ice rafting dominant sediments are very poorly sorted (average standard deviation 3.8ϕ) and show a very strong covariance with gravel content. Although the mean standard deviation places these materials in the very poorly sorted category, they range from very poorly sorted to extremely poorly sorted in those bottom samples with large gravel content (cores 16 and 27, and grab sample 7G).

The ice rafting dominant sediment has moderately negative skewness (mean skewness -0.206). It correlates strongly with sand content. Skewness becomes more positive downward in core 20 because of the higher sand content caused by increased current activity. These sediments are platykurtic (mean kurtosis -0.542).

Sediments dominated by water transport

The water transported sediments have the lowest mean gravel content (< 1%). There is a slight increase in gravel content at the bottom of cores 19 and 29 which may be the result of increased ice rafting at the time these sediments were deposited. The average sand content in the water transported sediments is also very low (4%). It shows a down core increase in only cores 21 and 29, which may also be related to ice rafting. Silt content (average 44%) is higher for dominantly water transported sediments than for any of the other three sediment types. The down core variations in silt content in the water transport facies have an inverse relationship with sand and gravel content, except for core 21 between 130 cm to 138 cm. Here the silt content decreases as clay content increases. The reason for this occurrence is not certain; however, a change in sediment source, water transport characteristics or bioturbation (as observed in radiographs) are possible causes.

Clay (mean, 52%) is the most abundant sediment present in water transport dominant sediments. Its decrease downward in core 29 is coupled with increased sand and gravel content. Clay shows an opposite trend to silt in core 30 (0 cm - 78 cm). This most likely results from changes in the grain size of the sediment found in the runoff from Inglefield Land, or perhaps in the nature of the dynamics of the water column (current regime, etc.).

The average mean grain size for the water transport dominant sediments is 7.9ϕ (0.0042 mm, very fine silts). The mean standard deviation of these sediments is 2.5ϕ (very poorly sorted). Even though they are classified as "very poorly sorted," they are the best sorted of any sediments collected during this study. This is due primarily to the small amounts of gravel and sand present in the water transport dominant sediments. Increased values of standard deviation in several intervals in cores 19, 21, 29 and 30 are caused by increased gravel content.

The water transport dominant sediments have a high negative average skewness (-0.325) because of the high percentages of the silt and clay fractions relative to the sand and gravel component. The average kurtosis value for these materials is 0.072 (leptokurtic) indicating less (relative to the other three lithofacies) of a bimodal aspect to

the sediment grain size distribution curves, in this environment of deposition.

Till 1

The mean gravel content of till 1 is 15%. It increases downward in core 24 and decreases downward in core 12. Gravel increase is irregular in cores 11 and 26 resulting in abrupt down core changes. Sand is the most abundant sediment type in till 1, (mean value equal to 33%). The average silt content is 29%, making it the second most abundant sediment size in this till. It decreases in abundance as the amount of coarse material (sand and gravel) present in a particular sediment sample increases. Silt is covariant with the clay fraction. The mean clay content in till 1 is 23%, exceeding only the gravel fraction in abundance. Clay generally increases downward in core 12 as does silt, with a concomitant decrease in sand and gravel. There is a marked increase in clay between 9 cm - 20 cm in core 26 which is probably related to an influx of finer material during the previously discussed reworking of the upper part of this core.

The mean grain size of till 1 is 4.0ϕ (0.062 mm, very fine sand). It is extremely poorly sorted with the highest mean standard deviation (4.2ϕ) of the four lithofacies. This is, in large part, due to the abundant coarse material in these sediments. The relative abundance of gravel also results in a skewness which is only slightly negative (-0.055). Because of the wide range of particle sizes (the "tails" of the sample curve are better sorted than the central portion) the sediment distribution curve is very broad (platykurtic) culminating in a larger mean negative kurtosis (-0.671).

Till 2

Till 2 has the largest mean gravel (22%) and sand (41%) contents and the smallest mean silt (23%) and clay (14%) contents of the four sediment types under discussion. Its average mean grain size is 2.7ϕ (0.165 mm [fine sand]) and its average standard deviation is 4.0ϕ , (extremely poorly sorted). The dominance of coarse grained material produces a positive skewness with a mean value of 0.153. The mean kurtosis is -0.445 (platykurtic).

The textural differences between till 2 and till 1 may be due to differences in the bedrock and soils from which the tills were derived. These differences will be discussed later. However, the differences between the textural parameters may be more attributable to the morphology of the Basin. Most of till 1 is found in the deeper water (~ 200 meters) of the western trough whereas till 2 is found in the relatively shallow part of Kane Basin, especially on the northern part of the topographic high, where water depths are 100 meters or less. This area is sometimes free of pack ice during August allowing wind-generated waves to occur. This would provide a greater opportunity for winnowing, by both wave and current action, thereby slightly improving the overall sorting compared to till 1, even though till 2 has a greater average abundance of both gravel and sand.

Originally till 2 may have been much closer to till 1 texturally, but the removal of fines in a higher energy environment resulted in a slightly modified till containing a larger coarse component, slightly better sorting, a more positive skewness and a grain size distribution curve which is less platykurtic, than till 1. In effect, the upper part of till 2 might now be considered a "lag" deposit.

The sediments identified as tills contain more abundant coarse fractions (sand and gravel), less clay, have a lower mean grain size, greater standard deviations (poorer sorting) and are less negatively skewed compared to the ice rafting dominant or water transport dominant sediments. The ice rafting dominant sediments in turn have a relationship similar to that just described, relative to the water transport dominant materials.

Friedman and Sanders (1978) plotted the cumulative-frequency curves of various tills in order to illustrate the textural character of these extremely poorly sorted materials (Figure 45). The cumulative-frequency curves of the four Kane Basin lithofacies were also plotted on this graph. Till 1 and till 2 have cumulative-frequency curves similar to the other tills, as does the ice rafting dominant sediment. However, the ice rafting dominant sediment has a lower coarse-grained fraction and higher clay content than the two tills. Its cumulative-frequency curve plots just above the fine-grained tills from the Valparaiso Moraine (Friedman and Sanders, 1978). The cumulative-frequency curve

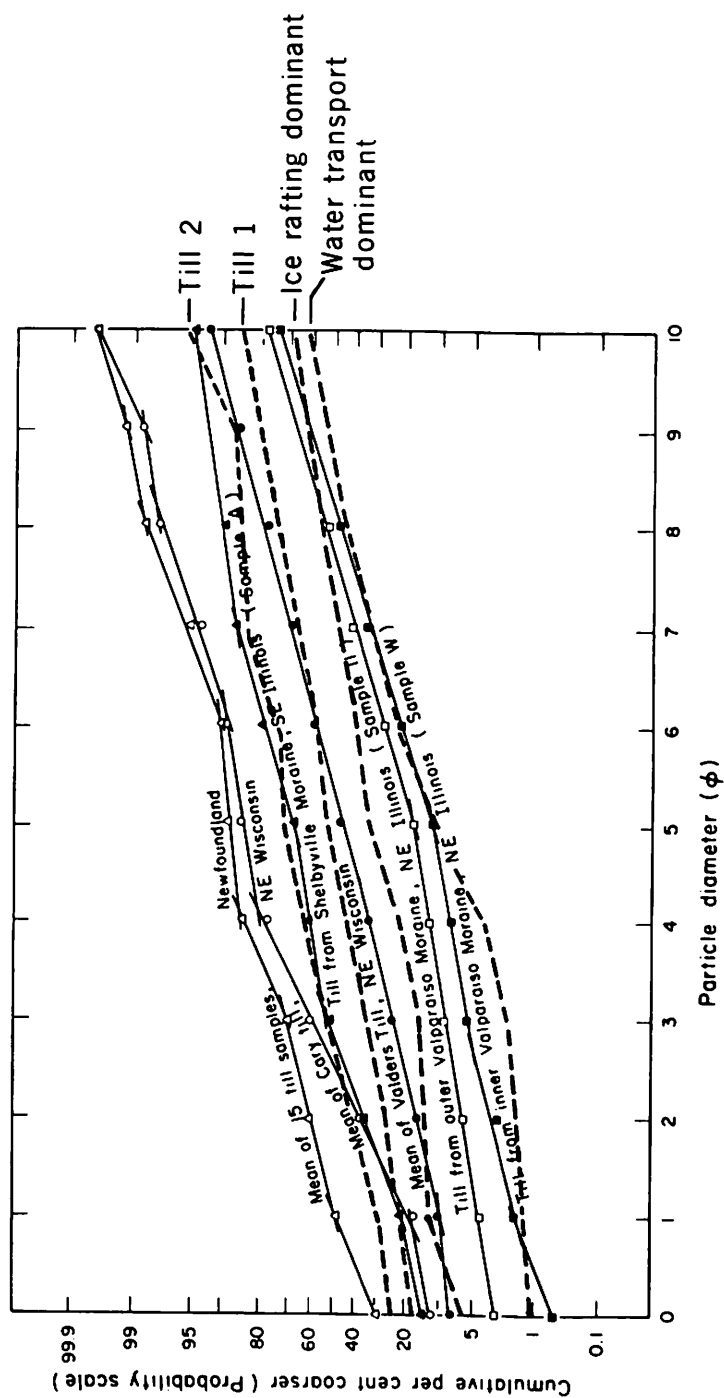


Fig. 45. Graph of cumulative-frequency curves of various tills and glacial marine sediments (after Friedman and Sanders, 1978).

for the water transported sediment falls, for the most part, below these Valparaiso tills. The finer-grained nature of both ice rafting and water transport sediments relative to till 1 and till 2 is apparent when examining this graph. Note that the ice rafting and water transported sediments are composed of approximately 35% and 40% respectively, of material finer than 10M ϕ (.001 mm). Whereas, the greater than 10M ϕ content of till 1 is < 15%; for till 2 it is approximately 5%.

In an attempt to differentiate tills and glacial marine sediments Frakes and Crowell (1973), plotted the mean grain size (M ϕ) vs. inclusive graphic standard deviation of assorted tills, and of glacial marine sediments from the Ross and Beaufort Seas (Figure 46). They reasoned that in a subaerially deposited till, all material is dropped as the ice melts, hence the typically poorly sorted and non-stratified till. In the formation of glacial marine sediments fine debris deposited from icebergs is subject to current action (in the present case this applies to fine water transported sediment as well) and, therefore, is widely dispersed as it settles to the bottom. Thus, subaqueously deposited (glacial) detritus should be somewhat better sorted than till. Except for a few overlapping Beaufort Sea samples the individualized clustering of the samples is quite apparent.

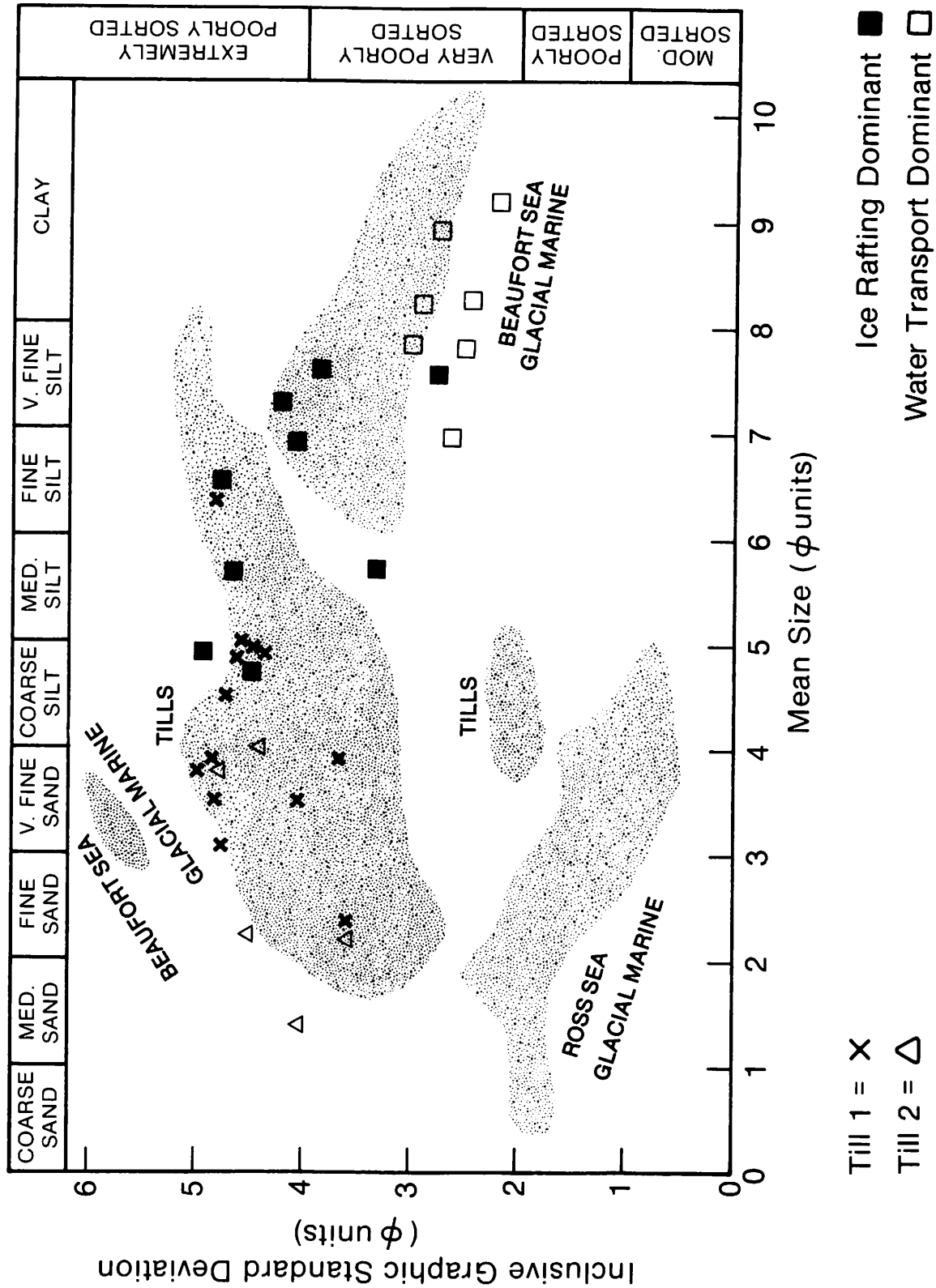
The average mean grain size (M ϕ) and standard deviation values of the four Kane Basin lithofacies have also been plotted on this graph (Figure 46). Note that the sediments identified as tills in the Kane Basin fall primarily into the till cluster. The sediment dominated by ice rafting falls within the tills and the glacial marine sediments of the Beaufort Sea. The sediment dominated by water transport plots within and just below the glacial marine cluster indicating a similar mean grain size but slightly better sorting.

It must be pointed out that the standard deviation values in this study are based on moment measures whereas Frakes and Crowell (1973) used Folk's (1966) Inclusive Graphic Standard Deviation. This difference, however, should not have a significant effect on the outcome.

Mass Physical Properties

In general the areal distribution of the mass physical properties of the surficial sediments of Kane Basin show low wet unit weight values

Fig. 46. Graph of $M(\phi)$ vs. inclusive graphic standard deviation of assorted tills and glacial marine sediments (modified after Frakes and Crowell, 1973). Shaded zones represent data plotted by Frakes and Crowell, 1973.



in the southern and eastern Basin because of the influence of the water transport dominant sediments, and high wet unit weight values in the northern and western Basin. Conversely the water content, void ratio and porosity parameters are highest in the eastern and southern Basin, and have their lowest values in the northern and western portions of the Basin, where the tills are dominant. In the eastern part of the Basin, in the vicinity of the Humboldt Glacier, the wet unit weight values increase while water content, void ratio, and porosity values decrease. This is because the bottom sediments are influenced by the glacier which is producing coarser ice rafted materials.

Sediments dominated by ice rafting

The mean wet unit weight value for the ice rafting dominant sediment is 1.75 gm/cm^3 . Except for cores 18 and 27, all cores containing primarily ice rafted sediment show an increase in wet unit weight values with depth. This is due primarily to a general increase in the coarse fraction down core and possibly to some extent, the effect of overburden pressure. The trend of the wet unit weight in cores 18 and 27 is dominated by marked, down core changes in the coarse fraction. The water content (mean 50%), void ratio (mean 1.36) and porosity (mean, 56%) vary in opposition to wet unit weight. As might be expected, the wet unit weight shows a strong positive covariance with sand and gravel content, while water content, void ratio and porosity all have a strong negative relationship with these size fractions. The opposite relationship exists relative to clay, mean grain size and the four mass physical properties. The relations mentioned here between grain size parameters and mass physical properties apply equally to all four lithofacies, and not only to the ice rafting dominant materials.

The average shear strength values (fall cone measurements) for those ice rafting dominant sediments suitable for testing, was 85 gm/cm^2 with the highest values occurring in the cores nearest Humboldt Glacier, possibly because of the presence of larger amounts of coarse sediment. In the sediments proximal to the Glacier, shear strength decreases down core. The reason for this is not apparent. In the other cores from this facies, no discernable down core shear strength trends were evident.

Those ice rafting dominant sediments fine enough to undergo Atterberg limits testing were found to have for the most part, low to medium plasticity. They were classified, according to Casagrande's plasticity chart (Figure 15) as; SC, SF, ML OL, and CL. The activity (Ac) value for these sediments was < 0.75 and in most cases < 0.40 (Figure 16). The A-line and activity (Ac) categorization of these materials shows them to be sediments with generally low plasticities and activities, typical of sediments derived in large part from glacial processes.

The exceptions to the classifications outlined above are the upper intervals in cores 22 (0 cm - 11 cm, 18 cm - 26 cm) and 23 (0 cm - 10 cm), which are classified as CH (inorganic clays of high plasticity). These cores are farther from Humboldt Glacier and closer to Inglefield Land (a major source of water transported sediments), than the other ice rafted sediment cores tested (5, 17, 18). Apparently the influence of these finer grained materials is greater in the vicinity of cores 22 and 23. This influence is obvious when examining Figures 13 and 14. The upper portions of both core 22 and core 23 have higher liquid limits and plasticity indices than their down core counterparts, and higher activities as well ($Ac > 0.75$ and $Ac < 0.75$, respectively).

Sediments dominated by water transport

The water transported sediments have the lowest average wet unit weight (1.48), and their average water content (101%), void ratio (2.59) and porosity (72%) values are much higher. This can be attributed to the finer grained nature of these sediments, coupled with their high rate of sedimentation and normally consolidated to underconsolidated condition (see Chapter IV).

Core 19 shows a gradual increase in unit weight and a decrease in water content, unit weight and porosity down core, without an accompanying increase in sand and gravel. These trends may, therefore, be due to overburden pressure resulting in some consolidation and dewatering of the material. However, the liquidity index (a rough indicator of consolidation) shows no down core trend which might verify this interpretation. In core 21 wet unit weight also increased down core to 134 cm. Between 134 cm - 150 cm there is a marked decrease in wet unit

weight and a sharp increase in water content. Within this zone is a significant increase in the clay fraction (Table 9 and Figure 61, in Kravitz, 1983). The reason for this increase is not known (see comments under Texture, this chapter). Below 150 cm the wet unit weight once again increases while water content decreases to the bottom of the core. Overall, there is a general coarsening, and increase in wet unit weight down core 21 (becoming finer upward). The down core coarsening is due to increased sand content, and the unit weight trend is related to this as well as to the probable effects of overburden pressure. Core 28, with the lowest wet unit weights and highest water contents of any sediment in Kane Basin is very uniform with water content and void ratio decreasing only slightly down core. This decrease may be due in some part to overburden pressure. The core also shows no significant down core variation in its grain size distribution. It appears to represent constant sedimentation conditions resulting in fairly homogeneous sediment. Bioturbation (Figure 42) could have contributed somewhat to this homogeneity.

Wet unit weight increases down core in cores 29 and 30 (0 cm - 78 cm) while water content, void ratio and porosity decrease. The trends can be attributable in both cases to increases down core in the coarse fraction (and possibly overburden pressure).

The mean shear strength value for the water transport dominant sediments is 38 gm/cm², the lowest of the four lithofacies. This is not surprising since in the Kane Basin shear strength is covariant with gravel and sand; and has a negative relationship with silt, mean grain size, water content and void ratio. The relationship is very obvious from examination of Figure 14. In some instances, low shear strength may have been the result of bioturbation in the sediments dominated by water transport. This process can lower the shear strength of unconsolidated fine grained sediment by destroying the sediments microstructure (Kogler, 1967).

The highest plasticity (LL > 50) of all materials in the Kane Basin is found in the water transported sediments. The plots of these materials on the plasticity chart (Figure 15) classifies them as: CH, MH, OH, and CL sediments, primarily of medium to high plasticity.

Their activities range from inactive ($Ac < 0.75$) to active ($Ac > 1.25$) with the vast majority falling into the normal ($Ac = 0.75$ to 1.25) category.

The distribution of the plots on the plasticity and activity charts strongly imply different sources for the sediments dominated by water transport (see discussion of Atterberg limits and activity characteristics of cores 14, 19, 21, 28, 29, 30 and 31, Chapter IV).

In core 14, these characteristics are the result of a temporal change in the nature of the sediments at this location; the water transported sediment in the lower part of the core reflecting the waning influence of sediments coming from Humboldt Glacier (and perhaps Washington Land) while in the upper part of the core this material is mixed with, and diluted by, sediment from Inglefield Land. This is similar to the previously discussed process affecting the upper portions of cores 22 and 23.

In the case of cores 19, 21, 28, 29, 30 and 31, there is an emerging pattern of temporal change. Smaller liquid limit, plasticity indices, and activity values as found in the sediments further down in the cores, compared to the sediments in the upper part of the cores. This indicates, along with the other mass physical and textural properties previously discussed, that conditions in the south, central and southeastern Basin have changed from an ice dominant regime to one where water transport (especially from Inglefield Land) plays a greater role (Figure 40).

The water transported sediments near Inglefield Land are predominantly micaceous or diatomaceous fine sandy or silty sediments and organic clays of medium to high plasticity (MH/OH). In terms of activity they are mostly normal ($Ac = 0.75$ to 1.25). The sediments are relatively rich in diatoms, plant fragments and organic carbon content. These features are characteristic of most of the materials in cores 28, 29, 30 (0 cm - 78 cm) and 31 (0 cm - 8 cm).

At greater distances from Inglefield Land there is a marked increase in the amount of inorganic clays of high plasticity (CH), with activities ranging from inactive to normal. These are characteristic of cores 19 and 21. Diatoms, plant fragments and high organic carbon values are still relatively abundant in the upper part of core 19 and

within core 21. In the water transport dominant portion of core 14 (0 cm - 90 cm), which is the most distant core from Inglefield Land containing this material, there are no MH/OH type sediments; only CH material whose activity ranges from inactive to normal. In this core diatoms are present only at the surface in rare to frequent quantities. No plant fragments were observed. The relatively high organic carbon content of this sediment can be attributed to the presence of sand and silt sized coal fragments.

Till 1

The till 1 sediments contain an average wet unit weight value of 2.06 gm/cm^3 ; an average water content of 23%; an average void ratio of 0.60; and an average porosity of 38%. Only till 2 has a larger average wet unit weight and lower water content, void ratio and porosity values.

The water content, void ratio and porosity values are opposite to wet unit weight in all till 1 cores, except in core 25, where the specific gravity of the sediments appears to significantly affect the wet unit weight down core distribution. As in the previous lithofacies (ice rafting dominant and water transport dominant), there is a strong correlation among the mass physical and textural properties of the sediment.

Only a limited number of shear strength measurements were made on till 1 sediments because of the coarse grained nature of the material. The mean shear strength value for those sediments measured was 68 gm/cm^2 which is more than the water transported sediments but less than the ice rafted material. This value is misleading, however, because much of the till 1 sediment was so coarse that it was impossible to test with the fall cone. Except for the 25 cm - 35 cm interval in core 11 the till 1 sediments were too coarse for Atterberg limits testing and therefore are considered non-plastic. This one test resulted in a liquid limit value of 26 (low plasticity).

Till 2

The till 2 sediments have the largest average wet unit weight value (2.15 gm/cm^3) and the smallest average water content (20%), void ratio (0.52) and porosity (33%) values of the four lithofacies. This

may be due in part to the effects of the winnowing of the surficial layer of till 2. Because of the shortness of the cores taken in this extremely resistant material no down core data was obtained. The material was too coarse for fall cone tests and Atterberg limits measurements, therefore, the gross shear strength estimate was based on core penetrability and determined to be greater than 300 gm/cm²; all till 2 materials are non-plastic.

Easterbrook (1964), and Boltunov (1970), utilized mass physical properties to differentiate between glacial (tills), and glacial marine till like sediments. Their independent studies in different areas of the world (Easterbrook in the Puget Lowland and Boltunov in Spitzbergen) concluded that void ratios are lower in tills and higher in glacial marine sediments and conversely wet unit weights (also termed bulk densities) are higher in tills and lower in glacial marine deposits. They further stated that it might be possible to expand these relationships to other areas where similar materials are found. Because of the success of these earlier investigations, the wet unit weights (Figure 47), and void ratios (Figure 48) of the four lithofacies in the Kane Basin were plotted.

It can be seen that in each case, with the exception of one crossover, the grouping of the tills, ice rafted sediments and water transported sediments are quite distinct. The crossover sample, core 13, is a very short core which was disturbed during the sampling process. This disturbance may have resulted in a lower wet unit weight. The sediment from core 13 is classified as a till, on the basis of factor analysis, which took into account a large number of parameters.

The grouping of the plots of ice rafted (glacial marine) sediments, and the grouping of the tills in Figure 46, and again in Figures 47 and 48 is quite obvious. This clustering of the samples provides strong evidence for their classification into separate facies.

Carbonate and Organic Carbon Distribution

Surface distribution

The large amount of carbonate in the surficial sediment off Ellesmere Island is the result of the erosion of the Paleozoic carbonate rocks (limestones and dolomites) found along the Island's east coast.

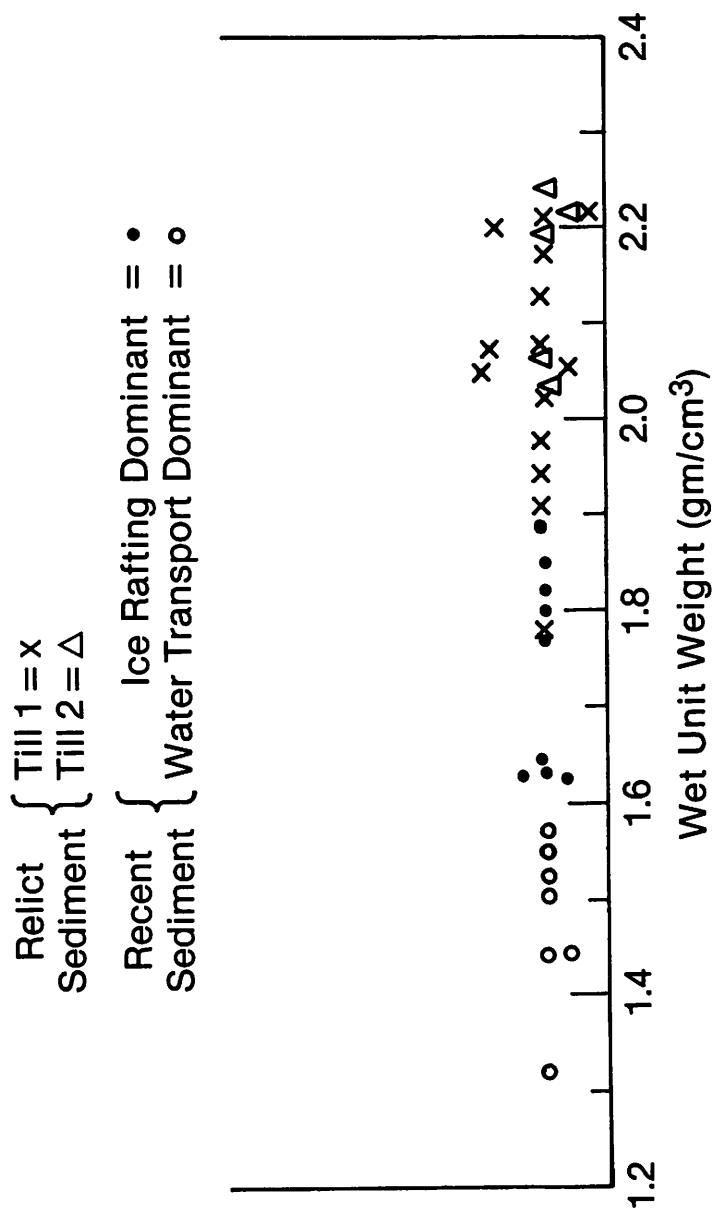


Fig. 47. Graph of wet unit weight values for the four lithofacies.

Relict { Till 1 = x
Sediment { Till 2 = Δ

Recent { Ice Rafting Dominant = •
Sediment { Water Transport Dominant = ○

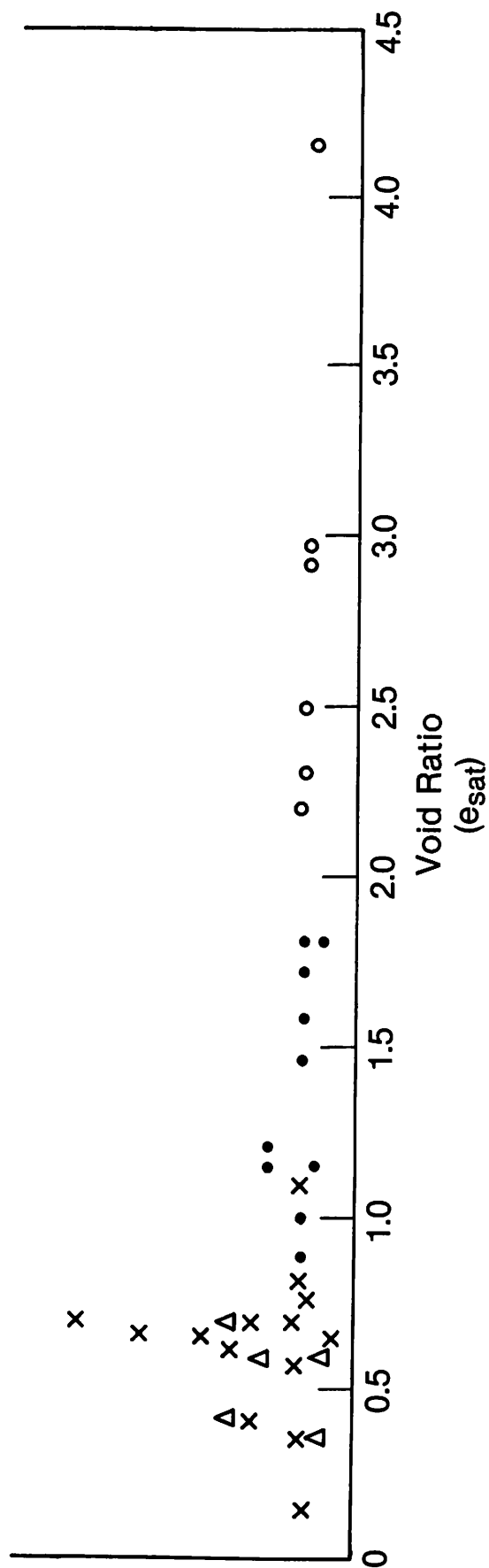


Fig. 48. Graph of void ratio values for the four lithofacies.

The relatively high zone of carbonate in the northeastern Basin is the result of erosion of the Lower Paleozoic carbonate sequences of Washington Land. Quite possibly the Humboldt Glacier is eroding similar carbonates along its northern boundary with Washington Land. The small pocket of high carbonate off Cape Leiper most likely comes from the Lower Paleozoic (Cass Fjord and Cape Kent Formations) which crops out along the coast of Inglefield Land in this vicinity. The tongue of low carbonate values directly off Humboldt Glacier reflects the low quantity of carbonate produced by erosion in this area and supports the view that the Humboldt Glacier is, for the most part, eroding igneous and metamorphic basement rocks (Kravitz, 1976).

The organic carbon distribution in the surficial sediment layer is governed by four components: 1. Cenozoic coal; 2. plant fragments; 3. marine micro-organisms (diatoms and foraminifera); 4. organic coatings on clays. The large high organic carbon zone in the northwestern portion of the Basin is produced by erosion of Cenozoic coal exposed on eastern Ellesmere Island. In addition, the presence of common to very common diatom abundances along the entrance to Kennedy Channel add to this area's concentration of organic carbon.

The other zone of relatively high organic carbon content is along the Inglefield Land coast. This area also contains abundant diatoms, as well as large amounts of terrestrial plant fragments brought into Kane Basin by the streams draining Inglefield Land. Coal particles are ubiquitous in almost all core and grab samples but to a much lesser extent compared to the sediments of the Western Basin.

Sediments dominated by ice rafting (carbonate)

The ice rafting dominant sediments have a mean carbonate value of 16%. Overall, carbonate shows no definite down core trends in these sediments. The ice rafted sediments do show an increase in carbonate content off Washington Land and in those sediments distal from Humboldt Glacier and closer to the western side of the Basin, translating to lateral variations but no apparent temporal change in carbonate content for the ice rafting dominant sediments. The reason for these lateral variations is the dominance of Paleozoic carbonate rocks on both Washington Land and Ellesmere Island.

Sediments dominated by water transport (carbonate)

The water transported sediments average carbonate content is 15%, which is very close to the average carbonate content of the ice rafting dominant sediments. Considering the precision of the analytical technique used there is no significant difference in the average carbonate values between the two lithofacies. Core 21 shows no down core trend but increases markedly at 150 cm. This increase is due to a large number of limestone fragments in the sand fraction of this core between 145 cm - 155 cm. Cores 14 (0 cm - 90 cm), 29 and 30 (0 cm - 78 cm) show slight down core increases in carbonate content. These down core increases in carbonate correspond to previously mentioned increases in the coarse fractions of these cores.

Till 1 (carbonate)

Till 1 has an average carbonate content of 25%, the largest of the four lithofacies. Most of this carbonate probably came from the Lower Paleozoic carbonate sequences on Ellesmere Island and an unknown quantity derived from the Tertiary deposits along the Ellesmere coast facing Kennedy Channel (Miall, in press).

Till 2 (carbonate)

The average carbonate content of till 2 is 18%, the second largest of the four lithofacies. The main source of this carbonate is probably the Lower Paleozoic carbonates of Washington Land. This interpretation is based on the proximity of the lithofacies to Washington Land, as well as its (exposed) distribution pattern on the floor of the Basin (Figure 17).

Sediments dominated by ice rafting (organic carbon)

The average organic carbon value for the ice rafting dominant sediment is 0.54%. The organic-carbon-down-core-distribution for all four lithofacies is quite irregular and it is not possible to establish a simple rationale for its temporal distribution. In some of the cores (e.g., core 18) there is a covariant relation with the abundance of clay; in other cores no apparent relationship to grain size exists. The limited organic carbon content in the ice rafting dominant sediments can

be attributed in varying degrees to marine micro-organisms (diatoms and foraminifera), coal, and organics related in some way to the clay fraction of the sediments.

Sediments dominated by water transport (organic carbon)

The water transported sediments have an average organic carbon content of 1.04%. Their down core distributions are also not systematic. The organic carbon in these sediments can be attributed to large amounts of diatoms, plant fragments from Inglefield Land, and to a lesser extent, coal fragments; all of which have been microscopically identified in these materials. Many of these sediments are found at water depths in excess of 300 meters, where the organic material, because of its light weight, tends to settle out along with the clay fraction, and where the organics are not as readily oxidized or biodegraded as are those organic materials deposited along with coarser sediments at shallower depths. The presence of bioturbation in the fine grained water transported sediments is proof of an active benthos, and another possible explanation for the erratic down core distribution of organic carbon.

Till 1 (organic carbon)

Till 1 sediments have an average organic carbon content of 1.07%, about equal to the water transport dominant sediment. The high till 1 organic carbon content, except for the large numbers of diatoms at the surface of cores 2, 3 and 4 and to a much lesser extent at the tops of cores 9 and 13, is due to the presence of coal. With the exception of the previously mentioned diatoms and a few foraminiferal tests near the top of core 11 the till 1 sediments contain no marine micro-organisms, but they do contain abundant coal particles. The down core distribution of the organic carbon once again displays an irregular pattern.

Till 2 (organic carbon)

The average organic carbon content of till 2 is 0.20%, the lowest of the four lithofacies. The presence at the till surface of rare to frequent diatom abundances provides one source of organic carbon and coal particles another source.

Gravel and Sand Composition

The distribution of gravel and heavy minerals in the surficial sediment layer of Kane Basin is discussed by Kravitz (1975). Briefly, the eastern half of the Basin is dominated by sediments whose gravel fractions contain crystalline rock fragments with lithologies similar to the crystalline basement rocks exposed on Inglefield Land, and those rocks presently being eroded by Humboldt Glacier. Carbonate rocks are the principal component of the gravels from Ellesmere Island eastward to the middle of the western trough. They are also dominant in a lobe extending from Kennedy Channel down to about 79°28'N, covering part of the northern topographic high.

Sediments with gravel fractions containing fragments of clastic rocks (sandstone, siltstone, etc.) occur in a strip extending from Kennedy Channel to Bache Peninsula, covering the eastern half of the western trough and the entire western edge of the topographic high. A concentration of highly friable and stained rock fragments, predominantly clastics, but including some carbonate rock fragments, occurs in the gravel fraction of the sediments found in a zone stretching in a southwesterly direction from Kennedy Channel to Buchanan Bay. This zone covers most of the western trough, and a large part of the western topographic high.

The gravel fractions of the ice rafted and water transported sediments are overwhelmingly of crystalline origin (see Table 8 in Kravitz, 1975). Samples closer to the western Basin and to Washington Land, and which show an increase in their overall carbonate content, also have more carbonate rocks in their gravel fraction.

The till 1 gravels are composed predominantly of carbonate and clastic rock fragments, many of which are stained (both brown and black) and friable. Many of these carbonates appear arenaceous. The clastics are siltstones composed of quartz and fresh feldspar in a clay and chlorite matrix, litharenites (containing basalt grains rich in plagioclase microlites), claystone, limestone, quartz, feldspar, and ferromagnesian minerals in a fine grained groundmass. When first discovered (Kravitz, 1975), the origin of these clastic components was unknown. However, Miall (in press) has reported on the results of field work conducted in 1977 which identified Tertiary clastic sedimentary rocks

which crop out along the northeast coast of Ellesmere Island, flanking Kennedy Channel (Figure 3). The composition of these Tertiary rocks and the materials making up till 1 are very similar, including the heavy mineral and clay mineral assemblages. The Tertiary rocks are therefore proposed as the origin of much of the material of till 1. The till 1 cores (10, 11, 12, 25) closer to Ellesmere Island contain relatively abundant carbonate rocks in their gravel fractions compared to clastics. The samples of till 1 farther to the east are rich in the clastic rocks just described.

Both crystalline rocks and carbonate rocks make up the gravel component of till 2, although carbonates dominate. The crystalline rocks dominate only in core 6, the till 2 sample closest to Humboldt Glacier. The provenance of the carbonate rocks is probably Washington Land with a minor contribution from Ellesmere Island. Further petrographic work is needed to resolve this question.

Sediments dominated by ice rafting

The ice rafted sediments contain the following heavy mineral suite: non-opaques (77%), alterites (5%), opaques (15)%, and aggregates (3%). The most abundant non-opaque minerals include garnet (44%), orthopyroxene (23%), clinopyroxene (9%), and amphibole (17%) (see Table 13). The total amount of accessory (secondary) heavy minerals comes to 7%.

The ice rafted sediments heavy minerals generally show no well defined down core trends. The cores nearest Humboldt Glacier (16, 17, 18) are an exception to this generalization. In these cores garnet content decreases down core while orthopyroxene content increases. The two minerals, the most prominent in the sediments dominated by ice rafting, show negative correlation with each other. This is probably caused by changes in the rocks undergoing erosion beneath the Humboldt Glacier. The garnet bearing rocks (schists and gneisses?) are presently being eroded and the rocks containing hypersthene (gabbros and tonalites?) are now less common and therefore less frequently in contact with the ice. Most of the minerals in the vicinity of the Humboldt Glacier are angular; in core 18 some of the hornblende is rounded, implying a secondary (albeit minor) sediment source in this area.

Core 22 (0 cm - 36 cm) has been classified as ice rafted sediment. Below 36 cm it has mass physical and textural properties more characteristic of till 2. The downward increase in amphibole and the concomitant decrease in garnet and orthopyroxene lends additional credence to this view. Core 30 (78 cm - 101 cm) contains many rounded orthopyroxenes and the few tourmaline grains present are also rounded. There are fresh appearing biminerallitic aggregates of garnet and orthopyroxene as well as an assortment of stained, corroded and rounded grains. Many of the non-opaques are etched. Considering the nature of these sediments and the proximity of Inglefield Land, it is apparent that many of the heavy minerals found in the lower part of core 30 originated from the tills and soils of this area (Tedrow, 1970). The sources then, of the sand fraction of the ice rafting facies, are predominantly the fresh materials produced by Humboldt Glacier and to a lesser extent the weathered tills and soils of Inglefield Land.

Sediments dominated by water transport

The water transported sediments contain the following heavy minerals suite: non-opaques (77%), alterites (6%), opaques (14%) and aggregates (3%). The most abundant non-opaque minerals include garnet (42%), orthopyroxene (23%), clinopyroxene (12%), and amphibole (16%). The composition of the heavy minerals in the ice rafting and water transport sediments are practically identical indicating similar source rocks. This is significant since a high proportion of the sediments dominated by water transport originate in Inglefield Land (see previous discussions on texture and mass physical properties). The heavy mineral analysis further substantiates an Inglefield Land origin. The large amounts of corroded, stained (brown and red), and rounded orthopyroxenes, clinopyroxenes, garnets, tourmalines, amphiboles and zircons (in some cases mixed with plant fragments), are typical of the heavy mineral suites in the tills and soils of Inglefield Land (Tedrow, 1970).

The difference between the mineralogy of the ice rafting facies and the water transport facies, therefore, is not in the presence/absence of certain species or in their relative concentrations, but in the physical character of the grains themselves. In the ice rafted sediment the vast majority of grains are angular to subangular, and fresh in appearance.

Only a very small proportion of grains, those near Inglefield Land, are rounded, stained, etched, etc. In contrast the sediments dominated by water transport contain a very large number of the grains which are weathered and rounded (contributed by Inglefield Land) as well as angular and fresh. The similarity of mineral species and their relative concentrations indicates that the rocks being eroded by the Humboldt Glacier and the basement rocks exposed on Inglefield Land are very similar.

Down core variations of the heavy mineral components in the water transported sediments provide little definitive information. Cores 14 (0 cm - 90 cm), 19, 21 and 28 show an increase in garnet in the surficial layer (as in cores 16, 17, 18). This is additional evidence in support of the present day erosion of garnet bearing rocks on the Greenland landmass which borders the eastern side of Kane Basin. In cores 28 and 29 there are high (anomalously high relative to the other cores) percentages of dolomite, especially between 14 cm - 45 cm (17%) in core 29. Tedrow (1970) reported large quantities of dolomite in the soils of Inglefield Land, which is possibly the source for dolomite in cores 28 and 29.

Till 1

The till 1 sediments contain the following heavy minerals suite: non-opaques (53%), alterites (7%), opaques (14%), and aggregates (26%). The most abundant non-opaque minerals include garnet (13%), orthopyroxene (7%), clinopyroxene (55%), and amphibole (15%). The combined total amount of the accessory (secondary) heavy minerals is 10%. The difference between the heavy mineral suite of till 1 and the ice rafted and water transported sediments is marked. Clinopyroxene is the major mineral species in till 1 with garnet and orthopyroxene subordinate. The non-opaque component is considerably lower and the percentage of aggregates much higher than the ice rafting and water transport facies. The high percentage of aggregates is believed to be due to the presence of the large clastic rock component of the gravel fraction in this till (Kravitz, 1975). There is 3% more accessory minerals in till 1 than in the ice rafted and water transported sediments. This is a large amount in view of the overall low percentages of these minerals in Kane Basin

sediments. Aggregates increase with depth in core in all till 1 cores. Except for core 12, garnet and orthopyroxene show upward increases while clinopyroxene decreases slightly. The non-opaques also tend to increase in abundance upward, or show no change. These trends indicate the addition (through reworking) of recent sediments into the upper portion of the till. There is some indication of this mixing in the upper few centimeters of core 11 due to the presence of foraminiferal tests, and in the upper few centimeters of core 26 which show current activity (Figure 44). It can also be seen in the mixing of factors I and II in cores 25 and 26 (Figures 182 and 183, respectively, in Kravitz, 1983).

From an examination of the character of the various heavy mineral fractions it is obvious that the provenance of till 1 differs considerably from that of the ice rafting and water transport facies. This is emphasized by the abundance of clinopyroxene, accessory (secondary) heavy minerals, and aggregates in the till 1 sediments. In previous work (Kravitz, 1975) the origin of the clinopyroxene in till 1 was unclear. It is now believed that much of the clinopyroxene was derived from the sand fraction of the Tertiary outliers found on Ellesmere Island and from the many basalt fragments found in the Tertiary litharenites. A positive correlation exists at the 99.0 level of significance between sphene, chlorite (sand-sized) and epidote inferring a common origin. This suite can occur as the result of low temperature metamorphism in limestone and dolomite terrain (similar to that found on Ellesmere Island) producing calc-schists. These three minerals also occur in phyllites, which are found as sedimentary clasts in the Tertiary outliers. The source of the phyllite component is considered to be the Proterozoic and Paleozoic rocks underlying the Tertiary in northeast Ellesmere Island (Miall, in press). The Ellesmere Island Tertiary outliers are, therefore, the origin of the majority of the heavy minerals, as well as the gravel fraction in till 1.

Of the till 1 samples, two are mineralogically distinct from the rest (core 4 and core 14 [108 cm - 132 cm]). These two samples are composed of a sediment rich in kaolinite and aggregates, and low in clinopyroxene, expanding lattice clays, and non-opaques. In the case of core 14 (108 cm - 132 cm) there are relatively large quantities of tourmaline, rutile, zircon and opaques present. Factor II has the

strongest loading values for these samples, however, the communality* of the samples is low, indicating that more factors would be required to properly account for the variance present in this sediment. The samples are mineralogically different from other samples of till 1 but similar in other physical parameters (thus the relatively high factor II loading values) which indicates a different provenance, but similar sedimentological processes (i.e., deposition by ice). Although the provenance of this sediment is unknown, certain aspects of the source area can be evaluated.

The large amount of kaolinite and the low Fe and Mg contents of these materials, compared to the surrounding sediments (Table 15, Kravitz, 1983), may indicate they originated in a fresh water acidic environment (Keller, 1970). The heavy mineral suite with abundant rounded tourmaline, zircon and rutile, as well as numerous aggregates indicates derivation from sedimentary source rocks. Based on the evidence available these source rocks could be siltstones or sandstones (polycyclic sediments). If Pelletier's (1966) interpretation of the Kane Basin as a drowned watershed is correct, perhaps the source rocks are highly weathered, clay rich interfluvial materials. Cambrian(?) sandstones have recently been discovered along the coast of Washington Land (John Peel, personal communication); however, they have not yet been studied.

Till 2

The till 2 sediments contain the following heavy minerals suite: non-opaques (79%), alterites (5%), opaques (13%), and aggregates (3%). The most abundant non-opaque minerals include garnet (33%), orthopyroxene (23%), clinopyroxene (8%), and amphibole (22%). The total amount of the accessory heavy minerals is 7%.

This heavy mineral suite is similar to that in the ice rafting and water transport facies except for a higher amphibole content (the highest of the four lithofacies). Based on the lithology of the gravels, primarily carbonates with some crystallines, I interpret the

* Communality represents that proportion of the variance of a variable accounted for by the number of factors used.

sources for this till to be the carbonate rocks of Washington Land and the basement rocks underlying Humboldt Glacier. The heavy mineral suite of till 2 supports the interpretation that the basement rocks are a source for this sediment. The contribution of Ellesmere Island to till 2 is unknown. The higher amphibole content in this part of Kane Basin was first reported by Kravitz (1975). The cause for this anomaly remains uncertain. However, since no source of amphibole has been found in the land mass bordering this part of the Basin (Peter Dawes, John Peel, personal communication), a relict sediment source is suspected.

The Character and Distribution of the $< 2 \mu\text{m}$ Fraction Mineralogy

Surface distribution of clay minerals

Illite is the dominant clay mineral in Kane Basin. Its greatest concentration occurs in the surficial sediment in the areas adjacent to the Humboldt Glacier and Inglefield Land. Keller (1970) considers one of the sources of illite to be glacial comminution of antecedent mica. The large concentration of illite near the Humboldt Glacier is attributed, therefore, to glacial erosion of the micaceous rocks underlying the Glacier. Since illite denotes a weathering product, most of the material found under the 10\AA peak in samples directly off the glacier might better be termed clay-sized mica. Tedrow (1970) reported illite in the soils of Inglefield Land as well as vermiculite, montmorillonite and kaolinite. The high concentration of illite adjacent to Inglefield Land may also be due to input from the glacial deposits which cover large segments of this landmass, since illite is abundant in many tills which overlie high rank metamorphic terrains (Piper and Slatt, 1977). The decrease in illite abundance in the surficial sediments to the north and west is caused by dilution by increased amounts of expanding lattice clays, kaolinite and chlorite in these areas. In addition, the effect of the southerly current in the western Basin interferes with the deposition of illite-bearing recent sediments.

The expanding lattice clay is the second most abundant clay mineral group in the Basin. Its greatest concentration is in the western Basin where it is associated with the Ellesmere Island till (till 1). The relatively large amount of expanding lattice clays in the surficial

sediment directly off Inglefield Land indicates derivation from the vermiculite (a mixed layered clay) and montmorillonite rich soils in this area. The high concentration of expanding lattice clay in the northeastern part of the Basin points to a possible source in the soils of Washington Land; however, the mineralogy of these soils is not known. The zone of expanding lattice clay (11% - 20%) directly off Humboldt Glacier may simply be due to the influence of nearby Inglefield Land. The area of low expanding lattice clay values in the eastern Basin is caused in part by the very high illite load carried by Humboldt Glacier.

Kaolinite in the surficial sediment is concentrated in the northern Basin as a result of the presence of relict sediment in this area. The origin and nature of these materials was discussed in the previous section.

The distribution pattern of chlorite is not easily explained. In the western Basin, chlorite occurs as the matrix of some siltstones and litharenites and it is often a constituent in the phyllites found in till 1. In the southern part of the Basin some of the chlorite is probably derived from the soils of Inglefield Land. In the rest of the Basin the origin of the chlorite is even less well defined. Several possible sources I suggest are the following: some of the chlorite may be the result of diagenetic changes; however, in Kane Basin the vast majority of this mineral is considered to be detrital. The configuration of the zone of high chlorite content across the northern part of Kane Basin, with lower values on either side, suggests a possible submarine origin (relict material? diagenesis?). Some of the cores near Humboldt Glacier show several high chlorite values down core identifying the glacier as a possible source of at least some chlorite. However, if the glacier is presently supplying chlorite, it is only a small amount.

Sediments dominated by ice rafting

The clay mineralogy in the ice rafted facies is as follows: illite 70%, expanding lattice clays 10%, kaolinite 8% and chlorite 12%.

In cores 5, 16, 17, and 22 there is a general increase in expanding lattice clays downward indicating lower amounts of this material in the most recent ice rafted sediments. Illite shows the opposite trend. In core 17 an inverse relationship exists between illite and chlorite.

When there is an increase in the amount of one mineral there is a decrease in the amount of the other, pointing to different sources or fluxuations in the same sources. Cores 23, 27, 30 (78 cm -101 cm), and 31 (8 cm - 41.5 cm) have a greater content of expanding lattice clays in their upper layers than lower in the core. This may be attributed to either the influence of the sediments coming from Inglefield Land or from the western Basin, since both areas contain more expanding lattice clay than the sediment originating from Humboldt Glacier. In all cases kaolinite is either more abundant in the lower portion of the cores or shows no down core variation; chlorite exhibits no apparent pattern.

Sediments dominated by water transport

The clay mineralogy in the water transported facies is as follows: illite 67%, expanding lattice clays 13%, kaolinite 8% and chlorite 12%. In core 14 (0 cm - 90 cm) the expanding lattice clay increases in abundance upward until approximately 20 cm from the top at which point illite increases and the expanding lattice clays decrease. This indicates a greater sediment input from Humboldt Glacier, or a reduction in the amount of expanding lattice clays available. The increased abundance of illite in core 19 from 76 cm to 83 cm corresponds to an increase in gravel and rock flour and denotes a slight increase in ice rafting at this location. Expanding lattice clay and kaolinite generally decrease in abundance upward as illite and chlorite increase. Core 21 exhibits a marked decrease in expanding lattice clay in the lower portion of the core. This correlates with an increase in illite, sand and silica rich rock flour which, along with the plasticity and activity (Ac) character of the materials, indicates deposition of sediment derived from the Humboldt Glacier. Cores 28, 29, 30 and 31 generally show an overall up core increase in expanding lattice clay which reflects deposition of sediments derived from Inglefield Land or from the western Basin. They have higher kaolinite concentrations down core indicating that past conditions were more favorable to its production than the present, and/or that kaolinite bearing materials were more available for erosion in the past. In these cores illite remains unchanged or increases in quantity upward, while chlorite has no obvious pattern.

Till 1

The clay mineralogy in till 1 is as follows: illite 51% (the lowest illite value in the four lithofacies), expanding lattice clay 22% (the highest value for the four lithofacies), kaolinite 15% (the highest value for the four lithofacies) and chlorite 12%.

Except for core 14 (108 cm - 132 cm) the expanding lattice clays increase in abundance down core. This pattern is at times obscured in the upper part of some till 1 cores because of mixing. The opposite relationship exists for illite. The downward increase in expanding lattice clays and decrease in illite simply reflects the dominance of illite in the Recent sediments. The lower portion of core 14 contains abundant kaolinite. Kaolinite has its greatest concentrations in the lower portions of most till 1 cores, or shows no trend. Chlorite, with the exception of core 12, increases up core or shows no trend at all.

Till 2

The clay content in till 2 is as follows: illite 72%, expanding lattice clays 8% (the lowest of the four lithofacies), kaolinite 8%, and chlorite 12%. As with the heavy minerals and gravel component the clay mineralogy most closely resembles the sediments dominated by ice rafting and water transport. Therefore, Greenland is identified as the source for this material.

In summary, illite is the dominant clay mineral in the Kane Basin sediments. It shows a general increased abundance upward in the cores. This pattern is especially obvious in the eastern Basin near the Humboldt Glacier, which is the main source of illite in Kane Basin. In the vicinity of Inglefield Land (where expanding lattice clays are present in the soil) the expanding lattice clays increase in abundance up core in the water transport dominant sediments. This may be due to the increasing influence of Inglefield Land as a sediment source for the Kane Basin. In the western Basin, where till 1 dominates, expanding lattice clay is relatively abundant. This material is probably derived from alteration of the volcanic material in till 1. In addition, expandable clay is abundant on Ellesmere Island in the Tertiary materials identified by Miall (in press). A large expanding lattice clay component is expected in till 1 since these Tertiary

sediments found in this till contain large amounts of these minerals (see previous discussions). The up core decrease in abundance of expandable clay reflects the influence of present day sedimentation dominated by illite. Kaolinite generally decreases in abundance up core, indicating that very little is being derived from present day sources. The kaolinite, like the expanding lattice clays, is considered relict (see section on Gravel and Sand, this chapter) rather than modern although the two were derived from different sources. The chlorite in the clay fraction, like the expanding lattice clays, is more abundant in the western Basin and has positive correlation with many of the same mineralogical components. In some cases chlorite shows concomitant up core increases with illite and is locally common near Humboldt Glacier (core 17) indicating possible derivation from present day sources. Diagenetic changes are also a possibility.

Surface distribution of rock flour

The distribution of rock flour in the surface sediment layer of Kane Basin identifies the Humboldt Glacier as its main producer with lobes of decreasing rock flour abundance extending westward from the glacier (Figure 23). The amount of rock flour in the surface layer decreases in a westerly direction and then increases along the Ellesmere Island coast. This is probably a result of the activity of valley glaciers on the Island. The elongate nature of this zone is considered to be due to the spreading action of the current which moves in a southerly direction down the western side of Kane Basin. This current is also the most likely reason for the thin elongate lobe of low rock flour content found in the western Basin. It may also be the reason why till 1 is still exposed; the current reduces the deposition of Recent sediments.

The concentration of silicates in the rock flour in the eastern Basin (Figure 24) and of carbonates in the western Basin (Figure 25) mirror the nature of the source rocks on either side of Kane Basin. In the east they are primarily igneous and metamorphic Proterozoic basement rocks and on the west, Paleozoic carbonates. The high concentration of carbonate in rock flour across the entrance of Kennedy Channel is due to the proximity of both Ellesmere Island and Washington Land. The unusual

pattern of the carbonate distribution in the western Basin is possibly an artifact of the current activity in this area. It is obvious from an examination of both the rock flour's distribution and its composition that silicates originating in Greenland strongly dominate this material in the surface sediment layer of Kane Basin.

Sediments dominated by ice rafting

Rock flour comprises 19% of the $< 2 \mu\text{m}$ fraction of the ice rafting facies. It contains quartz (41%), feldspar (41%), amphibole (3%), and carbonate (15%).

In core 5 rock flour decreases in abundance up core. In core 16 rock flour and illite are relatively abundant between 45 cm - 55 cm. In this interval clinopyroxenes, opaques and expanding lattice clays show correspondingly low abundances. This may reflect an increase in Humboldt Glacier activity. There is more rock flour in the upper part of core 18 while in cores 20, 22, 30 (78 cm - 101 cm) and 31 (8 cm - 41.5 cm) rock flour increases down core as does the $< 2 \mu\text{m}$ carbonate. The cores and grab sample nearest Humboldt Glacier are richer in $< 2 \mu\text{m}$ feldspar than in quartz.

Sediments dominated by water transport

Rock flour comprises 15% of the $< 2 \mu\text{m}$ fraction of water transported sediments. It contains quartz (51%), feldspar (40%), amphibole (3%), and carbonates (6%).

Core 14 (0 cm - 90 cm) sediments show a general upward increase in rock flour, most likely originating from Humboldt Glacier. This is supported by the fact that feldspar is more abundant than quartz in this material. Rock flour content is higher in the lower portions of cores 19, 21 and 29 than in their upper portions. This provides additional evidence that water transport processes are having increasingly greater influence (over ice rafting processes) on the sediments in this part of the Basin. Cores 28 and 30 show no down core trend relative to rock flour.

Till 1

Rock flour comprises 14% of the $< 2 \mu\text{m}$ fraction of till 1. It contains quartz (29%), feldspar (14%) and carbonate (57%). The quartz and feldspar content is the lowest of the four facies and the carbonate content is the highest. There is no detectable amphibole in this sediment. The high relative carbonate content in the rock flour in these sediments strongly supports Ellesmere Island as their source.

Cores 25 and 26 show an upward increase in rock flour until 35 cm and 24 cm respectively. From these intervals to the surface there is a decrease in rock flour abundance. This decrease in rock flour may be due to the previously discussed mixing (with sediment containing a larger clay mineral component) or winnowing because of current activity. Either process is the plausible reason since even though the % clay minerals in the $< 2 \mu\text{m}$ fraction increases while % rock flour decreases, the total % clay size shows a decrease. None of the other cores from till 1 have definite rock flour trends down core.

Till 2

Rock flour comprises 25% of the $< 2 \mu\text{m}$ fraction of till 2, the highest of the four lithofacies. It contains quartz (40%), feldspar (36%) and carbonates (24%). No $< 2 \mu\text{m}$ amphibole was identified in these sediments.

The till 2 sediment cores, with the exception of core 22 (36 cm - 44 cm), only penetrated approximately 20 cm below the sediment-water interface. This low penetration is due to the extreme resistance of the till to coring.

The greater abundance of carbonate in the $< 2 \mu\text{m}$ fraction corresponds to the larger carbonate content in the gravel component and the higher percent carbonate in the total sample, relative to the ice rafted and water transported sediments. This carbonate enrichment is attributed to the proximity of carbonate rich Washington Land.

The absence of amphibole in the $< 2 \mu\text{m}$ fraction is surprising since till 2 contains the largest sand sized amphibole content of the four facies.

The Humboldt Glacier is presently the main producer of rock flour in the Kane Basin. A lesser amount of this material is believed to be

coming from the glaciers on Ellesmere Island. Rock flour is also a component of the relict sediment (till 1) in the western Basin.

Chemical Elements in the $< 2 \mu\text{m}$ Sediment Fraction

The chemical elements analyzed for in the $< 2 \mu\text{m}$ fraction were; Fe, Mg, Mn, Cr, Co, Ni, Zn, Cu and Ti. These elements have their greatest concentrations in the western Basin. In the case of Fe and Zn the high concentrations are due to only two cores (10 and 27). All of the elements have their lowest concentrations in the northeastern Basin along the topographic high.

The distribution of Fe in the sediments of the Kane Basin is controlled by a number of factors. In the northeastern Basin its distribution is based on the lower values of Fe in the kaolinite rich sediments found on the topographic high. The low Fe concentrations directly off Inglefield Land generally correspond to areas of high silt and lower clay content (Kravitz 1975). It is possible that much of the Fe occurs as oxide coatings on clay sized particles (Gibbs, 1973) emanating from Inglefield Land, which are carried farther out to sea. Another possibility is that when the fresh water comes into contact with sea water the dissolved Fe precipitates out as clay- and colloid-sized particles. It is then swept away from the coast while suspended in the water column (Coonley et. al. 1971). An additional alternative is simply dilution caused by a high rate of deposition of Fe deficient sediments. The possibilities outlined above may also explain the lower Fe concentrations off Ellesmere Island near Dobbin Bay.

The reason for the high content of Fe and other elements (Mg, Mn, Cr, Co, Ni, Zn and Cu) in the surface layer of core 27 (0 cm - 16.5 cm) is unknown. Core 27 contains stained gravel and it does have a fairly high percentage of opaques (18%) as well as chlorite (13%), and amphibole (1%) in the $< 2 \mu\text{m}$ fraction. The stain may represent oxide coatings which scavenged other elements. The cumulative effect of these constituents may result in the high chemical element content.

Fe has a positive correlation ($> .4 - < .6$) with Mn, Cr, Co and Ni at the 99.9 level of significance. This is not a strong correlation, but it may indicate a relationship of Fe to basic igneous rock sources (Cr, Co, and Ni). Because the correlation includes Mn this relationship

may be due more to scavenging by iron and manganese oxide (MnO_2^-) coatings on sediment particles, than to the basic igneous rock sources.

The Mg distribution is marked by locally high concentrations (Figure 27). Mg is dominant in the western Basin and has its lowest concentrations (as does Fe) in the kaolinite rich sediments on the topographic high. The Mg content of the western Basin is primarily attributed to the influx of carbonates (dolomites) from Ellesmere Island and possibly to the chlorites present in the till 1 sediment.

Mg has a strong positive correlation ($>.7$) with Mn at the 99.9 level of significance. Mn can substitute for Mg in both limestones and dolomites and this may be a reason for the strong correlation. Mg shows a weak positive correlation ($.4 - < .6$) with Cr, Co, Ni and Cu at the 99.9 level of significance. Therefore, Mg sources attributed to both metamorphic and basic igneous rocks (such as those present in till 1) are a possibility. The covariance between Mg, spinel and clinopyroxene coupled with the correlations between Mg and the transition elements indicate a possible basic igneous rock source for at least some of the Mg in the Kane Basin sediments.

The most important source of Mn in the Kane Basin may be ferromanganese oxide coatings on the sediments of the western Basin. The strong positive correlation ($> .6$) at the 99.9 level of significance among Mn and the elements Cr, Co, and Ni indicates that the same major processes influence all four elements. The degree that this relationship is due to scavenging, or to a common basic igneous rock source is not known.

Ni with its high crystal field stabilization energy is capable of replacing many other elements in the crystal lattice of minerals. Therefore, it is not surprising to see it concentrated in the western Basin, since it readily replaces Mg and possibly Al in the montmorillonite lattice (Grim, 1968).

The strong positive correlations ($> .7$) among Cr, Co, Ni and Cu at the 99.9 level of significance indicate a communality of source. This natural grouping of elements is often associated with the minerals from ultrabasic and basic rocks.

The greatest concentration of Ti in the Kane Basin is found in the western trough. This, along with its covariance with Mn, Cr, Co, Ni and

Cu indicates a primary origin similar to these trace elements. Sources for Ti include the fragments of basalt found in till 1 as well as the resistates (i.e., rutile) found in most of the Kane Basin sediments.

Zn^{2+} has an ionic radius and charge similar to Mg^{2+} and it may, during the early magma stage substitute for this element in mafic minerals such as clinopyroxene (Rose, et. al. 1979). It would be reasonable to assume, therefore, that one likely, though not exclusive source for this element, is the basaltic material found in till 1. The main concentrations of Zn, however, are in the eastern Basin. In addition to its possible occurrence in the mafic minerals found on this side of the Basin there are two other potential sources; the soils and plants of Inglefield Land (Tedrow, 1970) and, to a lesser extent, the marine fauna and flora found in the eastern side of the Kane Basin.

The chemical element averages for the four lithofacies can be found in Table 6. Except for Fe and Zn the till 1 lithofacies has the highest chemical element values. The difference in the average Zn values between till 1 and the ice rafting facies is small, however, the large Zn values in till 1 are restricted to only a few samples whereas the high Zn values in the eastern Basin are more evenly distributed. The higher Fe values in the eastern Basin may be due to iron bearing minerals from Greenland's Proterozoic igneous and metamorphic basement and to the higher clay component in the sediments. The elevated percentages of the chemical elements in till 1 are due to sources previously mentioned namely the basaltic and metamorphic fragments in the till, the minerals derived from them, scavenging of elements by ferro-manganese oxides, and in the case of Mg, the primary source is probably the carbonate rocks (dolomites) of Ellesmere Island.

Diatom Distribution

The high concentration of diatoms in the sediment adjacent to Inglefield Land and across the entrance to Kennedy Channel is attributed to the availability of nutrients. In the case of Inglefield Land nutrients are found in the waters draining this land mass. The nature of these nutrients and their concentrations can be ascertained to some extent by reviewing the analysis conducted on the soils and plants of this area by Tedrow (1970). Generally they consist of nitrogen,

phosphorus and silica along with some of the major and minor elements previously discussed. The high diatom abundance in the northern Basin is probably caused by upwelling due to shoaling in the Kennedy Channel at the entrance to the Kane Basin.

The ice rafting sediment cores nearest Humboldt Glacier, except for core 16, have rare to frequent diatoms in their surface layer. No diatoms were found in the lower layers of these cores. This is believed to be the result of dilution by rapid sedimentation as well as inferred low nutrient levels in the waters found several kilometers from Humboldt Glacier. Core 16 and other cores containing sediment dominated by ice rafting contain rare to frequent diatoms and occasional foraminifera at various down core intervals below the surface layer.

The water transported sediment cores usually contain rare to frequent diatoms at the surface and common to very common diatom abundances as well as other shell material below the surface. Core 21 has common to very common diatom abundances from the surface to 90 cm and no diatoms from 130 cm to 138 cm. This interval shows a very high clay content previously attributed to a sudden influx of clay which may have diluted the diatom concentration, or represents conditions unfavorable for diatom production. Below this interval, in the coarser part of the core, diatoms are only rare to frequent in abundance. In cores 19 and 29 no diatoms were found below 130 cm, where other sediment parameters i.e., texture and mass physical properties indicate an increase in ice activity. Core 30 with its common to very common diatom abundances in its upper water transported sediment, and rare to frequent abundances in its ice rafted sediment (78 cm - 101 cm) adds further evidence to lower diatom production (or dilution by higher rates of deposition) during periods marked by greater ice activity.

With the exception of surface cores 2, 3 and 4 located in the upwelling area and the surface of cores 9 and 13, there are no diatoms in any of the till 1 sediment samples. The lack of diatoms in the upper portions of cores 10, 11, 12, 24, 25, 26 and grab sample 26G, which is reworked till, may well be due to low nutrient content of the arctic water flowing down the western side of the Basin. The absence of diatoms tests and shell material of any other marine organism below the upper few centimeters of all till 1 cores is added evidence that till 1

is a subaerial deposit, as opposed to a subaqueous till. Till 2 sediments contain some diatoms but since penetration of this material was limited to only a few cm below the sediment-water interface there is nothing known about the composition of the deeper material. However, no shell material of any kind was found in core 22 (36 cm - 44 cm) which is believed to consist in large part of till 2 sediment.

In summary, those areas of high nutrients contain abundant diatoms (common to very common) and in water transported sediments these abundances continue down core. Where ice rafting, past and present, is dominant the diatom abundances are less (rare to frequent) or, where deposition is high and nutrient levels low, dilution will result in extremely rare to no diatoms found at all. In both till 1 and till 2 no diatoms or tests of other marine organisms are present more than a few centimeters below the sediment-water interface. The shell material at the surface is a reflection of modern conditions.

CHAPTER VI

CONCLUSIONS

The sediments of Kane Basin were previously divided into two main categories (Recent and relict) found in three sedimentological provinces (Kravitz, 1976). These two categories can now be further subdivided into the following four lithofacies:

Recent

Sediments dominated by ice rafting

Sediments dominated by water transport

Relict

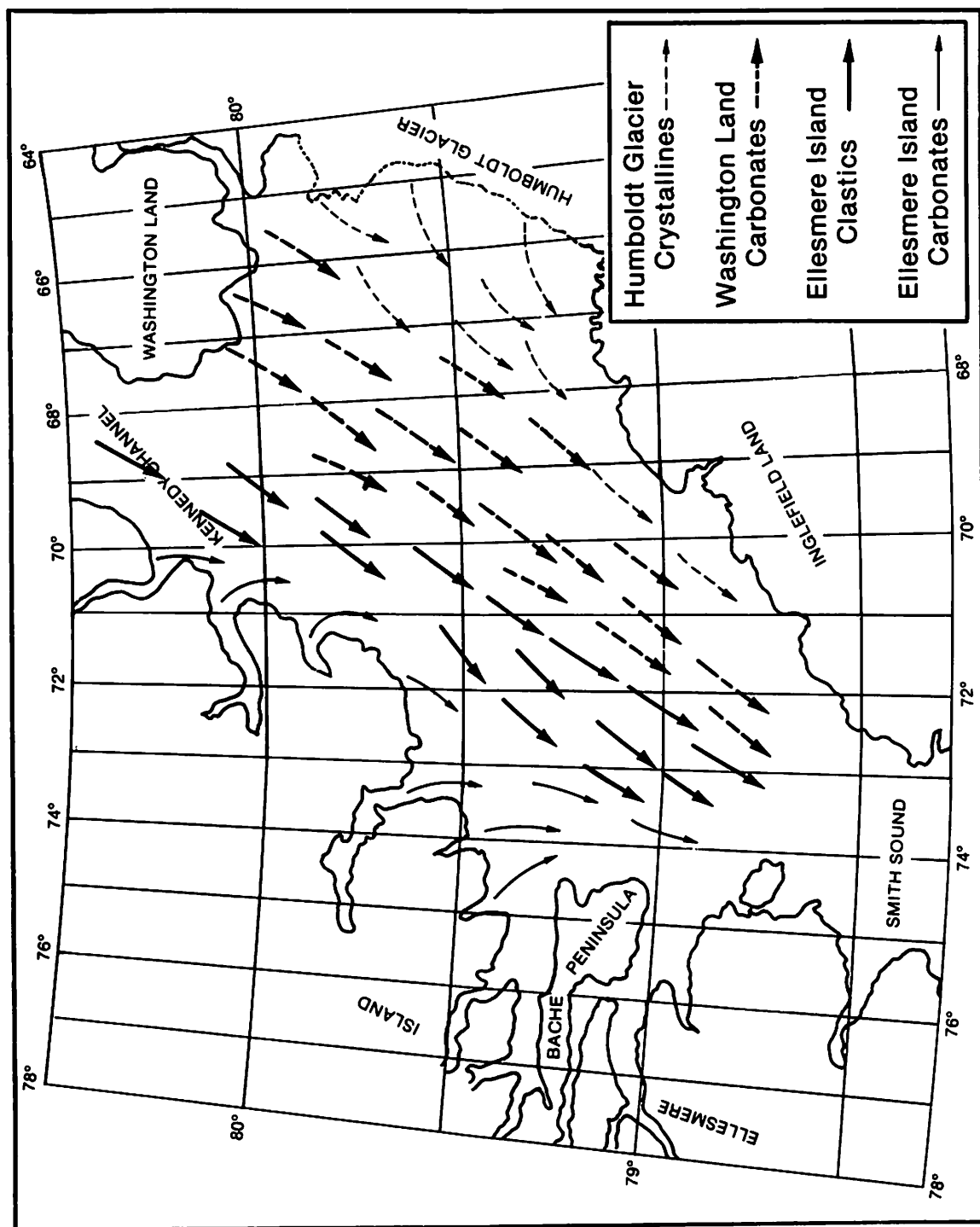
Ellesmere Island till

Greenland till

The following sequence of events may have led to the development of these lithofacies.

Ice advanced into Kane Basin from the north, west, and east bringing with it sediments from northeastern Ellesmere Island, from perhaps as far away as the Lady Franklin Bay area, from Washington Land, Greenland and from that part of Greenland between Washington Land and Inglefield Land now covered by Humboldt Glacier. In the western Basin the ice entered through Kennedy Channel, and as outlet glaciers through some of the fjords on the east coast of Ellesmere Island. Upon entering the Basin this ice was generally confined to what may have previously been a river valley and is now a bathymetric feature known as the western trough. In the east the ice entered the Basin from Washington Land and the area of the Humboldt Glacier. It presumably moved down another former river valley, presently the eastern trough, and overrode a broad interfluvium (the topographic high) between the two valleys. The ice moved south and coalesced in the lowlands at the south end of Kane Basin (Figure 49). As the ice retreated, its sediment load was released and deposited.

Fig. 49. Inferred direction of ice movement in Kane Basin.



Exposed in the western Basin is what I interpret to be a sub-aerially deposited melt out till, or a till deposited at the terminus of the ice in extremely shallow, quiet water, devoid of organisms. This interpretation is based on a number of the sediments characteristics. Texturally the sediment is extremely poorly sorted containing an admixture of gravel, sand, silt, and clay. It's grain size parameters are very similar to other tills (Frakes and Crowell, 1973, Friedman and Sanders, 1978). The sediment's mass physical properties, wet unit weight, void ratio, porosity and water content also are more typical of tills than ice rafted glacial marine sediment (Easterbrook, 1964; Boltunov, 1970). The lack of pebble orientation, the presence of large numbers of friable, oxide-stained pebbles and an overall sandy texture indicates that the sediment is an ablation till rather than a basal till (Goldthwait, 1971). The absence of sedimentary structures and marine fossils support the interpretation that it is a subaerially (or extremely shallow, quiet water) deposited till instead of a deeper water glacial marine deposit (Chriss and Frakes, 1972, and Edwards, 1978).

Three lithologic groups, two major and one minor, are found in the Ellesmere Island till (till 1). The material in the western part of the Basin contains abundant carbonate rock fragments and sparse heavy minerals (Kravitz, 1976). It was derived from that part of Ellesmere Island adjacent to the Kane Basin, where carbonate rocks are widely exposed. The ice, which entered Kane Basin through Kennedy Channel contained sediments dominated by litharenites (with basalt and phyllite fragments), many monomineralic and polymineralic aggregates, and a diverse heavy mineral assemblage. The heavy minerals are composed mostly of clinopyroxene, with subordinate amounts of garnet, orthopyroxene, and amphibole; apatite, epidote, chlorite (sand-sized), sphene, spinel and kyanite are also present. Illite is the most abundant clay mineral, however, expanding lattice clays and chlorite are also major constituents. Concentrations of the chemical elements, Mn, Cr, Co, Ni, Cu, and Ti are slightly higher in these sediments than in the other three lithofacies. This sediment was derived from Tertiary rocks exposed on the Ellesmere Island coast adjacent to the Kennedy Channel in the vicinity of Judge Daly Promontory and Lady Franklin Bay.

Farther to the east in the northern part of the western Basin, on and near the topographic high, the mineralogy of the till 1 (core 4 and core 14 [108 cm - 132 cm]) reflects another source. Compared to other till 1 sediments this source contains relatively abundant kaolinite and opaques. In addition, clinopyroxene is less abundant, and locally the heavy mineral suite is composed of rounded tourmaline, rutile and zircon (core 14 between 108cm - 132cm). The source is believed to be poly-cyclic rocks which may have originated under fresh water acidic conditions and may be reflective of conditions previously existing in now submerged river valleys and interfluves.

The Greenland till (till 2) is located along the topographic high. It is identified as a till on the basis of textural and mass physical properties. This material is extremely resistant to corer penetration and it was not possible to use x-radiography to ascertain the internal structure. The till is coarser and more compact (slightly greater wet unit weights and lower void ratios) than till 1. This may have been caused by winnowing action of waves and currents in this relatively shallow portion of Kane Basin, during the sea level rise following ablation. The sediment was derived from two primary sources. Carbonate pebbles, the dominant lithology in the gravel fraction, were derived from Washington Land. Pebbles composed of crystalline rocks, the dominant lithology in the easternmost area, were derived from the area of the Humboldt Glacier. Rocks eroded by the Humboldt Glacier were the primary source for the heavy minerals, which are dominantly garnet, orthopyroxene and amphibole, with subordinate clinopyroxene. The dominant clay mineral is illite, with expanding lattice clays, chlorite and kaolinite present in small amounts. To the east the till, if deposited, is presently covered by more recent sediments.

As the ice retreated, sea level rose filling the Basin. During this time ice rafting became the predominant sedimentary process. In general, the ice rafting dominant sediment can be differentiated from the tills by slightly better sorting, lower wet unit weights, higher void ratios, water contents and porosities, the presence of many drop-stones (which often distort underlying laminae), marine microorganisms (diatoms and foraminifera), and sedimentary structures resulting when current activity reworks the ice rafted materials.

Ice rafting in the eastern Basin is associated with the Humboldt Glacier. The gravels are composed mostly of crystalline rocks and the heavy minerals are dominated by garnet and orthopyroxene; the clays are mainly illite and the rock flour is composed predominantly of silicate minerals. The ice rafting dominant sediment covers the Greenland till throughout the eastern Basin except for the shallowest areas on the topographic high. As the ice retreated from the western Basin, a southerly current developed keeping the Ellesmere Island till largely exposed. Some reworking and mixing with more Recent sediments took place in the upper part of this till due to the increased current activity. This reworking is identified by factor profiles which indicate mixing in the uppermost layers, radiographs showing sedimentary structures, the presence of the tests of microorganisms in the surficial layers of a few of the cores, and slight increases in factor I type mineralogy (increases in illite, garnet and orthopyroxene).

As the ice continued to recede, sea level continued to rise and the influence of ice activity in Kane Basin began to decline. These conditions are manifest in the sediments by an upward increase in the water transport dominant materials. There is a decrease in the carbonate component of the rock flour in these sediments and an increase in the silicate component while overall the amount of rock flour decreased. The sediment activity (Ac) values are greater and the sediment is finer grained and better sorted. The textural changes are accompanied by lower wet unit weights and higher water contents, void ratios and porosities than those found in the previously deposited sediments (tills and ice rafted materials). Plant fragments are a significant component of the sediments, especially near Inglefield Land, together with relatively abundant diatoms, which occurred as a result of nutrients brought into the Basin by stream runoff. However, the mineralogy (except for the presence of slightly more expanding lattice clays) of these sediments shows little change from the ice rafting dominant sediments because the source rocks for both lithofacies are similar. The main differences are seen in grain geometry. Fresh, angular to subangular grains characterizes the ice rafted material, whereas rounded to subrounded, oxide-stained and often corroded grains are typical of the water transported sediments originating primarily from the soils and tills of Inglefield

Land. These water transported materials, while occasionally containing sedimentary structures are often bioturbated and, with the exception of some shell material and occasional dropstones, are featureless. This indicates a generally low energy environment of deposition. Table 8 lists the most salient parameters used in characterizing the lithofacies and identifying their provenances.

The modern sedimentological setting, therefore, presents the two exposed tills. The south flowing current retards Recent sediment deposition in the western Basin. Ice rafting accompanied by rock flour produced by Humboldt Glacier dominates the area near the glacier. Water transport dominates in the southeastern Basin, with these sediments blanketing the sea floor near Inglefield Land and spreading to the northwest (Figure 50).

The presence of the two undated tills found in Kane Basin raises some questions as to their place in the Quaternary stratigraphy of this part of the Arctic. Considerable evidence exists that substantial ice inundated the valleys exiting from the interior of Judge Daley Promontory, northeastern Ellesmere Island, approximately 28,000 to >35,000 years B.P. (England et al. 1978). However, the glaciers were believed to be thin and, therefore, formed small ice shelves upon entering Kennedy Channel, where they deposited shell rich till and other glacial marine sediments. Since England (1978) and England et al. (1981) found no stratigraphic evidence that these older deposits had been overridden by late Wisconsin/ Würm ice, England et al. (1981) concluded that the Wisconsin/Würm advance did not take place in the area under study. If they are correct then the Ellesmere Island till (till 1), much of which originated from this very area, could not have been formed by this most recent ice advance.

The existence of erratics believed to have been deposited by an earlier advance of the northwest Greenland ice sheet (tentatively 80,000 years B.P.), and which rest on ridges composed of Tertiary rocks (Christie, 1967, England and Bradley 1978) presents the possibility that this earlier advance may have continued through Kennedy Channel and into Kane Basin carrying with it the Tertiary materials derived from northeastern Ellesmere Island. The theory persists that a major ice ridge existed over Kennedy Channel, and that the northeast Ellesmere Island

TABLE 8

MAJOR PARAMETERS CHARACTERIZING THE FOUR LITHOFACIES

	Till 1 (Ellesmere Island Till)	Till 2 (Greenland Till)	Ice rafting dominant	Water transport dominant
Factors	II	III	I	I
Sedimentary structures	None	None	Coarse bedding Laminae Cross-laminae	Coarse bedding Laminae Cross-laminae
Pebble orientation	No	No	Yes	Yes
Bioturbation	None	None	Weak	Strong
Shell material	None	None	Yes	Yes
Diatoms	Surface only	Surface only	Surface and occasionally down core	Surface and common down core
% Gravel	15	22	7	< 1
% Sand	33	41	20	4
% Silt	29	23	31	44
% Clay	23	14	42	52
M(ϕ)	Very fine sand (4.0)	Fine sand (2.7)	Medium silt (5.8)	Very fine silt (7.9)

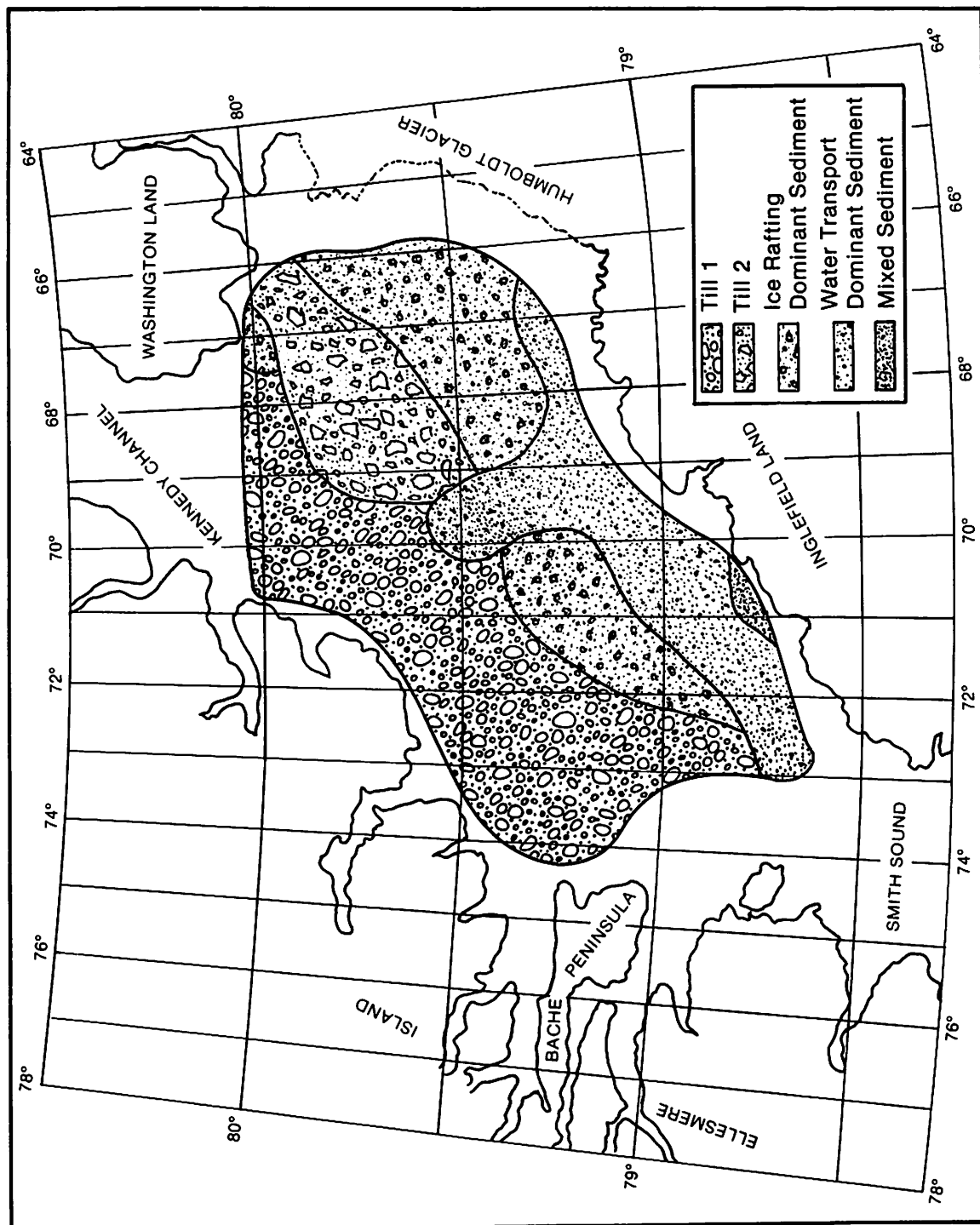
TABLE 8
(continued)

	Till 1 (Ellesmere Island Till)	Till 2 (Greenland Till)	Ice rafting dominant	Water transport dominant
Standard deviation	Extremely poorly sorted (4.2)	Extremely poorly sorted (4.0)	Very poorly sorted (3.8)	Very poorly sorted (2.5)
Skewness	Slightly negative (-0.055)	Positive (0.153)	Moderately negative (-0.206)	Highly negative (-0.325)
Kurtosis	Platykurtic (-0.671)	Platykurtic (-0.445)	Platykurtic (-0.542)	Leptokurtic (0.072)
Wet unit weight (gm/cm ³)	2.06	2.15	1.75	1.48
Water content (% dry weight)	23	20	50	101
Saturated void ratio	0.60	0.52	1.36	2.59
Porosity (%)	38	33	56	72
Total carbonate (%)	25	18	16	15
Illite(%)	51	72	70	67
Expanding lattice clays(%)	22	8	10	13

TABLE 8
(continued)

	Till 1 (Ellesmere Island Till)	Till 2 (Greenland Till)	Ice rafting dominant	Water transport dominant
Kaolinite(%)	15	8	8	8
Aggregates	26	3	3	3
% Silicate in rock flour	46	76	84	93
% Carbonate in rock flour	54	24	16	7
Dominant rock types in gravel fraction	Clastics and Carbonates	Carbonates	Crystallines	Crystallines
% Garnet	13	40	44	42
% Orthopyroxene	7	23	23	23
% Clinopyroxene	55	8	9	12

Fig. 50. Areal distribution of four lithofacies found in Kane Basin.



and northwest Greenland ice sheets were confluent (although not necessarily during the Wisconsin/Würm glaciation). This furnishes an attractive possible explanation for the concomitant deposition of the two tills of separate provenance which have been identified in Kane Basin.

The conclusions presented above are based on the interpretation that "till 1" and "till 2" were indeed deposited by subaerial melting of continental glaciers. Sediments similar to till can be produced by intensive ice rafting in an environment where very little or no reworking of sediments takes place (Chriss and Frakes, 1972). Such ice rafted sediments might texturally resemble glacial tills and this possibility exists. However, the evidence cited above strongly favors the interpretation that "till 1" and "till 2" are true tills and not glacial marine sediments.

- Casagrande, A., 1948, Classification and identification of soils: American Society of Civil Engineers. Transactions, vol. 113, p. 901-931.
- Chriss, T., and Frakes, L. A., 1972, Glacial marine sedimentation in the Ross Sea, p. 747-762: in Adie, R. (ed.), Antarctic geology and geophysics. Scandinavian University Books, Oslo, 876 p.
- Christie, R. L., 1964, Geological reconnaissance of northeastern Ellesmere Island, District of Franklin: Geol. Surv. of Canada Mem. 331, 79 p.
- _____, 1967a, Bache Peninsula, Ellesmere Island, Arctic Archipelago: Geol. Surv. of Canada Mem. 347, 63 p.
- _____, 1967b, Reconnaissance of the surficial geology of northeastern Ellesmere Island, Arctic Archipelago: Geol. Surv. of Canada Bull. v. 138, 50 p.
- Collin, A. E., 1965, Oceanographic observations in Nares Strait, northern Baffin Bay, 1963, 1964: Unpubl. Manuscript, Bedford Inst. Ocean., no. 65-5.
- Coonley, L. S., Baker, E. B. and Holland, H. D., 1971, Iron in the Mullica River and in Great Bay, New Jersey: Chem. Geol., v. 7, p. 51-63.
- Cooper, J. H. and Johnson, K. A., 1950, A rapid method of determining the liquid limit of soils: Materials Laboratory Rpt. no. 83, Washington State Highway Department.
- Dawes, P. R. and Soper, N. J., 1973, Pre-Quaternary history of north Greenland, p. 117-134: in Pitcher, M. G. (ed.), Arctic Geology, The Am. Assoc. Petrol. Geol. Mem. 19, 747 p.
- _____, 1976, Precambrian to Tertiary of northern Greenland, p. 248-303: in Escher, A. and Watt, W. S. (eds.), Geology of Greenland, The Geol. Surv. of Greenland, Copenhagen, 603 p.
- Day, C. G., 1968, Current measurements in Smith Sound, summer 1963: U.S. Coast Guard Oceanographic Report No. 16.
- Doeglas, D. J., 1940, The importance of heavy mineral analysis for regional sedimentary petrology: in Trask, P. D., chm., Report of the Committee on Sedimentation, Natl. Research Council, Div. Geology and Geography Ann. Rept. 1939-1940, App. D. Exhibit G, p. 102-121.
- Dunbar, M., 1971, Winter ice reconnaissance in Nares Strait, 1970-71: Defence Research Establishment Ottawa Technical Note no. 71-34, 29 p.
- _____, 1974, Ice regime and ice transport in Nares Strait: Arctic, v. 26, p. 282-291.

REFERENCES CITED

- Aksu, A. E., 1981, Late Quaternary stratigraphy, paleoenvironmentology and sedimentation history of Baffin Bay and Davis Strait. Ph.D. Dissertation, Dalhousie University, Halifax, Nova Scotia.
- Allison, L. E., 1935, Organic soil carbon by reduction of chromic acid: *Soil Science*, v. 40, p. 311-320.
- American Society for Testing Materials, 1964, Procedures for testing soils. Philadelphia, 540 p.
- Andrew, J. A., and Kravitz, J. H., 1974, Sediment distribution in deep areas of the northern Kara Sea, p. 231-256: in Herman, Y. (ed.), *Marine geology and oceanography of the Arctic seas*, Springer-Verlag, New York, 397 p.
- Arctic Pilot, 1976, Volume III: Hydrographic Department, Admiralty, London, England.
- Bailey, W. B., 1956, On the origin of deep Baffin Bay water: *Jour. Fisheries Research Board of Canada*, v. 13, no. 3, p. 303-308.
- Baker, S. R. and Friedman, G. M., 1973, Sedimentation in an Arctic marine environment: Baffin Bay between Greenland and the Canadian Arctic Archipelago: *Symposium on Offshore Eastern Canada*, collected papers, p. 471-498.
- Biscaye, P. E., 1964, Distinction between kaolinite and chlorite in Recent sediments by x-ray diffraction: *The Am. Mineralogist*, v. 49, p. 1281-1289.
- , 1965, Mineralogy and sedimentation of recent deep-sea clays in the Atlantic Ocean and adjacent seas and oceans: *Geol. Soc. Amer. Bull.*, v. 76, p. 803-832.
- Boltunov, V. A., 1970, Certain earmarks distinguishing glacial and moraine-like glacial-marine sediments, as in Spitzbergen: *Internat. Geology Rev.*, v. 12, no. 2, p. 204-211.
- Booth, J. D., and Burckle, L. H., 1976, Displaced Antarctic diatoms in the southwestern and central Pacific: *Pacific Geology*, v. 11, p. 99-108.
- Burmister, D. M., 1960, Strain-rate behavior of clay and organic soils, p. 88-105: *Symposium on time rates of loading in soil testing*. ASTM Special Technical Publication, no. 254, 375 p.
- Carver, R. E., 1971, Heavy mineral separation, p. 427-452: in Carver, R. E. (ed.), *Procedures in sedimentary petrology*, Wiley Interscience, New York, 653 p.

- _____, 1979, Fall ice drift in Nares Strait, as observed by sideways-looking airborne radar: *Arctic*, v. 32. no. 4, p. 283-307.
- Easterbrook, D. J., 1964, Void ratios and bulk densities as means of identifying Pleistocene tills: *Geol. Soc. America Bull.* v. 75, p. 745-750.
- Edwards, M. B., 1978, Glacial environments, p. 416-438: in Reading, H. G. (ed.), *Sedimentary environments and facies*, Elsevier, New York, 557 p.
- Emery, K. O., 1949, Topography and sediments of the Arctic Basin: *Jour. Geology*, v. 57, p. 512-521.
- England, J., 1978, The glacial geology of northeastern Ellesmere Island, N.W.T., Canada: *Canadian Jour. Earth Sci.*, v. 15, no. 4, p. 603-617.
- _____, and Bradley, R. S., 1978, Past glacial activity in the Canadian High Arctic: *Science*, v. 200, p. 265-270.
- _____, Bradley, R.S., and Miller, G.H., 1978, Former ice shelves in the Canadian high Arctic: *Jour. Glaciology*, v. 20, p. 393-404.
- _____, Bradley, R. S., and Stuckenrath, R., 1981, Multiple glaciations and marine transgressions, western Kennedy Channel, Northwest Territories, Canada: *Boreas*, v. 10, p. 71-89.
- Flanagan, F. J., 1973, 1972 values for international geochemical reference samples: *Geochim. Cosmochim. ACTA*, v. 37, p. 1189-1200.
- Folk, R. L., and Ward, W. C., 1957, Brazos River bar: A study in the significance of grain size parameters: *Jour. Sed. Petrology*, v. 27, p. 3-26.
- _____, 1966, A review of grain size parameters: *Sedimentology*, v. 6, no. 2, p. 73-93.
- _____, 1968, *Petrology of sedimentary rocks*: Hemphill's. Austin, Texas, 154 p.
- Frakes, L. A., and Crowell, J. C., 1973, Characteristics of modern glacial moraine sediments: application to Gondwana glacials, p. 373-380: in Campbell, K.S.W. (ed.), *Gondwana geology: 3rd Gondwana Symposium*, Canberra, Australia.
- Friedman, G. M., 1962, On sorting, sorting coefficients, and the log-normality of the grain-size distribution of sandstones: *Jour. Geology*, v. 70, p. 737-753.
- _____, and Sanders, J. E., 1978, *Principles of sedimentology*, Wiley, New York, 792 p.

- Galehouse, J. S., 1969, Counting grain mounts: number percentage vs. number frequency: Jour. Sed. Petrology, v. 39, p. 812-815.
- Gibbs, R. J., 1965, Error due to segregation in quantitative clay mineral x-ray diffraction mounting techniques: Am. Mineralogist, v. 50, p. 741-751.
- _____, 1973, Mechanisms of trace metal transport in rivers: Science, v. 180, no. 4081, p. 71-73.
- Goldthwait, R. P., 1971, Introduction to till, today, p. 3-26: in Goldthwait, R. P. (ed.), Till: A Symposium. Ohio State Univ. Press, Columbus.
- Grant, A. C., 1965, Distributional trends in the recent marine sediments of northern Baffin Bay: Bedford Inst. Ocean. Rpt. 65-9.
- Griffiths, J. C. and Rosenfeld, M. A., 1954, Operator variation in experimental research: Jour. Geology, v. 62, p. 74-91.
- Grim, R. E., 1968, Clay mineralogy, McGraw-Hill, New York, 396 p.
- Hansbo, S., 1957, A new approach to the determination of the shear strength of clay by the fall-cone test: Royal Swedish Geotechnical Institute Proceedings, no. 8, p. 1-59.
- Hill, D. E., and Tedros, J. C. F., 1961, Weathering and soil formation in the Arctic environment: Am. Jour. Sci., v. 259, p. 84-101.
- Hobbs, W. H., 1948, American and Eurasian glaciers of the past: Sci. Monthly, v. 66, no. 2, p. 99-106.
- Hvorslev, M. J., 1936, Conditions of failure for remolded cohesive soils: 1st Intern. Conf. on Soil Mechanics and Foundation Engineering Proc., v. 3, p. 51-53.
- _____, 1937, Über die festigkeitseigenschaften gestorter bindiger boden: Ingeniorridenskabelige Skrifter A, nr. 45, Danmark, Naturvid, Samfund. Copenhagen, 159 p.
- Imbrie, J., and Van Andel, T. H., 1964, Vector analysis of heavy-mineral data: Geol. Soc. America Bull., v. 75, p. 1131-1156.
- Jones, T. A., 1970, Comparison of the descriptors of sediment grain-size distributions: Jour. Sed. Petrology, v. 40, p. 1204-1215.
- Keller, W. D., 1970, Environmental aspects of clay minerals: Jour. Sed. Petrology, v. 40, p. 788-813.
- Kerr, J. W., 1967a, Stratigraphy of central and eastern Ellesmere Island, Arctic Canada, Pt. 1, Proterozoic and Cambrian: Geol. Surv. of Canada Paper 67-27, 63 p.

- _____, 1967b, Vendom Fiord Formation - a new red-bed unit of probable early Middle Devonian (Eifelian) age, Ellesmere Island, Arctic Canada: Geol. Surv. of Canada Paper 67-43.
- _____, 1968, Stratigraphy of central and eastern Ellesmere Island, Arctic Canada Pt. II, Ordovician: Geol. Surv. of Canada Paper 67-27.
- _____, 1976, Stratigraphy of central and eastern Ellesmere Island, Arctic Canada, Part III. Upper Ordovician (Richmondian), Silurian and Devonian: Geol. Surv. of Canada Bull. 260.
- Kindle, E. M., 1924, Observations on ice-borne sediments by the Canadian and other Arctic expeditions: Am. Jour. Sci., v. 7, p. 251-286.
- Klován, J. E., 1975, R and Q-mode factor analysis, p. 21-69: in McCammon, R. B. (ed.), Concepts in geostatistics, Springer-Verlag, New York, 168 p.
- Koch, L., 1929a, Stratigraphy of Greenland: Meddr Grnland, v. 73, lafd, no. 2, p. 205-320.
- _____, 1929b, The geology of the south coast of Washington Land: Meddr Grnland, v. 73, lafd, no. 1, 39 p.
- _____, 1933, The geology of Inglefield Land: Meddr Grnland, v. 73, lafd, no. 2, 38 p.
- Kogler, F. C., 1967, Geotechnical properties of Recent marine sediments from the Arabian Sea and the Baltic Sea,;. 170-176: in Richards, A. F. (ed.), Marine geotechniques, Univ. of Illinois Press, Urbana, 327 p.
- Kravitz, J. H., 1966, Using an ultrasonic disrupter as an aid to wet sieving: Jour. Sed. Petrology, v. 36, p. 811-812.
- _____, 1968, Splitting core liners with a mica undercutter: Jour. Sed. Petrology, v. 38, p. 1358-1361.
- _____, 1970, Repeatability of three instruments used to determine the undrained shear strength of extremely weak, saturated, cohesive sediments: Jour. Sed. Petrology, v. 40, p. 1026-1037.
- _____, and Sorensen, F. H., 1970, Sedimentological reconnaissance survey of Kane Basin: Maritime Sediments, v. 6, p. 17-20.
- _____, 1975, Textural and mineralogical characteristics of the surficial sediments of Kane Basin: M. S. Thesis, The George Washington University, Washington, D.C., 165 p.
- _____, 1976, Textural and mineralogical characteristics of the surficial sediments of Kane Basin: Jour. Sed. Petrology, v. 46, no. 3, p. 710-725.

- _____, 1983, Sediments and sediment processes in a high Arctic glacial-marine basin [Ph.D. dissert.]: The George Washington University, Washington, D.C., 487 p.
- Krumbein, W. C. and Pettijohn, F. J., 1938, Manual of sedimentary petrography. Appleton-Century-Crofts, New York, 549 p.
- La Fond, E. C., Dietz, R. S., and Prichard, D. W., 1949, Oceanographic measurements from the U.S.S. Nereus on Arctic cruise, 1947: U.S. Navy Electronics Lab. Report.
- Lambe, T. W., 1951, Soil testing for engineers: Wiley, New York, 165 p.
- Loring, D. H., and Nota, D. J. G., 1973, Morphology and sediments of the Gulf of St. Lawrence: Fisheries Research Board of Canada Bulletin 182, 147 p.
- Marlowe, J. I., 1968, Unconsolidated marine sediments in Baffin Bay: Jour. Sed. Petrology, v. 38, p. 1065-1978.
- McLaren, D. J., 1963, Goose Fjord to Bjerne Peninsula: in Geology of the north-central part of the Arctic Archipelago, Northwest Territories (Operation Franklin), Geol. Surv. of Canada. Mem. 320, p. 310-338.
- Medlin, J. H., Suhr, N. H., and Bodkin, J. B., 1969, Atomic absorption analysis of silicates employing LiBo_2 fusion: Atom. Abs. Newsletter v. 8, p. 25-29.
- Miall, A. D., (in press), Tertiary sedimentation and tectonics in the Judge Daly Basin, northeastern Ellesmere Island, Arctic Canada: Geol. Surv. of Canada Paper 80-30.
- Moynihan, M. J., 1972, Oceanographic observations in Kane Basin, September 1968 and July-September 1969: U.S. Coast Guard Oceanographic Report No. 55, 70 p.
- Muench, R. D., 1971a, The physical oceanography of the northern Baffin Bay region: Baffin Bay - North Water Project Scientific Rpt. 1, Arctic Institute of North America.
- _____, 1971b, Oceanographic conditions at a fixed location in western Kane Basin, May 1969, p. 1-5: in Moynihan, M. J. and Muench, R. D., Oceanographic observations in Kane Basin and Baffin Bay, May and August-October 1969: U.S. Coast Guard Oceanographic Report No. 44, 143 p.
- Neville, A. M., and Kennedy, J. B., 1964, Basic statistical methods for engineers and scientists. International Textbook, Scranton, Pa., 325 p.
- Okada, H., 1971, Classification of sandstone: analysis and proposal: Jour. Geology, v. 79, p. 509-525.

- Ovenshine, A. T., 1970, Observations of iceberg rafting in Glacier Bay, Alaska, and the identification of ancient ice-rafted deposits: Geol. Soc. America Bull., v. 81, p. 891-894.
- Pelletier, B. R., 1966, Development of submarine physiography in the Canadian Arctic and its relation to coastal movements: in Garland, G. D. (ed.), Roy. Soc. Canada, Spec. Pub. No. 9, p. 77-101.
- Pierce, J. W. and Siegel, F. R., 1969, Quantification in clay mineral studies of sediments and sedimentary rocks: Jour. Sed. Petrology, v. 39, p. 187-193.
- Piper, D. J. W., and Slatt, R. M., 1977, Late Quaternary clay-mineral distribution on the eastern continental margin of Canada: Geol. Soc. American Bull., v. 88, p. 267-272.
- Poulsen, C., 1946, Notes on the Cambro-Ordovician fossils collected by the Oxford University Ellesmere Island Expedition 1934-1935: Quart. Jour. Geol. Soc. London, v. 102, p. 299-337.
- Rose, A. W., Hawkes, H. E., and Webb, J. S., 1979, Geochemistry in mineral exploration, Academic Press, New York, 657 p.
- Ross, D. A., 1971, Sediments of the northern Middle America Trench: Geol. Soc. America Bull., v. 82, p. 303-322.
- Rubey, W. W., 1933, The size-distribution of heavy minerals within a waterlaid sandstone: Jour. Sed. Petrology, v. 3, p. 3-29.
- Rucker, J. B., and Stewart, R. A., 1966, Sediment size computer program; U.S.N. Oceanographic Office Informal Manuscript 66-11, 20 p.
- Sadler, H. E., 1976, The flow of water and heat through Nares Strait: Defence Research Establishment Ottawa Rept. 736, Ottawa, 184 p.
- Short, A. D., and Wiseman, W. J., 1975, Coastal breakup in the Alaskan Arctic: Geol. Soc. America Bull., v. 86, p. 199-202.
- Skempton, A. W., 1953, The colloidal activity of clays: 3rd Intern. Conf. on Soil Mechanics and Foundation Engineering Proc., v. 1, p. 57-61.
- _____, 1960, Terzaghi's discovery of effective stress: From theory to practice in soil mechanics, Wiley, New York, 425 p.
- _____, 1970, The consolidation of clays by gravitational compaction: Quart. Jour. Geol. Soc. London, v. 125, p. 373-411.
- Sverdrup, H. U., 1938, Notes on erosion by drifting snow and transportation of solid material by sea ice: Am. Jour. Sci., v. 35, p. 370-373.
- Tarr, R. S., 1897, The Arctic sea ice as a geological agent: Am. Jour. Sci., v. 3, p. 223-229.

- Taylor, D. W., 1948, Fundamentals of soil mechanics, Wiley, New York, 700 p.
- Tedrow, J. C. F., 1968, Soil investigations in Inglefield Land, Greenland Arctic Inst. of N. A. Research RPT, DA-AROD-31-124-6820.
- _____, 1970, Soil investigations in Inglefield Land, Greenland: Meddr Grnland, v. 188, no. 3, 93 p.
- Terzaghi, K., 1924, Die theorie der hydrodynamischen spannungsercheinungen und ihr erdbautechnisches anwendungsgebiet., Intern. Cong. Applied Mechanics Proc., p. 288-294.
- _____, and Peck, R. B., 1948, Soil mechanics in engineering practice. Wiley, New York, 566 p.
- _____, 1955, Influence of geological factors on the engineering properties of sediments: Economic Geology, 50th Anniversary Volume, 1905-1955, p. 557-618.
- Trettin, H. P., 1969, Pre-Mississippian geology of northern Axel Heiberg and northwestern Ellesmere Island, Arctic Archipelago: Geol. Surv. of Canada Bull. 171.
- Troelsen, J. C., 1950, Contributions to the geology of northwest Greenland, Ellesmere Island, and Axel Heiberg Island: Meddr Grnland, v. 149, no. 7, 86 p.
- Twenhofel, W. H., and Tyler, S. A., 1941, Methods of study of sediments. McGraw-Hill Book Company, Inc., New York, 183 p.
- Uchupi, E., 1964, Sediments and topography of Kane Basin: Oceanographic observations Kennedy Channel, Kane Basin, Smith Sound, and Baffin Bay, U.S. Coast Guard Oceanographic Report No. 5, p. 61-72.
- Van Andel, T. J. H., 1950, Provenance, transport, and deposition of Rhine sediments. H. Veenman and Sons, Wageningen, Netherlands, 129 p.
- _____, and Veevers, J. J., 1967, Morphology and sediments of the Timor Sea: Bull. Bur. Miner. Resour. Geol. Geophys. Aust., no. 83, 173 p.
- Walker, H. J., 1969, Some aspects of erosion and sedimentation in an Arctic delta during breakup: Actes du colloque de Bucarest, Hydrologie de deltas, Association Internationale d'Hydrologie Scientifique, p. 290-219.
- Young, E. J., 1966, A critique of methods for comparing heavy mineral suites: Jour. Sed. Petrology, v. 36, p. 57-65.
- Zubov, N. N., 1945, Arctic Ice: Northern Sea Route Directorate Press, Moscow 1945, Translation, U.S. Naval Oceanographic Office, Washington, D.C., 491 p.

**INSTITUTE OF ARCTIC AND ALPINE RESEARCH
OCCASIONAL PAPERS**

Numbers 1 through 5, and 9, 11, 12, 16, 17, 18, and 23 are out of print. A second edition of Number 1 is available from the author. Numbers 2, 3, 4, 5, 9, and 11 are available from National Technical Information Service, U.S. Department of Commerce. For details, please write to INSTAAR.

6. *Guide to the Mosses of Colorado*. By W. A. Weber. 1973. 48 pp. Order from the author, University of Colorado Museum, Boulder, Colorado 80309. \$2.50.
7. *A Climatological Study of Strong Downslope Winds in the Boulder Area*. By W. A. R. Brinkmann. 1973. 228 pp. Order from the author, Institute for Environmental Studies, University of Wisconsin, 1225 West Dayton Street, Madison, Wisconsin 53706.
- †8. *Environmental Inventory and Land Use Recommendations for Boulder County, Colorado*. Edited by R. F. Madole. 1973. 228 pp. 7 plates. \$6.00.
- †10. *Simulation of the Atmospheric Circulation Using the NCAR Global Circulation Model With Present Day and Glacial Period Boundary Conditions*. By J. H. Williams. 1974. 328 pp. \$4.75.
- †13. *Development of Methodology for Evaluation and Prediction of Avalanche Hazard in the San Juan Mountains of Southwestern Colorado*. By R. L. Armstrong, E. R. LaChapelle, M. J. Bovis, and J. D. Ives. 1975. 141 pp. \$4.75.
- †14. *Quality Skiing at Aspen, Colorado: A Study in Recreational Carrying Capacity*. By C. Crum London. 1975. 134 pp. 3 plates. \$5.50.
- †15. *Palynological and Paleoclimatic Study of the Late Quaternary Displacements of the Boreal Forest-Tundra Ecotone in Keewatin and Mackenzie, N.W.T., Canada*. By H. Nichols. 1975. 87 pp. \$4.00.
- †19. *Avalanche Release and Snow Characteristics, San Juan Mountains, Colorado*. Edited by R. L. Armstrong and J. D. Ives. 1976. 256 pp. 7 plates. \$7.50.
- †20. *Landslides Near Aspen, Colorado*. C. P. Harden. 1976. 61 pp. 5 plates. \$3.75.
- †21. *Radiocarbon Date List III. Baffin Island, N.W.T., Canada*. J. T. Andrews. 1976. 50 pp. \$2.50.
- †22. *Physical Mechanisms Responsible for the Major Synoptic Systems in the Eastern Canadian Arctic in the Winter and Summer of 1973*. By E. F. LeDrew. 1976. 205 pp. \$4.50.
- †24. *Avalanche Hazard in Ouray County, Colorado, 1877-1976*. By B. R. Armstrong. 1977. 125 pp. 32 plates. \$4.50.
- †25. *Avalanche Atlas, Ouray County, Colorado*. By B. R. Armstrong and R. L. Armstrong. 1977. 132 pp. 34 plates. \$6.00.
- †26. *Energy Budget Studies in Relation to Fast-ice Breakup Processes in Davis Strait. Climatological Overview*. R. G. Barry and J. D. Jacobs with others. 1978. 284 pp. \$7.00.
- †27. *Geocology of Southern Highland Peru: A Human Adaptation Perspective*. By B. P. Winterhalder and R. B. Thomas. 1978. 91 pp. \$6.00.
- †28. *Tropical Teleconnection to the Seesaw in Winter Temperatures between Greenland and Northern Europe*. By G. A. Meehl. 1979. 110 pp. \$4.00.
- †29. *Radiocarbon Date List IV. Baffin Island, N.W.T., Canada*. By G. H. Miller. 1979. 61 pp. \$4.00.
- †30. *Synoptic Climatology of the Beaufort Sea Coast of Alaska*. By R. E. Moritz. 1979. 176 pp. \$6.00.
- †31. *The North Pacific Oscillation and Eigenvectors of Northern Hemisphere Atmospheric Circulation during Winter*. By J. C. Rogers. 1979. 177 pp. \$6.00.
- †32. *Modeling of Air Pollution Potential for Mountain Resorts*. By D. E. Greenland. 1979. 96 pp. \$5.00.
- †33. *Baffin Island Quaternary Environments: An Annotated Bibliography*. By M. Andrews and J. T. Andrews. 1980. 123 pp. \$5.50.
- †34. *Temperature and Circulation Anomalies in the Eastern Canadian Arctic, Summer 1946-76*. By R. A. Keen. 1980. 159 pp. \$6.00.
- †35. *Map of Mixed Prairie Grassland Vegetation, Rocky Flats, Colorado*. By S. V. Clark, P. J. Webber, V. Komárková, and W. A. Weber. 1980. 66 pp., 2 plates. \$8.00.
- †36. *Radiocarbon Date List I: Labrador and Northern Quebec, Canada*. By S. K. Short. 1981. 33 pp. \$4.00.
- †37. *Ecological Studies in the Colorado Alpine: A Festschrift for John W. Marr*. Edited by James C. Halfpenny. 1982. 147 pp. \$10.00.
- †38. *Geocología de la Región Montañosa del sur Perú: Una Perspectiva de Adaptación Humana*. By Bruce P. Winterhalder and R. Brooke Thomas. 1982. 99 pp. \$6.00. (Previously published in English as Occasional Paper No. 27, 1978.)
- †39. *Sediments and Sediment Processes in Kane Basin, a High Arctic Glacial Marine Basin*. By J. H. Kravitz. 1982. 184 pp. \$8.00.

†Order from INSTAAR, Campus Box 450, University of Colorado, Boulder, Colorado 80309. Orders by mail add \$1.00 per title.

Occasional Papers are a miscellaneous collection of reports and papers on work performed by INSTAAR personnel and associates. Generally, these papers are too long for publication as journal articles or they contain large amounts of supporting data that are normally difficult to publish in the standard literature.